NASA Conference Publication 2116



# Operational Applications of Satellite Snowcover Observations

Proceedings of a final workshop
held at Sparks, Nevada
April 16-17, 1979

NASA

NASA Conference Publication 2116

# Operational Applications of Satellite Snowcover Observations

*Editors*
Albert Rango, *Goddard Space Flight Center*
Ralph Peterson, *General Electric Company*

Proceedings of a final workshop
sponsored by The National Aeronautics
and Space Administration and
The University of Nevada, Reno
and held at Sparks, Nevada
April 16-17, 1979

National Aeronautics
and Space Administration

**Scientific and Technical
Information Office**

1980

# FOREWORD

Research progress in extracting meaningful snow information from satellite data led to the 1975 initiation of a NASA Applications Systems Verification and Transfer (ASVT) project on the Operational Applications of Satellite Snowcover Observations. Nine operational water management agencies in the western United States participated in this ASVT in cooperation with NASA. In addition, the National Environmental Satellite Service provided snow data from various NOAA satellites. On August 18-20, 1975, the first Workshop on Operational Applications of Satellite Snowcover Observations was held at the Waystation in South Lake Tahoe, California, primarily to bring together the various cooperating agencies for an information exchange of analysis techniques, early results, and problem solving. The proceedings of the workshop were published as NASA SP-391. This first workshop was fruitful in that it assembled operational water management personnel and remote sensing specialists to discuss the common topic of the use of remotely sensed snowcover information for improving snowmelt runoff forecasts.

Using the first Workshop as a springboard for the evolution of various methods, the operational agencies each developed ways to interpret the satellite data and use the snowcover information in their water management operations. During the spring snowmelt seasons of 1978 and 1979, many of the agencies were using the satellite snowcover data in a quasi-operational mode. In order to conclude the project, the agency participants were brought together to exchange investigation results at the Final Workshop on Operational Applications of Satellite Snowcover Observations. In addition, in order to present the results of the ASVT to the snow management community as well as the participating agencies, the Final Workshop was held in conjunction with the 47th Annual Western Snow Conference on April 16–17, 1979, at Sparks, Nevada. This final meeting, the publication of the Workshop proceedings in this document, and publication of the agencies' final reports as NASA Technical Papers should insure widespread dissemination of the snow ASVT results so that other interested organizations can make decisions regarding the adoption of the new technology.

Seventeen scientific papers were presented over the 2-day period covering various techniques for interpreting Landsat and NOAA satellite data, the status of future systems for continuing snow hydrology applications, the use of snowcover observations in streamflow forecasts by both ASVT participants and selected foreign investigators, and the benefits of using satellite snowcover data in runoff forecasting. Session chairmen were P. Ffolliott, University of Arizona, Tucson, Arizona; D. Wiesnet, NOAA/National Environmental Satellite Service, Suitland, Maryland; J. Meiman, Colorado State University, Fort Collins, Colorado; and J. Washichek, USDA/Soil Conservation Service (retired), Denver, Colorado. J. Dunbar-Douglass, Conferences and Institutes/University of Nevada, Reno, Nevada, was the Program Coordinator of the Workshop.

The papers published in these proceedings are in the same order as presented at the Workshop. In order to expedite the publication of the proceedings, papers were prepared in camera ready format. Each author assumes full responsibility for the content of his paper.

Albert Rango
Workshop Director
NASA/Goddard Space Flight Center

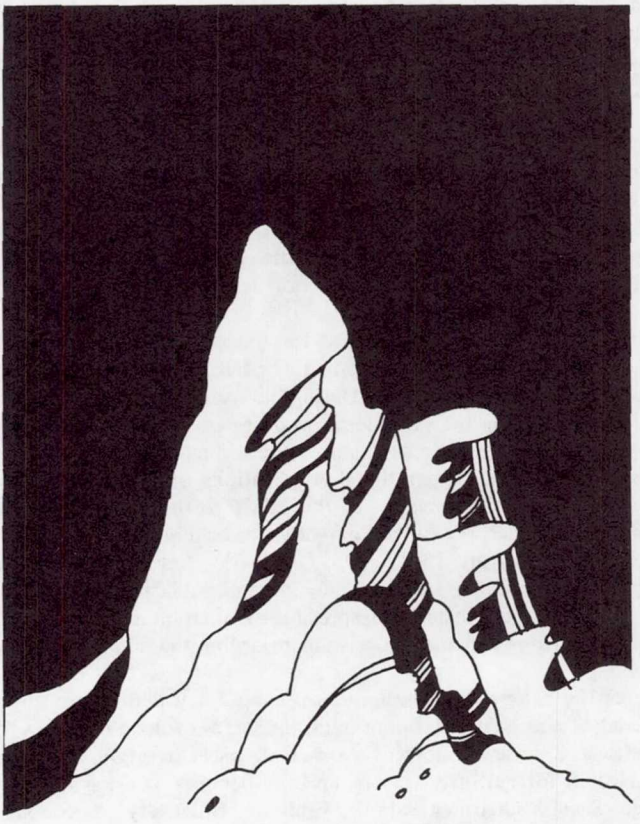

FINAL WORKSHOP ON
OPERATIONAL APPLICATIONS OF SATELLITE
SNOWCOVER OBSERVATIONS

TABLE OF CONTENTS

# THE EVOLUTION OF SATELLITE SNOW MAPPING WITH EMPHASIS ON THE USE OF LANDSAT IN THE SNOW ASVT STUDY AREAS

James C. Barnes and Clinton J. Bowley, Environmental Research & Technology, Inc., Concord, Massachusetts

## ABSTRACT

The potential of the satellite for mapping snow cover was recognized soon after the launch of the first United States weather satellite nearly 20 years ago. Since then, as improved satellite systems have been developed, an increasing use has been made of remote sensing from space to monitor snow. Maps showing percentage snow cover for selected river basins are now produced on a routine basis from the NOAA operational satellite imagery, and the data from Landsat have been shown to have practical application for snow mapping. This paper reviews the types of satellite data that have been used to map snow and the interpretive techniques that have evolved. The emphasis in the review is on the application of Landsat data in the four ASVT Snow Project study areas, and the development of methods to use snow cover area from Landsat in runoff prediction. The application of remote sensing in portions of the spectrum other than the visible is also discussed.

## INTRODUCTION

The year 1980 will mark the twentieth anniversary of the launch of the first United States weather satellite. As seen in Figure 1, the first television camera images from TIROS-1 were rather crude as compared to today's satellite data because of the relatively poor resolution and oblique viewing angle. These initial sensor systems were designed primarily to view clouds, and the resulting images showed patterns, such as spiral clouds associated with deepening storms, never before realized by the meteorologist.

It was not long after TIROS-1 returned its first images from space that efforts were underway to determine what information other than cloud patterns could be derived from weather satellites. In the early images, such as that shown in Figure 1, snow and ice were essentially the only terrestrial features that could be detected other than ocean-land boundaries, large lakes, and a few rivers. Thus, snow was perhaps the first "earth resource" observed from space, even before the term came into common use.

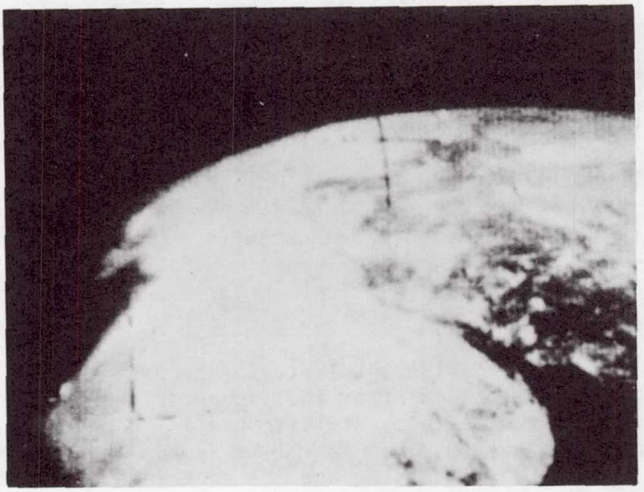

Figure 1 TIROS-1 image, 1 April 1960, viewing the mouth of the St. Lawrence River. Snow and ice can be seen in this very first image ever taken by a weather satellite.

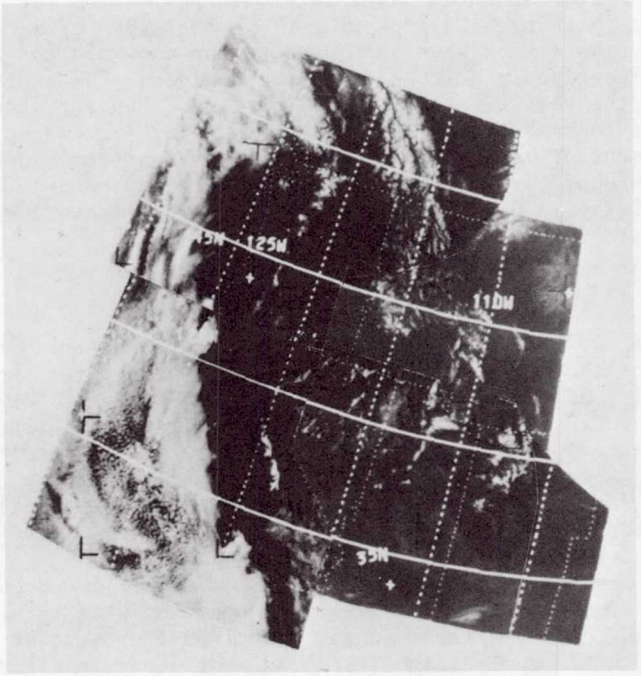


Figure 2 Cloud-free mosaic of the western United States compiled from ESSA-3 images taken in late May and June 1967. Snow cover can be seen in the Sierra Nevada, Colorado Rockies, Wind River Range, and other ranges.

Having recognized the potential of the earth-orbiting satellite to provide the hydrologist with useful information on snow cover, investigations were initiated in the mid-1960's to develop techniques to map snow from satellite images and determine the accuracy with which snow could be mapped. Following the introduction of improved spacecraft observational systems in the early 1970's, further studies were carried out to demonstrate that remote sensing from space could provide a more cost-effective means for monitoring snow cover. Moreover, these studies provided an indication that snow covered area, derived either by aerial or satellite surveys, can be employed as an additional parameter in the prediction of snowmelt-derived runoff. The positive research results in both mapping and runoff correlations led to the implementation in 1974 of the Snow Applications Systems Verifications Test (ASVT). An initial Snow ASVT workshop on applications of satellite snow cover observations was held in 1975 (Rango, 1975).

To assist personnel who would be involved in the Snow ASVT, a handbook of techniques for satellite snow mapping was prepared (Barnes and Bowley, 1974). The handbook included discussions of the various satellite systems with application to snow mapping, the techniques to identify and map snow from these data, and the problems inherent in using satellite observations. Now, at the completion of the Snow ASVT five years later, an updated handbook is in preparation (Barnes and Bowley, 1979). The purpose of the updated handbook is to document the snow mapping techniques used in the various ASVT study areas and the ways snow cover data have been applied to runoff prediction. Through documentation in handbook form, the methodology developed in the Snow ASVT can be extended to other areas.

## EARLY SATELLITE SNOW STUDIES

Using images from the very first satellites of the TIROS series, several early investigators showed that areas of snow cover could be delineated from space (Fritz, 1962; Singer and Popham, 1963; Tarble, 1963). Despite these studies, however, little operational application of snow cover mapping from satellite photography could be achieved with the earlier data, due in part to the uncertainty of obtaining an observation over a specified region from the TIROS series of satellites.

When satellites began to provide vertical-viewing imagery and daily global coverage, the first extensive research was carried out to assess the operational application of the data (Barnes and Bowley, 1968a). This work led to the preparation of an operational guide, applicable primarily to the Upper Mississippi-Missouri River Basins region (Barnes and Bowley, 1968b). Subsequently, studies were carried out emphasizing satellite surveillance of mountain snow in the western United States (Barnes and Bowley, 1969).

The early studies were concerned with how to identify snow in satellite imagery and, in particular, how to identify snow from cloud. Through interpretive keys, such as recognition of

terrestrial features, pattern recognition, uniformity of reflectance, shadows, and pattern stability, snow could be reliably distinguished from cloud. Using these keys and taking into consideration other factors, including the effects of forest cover, it was possible to begin monitoring snow cover extent on a regular basis. Mosaicked, cloud-free images showing typical snow cover distributions in the western part of the country, such as shown in Figure 2, were prepared for use as background charts to assist in the analysis of other images.

An excellent summary report on the status of satellite snow mapping using data in existence a decade after those first TIROS-1 images was prepared by an international committee for the World Meteorological Organization (McClain, 1973).

## CURRENT SATELLITE DATA WITH APPLICATION TO OPERATIONAL SNOW MAPPING

Three improved satellite systems introduced in the early 1970's have application to operational snow cover mapping: NOAA VHRR (Very High Resolution Radiometer), GOES (Geostationary Operational Environmental Satellite), and Landsat. Soon after observations from these satellites became available, researchers began investigations to evaluate the application of the improved data to snow hydrology (Wiesnet and McGinnis, 1973; Wiesnet, 1974; Barnes, et al, 1974; and McGinnis, et al, 1975). Subsequently, visible-channel data from these three satellite systems have been used to map snow cover in the Snow ASVT.

### NOAA Very High Resolution Radiometer (VHRR)

The NOAA series has been the operational meteorological satellite during the period of the Snow ASVT. The primary sensor on the NOAA satellites was the VHRR (Very High Resolution Radiometer), a dual-channel radiometer sensitive in the visible (0.6 to 0.7 μm) and thermal infrared (10.5 to 12.5 μm) spectral regions. The VHRR sensor was flown on each of the satellites from January 1973 until early 1979 (through NOAA-5). The spatial resolution of the VHRR is 900 m (0.5 nm).

The NOAA VHRR is designed primarily for direct readout use with three readout stations in use. Repeat coverage is provided twice daily; near local noon (visible and infrared), and again near local midnight (infrared), allowing both rapid and longer term changes in snow covered area to be monitored. The area that can be covered when the satellite passes directly overhead is a strip about 2,200 km (1,400 nm) wide and more than 5,000 km (3,000 nm) long.

A NOAA-5 VHRR image covering a large portion of the western United States is shown in Figure 3. The improvement in snow cover definition as compared to the ESSA mosaic shown in Figure 2 is obvious. Percentage of snow cover in several river basins in the ASVT study areas has been mapped on a routine basis from the VHRR images using a Zoom Transfer Scope (Schneider, 1975; Schneider and

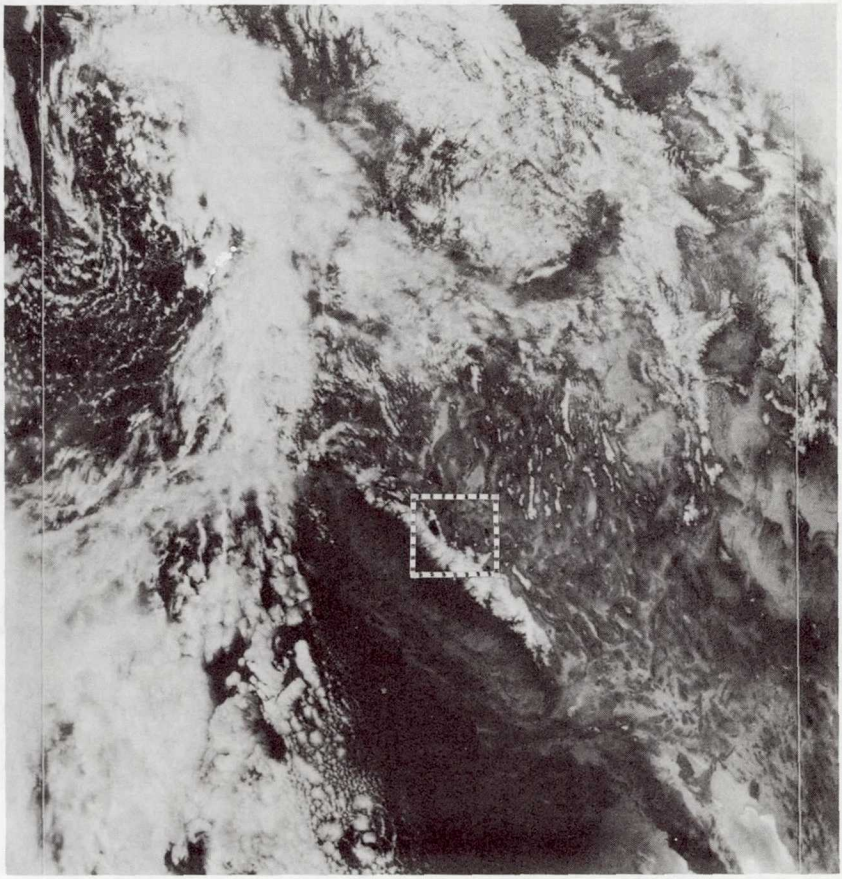

Figure 3 NOAA-5 visible-channel VHRR image, 22 April 1978, viewing the western United States. The area outlined over the Sierras is the area of the Landsat MSS scenes shown in later figures.

Matson, 1977).

Effective in early 1979, the NOAA satellite series has been replaced by the TIROS-N satellite series, the third generation of operational meteorological satellites. The primary sensor on TIROS-N is the AVHRR (Advanced VHRR), which has a spatial resolution similar to that of the VHRR, but is a four-channel instrument. The AVHRR will now be used for the National Environmental Satellite Service's routine snow mapping.

## Geostationary Operational Environmental Satellite (GOES)

Another satellite with application to snow mapping is the GOES system (Geostationary Operational Environmental Satellite). A geostationary, or so-called geosynchronous, satellite remains always above the same point on the equator, so always views the same portion of the earth. The altitude of a satellite to remain in geostationary orbit is 35,903 km.

Following NASA's experimental series of the late 1960's known as ATS (Applications Technology Satellite), came the GOES satellite program, which was initially called SMS (Synchronous Meteorological Satellite). The principal sensor on the GOES is the Visible and Infrared Spin-Scan Radiometer (VISSR), which provides the capability for acquiring observations every half-hour both day and night. The visible (0.54 to 0.70 μm) channel provides albedo measurements between 0.5 and 100 percent, and the infrared (10.5 to 12.5 μm) channel provides radiance temperature measurements between 180°K and 315°K.

The GOES data can be processed at different resolutions, ranging from 4 km (full-disc) to 1 km (sectorized) in the visible channel data. The maximum resolution for the thermal IR data is 8 km. Because the viewing angle of GOES becomes more oblique as latitude increases, the resolution of the imagery deteriorates with latitude. Therefore, GOES is more useful for mapping snow in the more southern areas, such as Arizona and the southern Sierra Nevada. An example of a GOES image on the same date as the NOAA VHRR image is shown in Figure 4.

## Landsat

High resolution, multispectral data from space first became available in the summer of 1972 with the launch of Landsat-1, called at that time the Earth Resources Technology Satellite (ERTS). Landsat-2 was placed in operation in January 1975, and Landsat-3 was launched in March 1978; data are now being collected by Landsat-2 and Landsat-3.

The Landsat spacecraft are polar orbiting satellites that view the earth from an altitude of approximately 900 km (500 nm). The primary sensor system carried by Landsat is the Multispectral Scanner (MSS). The MSS observes in four spectral bands, ranging from the visible to the near-infrared portions of the spectrum; the four bands are the MSS-4 (green: 0.5 to 0.6 μm), MSS-5 (red: 0.6 to 0.7 μm), MSS-6 (red to near-infrared: 0.7 to 0.8 μm), and

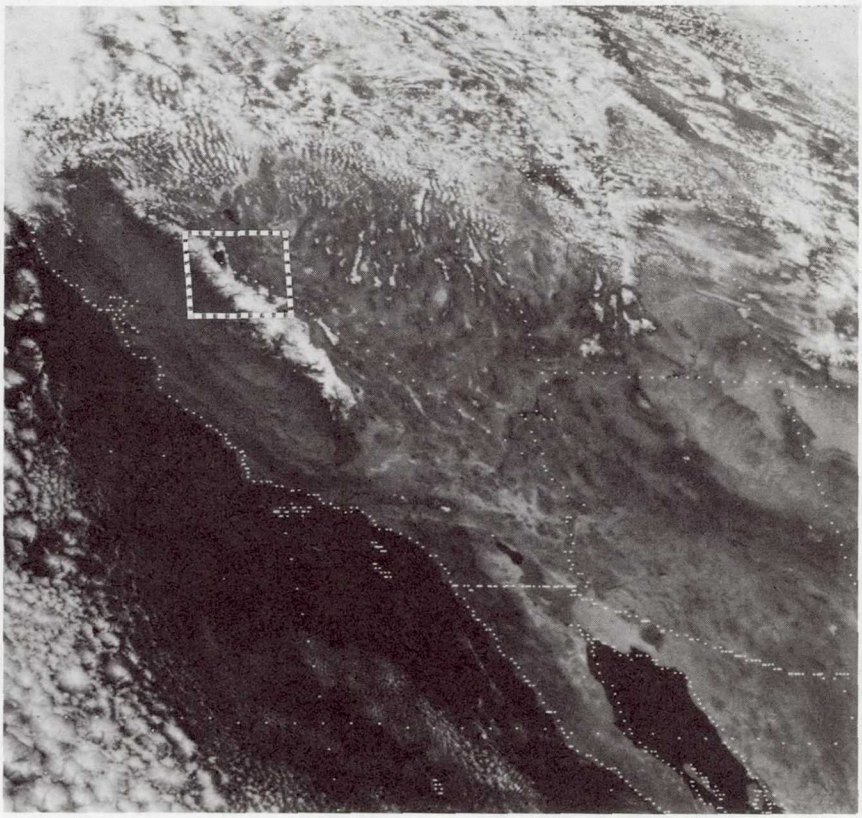

Figure 4 VISSR image from the western GOES satellite, 22 April 1978, 1945 GMT. Area covered by Landsat is indicated.

MSS-7 (near-infrared: 0.8 to 1.1 μm). Landsat-3 also carries a fifth MSS band, which measures in the thermal infrared portion of the spectrum (10.5 to 12.5 μm). Landsat views an area 185 km (100 nm) wide, and the MSS has a ground resolution of 80 meters (260 feet). Because of the relatively narrow swath viewed by Landsat, the satellite repeats coverage of the same area only once every 18 days.

Landsat MSS-5 images showing a striking difference in snow cover extent in the Sierra Nevada in April 1978 and April 1977 are shown in Figures 5a and 5b. The 1978 image is the same day as the VHRR and GOES observations.

The Landsat series of satellites has also carried a second sensor system, the Return Beam Vidicon (RBV). The RBV failed early in the life of Landsat-1 and was used very little on Landsat-2. The characteristics of the Landsat-1 and Landsat-2 RBV's in terms of sensor resolution and area viewed were similar to the MSS. The RBV on Landsat-3 is a single band instrument covering a spectral range of 0.50 to 0.75 $\mu$m, and has improved resolution (about 40 m as compared to the 80 m resolution of the MSS); the standard RBV product is at a scale of 1:250,000 as compared to 1:1 million for the MSS images. Since the RBV data have not been processed routinely, the data used for snow mapping applications have been almost exclusively from the MSS sensor; nevertheless, some excellent RBV images have been acquired. An example of an RBV image viewing the Lake Tahoe area is shown in Figure 6; the scale can be compared to that of the MSS images shown in the previous figures.

The results of studies to evaluate Landsat imagery (Barnes, et al, 1974) have shown that in areas such as Arizona and the southern Sierra Nevada the extent of the mountain snowpacks can be mapped from Landsat in more detail than is depicted in aerial survey snow charts. In four river basins of the southern Sierra Nevada, for example, the agreement between the percentage of the basin snow covered as mapped from Landsat and from the aerial survey charts is of the order of 5 percent. Moreover, in both areas, significant discrepancies between the Landsat and aerial survey data could usually be explained by changes in snow cover during the interval between the two observations.

Similarly, comparative analysis with high-altitude aircraft photography indicated that although small details in the snow line that cannot be detected in the Landsat imagery can be mapped from the higher-resolution aircraft data, the boundaries of the areas of significant snow cover can be mapped as accurately from Landsat as from the aircraft photography.

In a comparison between Landsat and NOAA VHRR Wiesnet (1974) found the snow cover area from VHRR imagery to be consistently less than that mapped from Landsat for the American River Basin. He attributed the observed difference to be due primarily to the fact that the VHRR tends to integrate the snowline and eliminates small snow patches that may be detected and mapped from Landsat. In a comparative analysis for the Conejos Basin in Colorado, however, the VHRR imagery indicated more snow than Landsat (Washichek, 1978).

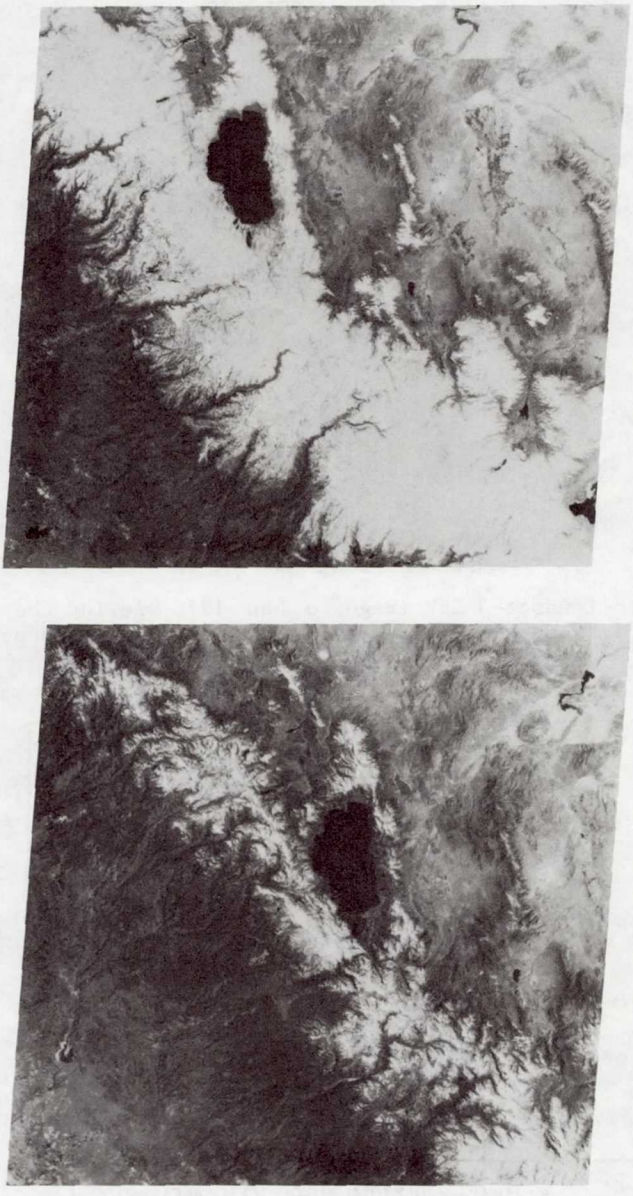

(a)

(b)

Figure 5 Landsat-2 MSS-5 scenes viewing the Lake Tahoe area. (a) 22 April 1978; (b) 15 April 1977. The snow cover area in 1978 is significantly greater than in 1977.

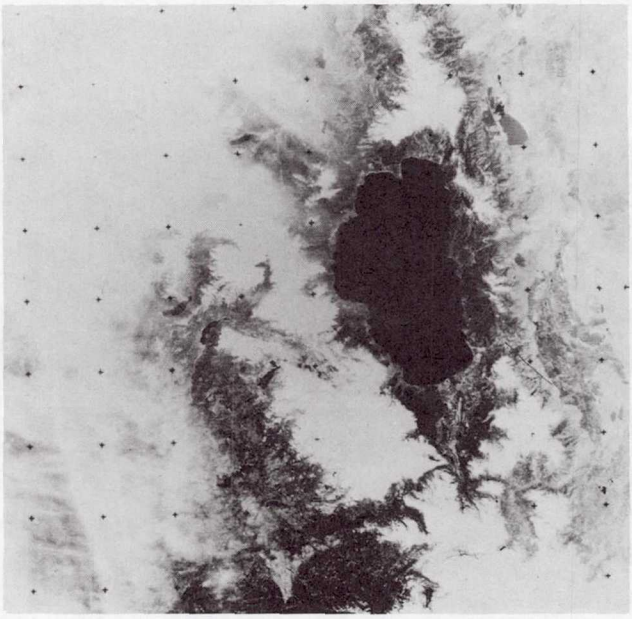

Figure 6 Landsat-3 RBV image, 6 June 1978 viewing the Lake Tahoe area. Some cloud obscures the snow cover west of the lake.

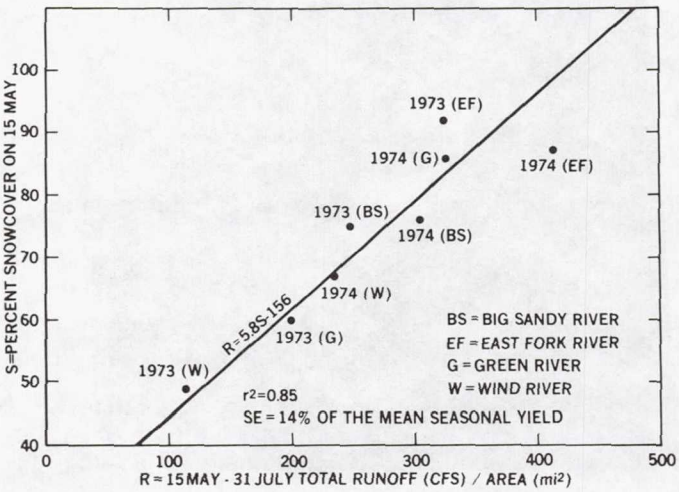


Figure 7 Landsat derived snow cover estimates versus measured runoff (1973 and 1974) for four watersheds less than 3,050 m mean elevation in the Wind River Mountains, Wyoming (from Rango et al, 1975).

Obscuration by cloud and identifying snow in heavily forested areas remain two major problems with all three types of satellite data used in the Snow ASVT. The cloud problem is more severe with Landsat, of course, because of its less frequent repeat coverage. In some years, such as 1972-73, useful data were fortunately acquired on nearly all Landsat passes over the Arizona and southern Sierras study areas; in other years, however, many of the passes have been cloud obscured. In the Arizona study area, where snow cover is extremely transient, the infrequent Landsat repeat coverage is also a drawback because significant changes in snow cover may occur between observations.

## USE OF SNOW COVERED AREA FROM LANDSAT IN RUNOFF PREDICTION

Regardless of the type of satellite system, visual-channel data have application only for mapping snow cover area. Although a relationship between reflectance and snow depth has been found in certain instances (McGinnis, 1975), operationally useful information on either the depth or water equivalent of mountain snowpacks cannot be derived from existing satellite systems. The question of how to relate satellite observations to runoff prediction has, therefore, been of prime concern.

At the time that techniques to map snow from satellites were being developed, other research related to runoff prediction was being carried out using aerial photographs. In studies of certain Colorado watersheds, Leaf (1969) found that a functional characteristic existed between extent of snow cover during the melt season and accumulated runoff, and that snow cover depletion relationships were useful for determining both the approximate timing and the magnitude of seasonal snowmelt peaks. This research would provide the basis for later studies to relate satellite snow cover area to snowmelt runoff.

Studies to employ satellite snow cover observations for seasonal streamflow estimation are described in a report by Rango, et al (1975). The initial attempts were made using low resolution meteorological satellite data to map snow covered area over the upper Indus River Basin in Pakistan. For the Indus River early spring snow covered area was extracted and related to April through June streamflow from 1967-1971 using a regression equation. Prediction of the April-June 1972 streamflow from the satellite data was within three percent of the actual total.

The results of further studies for two years of data over seven watersheds in the Wind River Mountains in Wyoming indicated that Landsat snow cover observations, separated on the basis of watershed elevation, could also be related to runoff in significant regression equations. The relationship between percent snow cover and runoff for the four lower elevation watersheds is shown in Figure 7. From these results, Rango et al (1975) concluded that satellite-observed snow covered area could be usefully employed as an additional seasonal runoff index parameter or as an input into certain hydrologic models.

The earlier studies were, in part, the basis for the imple-

mentation of the Snow ASVT, where the use of snow covered area in runoff forecasts has been evaluated in each of the four study areas. In the California study area, for example, snow covered area (SCA) from aircraft and satellite observations has been shown to be useful in reducing seasonal runoff forecast error on the Kern River watershed when incorporated into water supply forecast procedures (Rango et al, 1977). Similar analysis on the Kings River indicated that SCA-produced forecasts were generally as good as conventional forecasts but no significant improvement was noted. Based on the comparison of the Kings and Kern River watersheds, these investigators conclude that SCA will most likely reduce forecast procedural error on watersheds with: (a) a substantial degree of area within a limited elevation range; (b) an erratic precipitation and/or snowpack accumulation pattern not strongly related to elevation; and (c) poor coverage by precipitation stations or snow courses restricting adequate indexing of water supply conditions.

## OTHER TYPES OF SATELLITE DATA WITH APPLICATION TO SNOW MAPPING

Research has also been conducted to apply data from other satellite systems to snow hydrology. For example, data from the instruments of the Skylab Earth Resources Experiment Package (EREP) have been studied, as well as the hand-held camera photography taken by the Skylab-4 crewmen as part of the Visual Observations Project (Barnes and Smallwood, 1975; Barnes, et al, 1975). Snow mapping was also included as part of the Earth Observations Experiment of the Apollo-Soyuz Test Project (Smallwood, et al, 1979). Although not having application for collecting operational snow data, the color photography from the manned spaceflights has been shown to be very worthwhile for research purposes.

In addition to the use of satellite imagery and photography in the visual portion of the spectrum, the application of data from other spectral regions has also been investigated. Thermal infrared observations have been available routinely for a number of years from meteorological satellites; observations in the near-infrared were made from Skylab; and the Nimbus satellite series has carried microwave sensors since the early 1970's. Studies are continuing to evaluate and develop techniques for use of each of these types of observations.

### Near-Infrared Data

As reported by Barnes et al (1974) and Rango et al (1975), snow cover extent measured in the Landsat near-infrared spectral band (MSS-7) is consistently less than that measured in the visible bands because of the decreased reflectance of wet or refrozen snow in the near-infrared. In a more thorough examination of the characteristics of snow reflectance in the near-infrared using Skylab Multispectral Scanner (S-192) data, where measurements were made in several near-infrared spectral bands, Barnes and Smallwood (1975) found two potential applications to snow mapping of mea-

surements in the near-infrared spectral region: (1) the use of a near-infrared band in conjunction with a visible band to distinguish automatically between snow and clouds; and (2) the use of one or more near-infrared bands to detect melting snow.

The nearly complete reversal in snow reflectance between the visible and near-infrared bands observed in the S-192 data indicates that in certain portions of the near-infrared, snow surfaces are essentially non-reflective regardless of the condition of the snow. In contrast, the reflectance of clouds (water droplet) displays no decrease in the near-infrared bands. Therefore, a technique combining two spectral bands, one in the visible and one in the near-infrared, can be used to distinguish between snow and clouds. An example of this method to distinguish snow and clouds is shown in Figure 8.

The second potential application, that of detecting melting snow, is based on the observed behavior of snow in the intermediate S-192 bands from about Band 7 (0.78 - 0.88 μm) through Band 10 (1.20 - 1.30 μm). For two spring cases examined, the apparent snow extent decreases gradually from a maximum in the visible (Band 6) to a minimum in Band 11. It was concluded, therefore, that bands in the spectral range from about 0.8 μm to about 1.30 μm should provide the most information on the condition of the snow surface.

Thermal Infrared Data

The NOAA VHRR carried a thermal infrared channel (10.5 - 12.5 μm) with the same resolution as the visible channel. The thermal infrared scanner measures the radiative temperatures of the Earth's surface and cloud tops rather than the reflectances. Studies have indicated (Barnes and Bowley, 1974) that in most instances snow cover can be delineated in the VHRR thermal data because of its lower temperature, although the thermal gradients associated with snow boundaries are considerably better defined during the spring than during the winter. Caution must be exercised when interpreting infrared data over mountainous terrain, where temperature differences due to variations in elevation may obscure the temperature differences associated with snow cover.

Further studies of the application of thermal infrared measurements to snow hydrology are in progress using data from the Heat Capacity Mapping Mission (HCMM), launched in April 1978. The HCMM was the first of a planned series of Applications Explorer Missions (AEM) that involve the placement of small spacecraft in special orbits to satisfy mission-unique, data acquisition requirements. The HCMM sensor is a two-channel radiometer similar to the VHRR in its spectral ranges, but with somewhat better resolution. The primary purpose of the mission is to establish the feasibility of acquiring thermal infrared remote-sensor derived temperature measurements of the Earth's surface within a 12-hour interval at times when the temperature variation is a maximum, and applying the day/night temperature difference measurements to the determination of thermal inertia, that property of material to

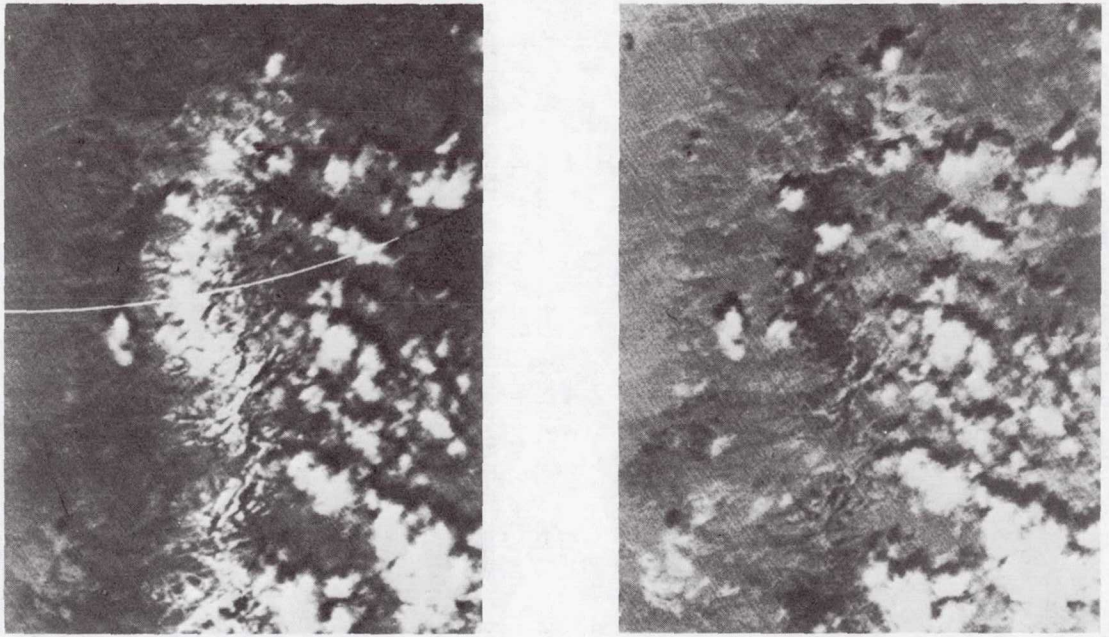

(a) Band 3 (b) Band 11

Figure 8 Comparison between Skylab S-192 visible and near-infrared data, viewing the White Mountains in California, 3 June 1973; (a) Band 3 (0.52 - 0.56 $\mu$m), (b) Band 11 (1.55 - 1.75 $\mu$m). Because of the decreased reflectance of the snow, clouds that cannot be detected in Band 3 are distinct in Band 11.

resist temperature changes as incident energy varies over a daily cycle.

Although the satellite was designed primarily for its geological applications, snow hydrology studies using the HCMM data are being carried out. The main purpose of the studies is to determine whether the thermal measurements from HCMM, and particularly the more precise day/night temperature difference measurements, can be related to snow conditions, such as areas of melting versus non-melting snow. Examples of HCMM visual and thermal infrared imagery are shown in Figures 9a and 9b.

### Microwave Data

Satellite observations in the visible, near-infrared, and thermal infrared portions of the spectrum are all affected by clouds. Microwave sensors, however, provide the capability for viewing the Earth's surface regardless of cloud conditions, so have great potential for snow mapping.

Studies of microwave properties of snow have been carried out for some time using ground-based and aircraft instruments. The microwave radiometers flown in space on the Nimbus satellites have not had sufficient resolution, however, to provide useful snow cover data, especially for mountainous terrain regions. Recently, using data from the improved Nimbus-6 Electrically Scanning Microwave Radiometer (ESMR), the utilization of space-borne microwave radiometers for monitoring snowpack properties has been investigated (Rango et al, 1979).

The results of this study show that snow accumulation and depletion at specific locations can be monitored from space by observing related variations in microwave brightness temperatures. Using vertically and horizontally polarized brightness temperatures from the Nimbus-6 ESMR, a discriminant function can be used to separate snow from no snow areas and map snow covered area on a continental basis. For dry snow conditions on the Canadian high plains significant relationships between snow depth or water equivalent and microwave brightness temperature were developed which could permit remote determination of these snow properties after acquisition of a wider range of data. The presence of melt water in the snowpack causes a marked increase in brightness temperature which can be used to predict snowpack priming and timing of runoff. The authors point out that as the resolutions of satellite microwave sensors improve, the application of these results to snow hydrology problems should increase.

## OUTLOOK FOR SATELLITE SNOW MAPPING

The Snow ASVT has provided a quasi-operational test of the use of satellite snow cover area in runoff prediction. Over the four-year period of the ASVT, each study center has found somewhat different methods for incorporating satellite data into runoff prediction models to be the most advantageous to the particular needs of their area. The overall results of the program indicate

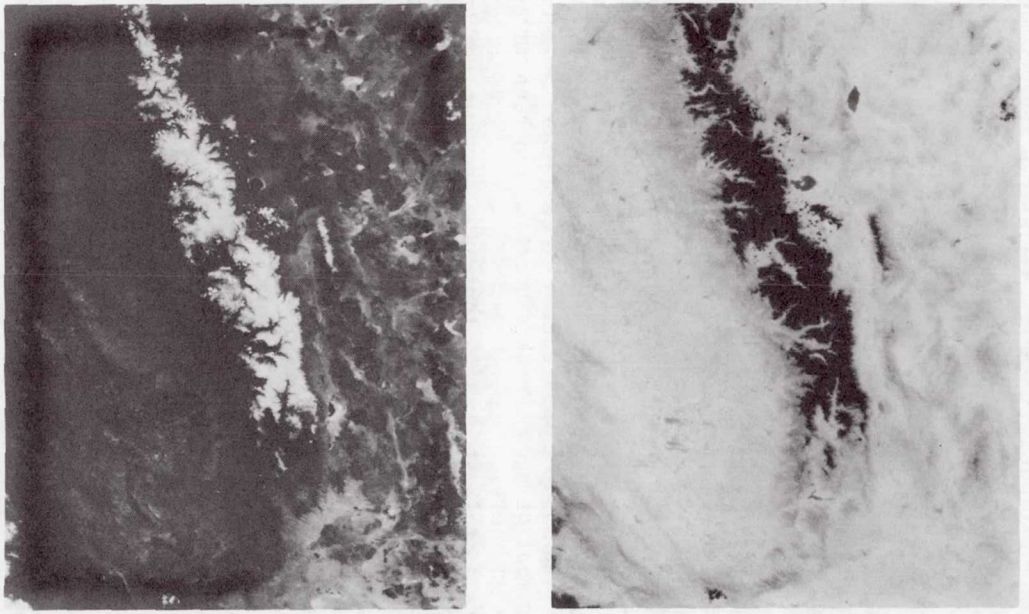

(a) (b)

Figure 9 Heat Capacity Mapping Mission (HCMM) images viewing the Sierra Nevada, 31 May 1978 (daytime). (a) visible-channel; (b) thermal infrared channel (lower temperatures are darker).

without doubt that the utilization of satellite data will continue to be an integral part of operational runoff prediction procedures.

Limitations, of course, exist in making use of satellite observations. Even after 20 years, the types of satellite data most readily available for operational use are still limited by clouds, and the highest resolution data, that from Landsat, are not always available in real time. Also, for the purposes of the Snow ASVT, photointerpretive techniques to map snow cover from the satellite images were found to be the most useful; nevertheless, further development of automated analysis techniques using digitized data is essential.

New satellite systems will be providing improved data. For example, the studies using Skylab near-infrared measurements have led to the development of the snow-cloud discriminator, an instrument to be flown on an operational Air Force meteorological satellite. Undoubtedly, much emphasis in coming years will be placed on remote sensing in the microwave; as technological advances allow space-borne microwave radiometers to provide better resolution data, these sensors will have greater application to snow hydrology.

This paper has reviewed the evolution of satellite snow mapping. The continued development of improved satellite systems and mapping techniques will lead to more reliable and more cost-effective means for monitoring snow cover distribution and predicting runoff.

REFERENCES

Barnes, J.C. and C.J. Bowley, 1968: "Snow Cover Distribution as Mapped from Satellite Photography", Water Resources Research, 4 (2), 257-272.

Barnes, J.C. and C.J. Bowley, 1968: Operational Guide for Mapping Snow Cover from Satellite Photography, Final Report under Contract E-162-67(N) for NOAA/NESS, Allied Research Associates, Inc., Concord, MA.

Barnes, J.C. and C.J. Bowley, 1969: "Satellite Photography for Snow Surveillance in Western Mountains", Proc. of 37th Western Snow Conference, Salt Lake City, Utah, April 1969, 34-40.

Barnes, J.C. and C.J. Bowley, 1974: "Handbook of Techniques for Satellite Snow Mapping", Final Report under Contract No. NAS 5-21803 to National Aeronautics & Space Administration/Goddard Space Flight Center, Environmental Research & Technology, Inc., Concord, MA, 95 pp.

Barnes, J.C. and C.J. Bowley, 1979: "Handbook of Satellite Snow Mapping and Runoff Prediction", Final Report Prepared for NASA Snow ASVT, Goddard Space Flight Center, Environmental Research & Technology, Inc., Concord, MA (in preparation).

Barnes, J.C. and M.D. Smallwood, 1975: "Synopsis of Current Satellite Snow Mapping Techniques, with Emphasis on Application of Near-Infrared Data", Proc. of Workshop on Operational Applications of Satellite Snowcover Observations, August 18-20, 1975, South Lake Tahoe, CA, 199-213.

Barnes, J.C., C.J. Bowley and D.A. Simmes, 1974: The Application of ERTS Imagery to Mapping Snow Cover in the Western United States, Final Report under Contract NAS5-21803, Environmental Research & Technology, Inc., Concord, MA, 77 pp.

Barnes, J.C., C.J. Bowley, J.T. Parr and M.D. Smallwood, 1977: "Snow Mapping Experiment", SKYLAB Explores the Earth, NASA SP-380, NASA Scientific and Technical Information Office, Washington, 191-224.

Fritz, S., 1962: "Snow Surveys from Satellite Meteorology", Rocket and Satellite Meteorology, North-Holland Publishing Co., Amsterdam, 419-421.

Leaf, C.F., 1969: "Aerial Photographs for Operational Streamflow Forecasting in the Colorado Rockies", Proc. 37th Western Snow Conference, Salt Lake City, Utah.

McClain, E.P., 1973: Snow Survey from Earth Satellites, World Meteorological Organization, WMO Pub. No. 353, Geneva, 42 pp.

McGinnis, D.F.Jr., 1975: "A Progress Report on Estimating Snow Depth Using VHRR Data from NOAA Environmental Satellites", Proc. of Workshop on Operational Applications of Satellite Snowcover Observations, August 18-20, 1975, South Lake Tahoe, CA, 313-324.

McGinnis, D.F.Jr., J.A. Pritchard and D.R. Wiesnet, 1975: Snow Depth and Snow Extent Using VHRR Data from the NOAA-2 Satellite, NESS Technical Memorandum, NOAA/National Environmental Satellite Service, Suitland, MD.

Rango, A. (Ed.), 1975: Proceedings of Workshop on Operational Applications of Satellite Snowcover Observations, August 18-20, 1975, South Lake Tahoe, CA, 430 pp.

Rango, A., A.T.C. Chang and J.L. Foster, 1979: "The Utilization of Spaceborne Microwave Radiometers for Monitoring Snowpack Properties", Preprint Nordic Hydrology, Vol. 10, No. 1, 29 pp.

Rango, A., J.F. Hannaford, R.L. Hall, M. Rosenzweig and A.J. Brown, 1977: "The Use of Snowcovered Area in Runoff Forecasts", Preprint X-913-77-48, NASA Goddard Space Flight Center, 29 pp.

Rango, A., V.V. Salomonson and J.L. Foster, 1975: "Seasonal Streamflow Estimation Employing Satellite Snowcover Observations", Preprint X-913-75-26, 34 pp.

Schneider, S.R., 1975: "The Operational Program of Satellite Snowcover Observations at NOAA/NESS, Proc. of the NASA Workshop on Operational Applications of Satellite Snowcover Observations, South Lake Tahoe, CA, 18-20 August, 1975, NASA SP-391, 87-101.

Schneider, S.R. and M. Matson, 1977: "Satellite Observations of Snowcover in the Sierra Nevadas During the Great California Drought", Remote Sensing of Environment, 4, 327-334.

Singer, S.F. and R.W. Popham, 1963: "Non-Meteorological Observations from Weather Satellites", Astronautics and Aerospace Engineering, 1(3), 89-92.

Smallwood, M.D., C.J. Bowley and J.C. Barnes, 1979: Snow Hydrology Studies Utilizing ASTP Photography, Final Report under Contract No. PC6-22331, Environmental Research & Technology, Inc., Concord, MA (in publication by NASA/Johnson Space Center).

Tarble, R.D., 1963: "Areal Distribution of Snow as Determined from Satellite Photographs", Publication No. 65, International Association of Scientific Hydrologists, 373-375.

Washichek, J.N., 1978: "Report on Operational Applications of Satellite Snow Cover Observations", Annual Report for 1977, to NASA Goddard Space Flight Center, by USDA, Soil Conservation Service, Denver, CO.

Wiesnet, D.R., 1974: "The Role of Satellites in Snow and Ice Measurements", Proceedings of Interdisciplinary Symposium on Advanced Concepts and Techniques in the Study of Snow and Ice Resources, National Academy of Sciences, Monterey, CA, December 2-6, 1973, 447-456.

Wiesnet, D.R. and D.F. McGinnis, 1973: "Snow-Extent Mapping and Lake Ice Studies Using ERTS-1 MSS Together with NOAA-2 VHRR", Proceedings of Third ERTS Symposium, December 1973, NASA SP-351, 995-1010.

**Page intentionally left blank**

# THE NOAA/NESS PROGRAM FOR OPERATIONAL SNOWCOVER MAPPING: PREPARING FOR THE 1980's

S. R. Schneider, National Environmental Satellite Service, Washington, D.C.

## ABSTRACT

The NOAA/NESS operational satellite snowmapping program is described at the end of its first 5 years. Supporting developmental efforts are reviewed.

## INTRODUCTION

Environmental satellites providing daily, high-resolution (1 km) imagery over North America became operational for the first time late in 1972. Shortly thereafter, hydrologists at the National Environmental Satellite Service (NESS) determined that imagery from these satellites could be used to create timely maps depicting snowcover over river basins of varying size, location and topography (Wiesnet and McGinnis, 1973). Snowmapping was upgraded to the status of an operational program at NESS during 1974 (Schneider et al., 1976) and has continued to expand in scope ever since. Indeed, areal snowcover measurements are now being routinely made at NESS for thirty critical basins in the United States and Canada. The data are disseminated to the user community by mail, teletype, and telecopier.

## SATELLITES AND SENSORS

### NOAA/VHRR

From 1973 to 1978, the primary sensor used to obtain data for the NESS snowmapping program was the Very High Resolution Radiometer (VHRR) onboard the NOAA series of polar-orbiting satellites. The VHRR is sensitive to two portions of the spectrum, a 0.6 to 0.7 $\mu$m (visible) and a 10.5 to 12.5 $\mu$m (thermal infrared) channel. Coverage over most basins is available once daily in the visible and twice each day in the thermal-infrared portions of the spectrum. Data from the satellite are received through the High Resolution Picture Transmission (HRPT) system at three NESS receiving facilities; Wallops Island, Virginia, Redwood City, California, and Gilmore Creek, Alaska. The raw, ungridded unmapped image signals are displayed through a film recorder which produces a 25 cm by 25 cm film negative. Each negative covers an area approximately 2100 km square with three frames usually available per pass. Prints from the image negatives, at

a normal scale of 1:10,000,000 and a resolution of 1 km (at nadir), are used in snowmapping. The VHRR achieves lateral coverage through continuous horizon-to-horizon scanning by a mirror oriented perpendicular to the forward motion of the spacecraft. Since the mirror rotates at a constant angular rate, the geometric resolution on the ground changes as the distance from the satellite subpoint increases. The resulting image produced from these signals will appear foreshortened in the area of the horizons. This foreshortening or distortion in the image can be corrected either through optical rectification or by further computer processing utilizing an algorithm described by R. L. Legeckis and J. Pritchard (1976).

SMS/GOES

Five satellites in the SMS/GOES series have been launched thus far. The first two Synchronous Meteorological Satellites, SMS-1 and SMS-2, were NASA sponsored prototypes. The most recent three, GOES-1, -2, and -3 were entirely NOAA funded (the acronym stands for Geostationary Operational Environmental Satellite). The satellites are termed "geostationary" because their position relative to the Earth's surface remains fixed. The satellite in this series that can currently be used to monitor the East Coast is GOES-2; it was launched on June 15,1977, and is stationed over the equator at 75°W longitude at an altitude of 37,500 $km^2$. GOES-3, which was launched on June 16, 1978, is stationed at 135°W and is currently the operational West Coast satellite. The imaging sensor on board the SMS/GOES is the Visible and Infrared Spin Scan Radiometer (VISSR). This sensor can provide imagery in both the visible and the infrared portions of the spectrum (as its name implies) as often as every half-hour. Imagery from the VISSR can be obtained in a variety of resolutions. Raw data is received from the satellite at a resolution of 1 km but can be averaged to produce images of larger spatial coverage at 2-, 4- or 8-km resolution (thermal infrared VISSR data is available only at a resolution of 8-km).

The 1-km VISSR images have been the data source for many of the operational snow maps produced since 1975. No computer programs presently exist to geometrically correct the distortion inherent in this type of imagery. However, small areas on the image may be rectified on a Bausch and Lomb Zoom Transfer Scope by optically stretching along the axis defined by the study area and the satellite subpoint.

## CURRENT METHODOLOGY

Snow maps are produced at NESS by first enlarging and rectifying a visible VHRR or VISSR image to overlay a hydrologic basin map. A Bausch and Lomb Zoom Transfer Scope (ZTS) is utilized for this purpose.

Registration of image to map on the ZTS involves aligning physiographic landmarks such as lakes, rivers and shorelines. After registration has been achieved the snow line on the image is traced onto the basin map and snowcovered areas are colored in. Percentage snowcover for the basin is then determined by using an electronic density slicer. The snow map is placed on the density slicer with a previously prepared opaque mask outlining the basin. The density slicer selectively color illuminates gray shades on the map. The colors are projected onto a display screen and percentage values for each color are read from a digital meter.

## PROGRAM DESCRIPTION

The areal snowcover data and/or snow maps are provided to water resource managers in numerous federal, state and local agencies. A map of the western United States showing many of the operational basins is presented in figure 1. A list of primary users and information on the precise location and size of each basin is given in the accompanying Table 1. The basins are similarly numbered on table and map.

The areal snowcover percentages are dispatched over the RAWARC teletype circuit to National Weather Service River Forecast Centers (RFC) in Sacramento, Fort Worth, Salt Lake City, Kansas City, and Portland as well as River District Offices in Great Falls, Phoenix, and Albuquerque. Snow maps are sent over telecopier or through the mail to other agencies including the U.S. Geological Survey, Bureau of Reclamation, Corps of Engineers, Soil Conservation Service, and U.S. Forest Service.

Not depicted in figure 1 but listed on the table are the St. John basin in Maine and New Brunswick, the Missouri River above Canyon Ferry Dam and the northeast U.S. snow map. The northeast U.S. analysis is first transmitted over telecopier to the National Weather Service Eastern Regional Hydrologist in New York and is then rerouted to RFC's in Hartford, Harrisburgh, and Cincinnati. Snow maps for the Missouri River above Canyon Ferry Dam were begun in November 1978, at the request of the Soil Conservation Service office in Bozeman, Montana.

Basin snow maps are made on an average of once a week beginning November 1st and terminate when the snowpack appears almost totally depleted on the imagery. The analyses can only be made when the basin is free of obscuring clouds. Accordingly, basins in the southwestern United States and California's Sierra Nevada are mapped more often than those in the less cloudfree Pacific Northwest.

Over six hundred snowcover measurements were made at NESS during the 1977-1978 snow season. Snowmapping totals for the past four years are as follows:

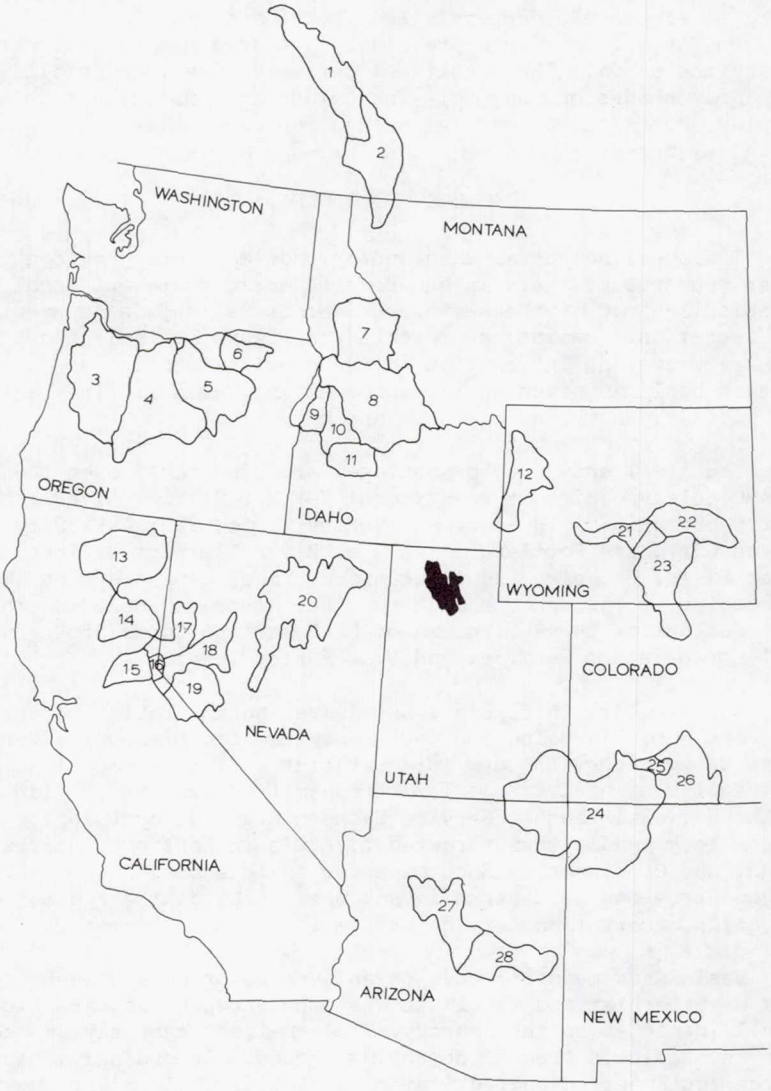


Figure 1. River basins for NESS operational snowmapping.

Table 1

Basins Being Mapped As Of 1978

| River Basin | Drainage Area in $Km^2$ | Primary Users |
|---|---|---|
| American above Fair Oaks (15) | 5,601 | Sacramento RFC |
| Boise above Lucky Peak (11) | 6,941 | Portland RFC, Columbia Basin Network |
| Carson (18) | 8,864 | Soil Conservation Service, Sacramento RFC |
| Clearwater above Peck (7) | 20,824 | Portland RFC, Columbia Basin Network |
| Columbia River above Mica Dam (1) | 21,290 | Portland RFC, Columbia Basin Network, B.C. Hydro & Power Authority, Environment Canada |
| Deschutes (4) | 27,195 | Portland RFC, Columbia Basin Network |
| Feather above Oroville (14) | 9,386 | California State Dept. of Water Resources |
| Humboldt above Comus (20) | 31,339 | Salt Lake City RFC, Soil Conservation Service |
| John Day (5) | 19,632 | Portland RFC, Columbia Basin Network |
| Kootenay above Libby (2) | 23,277 | Portland RFC, Columbia Basin Network |
| Missouri River above Canyon Ferry Dam | 40,714 | Soil Conservation Service, Great Falls RDO |
| North Platte between Alcova and Guernsey (22) | 12,198 | Bureau of Reclamation, Kansas City RFC, Soil Conservation Service |
| North Platte above Seminoe (23) | 15,274 | Bureau of Reclamation, Kansas City RFC, Soil Conservation Service |
| Northeast U.S. Snow Map | | NE Regional Hydrologist NWS |
| Payette above Emmett (10) | 6,941 | Portland RFC, Columbia Basin Network |
| Rio Grande above Colo.-New Mexico State Line (26) | 19,900 | Soil Conservation Service, Fort Worth RFC |
| Rio Grande above Del Norte (25) | 3,419 | Soil Conservation Service, Fort Worth RFC |
| Sacramento above Shasta (13) | 16,630 | California State Dept. of Water Resources |
| Salmon above Whitebird (8) | 35,095 | Portland RFC, Columbia Basin Network |
| Salt (28) | 16,141 | Salt Lake City RFC, Phoenix RDO, Salt River Project, U.S. Geological Survey |

## Table 1 (continued)

BASINS BEING MAPPED AS OF 1978

| River Basin | Drainage Area in $Km^2$ | Primary Users |
|---|---|---|
| San Juan (24) | 65,273 | Salt Lake City RFC |
| Snake above Palisades (12) | 13,340 | Portland RFC, Columbia Basin Network |
| St. John | 55,167 | Marine Bureau of Civil Emergency Preparedness, New Brunswick Dept. of Environment, Environment Canada, St. John Basin Task Force |
| Sweetwater above Pathfinder (21) | 6,027 | Bureau of Reclamation, Kansas City RFC, Soil Conservation Service |
| Tahoe-Truckee (16, 17) | 7,665 | Soil Conservation Service, Sacramento RFC |
| Umatilla (6) | 5,931 | Portland RFC, Columbia Basin Network |
| Verde (27) | 17,094 | Salt Lake City RFC, Phoenix RDO, Salt River Project, U.S. Geological Survey |
| Walker (19) | 9,241 | Soil Conservation Service, Sacramento RFC |
| Weiser (9) | 3,781 | Portland RFC, Columbia Basin Network |
| Willamette (3) | 26,159 | Portland RFC, Columbia Basin Network |

**********

Notes on Users:

1. The Columbia Basin Network includes the Soil Conservation Service, Bureau of Reclamation, U.S. Geological Survey, U.S. Army Corps of Engineers, National Weather Service, Bonneville Power Administration, B.C. Hydro and Power Authority, as weel as other state and local agencies.

2. Basins being done for the Bureau of Reclamation in Denver, Colorado, are retransmitted from the site to field offices in Caspar, Laramie, and Cheyenne, Wyoming.

3. The St. John Basin Task Force includes the National Weather Service, U.S. Army Corps of Engineers, U.S. Geological Survey, Environment Canada, and other state, provincial agencies.

4. Most basins are mapped twice weekly cloud cover permitting. The Salt, Verde and St. John basins are mapped daily cloud cover permitting. The Tahoe-Truckee, Carson and Walker basins are mapped only at the end of each month.

| Snow Year | Number of Snow Maps |
|---|---|
| 1974-1975 | 441 |
| 1975-1976 | 520 |
| 1976-1977 | 494 |
| 1977-1978 | 606 |
| | TOTAL 2061 |

The snowcover data are generally provided to users within 30 hours of a satellite overpass so they can be incorporated into watershed runoff forecast models. Quality control techniques used are described in Schneider et al (1976). They include checks of the operational snow maps with higher resolution Landsat satellite data, computer-enhanced imagery, ground-based snowpack measurements and aerial-survey maps. The data from aerial surveys are particularly useful for quality control purposes and are provided for basins in Arizona, Idaho, and British Columbia, respectively by the Salt River Project, Walla Walla District Corps of Engineers, and the British Columbia Hydro and Power Authority.

## USER EVALUATION

In an effort to streamline and improve snowmapping at NESS a detailed questionnaire was sent out to primary users of the snowcover data on October 24, 1978. The questions were directed towards user needs in terms of data timeliness, frequency, accuracy, and quality control. Of seventeen responses, three rated the snow maps as "excellent", fourteen rated them as "good" and two rated the maps as "fair" (in some cases more than one box was checked).

The following applications of the snowcover data were mentioned: runoff forecasting, flood prevention, water resource planning, research and development, reservoir/dam regulation, irrigation planning, and inclusion in State bulletins. Users reported that they were checking the satellite snowcover accuracy by using runoff data, snow-course data, hydromet networks, aerial surveys (both fixed and rotary wing) and mathematical models (SSARR and FLOCAST were mentioned).

Users requested coverage for over 30 additional basins. Several of the users requested that the data be transmitted to them in a more timely fashion, i.e., over telecopier rather than through the mail.

## NESS SUPPORT TO THE SNOW ASVT PROGRAM

According to Rango (1975) positive research results in both snowmapping and runoff correlations led to a decision at NASA in 1975 to operationally test the use of remotely sensed snowcovered area for improving runoff forecasts in a four-year duration Applications System Verification Test (ASVT). A contract was let

that same year to NOAA/NESS to promote a study in support of the snow ASVT. Since that time data from NOAA/NESS have been regularly shipped on request to the ASVT test sites in Arizona, California, Colorado and the Pacific Northwest. These data have been in the form of satellite imagery, digital tapes and completed snow maps. Daily NOAA snowcover data have been used at the four test sites to fill in gaps created by the less frequent coverage of Landsat-1 and 2.

As part of the ASVT Program a NESS representative was sent on a two-week training mission to all the ASVT test sites in January 1977. Mini-snowmapping workshops were conducted in Portland, Denver, and Placerville, California. A snow survey flight in Arizona was arranged by representatives of the U.S. Geological Survey and the Salt River Project to help the NESS analyst gain a "feel" for the appearance of snowcovered terrain in the Salt-Verde watershed.

Some of the NESS ASVT funds have been used to defray the cost of equipment purchased in support of the snowmapping study i.e., Zoom Transfer Scopes and density slicer vidicons. However, as the ASVT program now comes to an end, it becomes obvious that its major benefit to operational snowmapping at NESS has been to make the user community aware of the availability and usefulness of satellite snowcover data. In fact, several of the basins (Rio Grande, Feather, Sacramento) originally targeted for limited-duration study in support of the ASVT have now been added to the ongoing Operational Snowmapping Program at NESS.

## SELECTED CASES

### Sierra Nevada

Selected river basins in the Sierra Nevada have been operationally monitored at NESS since early 1973. In fact, one-hundred-seventy-eight (178) areal snowcover determinations were made alone for the American Basin (above Folsom) between January 1973 and June 1978. At the request of the California State Department of Water Resources, the Sacramento River basin above Shasta and the Feather above Oroville were added to the NESS operational snowmapping program in January 1977. In February 1978, the U.S. Soil Conservation Service office in Reno, Nevada, requested that operational coverage be extended to three river basins on the Eastern slopes of the Sierras: The Tahoe-Truckee, Carson and Walker.

The Sierra Nevada has served as an outdoor "laboratory" for snow-related research in the recent past. The NASA-sponsored Snow ASVT includes 38 major basins and sub-basins in the northern and southern Sierra (Brown and Hannaford, 1975). Film loops consisting of daily GOES satellite imagery have been constructed to dynamically depict seasonal melt off in the Sierras (Breaker

and McMillan, 1975). The feasibility of remotely determining snowpack density in the Sierras was explored by McMillan and Smith (1975). The Sierra Cooperative Pilot Project (SCPP), a winter orographic cloud seeding experiment, is now being designed by North American Weather Consultants and the Bureau of Reclamation for the Central Sierras (Foehner, 1978). The utility of areal snowcover measurements in runoff and water supply forecasting for Sierra basins is described in Hannaford (1977). A completely automated technique for snowmapping is currently being tested at NESS using six adjacent Sierra basins as the primary study area (Tarpley et al., 1979).

Of paramount interest was the two-year (1976-1977) drought in the Sierras, an event which was continuously monitored by NASA and NOAA satellites. Figure 2 depicts the entire Sierra Nevada Mountain Range as viewed by NOAA-3 during mid-April 1975. The Sierras can be seen as a broad white swath extending from the northwest (upper left) edge of the image to the southeast (lower right) edge. Figure 3 shows the same area as it appeared from the NOAA-5 satellite on a comparable date in 1977. Areal snowcover measurements for the entire mountain range, derived from the two images, revealed snowcover in 1977 to be less than one-third of what it was in 1975. In figures 4 and 5, snowcover in the Sierra Nevada (shown in black) for the two April cases is superimposed on a State outline of California. Through the use of the Zoom Transfer Scope and Density Slicer, areal measurements for selected Sierra basins were made from the imagery. Results showed that the ratio of 1977 to 1975 snowcover for basins in the lower elevation northern Sierras were approximately 1:8. Snowcover disparities were not as great (between 1:2 and 1:3) for basins in the high elevation central and southern sectors of the Sierras (Schneider and Matson, 1977).

Arizona

Three-hundred and four (304) snowcover measurements have been made at NESS for the Salt and Verde basins since November 1974. Owing to rapid snowmelt in Arizona, these basins must be monitored on a daily basis. In fact, rainfall and snowmelt combined to cause the Salt River to overflow its banks in both March and December, 1978. One such rapid snowmelt event took place in early March 1977, and was reported on in detail by McGinnis and Schneider (1978). An illustration from that paper is presented here as figure 6. The righthand side of the figure shows a Landsat-1 visible (band 5) image taken over Airzona at 1619 GMT on March 2, 1977. On the left is a ground-cover map for the same region. Ground cover strongly influences the appearance of snow in satellite imagery. Snowcover extends from the northeast corner of the image in a widening band until it stretches across the entire image at mid-image. The southward extent of the snow is limited to two bands: one, oriented northeast-southwest, ends midway between the Roosevelt and the San Carlos reservoirs: the

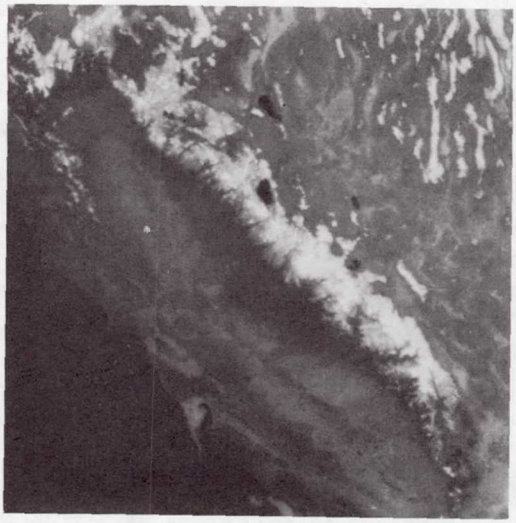

Figure 2. NOAA-3 satellite image showing snowcover in the Sierra Nevada mountain range on April 28, 1975.

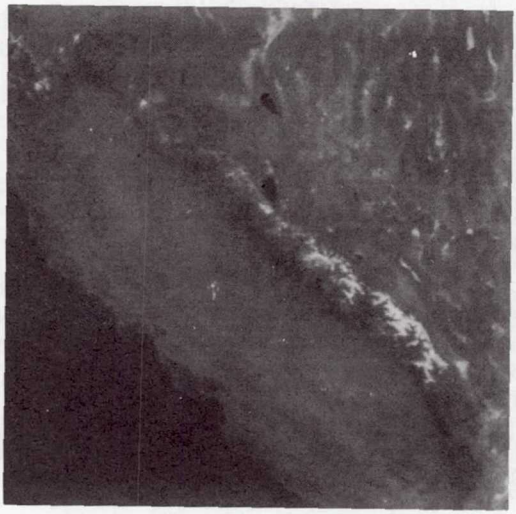

Figure 3. NOAA-5 satellite image showing snowcover in the Sierra Nevada mountain range on April 19, 1977.


Figure 4. Snowcover extent (in black) for the Sierra Nevada on April 28, 1975.


Figure 5. Snowcover extent (in black) for the Sierra Nevada on April 19, 1977.

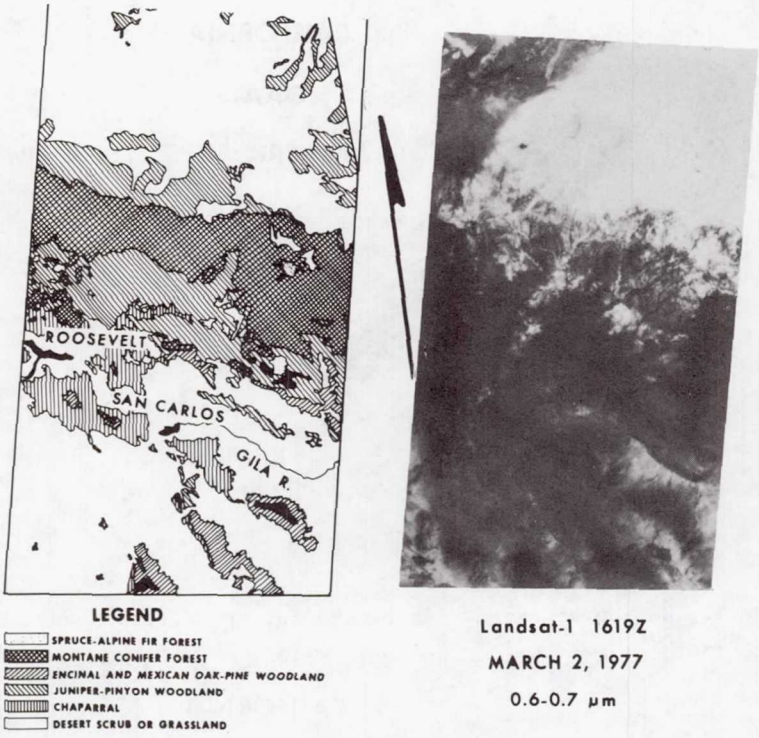


Figure 6

other, more blunt, ends just below the right center of the image. The snow scene appears brightest when the snow overlays desert scrub or grassland, as in the northern third of the image. At the higher elevations, where the forest canopy becomes more dense, the snow scene appears less reflective (grayer); e.g., note the protrusion of juniper-pinyon covered highlands into the open grasslands (upper center of image). Snow in the mountain conifer and spruce-alpine fir forests appear the least reflective. Most of the snowcover on the image was deposited as a result of strong convective activity over Arizona during the period 0000 to 1200 GMT, March 2, 1977.

Climatological data (NOAA, 1977) for Arizona show that 20 stations in or adjacent to the Salt Verde watersheds routinely report snowfall. Only seven of the 20 stations reported snowfall in this case. The greatest fall--10 cm--occurred at Hawley Lake (elevation 2493 m) and only two other stations measured as much as 2 cm of snow. Thus, the climatological data show not only that a very light snowfall occurred, but also how poorly the present network of stations delineates the areal extent of the snowfall. This failure to properly describe snowcover points to the need for mesoscale and synoptic-scale views available from satellite images.

Large areas of this extensive, but shallow snowcover had melted away when viewed by NOAA-5 on the morning of March 3. Using a compensating polar planimeter on the imagery, it was determined that the snow-covered area decreased by 18,850 $km^2$ between the mornings of March 2 and 3, an area almost as large as New Jersey.

St. John Basin

The St. John basin, which lies both in New Brunswick and Maine, has been the object of special study at NESS during the past few years. In 1975, the basin was selected as a desirable international study area for two different World Meteorological Organization (WMO) programs, the World Weather Watch and the WMO Snow Studies by Satellite project. The basin drains 58,500 square kilometers of which 36 percent lies within the United States and 64 percent lies within Canadian territory. Snowmelt-induced flooding in the spring is a common occurrence and over the last 60 years has accounted for approximately one million dollars of damage, annually. The April 1973 flood alone caused eleven million dollars of damage in New Brunswick. The snowmapping and river ice-reconnaissance techniques developed at NESS during the past few years have become an important part of the flood warning and forecasting network in the basin (Schneider, 1977).

The presence of dense coniferous forest throughout much of the St. John basin makes satellite detection of snowcover difficult. Figures 7A-D depict the St. John basin as it was viewed from the VHRR onboard NOAA-4 during various stages of snowmelt. On figure 7A the basin, which is outlined in white, has a very mottled and patchy look to it, even though it is 100-percent snow covered. The bright white features are frozen lakes and rivers as well as snow covered open terrain (of which there is very little in the basin). The forest covered areas appear in various shades of gray, the densest forests (darkest gray in appearance) being located in the western part of the basin. Figure 7B shows the eastern portion of the basin as mostly snow-free while cloudy in the west, and figure 7C, taken six days later, shows the basin with about 50 percent snowcover. Figure 7D depicts the basin as completely snowfree. Notice that on figure 7D, two heavily farmed regions, one south of Gagetown in the eastern part of the basin and one along the St. John River between Hartland and Grand Falls in the center of the basin, can be identified because of their very light gray tone.

As previously mentioned, figure 7A shows the St. John basin as completely snow covered. It also shows the entire St. John River along with every tributary and lake in the basin as completely frozen over. Ice conditions in the basin are much different in figure 7B, the VHRR image taken on 15 April 1976. In this image, almost all bodies of water in the basin east of the cloud bank have thawed out, save two ice-covered reaches of the

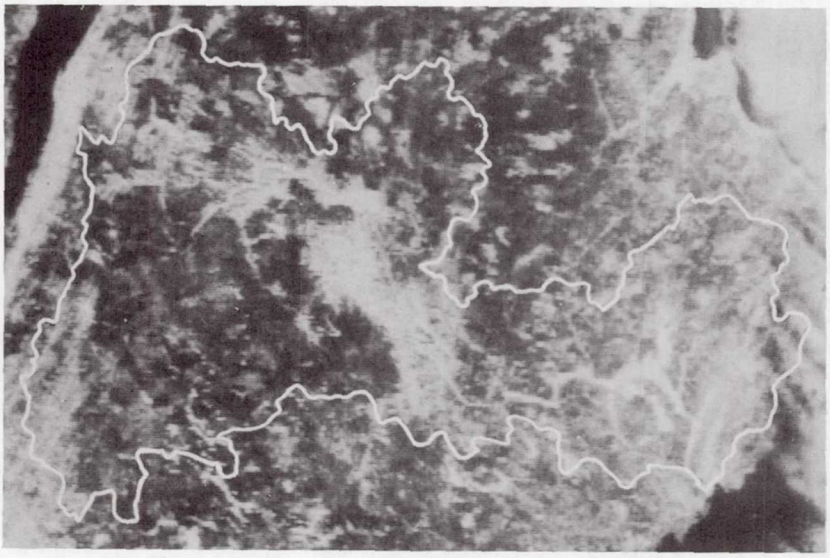

Figure 7A. VHRR image depicting St. John Basin on 9 March 1975. Basin is totally covered with snow and ice.

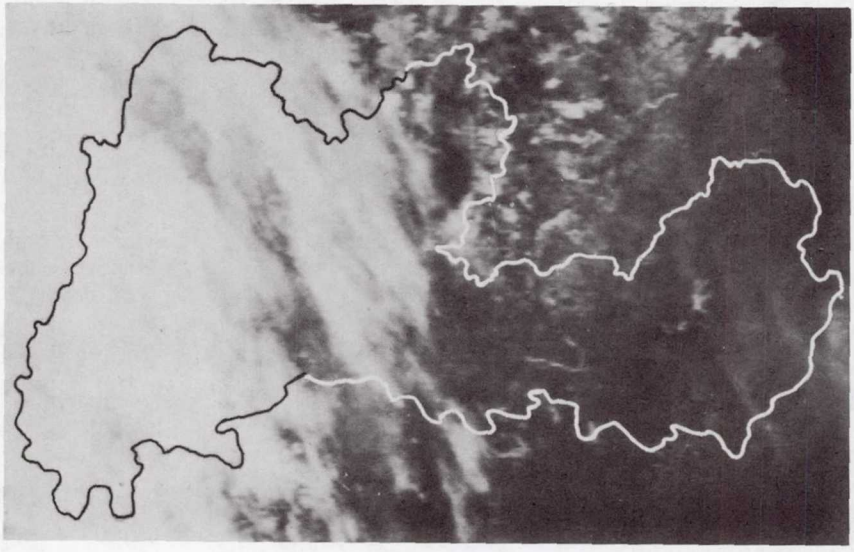

Figure 7B. VHRR image depicting the St. John Basin on 15 April 1976. The western part of the basin is covered by cloud; the eastern half is mostly snow free.

Figure 7C. VHRR image depicting the St. John Basin on 21 April 1976 with about 50 percent snowcover.

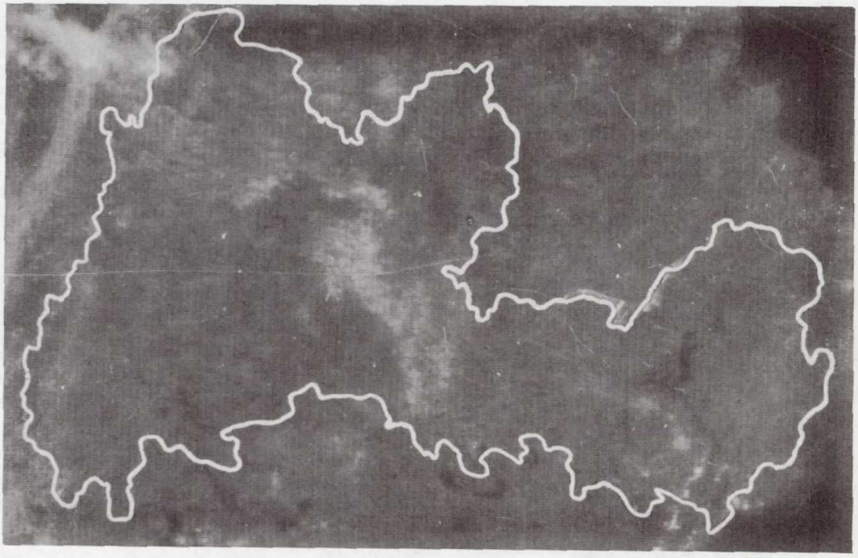

Figure 7D. VHRR image depicting a snow-free St. John Basin on 25 May 1975.

St. John River. These two ice-covered reaches include parts of Mactaquac Lake (nearest the cloud bank) and Grand Lake (to the northeast). An examination of the VHRR image taken six days later on 21 April 1976, reveals these two segments of the St. John River have completely thawed. Having a set of such imagery on hand, depicting the basin under all different snow and ice conditions, can greatly aid the photointerpreter in his work.

## DEVELOPMENT

### TIROS-N

The first of a new generation of polar-orbiting satellites, TIROS-N was launched on October 13, 1978. A second satellite in this series, NOAA-A will be launched in early 1979. Together, the satellites will be able to provide coverage four times daily (0300, 0730, 1500, 1930 Local Standard Time) over most areas in the United States and Canada. Each satellite will have an Advanced Very High Resolution Radiometer (AVHRR) onboard which will be able to provide coverage in the following five channels:

| | |
|---|---|
| Channel 1 | .58-.68 $\mu$m |
| Channel 2 | .725-1.0 $\mu$m |
| Channel 3 | 3.55-3.93 $\mu$m |
| Channel 4 | 10.5-11.5 $\mu$m |
| Channel 5 | 11.5-12.5 $\mu$m |

Several studies (Strong, et al., 1971; Wiesnet, et al., 1975; and O'Brien and Munis, 1975) have shown that it is often possible to detect metamorphosed (or melting) snow and ice by comparisons of simultaneous Landsat visible (MSS-5) and near infrared (MSS-7) imagery. These studies indicate that the reflectance of metamorphosed snow and ice is less in the near infrared than that of fresh non-melting snow. The availability of simultaneous AVHRR visible (Channel 1) and near infrared (Channel 2) imagery may in the future allow NESS investigators to give operational reports on the age and condition of river basin snow cover as well as its areal extent.

### High Resolution Film Loops

One-kilometer-resolution GOES images can be generated every half hour and strung together to make film loops. The loop can then be run continuously through a projector, displaying the same sequence of images over and over. These loops have been found helpful in discriminating between cloud and snow and in monitoring shadow effects on snow fields, fog dissipation, cumulus buildups and snowmelt.

### Interactive Snowmapping

Two new interactive computer systems named VIRGS (VISSR

Interactive Registration and Gridding System) were delivered to NESS in June 1978. A feasibility study concerning use of the VIRGS for operational snow mapping has already been carried out at the Madison campus of the University of Wisconsin (Gird, 1979). To use the system for snowmapping, basin perimeters drawn on standard aeronautical charts are first converted into grid points through the use of an electronic digitizing board, and are then read into the VIRGS. The basin outlines can then be displayed on the system video screen at any time by typing a single command on the keyboard. A joy-stick cursor is used to outline snowcover on the video screen; area statistics software on VIRGS are invoked to calculate and print out the basin snowcover percentages. Advantages of this system over pure photointerpretation include ease of basin registration and measurement of areal snowcover as well as the ability to display time-sequenced sets of images. Present disadvantages include lengthly set-up time, lack of hard-copy output and "jumpiness" of the joy-stick cursor.

### All Digital Snowmapping

A project is underway at NESS to check the feasibility of doing all digital snowmapping using 4-km visible GOES data. The test area includes nine contiguous basins in the Sierra Nevada. These basins offer a wide variety of terrain characteristics and ground cover for control purposes; they are also of ideal size and location as viewed from the West Coast geostationary satellite. Data used in this experiment are stored on computer disk packs for 24 hours. Snow maps for all nine basins can be done as often as five times daily: 1645Z, 1745Z, 2045Z, 2145Z and 0045Z. The model involves the thresholding of each individual basin pixel for snowcover and takes into account solar illumination angles as well as the nature of ground cover. Detailed description of this snowmapping model as well as preliminary results for the 1978-1979 snow season are presented in Tarpley et al. (1979).

## FINAL COMMENTS

An operational satellite snowmapping program for selected river basins is now in place at the National Environmental Satellite Service. Owing to the success of this program a larger number of requests for support have been received than can be handled given present manpower and fiscal restraints. Expansion of the program can therefore only come about through the development of more efficient (i.e., automated) techniques for snowmapping. This is the goal towards which satellite snow specialists must now direct their efforts.

## ACKNOWLEDGEMENTS

The author wishes to thank Mr. Russell Koffler for his support of the operational snowmapping program over the years. Meteorologists of the NESS Interactive Processing Group are

thanked for their diligent monitoring of snowcover in the various operational river basins. The author also expresses his appreciation to Mrs. Michele Head for her clerical and typing support of the snowmapping program including the expert preparation of this manuscript.

## REFERENCES

Brown, A. J., and Hannaford, J. F., 1975: Interpretation of Snowcover from Satellite Imagery for Use in Water Supply Forecasts in the Sierra Nevada, Proceedings of the NASA Workshop on Operational Applications of Satellite Snowcover Observations, South Lake Tahoe, California, 18-20 August 1975, NASA SP391, 39-51.

Breaker, L. C., and McMillan, M. C., 1975: Sierra Nevada Snow Melt from SMS-2, Proceedings of the NASA Workshop on Operational Applications of Satellite Snowcover Observations, South Lake Tahoe, California, 18-20 August 1975, NASA SP391, 187-198.

Foehner, O. H., 1978: Developing Techniques for Measuring Precipitation, Proceedings of the 46th Annual Meeting of the Western Snow Conference, Otter Crest, Oregon, 26-32.

Gird, R., 1979: Snow Extent Measurements from Geostationary Satellites Using an Interactive Computer System, Proceedings of the Final Workshop on the Operational Applications of Satellite Snowcover Observations, April 16-17, 1979, Sparks, Nevada, in press.

Hannaford, J. F., 1977: Investigation into the application of satellite imagery to hydrologic modeling of snowmelt runoff in the southern Sierra Nevada, Phase 1 Final Report, NAS5-22957, NASA, Goddard Space Flight Center, Greenbelt, Maryland, 48 pp.

Legeckis, R. and Pritchard, J., 1976: Algorithm for Correcting the VHRR Imagery for Geometric Distortions Due to the Earth Curvature, Earth Rotation, and Spacecraft Roll Altitude Errors, NOAA Technical Memorandum NESS 77, U.S. Department of Commerce, Washington, D.C., 31 pp.

McGinnis, D. F., and Schneider, S. R., 1978: Satellite Detection of an Extremely Light Snowfall in Arizona, Monthly Weather Review, 106 (9), 1380-1383.

McMillan, M. C., and Smith, J. L., 1975: Remote Sensing of Snowpack Density using Shortwave Radiation, Proceedings of the NASA Workshop on Operational Applications of Satellite Snowcover Observations, South Lake Tahoe, California, 18-20 August 1975, NASA SP391, 361-373.

O'Brien, H. W. and R. H. Munis, 1975: Red and Near-infrared Reflectance of Snow, U.S. Army Cold Regions Research and Engineering Laboratory, Research Report 332, Hanover, New Hampshire, 18 pp.

Rango, A., 1975: An Overview of the Applications System Verification Test on Snowcover Mapping, Proceedings of the NASA Workshop on Operational Applications of Satellite Snowcover Observations, South Lake Tahoe, California, 18-10 August 1975, NASA SP391, 1-12.

Schneider, S. R., Wiesnet, D. R., and McMillan, M. C., 1976: River Basin Snowmapping at the National Environmental Satellite Service, NOAA Technical Memorandum NESS 83, U.S. Department of Commerce, Washington, D.C., 19 pp.

Schneider, S. R., 1977: Operational Satellite Assessment of Snow Cover and River Ice in the Saint John River Basin, WMO SJRB Task Force Report No. 6.2, National Environmental Satellite Service, NOAA, Washington, D.C., 26 pp.

Schneider, S. R., and Matson, M., 1977: Satellite Observations of Snowcover in the Sierra Nevadas During the Great California Drought, Remote Sensing of Environment 4, 327-334.

Strong, A. E., E. P. McClain, and D. F. McGinnis, 1971: Detection of Thawing Snow and Ice Packs through the Combined use of Visible and Near-infrared Measurements from Earth Satellites, Monthly Weather Review, Vol. 99, No. 11, pp. 828-830.

Tarpley, J. D., Schneider, S. R., and Danaher, E. J., 1979: An All Digital Approach to Snow Mapping Using Geostationary Satellite Data, Proceedings of the Final Workshop on the Operational Applications of Satellite Snowcover Observations, April 16-17, 1979, Sparks, Nevada, in press.

Wiesnet, D. R., and McGinnis, D. F., 1973: Snow-Extent Mapping and Lake Ice Studies Using ERTS-1 MSS together with NOAA-2 VHRR, Third Earth Resources Technology Satellite-1 Symposium, December 10-14, 1973, Goddard Space Flight Center, Washington, D.C., pp. 995-1009.

Wiesnet, D. R., D. F. McGinnis, and M. C. McMillan, 1975: Evaluation of ERTS-1 Data for Certain Hydrological Uses, Final Report, NASA, Goddard Space Flight Center, Contract No.432-641-14-04-03.

**Page intentionally left blank**

# NEW GOALS FOR SNOW MONITORING BY SATELLITE

D.R. Wiesnet, National Environmental Satellite Service, Washington, D.C.

## ABSTRACT

The success of the snow mapping ASVT program has encouraged me to contemplate what new research and operational goals we hydrologists ought to be setting for ourselves. Short-term research goals should include: 1) testing of a snow/cloud discrimination satellite sensor; 2) field studies in situ of spectral reflectance of snow under diverse conditions; 3) development of techniques to estimate albedo of snow from satellite sensors; 4) determination of the effects of physical properties and substrate on snow spectral reflectance; and 5) determination of the effect of atmospheric attenuation on snow spectral response.

Achievement of these short-term goals ought to lead us to our long-term goals: 1) estimation of density and/or water equivalent of snow; 2) an understanding of spectral reflectance and albedo of snow throughout seasonal metamorphosis.

Short-term operational goals must be: 1) to reduce the time required for receipt of satellite data; 2) to optimize the MSS type sensors for snow studies; 3) to test empirical models relating snow-covered area to runoff; 4) to understand the snowmelt process well enough to model it with satellite data input; 5) to develop a digitized automated snowmapping program; 6) to revamp existing models to accept satellite data; and 7) to deposit snow-cover data in existing international repositories.

Achievement of these short-term goals should result in approaching our long-term operational goals: 1) a near-real-time, semi-automated computerized preparation of snowmelt-runoff calculations; 2) accurate seasonal hydrologic forecasts of basin water supply based on snow-runoff data.

## INTRODUCTION

Every ending is also a beginning. The end of the Applications Systems Verification and Transfer (ASVT) program in snow-cover observations is the appropriate time for us to look ahead and plan ahead. The success of the ASVT program will certainly engender new efforts in snow monitoring. The fact that NASA had invited me to speak to this select audience on a subject of great personal interest is appreciated, especially as I have been an unreimbursed but very interested observer and a strong supporter of the ASVT effort.

I would not quarrel with those who might say that this paper is a profound statement of the obvious. Nontheless, statements need to be made, and the obvious is not always obvious to everyone. The purpose of the paper is to present my point of view on the relative merits of future research and operational efforts that involve snow monitoring by satellite. If the goals here stated encourage only one graduate student to attack an unsolved snow monitoring problem, the paper would, in my view, have some redeeming research value.

## OPERATIONAL GOALS

Table 1 shows both the short- and long-term operational goals, and Table 2 lists the research goals. These lists are certainly not complete. However, achievement of any of the goals represents a noteworthy milestone in the progress of satellite snow studies.

Table 1--Operational Goals

Short-Term

1. Reduce the lag time for receipt of data.
2. Optimize MSS-type sensors for snow studies.
3. Test empirical models relating snow-cover area to runoff.
4. Understand the snowmelt process well enough to model it with satellite-data input.
5. Develop a digitized automated snow mapping program.
6. Revamp existing models to accept satellite data.
7. Deposition of data in international data repositories.

Short-Term

1. Near-real-time, semi-automated computerized preparation

of snow melt-runoff calculations or forecasts.

2. Accurate seasonal hydrological forecasts of basin water supply based on snow-runoff data.

Table 2--Research Goals

Short-Term

1. Test a snow/cloud discrimination sensor.

2. Field (in-situ) studies of spectral reflectance of snow under diverse conditions.

3. Develop techniques to estimate albedo of snow from satellite sensors.

4. Determine effect of physical properties of snow and substrate on spectral reflectance.

5. Determine effects of atmospheric attenuation of snow spectral response.

Long-Term

1. Estimation of density and/or water equivalent of snow.

2. An understanding of spectral reflectance and albedo of snow throughout seasonal metamorphosis.

Short-Term Operational Goals

1. Reduce the lag time for receipt of data.

This long-standing goal was mentioned as an original objective of the ASVT (Rango, 1975). If NOAA and NASA are serious about providing coverage for operational hydrologic studies, they must insure timely delivery of their products. Snow hydrology is simply too dynamic to do otherwise. Although NOAA/NESS has a system of image receipt and dissemination that is rapid, NASA has not always been successful in getting Landsat images to operational snow mappers in time to be used in forecasts.

2. Optimize MSS-type sensors for snow studies

What is the best spectral band to observe snow? What advantages do multiband data provide for snow studies? Are currently used bands optimum? I have difficulty with these questions.

Landsat's MSS-5 (0.6-0.7μm) provides the best contrast between snow-covered and snow-free terrain (Barnes and Bowley,

1974). The NOAA VHRR sensor utilized the same band. However, measured snow-covered area is a function of the spectral band (Schneider and McGinnis, 1976). It is also a function of spatial resolution. Results from pixel-count digital classification techniques can be rather different from those from photo-interpretive techniques (Table 3).

Table 3--Comparison of Conventional Analysis vs. Computer-Generated Analysis (from McGinnis et al., in preparation; data from the American River basin, Calif.)

| Date | Percent Snowcover Conventional Analysis (MSS 5) | Percent Snowcover Computer by GE Image 100 | Ratio GE Image 100/ Conventional |
|---|---|---|---|
| 8 May 1975 | 45 | 27 | 0.60 |
| 17 May 1975 | 40 | 20 | 0.50 |
| 13 Jun 1975 | 16 | 5 | 0.31 |
| 22 Jun 1975 | 12 | 2 | 0.17 |
| 1 Jul 1975 | 7 | 1 | 0.14 |
| 14 Apr 1976 | 41 | 21 | 0.51 |
| 23 Apr 1976 | 26 | 8 | 0.31 |
| 20 May 1976 | 7 | 1 | 0.14 |
| 29 May 1976 | 6 | < 1 | 0.08 |

Mountain snowcover, especially during melt, includes elements of bare rock, shadows, forests, open water, roads, man-made structures, etc., all of which have an effect on the total spectral response from the area represented by a single pixel. Other workers (e.g., Itten, 1975), have reported similar difficulties when working at full pixel resolution and using various classifications of snow. Snow itself has a wide range of spectral response depending on not only its physical characteristics but also on the solar zenith angle. Polar-orbiting satellites cannot view the same pixel from pass to pass. However, as others will later demonstrate (Tarpley et al., 1979), geostationary satellites are more nearly able to view the same pixel from day to day.

The thematic mapper (TM) in Landsat D has two new spectral bands at 2.0-2.35μm and 1.55-1.75μm. They were designed to detect hydrothermal alteration of rocks. Both these bands should be investigated as possible indicators of snow physical properties. The 1.55-1.75μm band will permit cloud/snow discrimination (Barnes and Smallwood, 1975; Salomonson, 1978).

3. Test Empirical Models relating Snow-Covered Area to Runoff

Many readers would argue that this goal is (1) already attained for certain individual basins; and (2) should be a long-term goal, rather than a short-term goal. For some, the ultimate long-range goal is a universally accepted snowmelt runoff model based on snow-covered area. Whatever our individual goals, if we consider the field of satellite hydrology as a bona fide discipline, then we ought to strive for a whole new approach to hydrologic forecasting based on parameters that can be readily gathered by satellite. The work of Leaf (1975) and Martinec (1975) as well as Rango and Salomonson (1976) is noteworthy in that satellite-derived snow-covered area is used directly as an input in combination with conventional snow survey data for making residual volume streamflow forecasts.

4. Understand the Snowmelt Process well enough to Model it with satellite-data input

Many studies of snowmelt are carried out in areas of permanent snow packs or on glaciers. Studies of the transient snow of the temperate zones are less common. The physics of snowmelt is basically understood, but the challenge is to develop a technique from the perspective of the satellite. Thermal sensing provides a measure of temperatures, but the latent heat required for a change of state from solid to liquid makes zero-degree isotherm mapping less attractive. "Ripeness" of the snowpack is a term that is rather qualitative, but generally refers to an advanced state of metamorphosis in which the water-soaked snow is at or approaching zero degrees Celsius and is ready to contribute to runoff. If we could detect and identify this water-soaked "ripe" phase of the snowpack, perhaps we could relate time of runoff inception or water equivalent to it and thereby improve our hydrologic forecasts.

5. Develop a Digitized, Automated Snow-Mapping Program

The 1975 ASVT meeting referred to the desirability of digitized snow mapping (Itten, 1975; Algazi and Suk, 1975; Dallam and Foster, 1975; Luther et al., 1975; Bartolucci et al., 1975). Using DMSP data, the Air Force now produces a daily Northern Hemisphere 1:30,000,000 polar stereographic printout of snowcover. NOAA/NESS plans for digitized snow mapping from GOES are presented elsewhere in this volume by Schneider. Tomorrow, Ron Gird of NESS will discuss his latest efforts to develop the "automated digital snowcover map." Also this afternoon Prof. Haefner from Zurich will display examples of digital snow maps showing great detail, quite unlike the large-pixel GOES/VISSR data.

6. Revamp Existing Forecast Models to Accept Satellite Data

This goal is closely related to 3 and 4 above and need not be discussed again here.

7. Deposition of Data in International Data Repositories

World Glaciology Centre A is located in Boulder, Colorado. Its Director, Dr. Roger Barry, will now accept snow-covered-area measurements. Publications on river basin snowcover should be sent to this archive. His address is:

World Data Centre A for Glaciology
(Snow and Ice)
Institute of Arctic and Alpine Research
University of Colorado
Boulder, Colorado 80309 U.S.A.

Landsat satellite images and tapes are archived routinely at the EROS Data Center, Sioux Falls, S.D., and NOAA satellite images and tapes are routinely archived at EDIS, Camp Springs, Md.

Long-Term Operational Goals

If satellite hydrology is to become a bona fide sub-discipline of hydrology, it seems to me that these two goals:

1. Near real time, semiautomated computerized preparation of snowmelt-runoff calculations, and

2. Accurate long-term seasonal hydrological forecasts of basin water supply based on snow-runoff data

represent worthwhile goals. I believe that satellite data will be needed to accomplish these goals in part or in full. Operational hydrologists will--properly--be chary of accepting new techniques unless they have been tried, tested, and proved. The first long-term goal stresses quickness; the second stresses "accuracy." My own work in examining continental and hemispheric snowcover variations leads me to believe that long-range seasonal hydrologic forecasts where snow is an important variable may be significantly improved as a result of the continued collection of snowcover data. Because many of these techniques of forecasting require a fairly large set of data for statistical analysis, it may take a decade or two before we can fully assess the impact satellite data collection is having on hydrologic forecasting.

## RESEARCH GOALS

### Short-Term Research Goals

1. Test a Snow/Cloud Discriminator Sensor

This goal will be achieved in 1982 when Landsat-D's mapper (TM) begins to transmit data. Dr. Salomonson's paper, which will be given tomorrow afternoon, will provide complete details on this significant, new sensor. As previously indicated the seven-band TM includes a 1.55-1.75μm band, which as Barnes and Smallwood (1975) have pointed out, has a low reflectance for snow but a high reflectance for clouds, thereby permitting snow/cloud discrimination.

2. Field (in-situ) Studies of Spectral Reflectance of Snow under Diverse Conditions

If there is a weakness in our efforts to advance the science of remote sensing of snow, it is in the lack of attention paid to advancing our knowledge of in-situ natural snow metamorphosis with respect to the spectral variations in irradiance under diverse atmospheric conditions, at diverse sun angles, with various substrates, and as a function of physical properties of the snow. The work of O'Brien and Munis (1975) and the newer microwave studies being done at the National Bureau of Standards and at NASA/GSFC under Dr. Rango's general supervision are notable exceptions. The often-cited capability of microwave sensors to penetrate cloud cover makes this sensor of enormous--yet presently potential--value.

3. Develop Techniques to Estimate Albedo of Snow from Satellite Sensors

NOAA/NESS prepares an experimental daily albedo estimate and prepares maps of albedo using an automated program from the scanning radiometer aboard NOAA polar-orbiting satellites. These values are mapped in a $2.5^{o}$ latitude-longitude array. However, these values include cloud tops and thus are not useful for localized snow-covered river basins. Snow albedo estimates mapped for snowcover in river basins would materially aid the forecasting hydrologist.

4. Determine Effect of Physical Properties of Snow and Substrate on Spectral Reflectance

This goal follows naturally from controlled and uncontrolled lab and field studies of snow as discussed in goal 2. Research efforts in the microwave spectrum have been made (Meier and Edgerton, 1971) and continue to be made (Chang and Choudhury, 1978), but an attempt to study snow substrates at CRREL (funded by NOAA/NESS) has met with difficulties (Fig. 1).

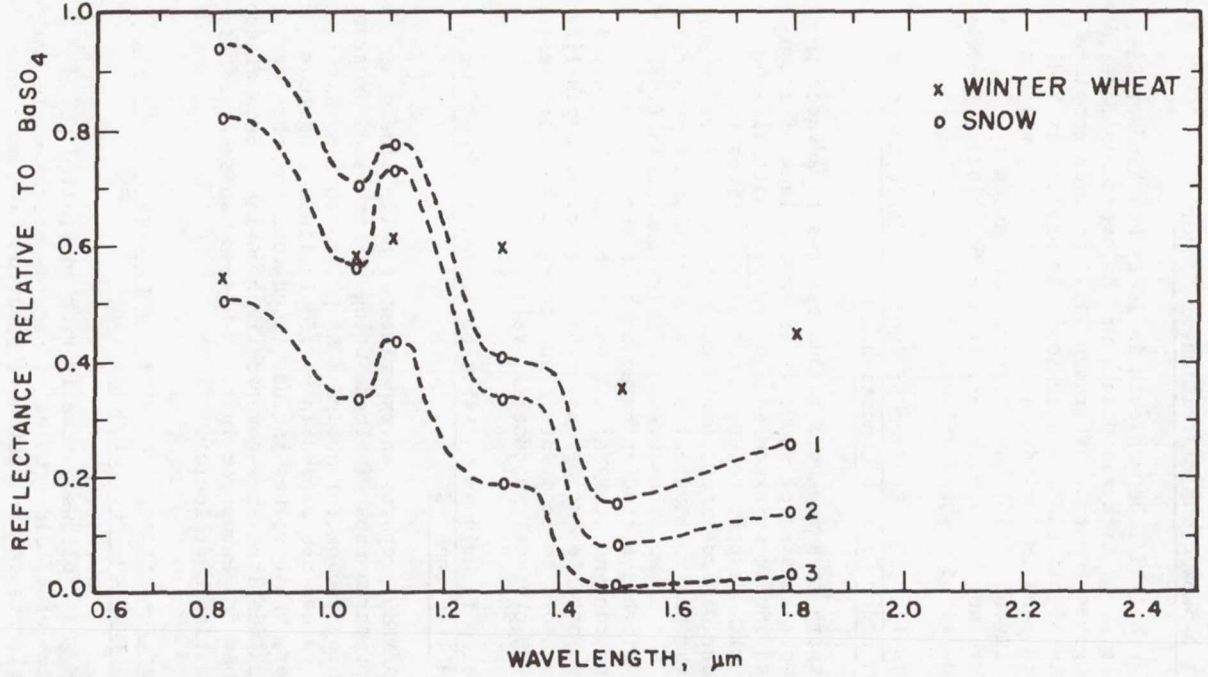


Figure 1. Spectral reflectance of snow melting in situ under solar irradiation. Curves are interpolated from data points. Curve 1 is based on measurements taken at 1040 LST, 11 April 1979, at Hanover, N.H., over 6.5 cm of snow that fell on 9 April 1979. Curve 2 is based on measurements taken at 1113, snow depth 5.5-6.0 cm; curve 3 is based on measurements taken at 1400 hours, snow depth 0.8-1.2 cm. The snow melted completely by 1445 hours. (Data from H. O'Brien, CRREL)

However, these efforts, under the direction of Mr. H. O'Brien, are continuing.

The Landsat-D TM bands, 1.55-1.75μm, and 2.08-2.35μm, ought to provide fresh insight into snow physical properties. Snow density, the presence of free water, grain size, hardness, and snow depth are parameters of interest.

5. Determine the Effects of Atmospheric Attenuation on the Spectral Response of the Snow

The superiority of band 5 (0.6-0.7μm) on Landsat-1 for snow mapping and general observation was quickly established, while band 4 was found to be obscured by haze and thin clouds. For serious research in multispectral investigations, atmospheric attenuation must be considered, especially where subtle differences in irradiance are presented as being definitive or diagnostic of snow types or metamorphic condition of the snow.

The most devastating attenuation of the spectral response of Landsat-obtained data was in fact not atmospheric but was bureaucratic. I refer to the arbitrary cutoff of high values of reflectance in Landsat MSS values in bands 4-6. This condition should be alleviated, but not completely cured by Landsat-D's Thematic Mapper (V. Salomonson, personal communication).

Long-Term Research Goals

1. Estimation of Density and/or Water Equivalent of Snow

Water balance equations are simply accounting procedures for keeping track of the water within the system and for determining the water in storage at any given time. The water equivalent of the snow is precisely the volumetric quantity that hydrologists need to know. If we could make an accurate daily assessment of water equivalent, snowmelt analysis problems would be virtually solved. No other quantity is more important in snow hydrology than water equivalent.

Is it realistic to expect that satellite sensors can give us this parameter? Depth, density and areal extent of snow are required. Spectral analysis may someday yield a density approximation. Snow depths can be averaged from ground stations with fair accuracy. Areal extent can indeed be obtained from satellite readings. In my opinion, snow density determinations will be made from Landsat-D's thematic mapper, if research continues at its present pace.

2. An Understanding of Spectral Reflectance and Albedo of Snow throughout Seasonal Metamorphosis

The goal of any research is ultimately to understand the phenomenon under study. The current textbook curves showing the spectral reflectance of snow are quite inadequate. The

textbook curves relating snow albedo values to variation in time are not adequate for use with spectrally selective satellite sensors. This lack of basic physical measurements hampers the hydrologist as well as the remote-sensing specialist. Unless and until the problems cited here are given serious consideration our understanding of the basic physical relations governing snowmelt and its attendant radiometric effects on the snow surface will remain scant.

On one hand we are viewing the successful completion of a remarkable project: the verification of the need for and importance of snow-cover mapping in river basins for practical operational hydrology. On the other hand, we stand on the threshold of a new challenge: to add to our knowledge and understanding of the snowmelt process and to contribute toward development of improved hydrologic forecasts from the use of new sensors.

REFERENCES

Algazi, V.R. and Suk, Minsoo, 1975, An All Digital Approach to Snow Areal Mapping and Snow Modeling, in Rango, A., ed., Operational Application of Satellite Snowcover Observations, NASA SP-391, p. 249-257.

Barnes, J.C. and Bowley, C.J., 1974, Handbook of Techniques for Satellite Snow Mapping, ERT Document No. 0407, NASA Contract No. NA55-21803, 101 p.

Barnes, J.D. and Smallwood, M.D., 1975, Synopsis of Current Satellite Snow Mapping Techniques with Emphasis on Near Infrared Data, in Rango, A., ed., Operational Application of Satellite Snowcover Observations, NASA SP-391, p. 199-213.

Bartolucci, L.A., Hoffer, R.M., and Luther, S.G., 1975, Snow-cover Mapping by Machine Processing of Skylab and Landsat MSS Data, in Rango, A., ed., Operational Application of Satellite Snowcover Observations, NASA SP-391, p. 295-311.

Chang, A.T.C. and Choudhury, B.J., 1978, Microwave Emission from Polar Firn, NASA Tech. Paper 1212, 20 p.

Dallam, W.C. and Foster, James, 1975, Digital Snow Mapping Technique using Landsat Data and General Electric Image 100 System, in Rango, A., ed., Operational Application of Satellite Snowcover Observations, NASA SP-391, p. 259-278.

Itten, K.I., 1975, Approaches to Digital Snow Mapping with Landsat-1 Data, in Rango, A., ed., Operational Application of Satellite Snowcover Observations, NASA SP-391, p. 235-247.

Leaf, C.F., 1975, Applications of Satellite Snowcover in Computerized Short-Term Streamflow Forecasting, in Rango, A., ed., Operational Application of Satellite Snowcover Observations, NASA SP-391, p. 175-186.

Luther, S.G., Bartolucci, L.A., and Hoffer, R.M., 1975, Snow-Cover Monitoring by Machine Processing of Multitemporal Landsat MSS Data, in Rango, A., ed., Operational Application of Satellite Snowcover Observations, NASA SP-391, p. 279-294.

Martinec, J., 1975, Snowmelt-Runoff for Stream Flow Forecasts, Nordic Hydrology, v. 6, p. 145-154.

McGinnis, D.F., Jr., Matson, M., and Wiesnet, D.R., in preparation, Selected Hydrologic Applications of Landsat-2 Data, Final Report NASA Contract No. NAS-53991A, 182 p.

Meier, M.F. and Edgerton, A.T., 1971, Microwave Emission from Snow--A Progress Report, Proceed. 7th Internat. Sympos. on Remote Sensing of Environment, v. 2, p. 1155-1163.

O'Brien, H.W. and Munis, R.H., 1975, Red and Near-Infrared Spectral Reflectance of Snow, in Rango, A., ed., Operational Application of Satellite Snowcover Observations, NASA SP-391, p. 345-360.

Rango, A., 1975, An Overview of the Applications Systems Verification Test on Snowcover Mapping, in Rango, A., ed., Operational Application of Satellite Snowcover Observations, NASA SP-391, p. 1-12.

Rango, A. and Salomonson, 1976, Satellite Snow Observations and Seasonal Streamflow Forecasts, Final Report: NOAA Contract No. NA-776-74, 19 p.

Salomonson, V.V., 1978, Landsat-D, a Systems Overview, 12th Internat. Sympos. on Remote Sensing of Environment, Quezon City, Phillipine Republic, Proceed., Environ. Res. Inst. Michigan, p. 371-385.

Schneider, S.R. and McGinnis, D.F., Jr., 1977, Spectral Differences between VHRR and VISSR Data and their Impact on Environmental Studies, Proceed. Amer. Soc. Photogramm., 43rd Ann. Mtg., Feb-Mar. 1977, Washington, D.C., p. 470-480.

**Page intentionally left blank**

# MAPPING NEW ZEALAND AND ANTARCTIC SNOWPACK FROM LANDSAT

I.L. Thomas*, with T.D. Prowse@ and I.F. Owens@

* Physics and Engineering Laboratory, Department of Scientific and Industrial Research, Private Bag, Lower Hutt, New Zealand.

@ Geography Dept., Univ. Canterbury, Christchurch, New Zealand.

## ABSTRACT

Computer mapping, based on the Landsat digital data, can aid the efficient management of one of New Zealand's resources - the annual snowpack. The same techniques are effective in supporting Antarctic cartography, glaciology, and surface operations. The development of digital analysis and enhancement techniques for the routine semi-automated evaluation of Landsat data is illustrated. The 1979 field programme will concentrate on an instrumented snow basin for a water yield study. An outline of this satellite/ground programme is presented.

## INTRODUCTION

The annual snowpack is an important natural resource for New Zealand:

1. 50% of New Zealand's electricity consumption in 1976 was derived from hydro power, fed in part from melting snowpack (New Zealand Official Year Book, 1977).

2. Irrigation is increasing in importance as most New Zealand soils have a seasonal moisture deficiency. In the central South Island an irrigation scheme, fed by snow melt, was completed in 1970. It serves 2000 hectares. Construction of an extension to this scheme to serve an additional 14 000 hectares is proceeding (NZ Year Book, 1977).

3. Control of flooding, siltation and erosion is of importance to New Zealand - a country generally of steep unstable hillsides. An assessment of melt potential can allow more efficient control through the dams.

4. Skiing is increasing in popularity.
New Zealand's snow capped mountains receive wide tourist interest; in 1976 over 312 000 international visitors spent NZ$143M in the country (excluding fares) (NZ Year Book, 1977).

In Antarctica, New Zealand has an international mapping commitment in the Ross Dependency. Monitoring of the classes and textures of the different types of snowpack is easily accomplished from Landsat. The resolution (57*79 m), large area coverage in 26 seconds (185*185 km), and near orthographic imagery ($\pm$5.8° off vertical), make the system corrected data ideally suited to support mapping down to scales of 1:100 000.

The emphasis in New Zealand has been on developing the capability for routine mapping of this snowpack resource from the digital Landsat data. Such mapping must classify and delineate the various types of snowpack. The techniques used are supervised histogram parallelepiped classification for thematic mapping, and subtractive box filtering for textural enhancement. The modules that accomplish this are contained within the Landsat ANalysis SYStem version 1(LANSYS 1) package programmed for an IBM 370/168 in Programming Language 1 (PL/1) (Thomas, 1979). Data is transferred via image tape from the IBM 370/168 to an in-house Varian V76 where histogram equalization is commonly used to further enhance texturally enhanced imagery, in radiance space, before the image data is written out on an Optronics Colorwrite as a positive colour transparency (McDonnell, 1979).

The first New Zealand use of Landsat for snowpack monitoring took place in 1977 during the evaluation of a proposed skifield (Six Mile Creek basin - 41.88°S, 172.85°E) (Thomas et al, 1978). This study was based on a non-automated comparison of the four band MSS radiances along representative transects. It was found possible to map three different types of snowpack using the technique. This study evaluated Landsat data for snowpack studies, indicated manpower time restrictions on analysis techniques and highlighted the problems induced by the terrain.

As a result of this pilot skifield evaluation a snowpack to water yield study was set up in the instrumented Camp Stream basin (43.13°S, 171.70°E) for the 1978 southern winter. This small (50 ha) basin was chosen because:

(i) its "spoon" shaped terrain reduced specular reflection anomalies;
(ii) its geology and geomorphology permitted the water yield to be measured readily at the egress free from seepage effects into, or out of, the catchment;
(iii) its history of snowpack, meteorological, and water yield statistics is known (e.g. Morris and O'Loughlin, 1965; O'Loughlin, 1969);
(iv) its small size allows every Landsat pixel to be considered individually by manual techniques if the need arises (~ 100 pixels over usual snow covered area);
(v) it has both east and west facing slopes to include sunlit and shaded surfaces at Landsat overpass time;
(vi) it has terrain that included tussock and scree surfaces permitting studies on the influence of the basal material on snowpack characteristics;
(vii) there is a 600 m range in elevation from the bushline (at 1070 m) to exposed ridge tops (at 1670 m);
(viii) it is near lesser instrumented skifield basins;
(ix) it is free from casual human influences - well away from ski trails, etc.;
(x) it is near to a serviced field station;
(xi) it appears on the same Landsat scene that covers the site used for a similar agricultural applications investigation. This reduces the New Zealand imagery scheduling load at NASA.

The 1978 programme was inhibited by a lack of Landsat imagery, so the main analytical emphasis has been on the development of the digital processing techniques outlined earlier. These techniques were developed to support time efficient semi-automated reduction of multi-channel Landsat data to single factor products for the management process. Examples of these techniques, applied to the Six Mile Creek, Camp Stream, and McMurdo Sound region of Antarctica (77.40°S, 163.53°E), are presented here.

Field measurements taken during the 1978 season were used to refine the ground support programme and those measurements scheduled for the 1979 season are outlined.

## OPERATIONAL ANALYSIS FACILITIES FOR LANDSAT DATA IN NEW ZEALAND

The best analysis package appears to be:

1. Ground Truth (GT) data taken in the test areas with all the variables being monitored that may influence the results. (New Zealand experience with metamorphosing snowpack indicates that the GT data is useless if taken outside "Landsat overpass time ±1 hour".)

2. The discipline oriented user, who will later perform the analysis, should participate in the GT programme. The software technologist should also participate, but less regularly. (This technologist is usually more familiar with the limitations of the data, and applicability of various computing options to the analysis task, than is the discipline oriented user.)

3. First generation texturally enhanced histogram equalized, or stretched, hue enhanced colour composite positive transparencies of the control and test areas should be prepared on the Colorwrite. Such transparencies allow the analyst to assess the subtleties of terrain modification to snowpack characteristics that thematic mapping cannot adequately portray.

4. Colour coded thematic maps in transparency form should be produced on the Colorwrite. The unclassified terrain data can be beneficially incorporated as a black and white background. These thematic maps may be straight classified (e.g. histogram parallelepiped) or include spatial massaging.

From these processed data products a final composite thematic map may be readily prepared, bringing the best of all systems to bear on the analysis.

The New Zealand programme has two major research objectives:

A. To evaluate Landsat snowpack data for incorporation in water yield research and operational management.

B. To provide rapid and low cost topographic mapping of parts of Antarctica to scales of 1:100 000, with low field manpower involvement.

The other objective - the monitoring of snowpack on the Mt. Robert and Six Mile Creek skifields - would be operational if Landsat coverage is obtainable.

Both major research objectives have similar computing needs - texturally enhanced imagery and thematic maps of snow/ice types. They differ in the Ground Truth support that is needed.

The textural enhancement process uses the following equation for each picture element in turn:

$$R' = R - 0.8\bar{R} + 20 \qquad (1)$$

where $R$ is the radiance, in the selected band, for the central pixel

$\bar{R}$ is the average radiance for the N*N nearest neighbour matrix surrounding, but excluding, the central pixel

$R'$ is the synthesized radiance for the pixel considered.

This is programmed in PL/1, uses integer arithmetic, minimal core storage, and is routinely available on a nationwide IBM 370/168 network. Commonly a 3*3 nearest neighbour matrix is used. This textural enhancement is applied to each MSS band in turn.

Once an image tape has been prepared on the IBM 370/168 it is passed to the in-house Varian V76. A sample area for the particular form of enhancement is selected (e.g. for snow or sea or forest, etc.) and the CCT radiance level occurrence statistics for that sample are compiled. From these a histogram equalized or stretch hue enhancement "look-up" table is prepared. The texturally enhanced data is then passed through the look-up table and written to the Colorwrite. Usually MSS 4 is written through a blue filter, MSS 5 through green, and MSS 7 through red, for the standard colour composite. (For further details of the PEL Colorwrite system see McDonnell (1979). Simpson (1978) provides a concise outline of the various usual enhancement options.)

Figure 1 is an example of this textural and hue enhancement applied to a part of Landsat scene 2192-21265 recorded over Central Canterbury, New Zealand, on 2 August 1975 (GMT). The subscene contains the Craigieburn Range with the Camp Stream basin being the southward opening "V" catchment situated on the second from the north, eastward extending ridge. The detail in the snowpack (and all terrain) has been enhanced over the standard product. The composite of MSS bands 4,5,7 has been found to be as effective as the composite of MSS bands 5,6,7 for revealing detail in the New Zealand snowpack.

For some applications, e.g. delineation of boundaries in Antarctic pack ice, etc., it is desirable to scale all regions of uniform radiance to a common level and to highlight departures from this uniformity. The same module in the LANSYS1 package is used but equation 1 is replaced by

$$R' = 0.01(R - \bar{R})^5 + 100 \qquad (2)$$

A 5*5 nearest neighbour matrix is presently being tested. Figure 2 presents results using this boundary enhancement module for a region of sea ice in scene 1174-19433 recorded over McMurdo Sound Antarctica on 13 January 1973 (GMT). The leads and brash ice are clearly delineated.

Thematic maps are also processed initially on the IBM 370/168 to image tapes. Rango and Itten (1976) compared the results of several different classification schemes for the computerized mapping of snowpack. They found little difference between histogram parallelepiped and maximum likelihood results. This finding has been confirmed for other types of target (Honey, 1978). The major influence on the success, failure, or indeterminancy, of any classification process is the accuracy of spectral signature determination for the different target types: in short - good ground truth. The PEL LANSYS1 thematic mapping package is presently based on histogram parallelepiped classification. Multi-date analyses, such as outlined by Luther et al (1975) should dramatically improve

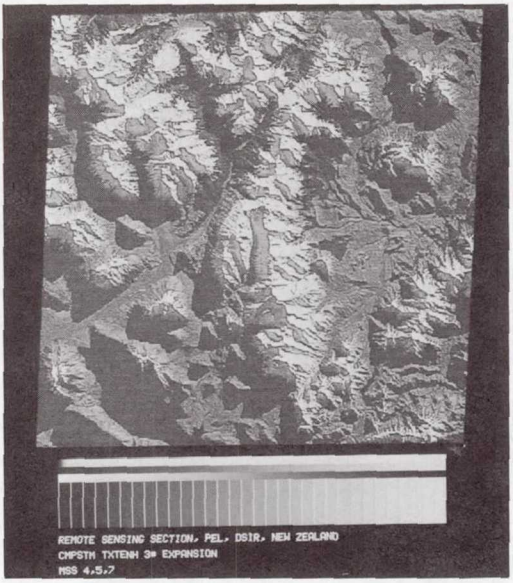


Fig. 1: A texturally and hue enhanced treatment of the Craigieburn Range, including the Camp Stream basin, from Landsat scene 2192-21265 recorded on 2 August 1975.

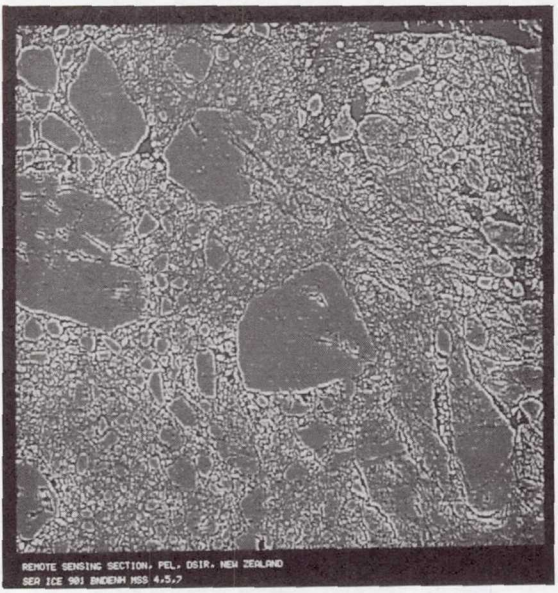


Fig. 2: A region of sea ice in McMurdo Sound, Antarctica (Landsat scene 1174-19433) has been boundary enhanced to highlight edge effects associated with leads and brash ice.

classification accuracy, but currently place quite a time and storage load on computing systems.

The first step in preparing a thematic map is the determination of the spectral signature ranges for each target type. Modules within the LANSYS1 package permit both unscaled and scaled coded lineprinter outputs to be prepared. The unscaled outputs have no compensation for scale differences brought about by the differing 'along-line' and 'across-line' spacing between characters extant on most computer lineprinters. The scaled output module resamples the data along a Landsat scan line. For the New Zealand system, the final product is scaled to approximately 1:18 810. Non-overprinted characters are used so that the radiance level range associated with each character may be clearly determined. A 57 character set is employed with the range of the set adjustable both by varying the lower limit, so the full range may be covered with a CCT level resolution of 1 level, or by varying the step increment. The work of Gordon (1978a,b) indicates that atmospheric variations, together with quantization and decompression uncertainties, may account for $\pm 1$ to 2 CCT levels. Hence a step increment of 2 is usually suggested.

Scaled lineprinter maps are a cost and time effective way of routinely monitoring snowpack state in regions like the Mt. Robert and Six Mile Creek basins. Figure 3 presents the scaled results for the Six Mile Creek basin recorded by Landsat in scene 2984-21002 on 2 October 1977. The base snowpack had just been overlaid by fresh powder snow - hence the apparent uniformity and high radiance levels in the illustrated channel.

Trial spectral signatures are determined from such lineprinter outputs for the different types of snowpack to be thematically mapped. These signatures are then inserted into the supervised histogram parallelepiped module and test areas classified. Output to the lineprinter are: areas in each class, a coded thematic map, occurrence statistics for the spectral signature range for each band for each target class, the mean and standard deviation for each range, a new suggested spectral signature range (based on the mean $\pm 1$ standard deviation), and the occurrence statistics expressed in radiance (mw/ster/cm$^2$/bandwidth) terms - to facilitate snowpack reflectance intercomparisons between channels and target types. This process is repeated until satisfactory signature ranges have been determined for each snowpack type.

This supervised histogram parallelepiped classification proceeds in a preselected target order and can be exploited for snowpack studies by classifying in decreasing radiance 'gate' order. This facet 'comb-filters' snowpack classes and can improve classification discernment in regions of many different snowpack types or terrain variations.

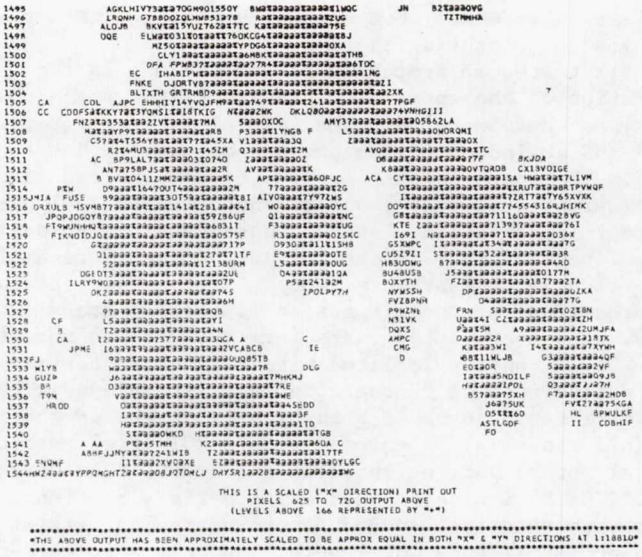

Fig. 3: An example of a coded lineprinter output used to monitor the area of snowpack for potential skifield evaluation. Portrayed here is the Six Mile Creek basin on scene 2984-21002 shown in MSS 5 where the "@" symbol indicates a CCT level range of 126-127. The alphanumeric characters indicate lower (~120) radiance levels. The lineprinter output has been resampled to a scale of 1:18 810.

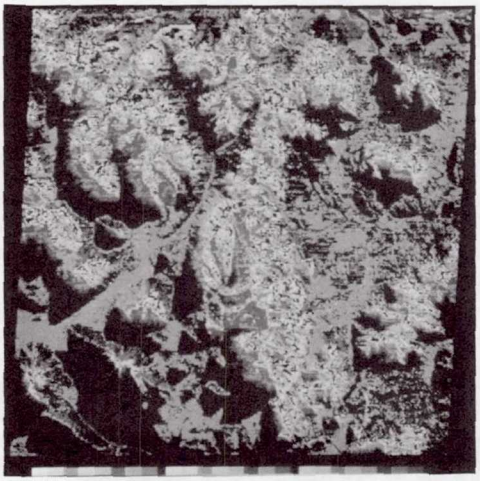

Fig. 4: The Craigieburn Range has here been classified for different snowpack types using straight supervised histogram parallelepiped classification. The colour codes are presented in Table 1. (Landsat scene 2192-21265.)

The final step in creating the image tape for the Varian V76 is the allocation of a number, and hence colour on the Colorwrite, to each target class. The user selects appropriate colours and allocates the numbers in one of the LANSYS1 modules.

In Figure 4 the Craigieburn Range region, shown texturally enhanced in Figure 1, is presented classified for ten different terrain modified snowpack types. It has been classified with the straight supervised histogram parallelepiped module. The unclassified sections of the MSS 5 band are usually laid down as a background black and white image. This background usually has the dual advantages of (i) assisting in relating the classified areas to topographic detail, and (ii) enabling the user to assess how appropriate to actuality were his choice of spectral signatures. In the classification examples presented here the MSS5 background is omitted as: most of the scene is classified, thus reinforcing the need to refer to the texturally enhanced colour composite to check the validity of the classification; and little of the remaining scene would be occupied with MSS5 data.

The histogram parallelepiped classifier, like many other classifiers, considers each pixel as a separate entity without recourse to the classification results for the surrounding elements. The LANSYS1 package includes a spatial massaging module which permits a central pixel to be reclassified (or declassified) depending on the classification status of its immediately nearest orthogonal neighbours (see Thomas, 1979, for a fuller discussion). The spatial massaging process aggregates classified pixels of like type or rejects those that have been thrown up perhaps as 'noise' in the classification process.

For some applications maximum detail may be required to study the high frequency contribution of the terrain to the classification of the lower frequency overlying target class. Snowpack studies may be such an application. Consequently both forms of computer produced thematic map are used: one with spatial massaging, to emphasize the overlying snowpack type; and one without, to highlight the contribution of specular variability to the resultant spectral signature.

Figure 5 presents the results of a spatial massaging process applied to the Craigieburn Range results given in Figure 4. The same scene, spectral signatures and colour allocation were used in both figures. The aggregation of snowpack types and reduction in solitary classified pixels is evident.

The classification leading to Figures 4 and 5 has proceeded without Ground Truth. The figures demonstrate the technique rather than ground actuality. It is hoped that concurrent Landsat overpasses and Ground Truth programmes will occur in Canterbury in 1979.

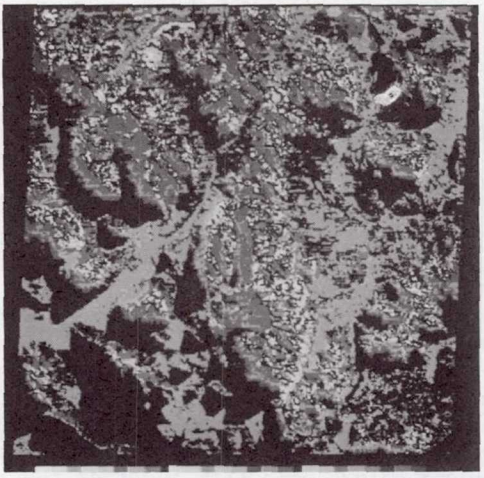

Fig. 5: The same classification has been applied as in Fig. 4 but spatial massaging has been implemented to reduce "noise" and aggregate snowpack conglomerates.

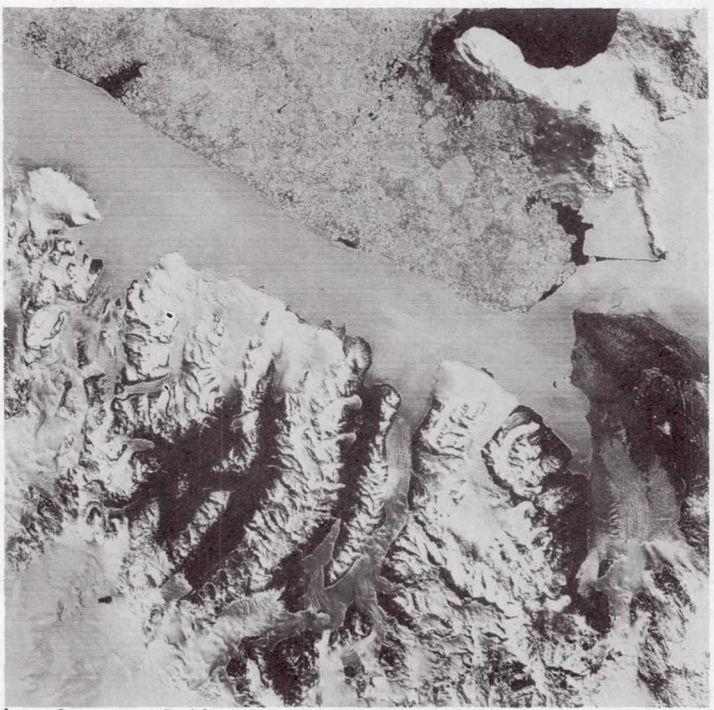

Fig. 6: The full Landsat scene 1174-19433 of McMurdo Sound Antarctica has here been texturally, and then hue, enhanced for snow and ice.

Most of the needs for Antarctic mapping that can be satisfied by Landsat data can be met by the LANSYS1 package. Figure 6 is a textural and hue enhancement, for ice, of scene 1174-19433, recorded over McMurdo Sound on 13 January 1973 (GMT).

A subscene of Figure 6 was overlaid with the best available cartographic linework for Ross Island and is presented as Figure 7. This is accomplished easily photographically and provides quick and cost effective mapping to the limit of the system corrected Landsat imagery - 1:100 000.

The surface traveller can obviously benefit from such texturally enhanced imagery. He can be further aided by thematic mapping of different snow and ice types. In Figure 8 such a thematic map for the piedmont at the mouth of New Harbour is presented. It differentiates snow/ice types into like radiance regimes. Again it is a demonstration of technique rather than actuality - ground truth was not available for this image.

## THE GROUND TRUTH PROGRAMME

Ground Truth (GT) programmes have evolved to support both the skifield evaluation in the Six Mile Creek basin and the snowpack to water yield study in the Camp Stream basin. During the 1977 and 1978 southern winters the research GT programme has developed to that presented below - scheduled for the 1979 season, principally for Camp Stream.

Three common-altitude survey lines have been permanently located around the basin. All three courses will be used when elevational differences in snow properties are found to exist. In periods of relative homogeneity only the central course will be monitored.

GT data will be collected on an areal scale compatible with the Landsat pixel resolution. Supplementary measurements will be made to refine the various data as the snowpack changes.

Snow depth and density measurements will be taken along the courses using a Mount Rose snow sampler and depth probes. Snow depth will normally be sampled every 20 m and density every 100 m - as the density has been found to be more spatially consistent than depth. The Mount Rose sampler, apart from permitting a coarse integrated density to be derived for the snow column, will also provide data to extrapolate the detailed layering and density data obtained from the snowpits.

The snowpits will be dug along or between the snowcourses, depending on conditions. The basic control sampling will be: two snowpits on the sunlit and shaded faces along the central snow course. Of these, two pits will be dug on a scree base and two on a tussock base. Special


Fig. 7: Part of scene 1174-19433, covering Ross Island, Antarctica, - from Fig. 6 - has been overlaid by cartographic line work to support New Zealand's Antarctic mapping programme.

Fig. 8: A region of the sea ice, ice shelf, piedmont, and shore snowpack at the mouth of New Harbour in McMurdo Sound (scene 1174-19433) has here been thematically mapped (histogram parallelepiped + spatial massaging) using the colour codes listed in Table 1 for the different ice types.

emphasis will be placed on the upper 20 cm of the snowpack - the zone which most influences the Landsat data.

The following measurements will be taken at each snowpit:

(i) A depth probe.

(ii) A Mount Rose density profile.

(iii) A normal 1 kg rammsonde profile.

(iv) A lightweight rammsonde (0.25 kg mass for both the ram mass and ram block, 60° ram apex angle) profile of the upper 20 cm. (Both rammsonde profiles will quantify the 'vertical' hardness of the snowpack.)

(v) A Brinell hardness assessment of the ice bonding of the surface snowpack layer - see Appendix A.

(vi) An analysis of snow grain type, size and interrelated structure at the surface and for each subsequent layer. This analysis will be initially based on the International Snow Classification for falling snow (Figure 4, La Chappelle, 1969) and on the scheme of Magono and Lee (Figure 5, La Chappelle, 1969) for both precipitated and falling snow. Further data on grain size, etc., will be classified according to the scheme reported in Appendix B of Perla and Martinelli (1976). These measurements will be supported by a micro-photographic system.

(vii) Volume/weight measurements of each snow layer will be taken to produce a detailed vertical density profile.

(viii) Temperatures will be measured in the air - 10 cm and 1 cm above the snowpack - in the surface and succeeding layers, and at least every 10 cm through the snowpack to produce a temperature gradient profile (2.5 cm near surface).

(ix) Horizontal 'hardness' of the snowpack will be quantified using hardness gauges modelled on those of the National Research Council of Canada - these are similar to soil hardness gauges.

(x) Free water content will be assessed using the method outlined in Appendix B of Perla and Martinelli (1976) and quantified by using a melting calorimeter.

(xi) Thermal quality - the percentage by weight of the snowpack's water equivalent which is in the form of ice - will also be measured using the melting calorimeter. The amount of energy required to move the composite snowpack at 0°C to water at 0°C, per gram, may then be quickly assessed from the latent heat of fusion of ice (O'Loughlin, 1969).

In addition the Camp Stream basin will carry the following instrumentation to support the programme:

1. A recording weir at the egress for monitoring water yield.
2. A snow lysimeter to estimate snowcover run off from a single plot (25 $m^2$).
3. A recording three point distance thermograph to monitor snowpack temperatures.

4. A thermograph and barograph for recording air temperature and barometric pressure.
5. A totalizing anemometer.
6. Snow deposition will be continuously recorded in the basin.
7. A snow ablation/evaporation study.

As part of the wider New Zealand monitoring programme the Forest Research Institute continuously records air, snow and soil temperatures over a 600 m elevation range on the nearby Mt. Cheeseman (8 km southwest).

It is envisaged that during the 1979 season (May-October) the Camp Stream basin will be monitored collaboratively by personnel from the Geography Dept., University of Canterbury, Forest Research Institute, NZ Forest Service, and DSIR. Intensive monitoring is scheduled for each Landsat 3 overpass date, with back-up monitoring for the Landsat 2 overpass dates (brought on by unfavourable weather conditions).

## COMPARISON OF SNOW/ICE RADIANCE RANGES BETWEEN NEW ZEALAND AND ANTARCTICA

New Zealand and Antarctica have obvious climatic differences that lead to different types of ice and snow being sensed by Landsat over the two regions.

The New Zealand snowpack is more likely to have liquid water coating the crystals or moisture freezing to form ice layers and coatings within the crystalline snowpack. O'Brien and Munis (1975) noted that the reflectance of wet or refrozen wet snowpack was less than snowpack that had no melt or free water associated with it. The densities of the wet and/or refrozen snowpack were higher than those samples free from melt. Antarctica, even on the coast, is usually free of such wet conditions. Consequently we would expect Antarctic snowpack to generally have higher reflectances than New Zealand snowpack.

O'Brien and Munis (1975) also found that snowpack reflectance decreased with increasing density, induced by increasing snowpack age. Mellor (1961), working with surface snowpack in the Antarctic, found lower densities to be related to lower mean annual temperatures, below -10°C. He cited a mean annual temperature for the McMurdo Sound region of -4°F (-20°C).

Consequently, on comparing surface snowpack between New Zealand and Antarctica as a function of both free water accretion and density, one would expect less dense surface snowpack to prevail in Antarctica with consequently higher radiances being recorded by Landsat.

These contentions are borne out by the results cited in Table 1. Presented there are the spectral signature upper and lower limit values for the supervised histogram parallelepiped classifiers that led to the thematic maps of Figures 4, 5 and 8. The values, presented in CCT level terms as they were used in the classification, may be readily converted to radiances in

| Snow/Ice Type | Scene/Date | Sun Az/El | %** Total Area | CCT Level Radiance Ranges MSS 4 | MSS 5 | MSS 6 | MSS 7 |
|---|---|---|---|---|---|---|---|
| Maximum Value | | | | 127 | 127 | 127 | 63 |
| New Zealand | | | | | | | |
| Fresh powder snow | 2984-21002 771002 | 62°/32° | - | 126-127 | 126-127 | 126-127 | 62-63 |
| Snow 1 (Mauve*) | 2192-21265 | 46°/15° | 1.3+ | 126-127 | 126-127 | 126-127 | 62-63 |
| Snow 2 (Yellow) | 750802 | | 0.3 | 114-126 | 126-127 | 126-127 | 62-63 |
| Snow 3 (Purple) | | | 0.4 | 106-114 | 120-127 | 120-127 | 55-62 |
| Snow 4 (Lt Yellow) | | | 2.0 | 90-106 | 120-127 | 120-127 | 44-55 |
| Snow 5 (Orange) | | | 3.3 | 69-90 | 90-118 | 90-118 | 30-48 |
| Snow 6 (Red) | | | 6.6 | 40-71 | 55-93 | 53-94 | 20-37 |
| Snow 7 (Lt Green) | | | 7.8 | 21-47 | 24-56 | 24-58 | 8-24 |
| Snow 8 (Dk Green) | | | 19.1 | 10-25 | 10-25 | 7-25 | 2-14 |
| Snow 9 (Lt Blue) | | | 40.9 | 6-12 | 4-15 | 5-15 | 0-10 |
| Snow 10 (Dk Blue | | | 18.1 | 6-19 | 3-16 | 2-13 | 0-2 |
| Total Area Classified as Snow 477.1 $km^2$ | | | | | | | |
| Antarctica | | | | | | | |
| Ice 1 (Dk Blue*) | 1174-19433 | 87°/22° | 5.7++ | 126-127 | 117-127 | 99-111 | 36-42 |
| Ice 2 (Dk Blue/Green) | 730113 | | 10.0 | 123-127 | 108-127 | 93-108 | 33-39 |
| Ice 3 (Lt Blue/Green) | | | 12.9 | 120-127 | 111-120 | 93-102 | 33-36 |
| Ice 4 (Dk Purple) | | | 52.6 | 114-126 | 108-117 | 87-96 | 30-36 |
| Ice 5 (Yellow/Green) | | | 6.0 | 111-120 | 102-111 | 84-93 | 30-36 |
| Ice 6 (Orange) | | | 0.1 | 111-120 | 99-114 | 81-93 | 30-36 |
| Ice 7 (Lt Purple) | | | 12.7 | 99-114 | 87-108 | 69-87 | 24-30 |
| Total Area Classified as Ice 870.7 $km^2$ | | | | | | | |

* The colours are those portrayed in the thematic map products - Figures 4,5,8
** Area percentages calculated from spatially massaged classification
+ For region covered in Fig. 5. ++ For region covered in Fig. 8.

TABLE 1 A comparison between the radiance ranges in CCT level terms, for snow/ice types between New Zealand and coastal Antarctica.

mw/ster/$cm^2$/bandwidth on recourse to the "Landsat Data Users Handbook" (1976). The colour codes employed in the thematic mapping are indicated. In the absence of detailed ground truth no more than a demonstration of the technique is possible and no attempt has been made to compensate the classification types for terrain modification. Also in Table 1 are given the areal percentage occurrence figures for each type of the classified snowpack. The figures are based on the spatially massaged classification results portrayed in Figures 5 and 8. The preponderance of lower radiance snowpack in the New Zealand test area is evident. One could conclude that the Camp Stream snowpack possessed a higher density and had, possibly, a closer association with free water than the Antarctic snowpack.

Glacial ice in its movement is subjected to pressure differentials. Mellor (1961) cites bore hole results in glacial ice of increasing density with depth (or pressure). (The crystal size was also noted to increase with depth.) The results O'Brien and Munis (1975) presented indicated (i) that denser snowpack was associated with lower reflectances, and (ii) the reflectance in the 0.8-1.1 $\mu$m region was less than that between 0.5 and 0.7 $\mu$m. Consequently we would expect glacial flow ice to have lower reflectance than stable surface snowpack. Such glacial ice is expected to be cyan to blue in colour in the standard false colour composite of MSS 4, 5, 7 printed, additively, through blue, green, and red filters respectively. The colour may be quickly deduced from the expected radiance levels in each MSS band, the printing filters for the respective channels, and an additive colour wheel (e.g.

Rib, 1968). Again, by extrapolating the results of O'Brien and Munis (1975), we would expect that as the ice density increased, the colour in the composite would progress from white through cyan to dark blue. Thus the colour may be used to indicate pressure fields in glacial icepack. An inspection of Figure 6 illustrates these contentions.

## TERRAIN MODIFICATION OF SPECTRAL SIGNATURES

It has been tacitly assumed in all New Zealand classification work that the semi-automated classifiers interpret gross terrain modification of the signature from the same target type, as being assigned to different classes. For example, snowpack of type 1 in direct sunlight is regarded as class 1, the same snowpack in partial shadow as class 2, and in deep shadow as class 3. An inspection of the texturally and hue enhanced colour composite together with the colour coded thematic map quickly allows the final thematic map to be compiled aggregating all three classes as the one snowpack type.

Band ratioing will be implemented after acquisition of an intelligent graphics terminal (a Hewlett Packard 2647A) in mid-1979. This will permit various empirical band ratio formulae to be quickly developed and evaluated for different types of study. Without such distributed processing it has not been time-effective to pursue this work with the present systems. Band ratioing is expected to further reduce the influences of terrain modification upon the classifiers.

## PROJECTED DEVELOPMENTS FOR THE 1979 SEASON

Detailed mapping of the Camp Stream basin is presently underway to prepare a base map to support hydrologic modelling of the basin. The map is to be at 1:5000 scale with 10 m contours.

A multi-channel, including thermal, scanner may be flown over the Camp Stream basin in early spring to evaluate the applicability of such an airborne multi-channel digital scanner to snowpack studies in New Zealand.

During the season it is expected that spectrophotometric scans will be taken of a variety of snowpack types 'in situ' in Camp Stream basin. The prime objective is to acquire more data on moisture/age/density influences within different snowpack classes upon the spectral reflectance characteristics. Specular and goniometric studies on the undisturbed field snowpack will also be conducted.

Band ratioing studies will be pursued on the intelligent terminal.

Ground truth programmes will be mounted to support Landsat data acquisition over both Camp Stream and McMurdo Sound (NASA Path 078 Row 090, and NASA Path 056 Row 116, respectively).

## CONCLUSION

An analysis package has been developed that supports the semi-automated assessment of snowpack. It works directly from the linear digital Landsat CCT data to both delineate and classify different classes of snowpack.

The routine comparison of two skifields is proceeding from the Landsat data, based on coded lineprinter outputs.

A combination of cartographic linework with texturally and hue enhanced imagery, or with a colour coded thematic map, is now routinely available to support Antarctic mapping to 1:100 000 scale. The research into snowpack/water yield is now supported by semi-automated analysis techniques together with a detailed ground truth programme. All is ready for the 1979 season.

Fundamental to any operational implementation of Landsat in this application are two factors: (i) frequent coverage, and (ii) rapid throughput of data to the user.

Frequent coverage is the only way valid area/type measurements may be implemented in a hydrologic forecasting model. New Zealand suffers from the very factor that nurtures the natural resource considered here - the native name for the country, Aotearoa means "land of the long white cloud"!

Rapid transmission of the data to the user is necessary for its incorporation in time-effective analysis and management procedures. Currently, April 1979, New Zealand is awaiting the arrival of MSS CCT products acquired over the test areas in July 1978.

To partially alleviate both these problems in the implementation of Landsat into the management scene, New Zealand is presently seriously considering the establishment, in stages, of a national Landsat receiving station and processing installation. This would permit imagery to be acquired of regions that are cloud free.

## APPENDIX A

### Monitoring Surface Snowpack Bonding Via the Brinell Hardness Parameter

Landsat senses mainly the surface layer of snow/ice crystals. Of vital importance to the problem of relating Landsat recorded radiances to snowpack data is the study of the composition and structure of this top layer. The crystal shape, structure, size and state are to be monitored in the Camp Stream programme.

As the snowpack metamorphoses, either through temperature or age, the surface structure can change. Ice bonding between individual crystals can lead to the thin surface layer, generally known as the 'crust'. The formation of this crust can change the recorded spectral signature dramatically - as we have discussed comparing the New Zealand and Antarctic snowpacks. In order to quantify this ice bonding several

'hardness' rigs were tested and one based on the Brinell parameter will be used during the 1979 programme.

Batson and Hyde (1931) indicate that the hardness of a body should be measured by the normal pressure per unit area which must act at the centre of a circular surface of pressure in order that at some point in the surface the stress may just reach the perfect elastic limit. This elastic limit is the maximum stress per unit area to which the surface layer may be subjected and still be able to return to its original form, on removal of the stress. The apparatus used in the New Zealand programme presently consists of an inverted hemi-spherical cap which is placed, rounded side down, on the snowpack and loaded by set masses. The diameter of the indentation left by the spherical segment (marked with washing blue) is then measured. The loading is chosen to allow the surface to perform elastically. In this way a measure of the surface bonding property is obtained, rather than the resistive forces of the underlying layers.

As $H_B = \frac{P}{A}$

and $A = \pi Dh$

$h = \frac{1}{2}(D - \sqrt{D^2 - d^2})$

then $H_B = \frac{P}{\pi \frac{D}{2} (D - \sqrt{D^2 - d^2})}$

where: D is the diameter of the sphere (mm)
d is the diameter of the indentation (mm)
h is the depth of the indentation (mm)
P is the total mass (kg)
A is the spherical area of the indentation ($mm^2$)
$H_B$ is the Brinell Hardness number

This technique has the advantage of quantifying the crust, for intercomparisons, irrespective of whether the crust is supported by other layers, or bridges an air pocket. Standard rammsonde techniques are affected by this crustal ice bonding, supporting layer resistive forces, and oblique cone forces, etc., as they break through the surface layer - the layer that influences the Landsat data the most.

Currently the equipment is being tested for use on sloping surfaces. It will be developed further during the 1979 season.

ACKNOWLEDGEMENTS

A programme such as this relies heavily on the distributed expertise of many people exercised often under arduous physical conditions. The field programmes have only been possible with the dedicated support of Mr. G. Baker of the Forest and Range Experimental Station and Drs. C. O'Loughlin, A. Pearce and Mr. P. Hinshy of the Forest Research Institute; Mr. A. Stephens of the NZ Forest Service; Mr. J. Waugh of the Ministry of Works and Development - for the Camp Stream operations: and Messrs. C. Wishart, D. Cordes, P. Farley and C. Maplesden - for the Six

Mile Creek project. The overall NZ Forest Service programme has been co-ordinated in Wellington by Mr. N.P. Ching and has been greatly supported by Mr. A. Neale of the NZ Meteorological Service, Dr. C. Bassett, Director, Forest Research Institute, and Mr. A.P. Thomson previous Director General NZ Forest Service - who initiated the application of Landsat to these studies in New Zealand.

Of vital assistance in preparing the Colorwrite products discussed here have been the software systems for hue enhancement and Colorwrite control written by Dr. M.J. McDonnell of PEL. The imagery has been run through the system by Mr. A. Hinton and processed by Mr. A.D.W. Fowler.

It is a pleasure to acknowledge the discussions with colleagues, Drs. W.H. Robinson, P.J. Ellis, and Mr. G.M. Allcock, at PEL that have strengthened the study.

In the preparation of this report the authors are grateful for the help of Miss V.M. Benning and Mr. R.C. Barrett of the Dept. of Lands and Survey for assistance with the mapping and cartography; to Messrs. J. Brownlie and T. Ransfield for photographic support; and to Mrs. S. Coburn, Mrs. C. Keppel, and Ms. P. Humphries for processing the report to legibility.

The work has been supported in part by DSIR/University contract No. UV/2/25.

REFERENCES

Batson R.G. and Hyde J.H. (1931) "Mechanical Testing - Vol. 1: Testing of Materials of Construction" p.292, publ. by Chapman and Hall, London, UK.

Gordon H.R. (1978a) "Removal of atmospheric effects from satellite imagery of the oceans", Applied Optics 17, 1631.

Gordon H.R. (1978b) "Remote sensing of optical properties in continuously stratified waters", Applied Optics 17, 1893.

Honey F.R. (1978) CSIRO Land Use Research, West Australia - private communication.

La Chappelle E.R. (1969) "Field guide to snow crystals", Univ. of Washington Press, Seattle, USA.

"Landsat Data Users Handbook" (1976) Published by NASA Goddard Space Flight Center, Maryland, USA. Document No.76SDS4258.

Luther S.G., Bartolucci L.A. and Hoffer R.M. (1975) "Snow cover monitoring by machine processing of multitemporal Landsat MSS data" in "Operational applications of satellite snowcover observations" Ed. A. Rango, NASA Report No. SP-391, p.279.

Mellor M. (1961) "The Antarctic ice sheet" Report I-B1 US Army Cold Regions Research and Engineering Laboratory, Feb. 1961.

McDonnell M.J. (1979) "Computer image processing and production at PEL" presented at 49th ANZAAS Congress, Auckland, NZ, 22-26 Jan. 1979.

Morris J.Y. and O'Loughlin C.L. (1965) "Snow investigations in the Craigieburn Range" Jour. of Hydrology (NZ) 4, p.2.

New Zealand Official Yearbook (1977) Department of Statistics, Wellington, New Zealand, September 1977.

O'Brien H.W. and Munis R.H. (1975) "Red and near-infrared spectral reflectance of snow" in "Operational applications of satellite snowcover observations" Ed. A. Rango, NASA Report No. SP-391, p.345.

O'Loughlin C.L. (1969) "Further snow investigations in the Craigieburn Range" Protection Forestry Report No.52, NZ Forest Service.

Perla R.I. and Martinella M. (Jun.) (1976) "Avalanche Handbook" publ. by US Dept. of Agriculture, Forest Service, Ft. Collins, Colorado, USA. Agriculture Handbook No.489.

Rango A. and Itten K.I. (1976) "Satellite potentials in snowcover monitoring and runoff prediction" Nordic Hydrology 7, p.209.

Rib H.T. (1968) "Color Measurements", sub-chapter 1.2, "Manual of Color Aerial Photography", ed. J.T. Smith, published by American Society of Photogrammetry, Virginia, USA.

Simpson C.J. (1978) "Landsat: developing techniques and applications in mineral and petroleum exploration" J. of Australian Geology and Geophysics 3, p.181.

Thomas I.L., Lewis A.J., Ching N.P. (1978) "Snowfield assessment from Landsat" Photogramm. Eng. and Rem. Sens. 44, p.493.

Thomas I.L. (1979) "User's guide to the Landsat ANalysis SYStem version 1 (LANSYS1) package", Physics and Engineering Laboratory Report (in preparation) April 1979.

# DIGITAL MAPPING OF MOUNTAIN SNOWCOVER UNDER EUROPEAN CONDITIONS

Harold Haefner, Department of Geography, University of Zurich,
CH-8006 Zurich, Switzerland

## ABSTRACT

A method was developed for monitoring the snowcover in high mountain terrain such as the Swiss Alps which fulfills the specific needs of Europe and whose results are suitable as input into the runoff model by Martinec. The procedure includes the rapid classification of multitemporal data for small watersheds with very high accuracy under all modifications caused by different illumination, sun angle, shadow effects, slope angle, exposure, terrain cover, etc. The method is based on a supervised classification technique, using a PPD-algorithm in general. In addition to the four Landsat-channels, a fifth artificial channel was created containing the average altitude information of each pixel and allowing a subdivision of the watershed in accordance to the requirements of the runoff model. Even in very small watersheds of about 40 $km^2$ the results achieved from Landsat data are at least as accurate as the ones gained from measurements of orthophotographs.

## INTRODUCTION

During recent years, the importance of earth resources satellites as a potential source for accurate and timely information has been recognized more and more in Europe. Under the leadership of the "European Space Agency" (ESA), in conjunction with its "Remote Sensing Working Group" (RSWG), the mission objectives were studied to identify specific demands and eventual contributions. ESA points out that the "main European emphasis is placed on the management and the conservation of known resources, rather than on the exploration and exploitation of new resources at national level" (ESA, 1977, p. 2). Even for developed regions such as Europe with reasonably complete resources information, earth observation satellites may play an important function in such areas as:

- monitoring the changing features of the European landscape (e.g., agriculture, land use, water resources)
- monitoring the coastal ocean areas (ESA, 1978, p. 1).

Within the field of water resources management, one of the most important potential applications to Europe is the operational monitoring of mountain snowcover. Mapping of the areal extent of the snowcover in its seasonal variations is closely correlated with surface runoff and, hence, is primarily undertaken for reservoir management and hydroelectric power station operations. Main attention has to

be given to mountain ranges such as the Alps, the Scandinavian mountains, the Pyrenees, etc., with their rugged topography, in and around which most of the hydroelectric power plants are located. For example: in Switzerland, 77.5%[1] of the total electric energy is produced by hydroelectric power plants, while in Norway, practically all electric energy is produced by hydroelectric power stations[2].

It is the purpose of this paper to briefly review problems of digital snowmapping under the above mentioned specific European conditions and demands, using the Swiss Alps as the example, and to demonstrate the methods developed at the Department of Geography, University of Zurich, in collaboration with the Department of Photography, Swiss Federal Institute of Technology, Zurich. In addition, critical aspects and unsolved problems still under investigation shall be mentioned to meet the objectives of a truly operational snowmonitoring system.

## EUROPEAN REQUIREMENTS

The critical problem areas in applying satellite data to water resources application in the European high mountain ranges are:

- The need for guaranteed repetition coverage in a specific time sequence:
  In the long run, this problem can only be solved definitely by introducing an all-weather data acquisition system. At present the problem has to be tackled by extensive studies on the cloud coverage and in particular by developing methods to classify partly clouded Landsat scenes. Having gained a long-term knowledge on the position and the changes of the transient snowline of the study area, it should be possible to extrapolate the course of the snowline where it is cloudcovered from the situation in the cloudfree parts.

- The continuous and rapid transfer of the data to the user in almost real time:
  This problem was solved in principle for Europe with the establishment of the EARTHNET data acquisition and distribution system by the European Space Agency (ESA).

- The increase in the repetition rate up to a 6- to 9-day cycle:
  This could be achieved, disregarding the cloud problem, by either receiving Landsat-2 and -3 simultaneously (which has not been undertaken regularly at present over Europe) or by combining Landsat with very high resolution weather satellite data.

- The variability of the mountain terrain and the smallness of the individual catchment areas in relation to the high demands of accuracy standards:
  Very accurate classification methods are required which are applicable under all different modifications of sun position, sun angle, illumination, slope angle, exposure, shadow effects, terrain cover, etc., as well as very precise measurement techniques.

(1) Valid for the hydrologic year 1977/1978, as reported in NZZ, No. 275, November 25, 1978.
(2) Odegaard and Ostrem, 1977, p. 5.

- The incorporation of automatic change detection methods:
  To directly compare multitemporal data-sets, geometric as well as radiometric corrections are needed. Weather conditions in the Alps vary greatly even within the same Landsat scene. Therefore a standardization of the data prior to a classification is of upmost importance(1).

- The combination with data received from other data acquisition systems:
  Data from various acquisition sources should be united in such a way that they become directly comparable; e.g., by geocoding the various data and by its organization in geographic information systems, spatially-oriented processing can be performed or the data can be used as input into environmental models (e.g., runoff models). This enables not only the combined utilization of a variety of information from different origin, but also the fast retrieval of the needed information for specific applications.

In conclusion, future operational snowcover measurement techniques will have to incorporate the following facilities (ESA, 1977, p. 15):

- automatic change detection
- correlation with terrain models
- optimum combination of meteorological and earth resources satellite data
- input of satellite data into environmental models (e.g., runoff model).

## STUDY AREA

The representative basin, the Dischma Valley, as used and surveyed for years by the Swiss Federal Institute for Snow and Avalanche Research, Weissfluhjoch/Davos, was chosen as the main study area. The Dischma Valley lies in the central part of Grisons and extends from Davos toward the southeast. The part above the water gage at 1668 m MSL (Figure 1) covers an area of 43.7 $km^2$. The highest surrounding peaks reach altitudes of more than 3000 m MSL.

In a further step, the study area was extended to the upper drainage basin of the Landwasser in the region of Davos to get results from a larger watershed. It covers an area of approximately 290.5 $km^2$ with altitudes between 1,000 - 3,100 m MSL.

## METHODOLOGY

Methodological aspects of snowmapping from satellites are discussed by Rango and Itten (1976) and Haefner and Muri (1978). In an operational system there always has to be a tradeoff between accuracy and time. In snowmapping, priority irrevocably has to be given to time, since no delay in the transference of the vital information to the user can be accepted. On the other hand, the demands for high accuracy and for detailed statistical documentation have been established clearly in Europe and consequently have to be considered as well. In addition, emphasis has to be given to the processing of multitemporal data acquired under very different atmospheric and illumination conditions. All these aspects have to be taken into account, setting up a compatible automated classification system in accordance to the available equipment and the financial funds.

(1) Research in this direction was undertaken by Staenz (1976/78) etc.

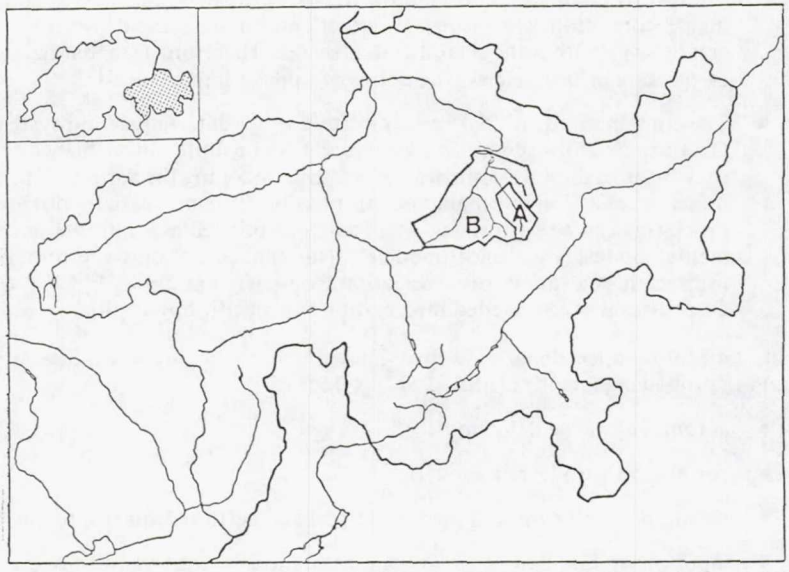


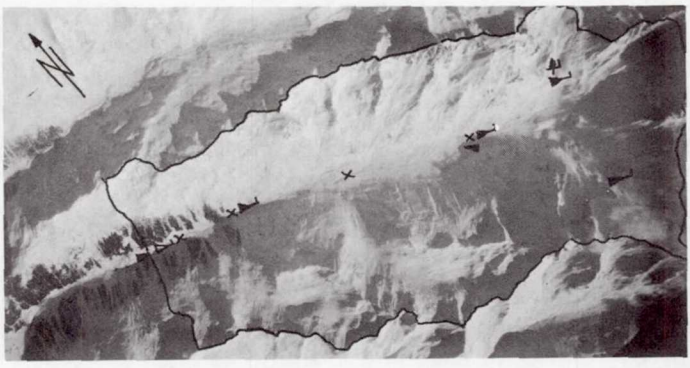


Dischma Valley: airphoto approx. 1:140,000 of Febr. 20, 1976

representative basin

precipitation gage

totalizer

stream flow gage

automated meteorological station

snow marker

Figure 1. Test sites Dischma Valley (A) and Landwasser (B), Davos – Grisons – Switzerland

Finally, the data processing has to be accompanied by various supporting activities, such as:

- ground observations and measurements
- studies of the spectral characteristics of snow
- aerial underflights, etc.

These supporting activities are indispensible for a better understanding of the study area and of the study object - snow - in its diurnal and seasonal variations, for an optimal selection of the training samples (in a supervised classification system) and for a verification of the results.

## DIGITAL DATA PROCESSING

### Approach

To meet the criteria as set up in the previous chapters, as well as the requirements for an input into a runoff model(1), the following concept was realized:

- supervised classification technique based on a very careful selection of the training samples
- specific determination of the transition zone between the totally snow-covered and the snowfree area
- construction of a fifth "artificial" Landsat channel containing the digital terrain model
- presentation of the results in maplike and tabular form.

### Preprocessing

Several preprocessing steps are undertaken including:

- reformating of the data in such a way that they are best organized for the available hardware and software
- radiometric corrections of the sixth line effect (scanline standardization)
- presentation of the digital data in geometric corrected images with the OPTRONICS-Photomation P-1700.

### Data Classification

An interactive image interpretation system, IBIS (Interaktives Bild-Interpretations-System), was developed to satisfy the specific needs as discussed (Fasler, 1978). The system (Figure 2) is structured in modular form, which enables an easy addition of new components or the use of a subset only. It consists of three parts:

(1) Runoff model developed by Martinec (1977) asking for a delineation of the watershed into different altitudinal zones.

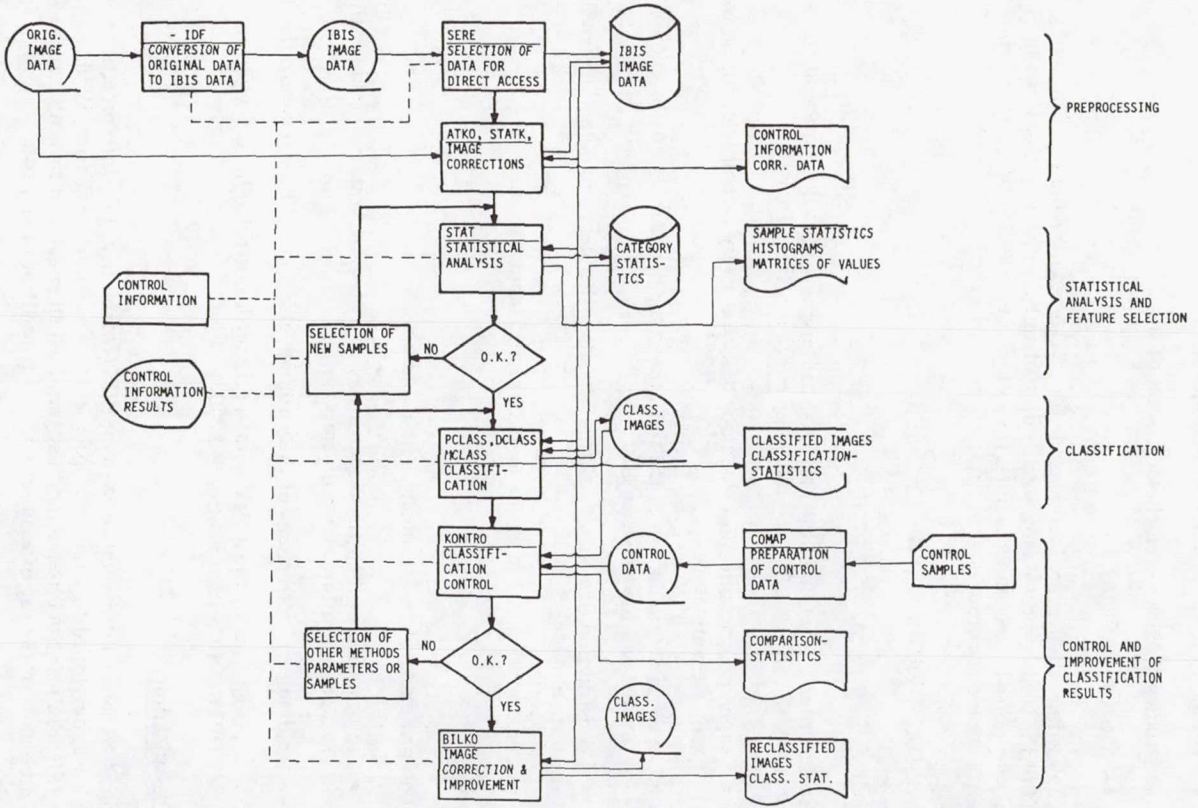


Figure 2. IBIS – Interactive Image Interpretation System (after Fasler, 1978)

- preprocessing as discussed in the previous chapter
- statistical analysis of the training samples (or groups of samples)
- classification based on the results of the previous steps with different algorithms such as:
  - parallel epiped mode (PPD)
  - maximum likelihood
  - euclidean distance (D-class).

In a supervised classification system the most critical item on which the quality of the results depends entirely is the selection and definition of the training samples. Therefore, specific care has to be given to this problem. To allow a precise measurement of the snowcover, three final categories are defined:

- totally snowcovered area
- transition zone
- totally snowfree area.

To achieve a clear separation, these three categories have to be subdivided into various sub-categories as shown in Figure 3. A first selection of the sub-categories is undertaken with reference to the well-known surface features. They are exactly located by using topographic and thematic maps and rechecking in the field.

The exact location of the training samples within the data-set is done by using geometric corrected satellite images enlarged with the Photomation system to such an extent that each individual pixel is recognizable. At the same time, the image is overlayed with a grid (20 x 20 pixels) to facilitate the location of the image coordinates. All training samples are tested regarding their statistical characteristics (Figure 4). If necessary, corrections such as shifts in the extension or position of the training samples, etc., are made to reach a final selection.

Several tests showed that a definite classification can be undertaken by using band 5 and 7 (Gfeller, 1975; Stirnemann, 1976). This remains valid as long as no bright objects such as concrete, white rocks, etc., or snow under dense needleleaf forest[1] are found in the test area and no classification of the snowcover into different snowtypes is desired. To test the separability of the selected training samples, they are represented in graphical form (program ELLPLT for HP 9830). Ellipses are drawn around the center of the meridian of each sample with the half-axis proportional to the standard deviation (Figure 5). This presentation illustrates the orientation of the training samples in a two-dimensional feature space and allows the determination of the boundaries for the PPD-classification. Figure 5b shows that if a larger part of the snowcover lays in shadow, the accuracy of the classification will be affected considerably.

The PPD-algorithm – by far the simplest and most economical one – offers good possibilities as long as not too many different variables (spectral bands) and not too many

(1) Itten (1977) used bands 4, 5, and 7 to overcome this problem.

| No. | sub-category | category | portion of snowcoverage |
|---|---|---|---|
| 1 | snow, dry, in sun | totally snowcovered area | |
| 2 | snow, metamorphic, in sun | | |
| 3 | snow, in shadow | | |
| 4 | snow, intermixed with few rocks, in sun | | 100 % |
| 5 | snow, intermixed with some snowfree spots | | |
| 6 | snow, half intermixed with rocks | transition zone | |
| 7 | snow, intermixed with snowfree spots ( 50 %) | | 50 % |
| 8 | snow, intermixed with snowfree spots ( 50 %) | | |
| 9 | dense needleleaf forest, snow-free, in sun | totally snowfree area | |
| 10 | open needleleaf forest and shrubs, snowfree, in sun | | |
| 11 | shrubs with some trees, snowfree, in sun | | 0 % |
| 12 | alpine zone, snowfree, in sun | | |
| 13 | alpine pastures with shrubs, snowfree, in sun | | |
| 14 | meadows, snowfree, in sun | | |
| 15 | settlements, snowfree, in sun | | |
| 16 | open water, in sun | | |

Figure 3. Training samples for snow classification

June 8th, 1976

| Sub-categ. | channel 4 $\bar{x}$ | channel 4 $\sigma$ | channel 5 $\bar{x}$ | channel 5 $\sigma$ | channel 6 $\bar{x}$ | channel 6 $\sigma$ | channel 7 $\bar{x}$ | channel 7 $\sigma$ |
|---|---|---|---|---|---|---|---|---|
| 1 | 127.00 | 0.00 | 127.00 | 0.00 | 127.00 | 0.00 | 62.90 | 1.93 |
| 2 | 126,27 | 2.05 | 127.00 | 0.00 | 127.00 | 0.00 | 45.75 | 3.97 |
| 4 | 118.10 | 17.44 | 122.31 | 11.88 | 121.17 | 13.74 | 44.19 | 7.39 |
| 5 | 118.78 | 11.40 | 125.61 | 4.37 | 125.19 | 4.18 | 45.94 | 5.64 |
| 6 | 70.67 | 19.25 | 81.11 | 23.02 | 74.86 | 21.50 | 23.54 | 6.98 |
| 7 | 68.83 | 16.60 | 84.38 | 20.17 | 83.69 | 17.48 | 28.75 | 4.58 |
| 8 | 52.04 | 11.75 | 62.96 | 14.33 | 68.83 | 11.70 | 26.27 | 3.87 |
| 9 | 13.30 | 1.51 | 12.28 | 2.09 | 24.32 | 5.19 | 11.20 | 2.83 |
| 10 | 20.65 | 3.34 | 23.07 | 5.18 | 50.45 | 9.53 | 28.84 | 5.73 |
| 11 | 16.64 | 1.59 | 16.62 | 2.53 | 38.11 | 6.33 | 19.04 | 4.17 |
| 12 | 32.70 | 3.31 | 41.61 | 4.60 | 68.29 | 6.07 | 33.80 | 3.74 |
| 13 | 22.55 | 2.66 | 25.74 | 3.94 | 51.99 | 10.55 | 26.50 | 6.71 |
| 14 | 20.70 | 2.19 | 19.77 | 2.83 | 79.30 | 14.93 | 44.49 | 9.45 |
| 15 | 27.98 | 3.34 | 31.33 | 4.83 | 53.44 | 8.11 | 24.56 | 5.76 |
| 16 | 17.21 | 0.83 | 10.04 | 0.46 | 5.79 | 1.10 | 0.00 | 0.00 |

August 7th, 1976

| Sub-categ. | channel 4 $\bar{x}$ | channel 4 $\sigma$ | channel 5 $\bar{x}$ | channel 5 $\sigma$ | channel 6 $\bar{x}$ | channel 6 $\sigma$ | channel 7 $\bar{x}$ | channel 7 $\sigma$ |
|---|---|---|---|---|---|---|---|---|
| 1 | 127.00 | 0.00 | 127.00 | 0.00 | 127.00 | 0.00 | 60.38 | 1.93 |
| 2 | 112.14 | 11.17 | 124.89 | 5.47 | 123.16 | 7.93 | 40.65 | 4.62 |
| 3 | 14.80 | 2.31 | 13.03 | 2.70 | 11.97 | 3.05 | 2.93 | 1.34 |
| 4 | 106.90 | 10.37 | 124.05 | 5.62 | 123.15 | 6.96 | 46.40 | 4.03 |
| 6 | 73.60 | 12.65 | 88.63 | 17.05 | 83.07 | 16.42 | 25.87 | 5.49 |
| 8 | 50.09 | 18.41 | 61.08 | 23.15 | 73.30 | 18.39 | 30.15 | 7.05 |
| 9 | 11.04 | 1.51 | 9.45 | 1.92 | 20.23 | 5.29 | 9.31 | 3.04 |
| 10 | 16.23 | 3.95 | 15.75 | 5.17 | 41.67 | 7.32 | 21.37 | 3.99 |
| 11 | 11.76 | 0.80 | 10.21 | 0.87 | 26.38 | 2.32 | 13.01 | 1.40 |
| 13 | 18.60 | 3.32 | 20.34 | 4.47 | 50.90 | 5.51 | 26.54 | 3.86 |
| 14 | 19.34 | 1.77 | 18.43 | 1.72 | 81.00 | 6.94 | 46.46 | 4.48 |
| 15 | 24.53 | 2.90 | 27.22 | 3.93 | 47.49 | 6.45 | 21.99 | 4.45 |
| 16 | 16.93 | 0.92 | 9.43 | 0.67 | 6.71 | 1.35 | 0.62 | 0.80 |

Figure 4. Statistics (mean value and standard deviation) for sub-categories (Numbers as in Figure 3) (after Urfer, 1978)

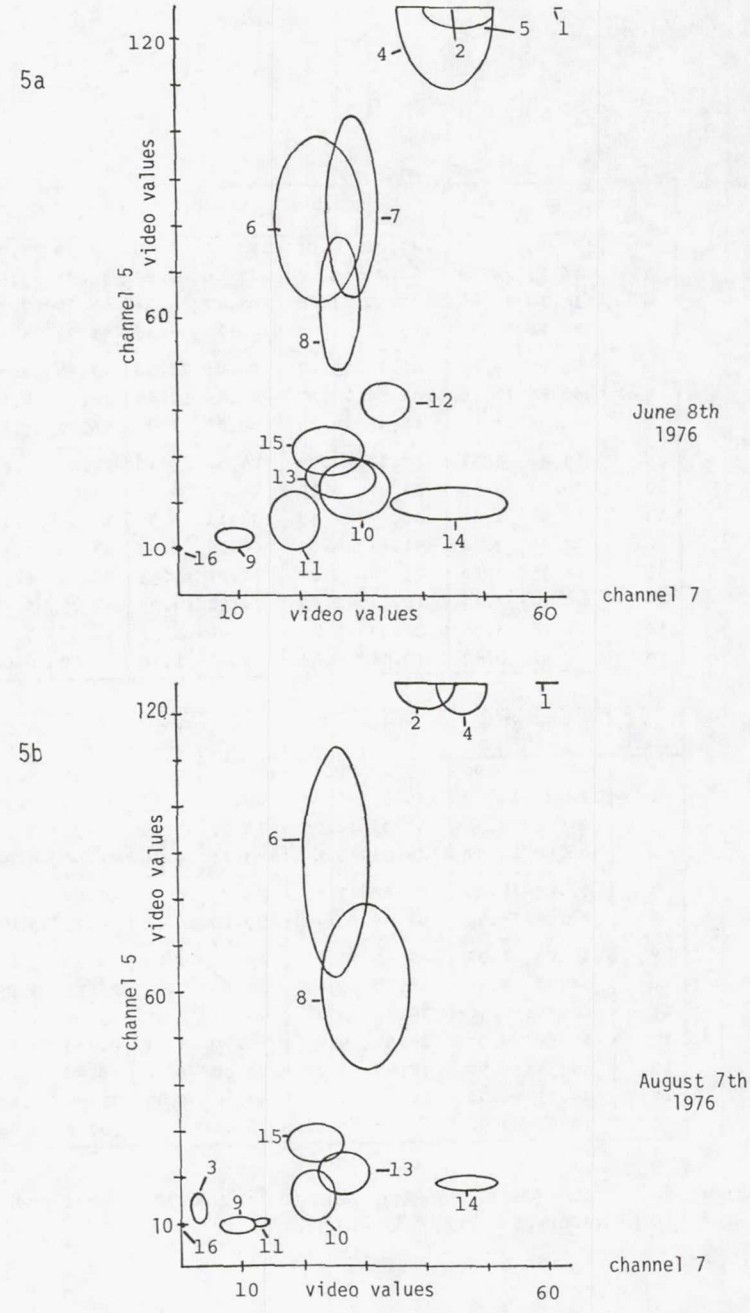


Figure 5. Graphical presentation of sub-categories (as in Figure 3) in two-dimensional feature space: Ellipses represent one standard deviation from mean values (after Urfer, 1978)

different sub-categories are used. The determination of the boundaries becomes very difficult if more than three variables and more than ten sub-categories are included. Under these circumstances, other algorithms than PPD should be used.

The snow-classification for the Dischma Valley test site is demonstrated in Figure 6 for June 8 and August 7, 1976, and for the Landwasser test site in Figure 7 for June 8, 1976.

Altitude Zone Channel

The basic idea was to create a fifth artificial Landsat channel, which adds to each pixel the information on the altitude zone to which it belongs(1) (to be called "altitude zone Landsat channel").

In a first step, the boundaries of the drainage basin as well as of the selected contour lines dividing the altitude zones (Figure 8) have to be delineated. This information is retrieved from a topo-map (1:50,000). To perfectly match the satellite image with the map, geometric corrections are necessary. Specific software was developed adaptable to the available equipment (OPTRONICS Photomation P-1700)(2). Afterwards, the corrected image is enlarged to the map-scale.

To precisely superimpose the satellite image onto the map, striking terrain points such as corners of woods, river outlets or junctions, mountain peaks, etc. are used, which are easy to identify on both presentations and which can be marked by map as well as satellite coordinates(3).

In a second step, the drainage basin is delineated and the terrain digitized by transferring the boundaries of the basin and of the altitude zones from the map onto the maplike satellite image (scale 1:50,000) and by orienting the scanline along the main axis of the digitizer plate. First, two reference points are registered with their satellite coordinates. Then the boundaries are digitized in form of satellite coordinates and stored in the HP-9800 computer.

It certainly would be possible to gain the digitized information directly from the map and to use the satellite image only for the determination of the reference points and the orientation of the digitizer. But to achieve maximum accuracy, the described technique is more feasible.

(1) Instead of altitude, other subdivisions of the study area, into natural or administrative units, etc., would be possible.

(2) We are aware that much more sophisticated equipment and techniques exist to fulfill this purpose, e.g., developed for the IMAGE-100 (Dallam, 1975). Similar developments are underway at Zurich, based on the interactive PDP-11/RAMTEK interactive image-analysis system.

(3) Satellite coordinates mean the position of a pixel in a Landsat scene expressed by line and column numbers.

June 8, 1976

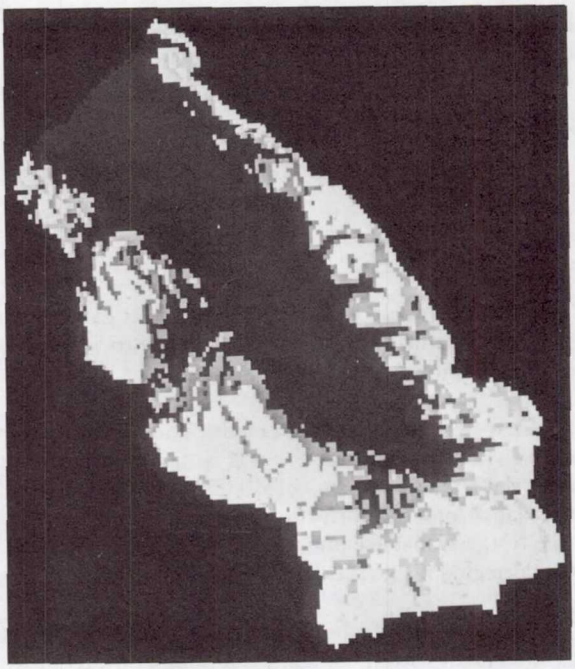

August 7, 1976

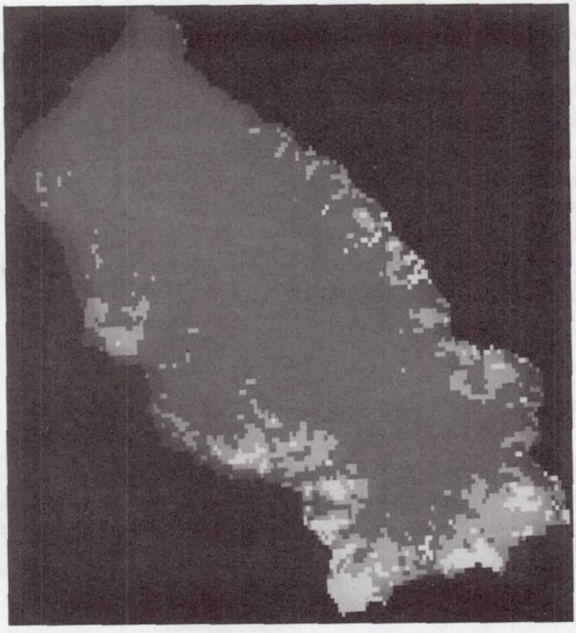

white = totally snowcovered

gray = transition zone

black = totally snowfree

Figure 6. Snow classification of Dischma Valley test site (after Urfer, 1978)

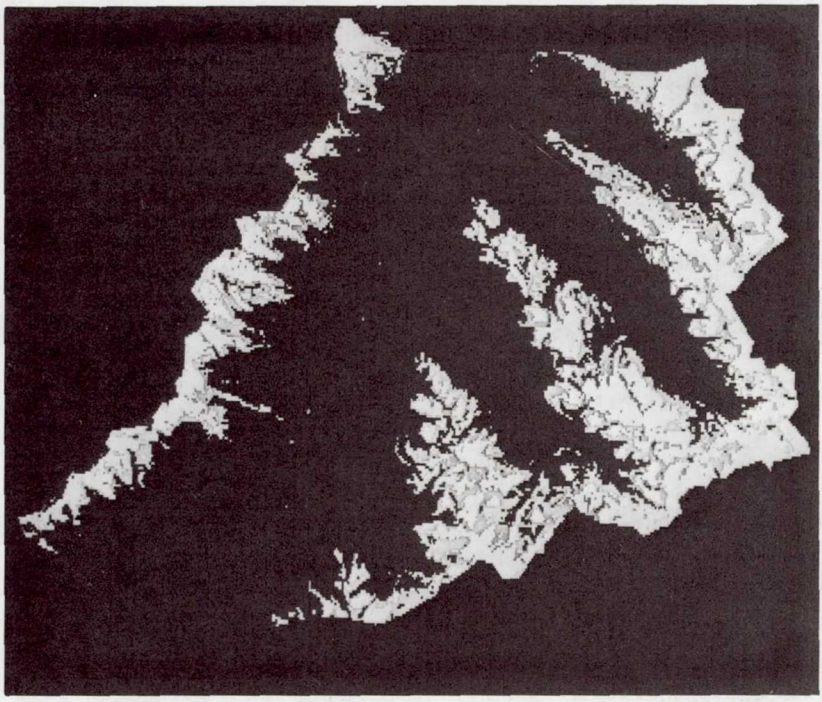

Figure 7. Snow classification of Landwasser test site, June 8, 1976 (after Urfer, 1978)

In a third step, the polygonal boundaries as registered are transferred from satellite coordinates into a grid system. The area within a polygon receives a binary figure and by its combining, the specific code for each altitude zone is established as follows:

- the highest zone above 2,600 m: 0 0 1
- the medium zone between 2,600 – 2,100 m: 0 1 1
- the lowest zone below 2,100 m: 1 1 1
- all parts not included in the test site: 0 0 0

In a last step, this information has to be added pixelwise to the video data of the four Landsat channels. Now, each pixel is attached to a specific altitude zone. All other pixels, which do not belong to one of these zones, are not taken into account in the classification or the output.

This method allows a very precise delineation and subdivision of test sites of any shape at will and an individual calculation of the extent of the snowcover for each areal unit. With the Photomation system, the altitude zones are presented in different graytones, as shown in Figure 9 for the Dischma Valley and in Figure 10 for the Landwasser test site. Comparisons were made between different Landsat scenes and

| | DISCHMA | | | LANDWASSER | | |
|---|---|---|---|---|---|---|
| | Pixels | % | $km^2$ | Pixels | % | $km^2$ |
| 1. high zone 2,600 m MSL | 2,176 | 22.5 | 9.82 | 6,605 | 10.3 | 29.81 |
| 2. medium zone 2100-2600 m MSL | 5,467 | 56.5 | 24.68 | 29,338 | 45.6 | 132.43 |
| 3. low zone 2,100 m MSL | 2,038 | 21.0 | 9.20 | 28,409 | 44.1 | 128.24 |
| Total test site | 9,681 | 100.0 | 43.70 (16.87 $mi^2$) | 64,352 | 100.0 | 290.48 (112.18 $mi^2$) |

Figure 8. Altitude zones of Dischma Valley and Landwasser test sites

with measurements from orthophotos. They produced an accordance in the size of the altitude zones of 0.1% between three Landsat scenes and of 0.5% with the orthophoto measurements.

Results

The areal measurements of the snowcover for June 8 and August 7, 1976, are summarized in Figure 11. Comparisons with a visual interpretation of orthophotos (1:50,000) and areal measurement with a Quantimet showed a very good accordance in the lower and medium altitude zone. The maximum difference in the portion of the snowcovered area was 1.8%. For the highest zone, the results differed up to 13.5%; but a careful evaluation lead to the conclusion that the Landsat measurements are more reliable.

The Landsat-altitude-channel as described has just to be produced once and can be used again for each new scene. The test area in the new image is shifted and rotated until it matches the one in the original image. The same reference points are utilized. The difference between the satellite coordinates of the new scene and the coordinates of the original image gives the shifting and rotating vectors. The more reference points used, the more accurate the calculation becomes.

An additional advantage means that part of the training samples (e.g., open water, settlements, snowfree forests, shrubs, pastures, etc.) can be used again directly. Their satellite coordinates are already registered. Other samples have to be newly established every time, especially the ones for the transition zone between the snowfree and snowcovered areas.

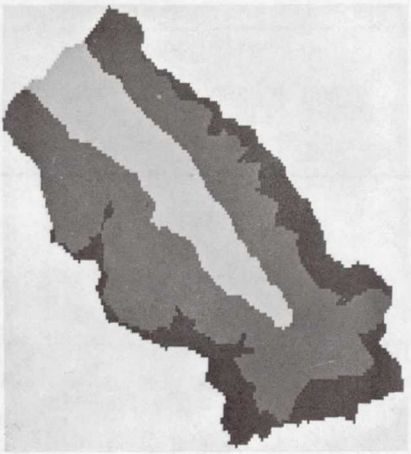

Figure 9

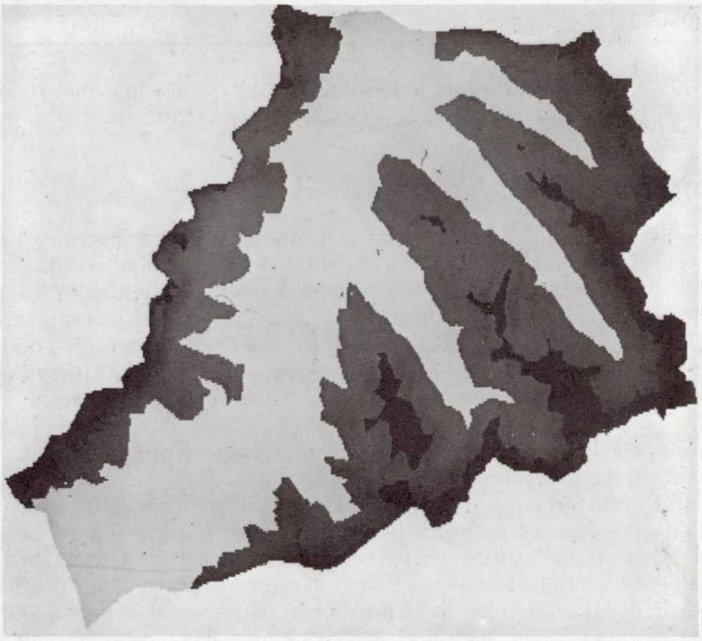

Figure 10

Figures 9 and 10. Altitude zone channel of Dischma Valley and Landwasser test sites (after Urfer, 1978)

| | Altitude zone | | | Test site |
|---|---|---|---|---|
| | > 2,600 | 2600-2100 | <2,100 | total |
| | % | % | % | % |
| DISCHMA June 8, 1976 | | | | |
| Landsat | 80.2 | 44.1 | 0.2 | 43.3 |
| Orthophoto | 72.9 | 42.3 | 0.0 | - |
| DISCHMA August 7, 1976 | | | | |
| Landsat | 36.0 | 5.4 | 0.0 | 11.1 |
| Orthophoto | 22.5 | 5.4 | 0.3 | - |
| LANDWASSER June 8, 1976 | | | | |
| Landsat | 78.4 | 37.9 | 0.0 | 25.3 |
| Orthophoto | - | - | - | - |

Figure 11. Extent of snowcover in the three altitude zones and comparison with measurements on orthophotographs (after Urfer, 1978)

Time Expenditure

Since time has been designed as the most critical factor, some considerations shall be added on the time requirements for the different parts of the digital data processing system. As a reference basis, the larger test site, Landwasser (Figure 1), of approximately 300 $km^2$, is taken and assumed that an experienced interpreter is carrying out the classification. The average time expenditures for the different operations are listed in Figure 12. In principle, they reveal that the method may satisfy the time requirement for a fast classification as well as the demand for high accuracy.

But it has to be pointed out clearly that quite a few aspects are not considered, which may slow down the procedure. First, the transference of the data from the ground station to the user (formating of the CCT's) is not taken into account. Secondly, the average time of 14 hours can be greatly shortened on one side and extended on the other. In an operational system where the altitude channel and part of the training samples do not have to be newly established, the time requirements could be reduced to about half. Contrarily, it has to be mentioned that immediate access to the computer is not always granted and longer waiting periods may have to be included. So, the figures as stated in Figure 12 cover just the time of active work for the interpretation.

| Operation | approximate time expenditure in hours |
|---|---|
| A preprocessing | 1 |
| B preparation of altitude zone channel | 5 |
| C combination of four Landsat-channels with altitude zone channel | 1/4 |
| D selection and location of training samples | 3 |
| E statistics, corrections, etc. | 2 |
| F classification and presentation in a geometric corrected image | 3 |
| t o t a l | 14 1/4 |

Figure 12. Time expenditure for the different operations of the snow classification system for the Landwasser test site (approximately 300 $km^2$) (after Urfer, 1978)

## CONCLUSIONS AND OUTLOOK

Today, the space segment for an automated monitoring of the snowcover in Europe can be regarded as operational. The severest restrictions originate from the cloud problem. Therefore, a classification of partly clouded Landsat scenes has to be reached, which asks for a perfect separation of snow and clouds under all different modifications by illumination, atmospheric effects, and terrain characteristics. To achieve this objective, a channel in the 1.55 – 1.75 $\mu$m region is essential. In addition, the repetition cycle has to be shortened during the critical days of the melting period to about 6 days.

Regarding the ground segment, a rapid production of the CCT's and their transference to the user still should be improved. The methodology for an operational classification of the data has to be developed and rationalized further toward:

- automatic change detection
- faster and more economical procedures
- combining the results with other information (e.g., input into a geographic information system)

- separating not only the snow from the background but subdividing the snowcover itself (e.g., wet/dry snow; freezing/thawing line; thick/thin cover, etc.

In doing so, the high accuracy standards as needed in Europe have to be preserved. This becomes especially important when classifying larger watersheds than investigated at present.

ACKNOWLEDGEMENT

For our snowmapping program from satellite data, NASA granted us a project for Landsat-1 and Landsat-2 as well as for Skylab-EREP. The research work was funded by the Swiss National Science Foundation. I wish to thank both institutions for their support.

Quite a few colleagues, research assistants, and graduate students participated in the program and contributed to its success. I am most grateful to all of them for their highly valuable assistance, enormous efforts, and encouragements; without them, this paper would not have been possible. In particular, I should like to mention Prof. Dr. W. F. Berg (Department of Photography, Swiss Federal Institute of Technology), Dr. K. Seidel (Department of Photography, Swiss Federal Institute of Technology), and Dr. K. I. Itten (Department of Geography, University of Zurich). Special thanks are extended to Mrs. E. Kupka and Mr. R. Muri for their help in preparing the paper.

REFERENCES

ESA: European Remote Sensing Space Programme. Mission Objectives and Measurement Requirements. ESA/EXEC(77)3, Paris, April 1977.

ESA: Interim Remote Sensing Programme Board – European Remote Sensing Programme. ESA/C(78)102, Paris, September 1978.

Fasler, F.: IBIS – an Interactive Image Interpretation System. Proc. ISP-IUFRO Int. Symp. on Remote Sensing, Freiburg i.Br., FRG, July 1978 (to be published).

Haefner, H.: Snow Mapping and Land Use Studies in Switzerland. Landsat-2 Final Report to NASA, Zurich 1977.

Haefner, H.: Snow Cover Monitoring from Satellite Data under European Conditions. Proc. ISPRA-Course, JRC, Italy 1978 (to be published).

Haefner, H., and R. Muri: Methodology of Snowmapping. Proc. ISP-IUFRO Int. Symp. on Remote Sensing, Freiburg i.Br., FRG, July 1978 (to be published).

Itten, K. I.: Approaches to Digital Snow Mapping with Landsat-1 Data. Proc. NASA Workshop on Operational Applications of Satellite Snowcover Observations, South Lake Tahoe, Calif., Washington, D.C., 1975.

Martinec, J.: Hydrologic Basin Models. Proc. ISPRA-Course, JRC, Italy 1978 (to be published).

Ødegaard, H. A. and G. Østrem: Application of Satellite Data for Snow Mapping. Norges Vassdrags - og Elektrisitetsvesen, Rapport 9-77, Oslo, 1977.

Rango, A., and K. I. Itten: Satellite Potentials in Snowcover Monitoring and Runoff Prediction. Nordic Hydrology, 7, 1976;

Seidel, K.: Digitale Bildverarbeitung. Technical Report, Swiss Federal Institute of Technology, Zurich, 1976.

Staenz, K.: Radiometrische Untersuchungen über das Reflexionsverhalten von Schnee. M.S.-Thesis, Department of Geography, University of Zurich, 1976 (unpublished).

Staenz, K.: Atmosphärische Korrekturen von Multispektraldaten des Erderkundungs-satelliten Landsat-2. Ph.D.-Thesis, University of Zurich, 1978.

Stirnemann, H.-P.: Schneedecke und Schneegrenzzone in Satelliten-aufnahmen. M.S.-Thesis, Department of Geography, University of Zurich, 1977 (unpublished).

Urfer, H.-P.: Routinemässige Schneekartierung in hydrologischen Einzugsgebieten mit Landsat-Daten. M.S.-Thesis, Department of Geography, University of Zurich, 1978 (unpublished).

**Page intentionally left blank**

# APPLICATION OF SATELLITE DATA FOR SNOW MAPPING IN NORWAY

H. A. Ødegaard[1], IBM, Oslo, Norway

T. Andersen and G. Ostrem, Norwegian Water Resources and Electricity Board, Oslo, Norway

## ABSTRACT

The total volume of meltwater runoff from a given mountain watershed in the spring is related to the extent of snowcover. Data acquired from space are valuable if they are received by the user within a few days and if an operational use of the data is possible.

A diagram showing the relation between subsequent meltwater runoff and remaining snowcover has been established for several given catchment areas. It seems that the same curve can be used also for other high-mountain drainage basins. A curve of this type can be used directly for runoff forecasts as soon as snowmelt has started.

A method for use of digital NOAA/TIROS imagery for snow mapping is described.

## INTRODUCTION

The Norwegian Water Resources and Electricity Board (NVE) annually produces 23,000 GWh or 30 percent of the electric energy in Norway and operates 45 hydroelectric power plants in the country. The rest of the electric power is produced in hydroelectric power plants owned by communities or private companies. No electricity is produced by thermal or nuclear methods. Therefore, snow surveys in high-mountain catchment areas are of vital concern to the management of power plants in Norway (Figure 1).

The winter production of power and the resulting draw-down of the reservoirs start in November. Ordinarily, snow surveys are made in the first week of February and the first week of April, before snowmelt starts. When the result of the first snow survey is available in the beginning of February, the first corrections in the production plans are made. Decisions are then made on how to distribute the total load between various power plants located in different parts of the country, relative to the size of their snow reservoir and ability to store the water during the following summer.

[1] H. A. Ødegaard was employed as senior hydrologist with the Norwegian Water Resources and Electricity Board (NVE) until October 1977, when he joined IBM.

Figure 1. Location Map

This means that a power plant with a large amount of snow in February will run on high load to make room in the reservoir for the expected large water volume. The plants with little snow will aim at a lower production in February through July. This "direction of production" takes place in a free market with buyers and sellers and is made possible by a well-developed network of transmission lines.

When the results of the April snow survey are available, new production plans are prepared and the load on the different power plants is reconsidered. From the start of snowmelt (about May 5) until it ends (about August 1), very little information is available on snow conditions. Some years a large amount of water may disappear due to evaporation or the filling up of the groundwater reservoir; other years the snow melts rapidly and only small losses are encountered. In this period, precipitation is recorded and the data are used to adjust the production plan. However, the main problem is the fact that very little information is available on snow conditions within the snow-covered areas for 3 months.

Implementation of thermal or nuclear energy into the present pure hydroelectric production system will increase electric energy prices and necessitate improvement of the daily management of the entire system. Accurate snow measurements will play an important role and contribute to increasing the overall efficiency of the power plants.

## SNOWMELT - SNOW LINE

The winter snow covers the landscape almost down to sea level in most of the country. A snow line (border between covered and uncovered ground) does not exist in the catchment areas during the winter. Therefore, the area of snow cover cannot be estimated from imagery before the snowmelt has started and the snow line is well above the lowest point in the catchment basin. A "strand zone" then develops parallel to the shoreline of the reservoir.

The catchment area for all the major power plants is a rolling mountain terrain without or with a sparse forest cover.

## RATE OF RUNOFF

After runoff has started, the snowcover remains close to 100 percent for some time. The volume of meltwater from the area during this first period varies according to the temperature pattern. The snowcover gradually decreases until the end of the snowmelt season. The daily amount of meltwater from the basin, or the basin snowmelt rate, starts declining before the summer temperature reaches its maximum value. The characteristic form of the snowcover depletion curve will be related to the hypsographic curve of the basin.

It was shown by Leaf (1967) that

$$A = \frac{100}{1 + e^{-bt}}$$

where

A = percentage of area without snow
t = time (days) measured from an arbitrary origin
b = a coefficient
e = the base of natural logarithms

For the Røssåga area, one of the largest basins in North Norway (Figure 2), the following expression (Figure 3) was found best to describe the observations:

$$S = \frac{200}{1 + e^{0.055t}}$$

S = percentage of snow cover

This expression will give the snowcover in percent for a given area t days after the reduction of the snow-covered area started, and may be used to estimate subsequent runoff.

## RESULTS

Landsat data (Figures 4 and 5b) have been analyzed for a number of catchment areas. Aircraft data (Figure 5a) are used to provide detailed ground information of the area. The measured area of snowcover and the registered and corrected subsequent runoff were plotted separately for each test area. It was soon found, however, that data for different areas could be plotted advantageously on the same graph. A curve could be fitted through these points with relatively small deviations. The basins in the south had nearly the same runoff characteristics as those in the north, although the climate is entirely different.

Figure 2 Oblique photograph showing part of Lake Røssvatn for the power plant Røssåga in North Norway. This picture is typical of most mountain drainage basins in Norway. More snow remains at higher elevations, where the snowcover is almost continuous. There is obviously no clearcut snowline.

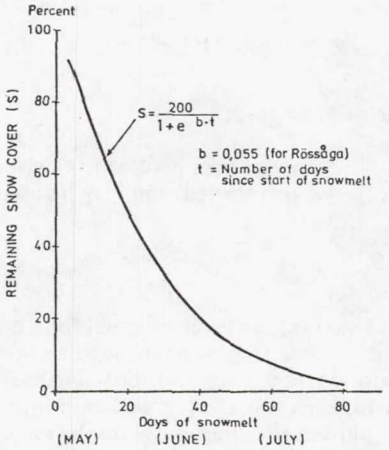


Figure 3 The diagram shows the typical decrease in snowcover, given in percent of the total catchment area, for the Røssåga drainage basin in northern Norway. The snow starts to melt in May. The snow-covered area decreases rapidly during late May and early June. In July there is a slower decrease in snow-covered area, possibly due to heavy snow accumulation in snow banks or patches of heavy snow caused by wind drift during the winter. There is almost no snow left in the area at the beginning of August.

Figure 4 The Landsat image 2168-10032 MSS 5, obtained July 9, 1975, shows the mountain plateau Hardangervidda, which is the main water source for many hydroelectric power plants in this part of southern Norway. The elevation ranges between 800 and 1800 m a.s.l. In spite of the low sun elevation (49 degrees), very few shadows are found on the mountain plateau. Most shadows are in the deep fjords on the western side and in the steep valleys on the eastern side of the main catchment areas. Power stations are mainly located in these depressions in the landscape.

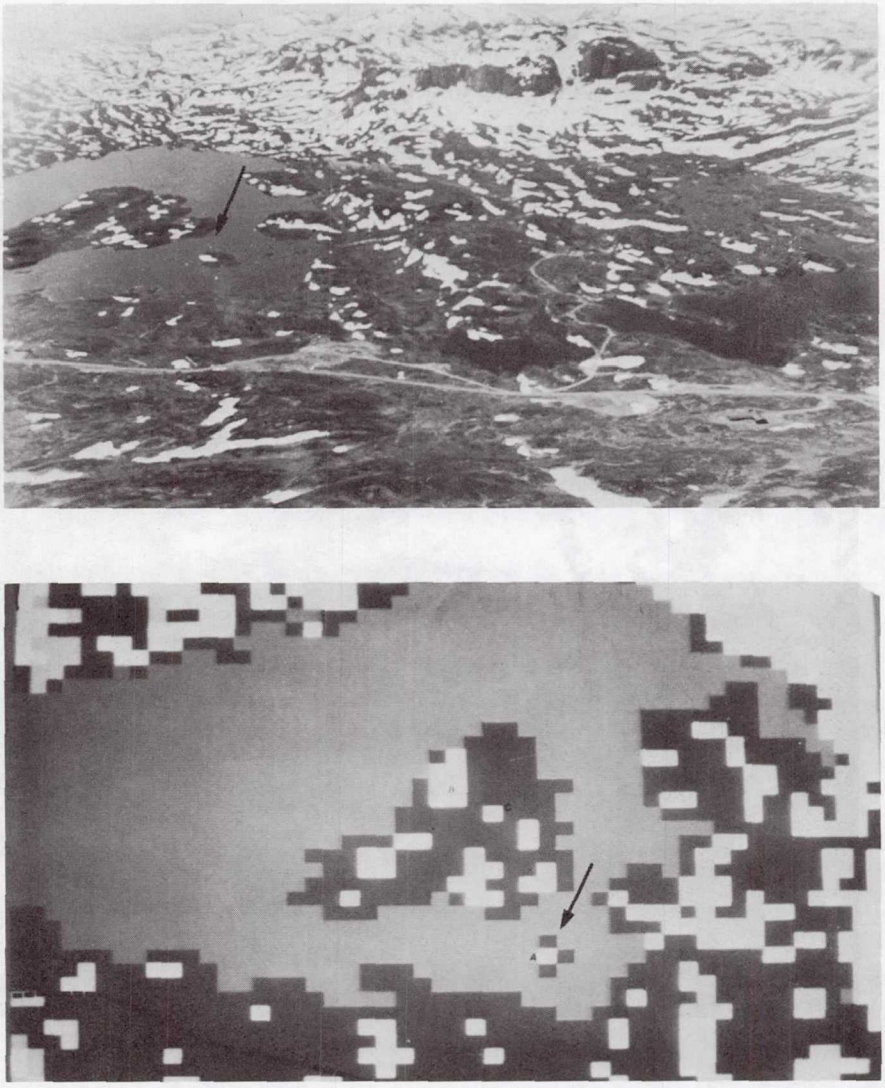

Figure 5 a. Oblique photograph from aircraft of the test area Kjela, taken on July 8, 1975. Typical landmarks are the highway and islands in the lake.

b. On the following day, July 9, the same area was imaged by Landsat for the purpose of determining the exact location of the snow limit. When the Landsat data is reproduced at full resolution (60 x 80 m), individual patches of snow on the two islands can almost be recognized (2168 - 10032).

The result of this work is shown in Figure 6, and the curve best fitted to the data can be expressed:

$Q = 128 (e^{0.0018 R} - 1)$

Q = subsequent runoff ($10^6 m^3$)

R = snow-covered area ($km^2$)

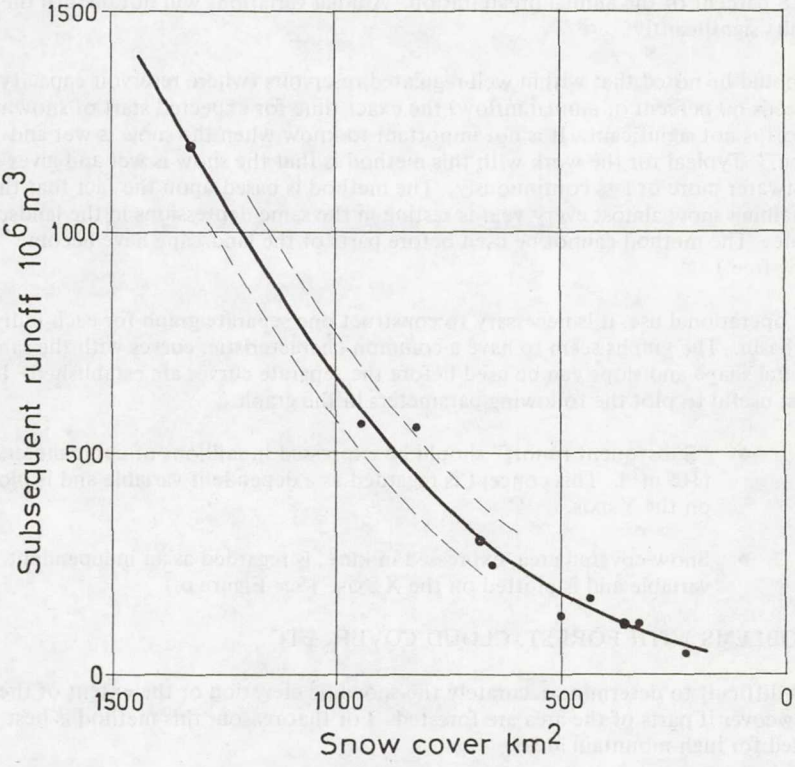


Figure 6 Experience has shown that it is possible to combine results obtained at various power plants in Norway in the same diagram. Subsequent runoff is plotted as a function of snowcover. Instead of calculating the percentage of snowcover in the catchment, it seems sufficient to determine the snow-covered area in square kilometers. The expected subsequent meltwater runoff can then be found directly from this generalized graph (heavy line) independent of the size of the total catchment area.

It is necessary to draw several more or less parallel lines in the same diagram – the upper of which would indicate the situation during years of exceptionally heavy snowcover. The lowermost would show the situation in years of very thin snowcover.

The subsequent runoff (Q) can then be determined when the snow-covered area (R) is known, for any area with the same characteristics as the test areas.

Experience has shown that if the extent of snowcover is determined from all four Landsat bands, there are significant differences in the results. MSS 4 gave the largest snowcover, but only slightly more than MSS 5. MSS 6 and MSS 7 gave the smallest snow areas. MSS 5 was selected as the best band for snow mapping.

All measured runoff values should be corrected so that they express the runoff with a "normal" precipitation included, as this will make future use of the graphs simpler and quicker. In June and July, the precipitation is normally low, on the order of 14 to 18 percent of the annual precipitation. Annual variations will not disturb the results significantly.

It should be noted that within well-regulated reservoirs (where reservoir capacity exceeds 60 percent of annual inflow) the exact time for expected start of snowmelt runoff is not significant. It is not important to know when the snow is wet and "ripe." Typical for the work with this method is that the snow is wet and gives off meltwater more or less continuously. The method is based upon the fact that the remaining snow almost every year is resting in the same depressions in the landscape. (Note: The method cannot be used before parts of the landscape have become snow-free.)

For operational use, it is necessary to construct one separate graph for each individual basin. The graphs seem to have a common characteristic; curves with the same general shape and slope can be used before the separate curves are established. It is most useful to plot the following parameters in the graph:

- "Subsequent runoff" should be expressed in millions of cubic meters ($10^6 m^3$). This concept is regarded as a dependent variable and is plotted on the Y-axis.

- Snow-covered area, expressed in $km^2$, is regarded as an independent variable and is plotted on the X-axis. (See Figure 6.)

## PROBLEMS WITH FOREST, CLOUD COVER, ETC.

It is difficult to determine accurately the snowline elevation or the extent of the snowcover if parts of the area are forested. For that reason, this method is best suited for high-mountain areas.

With little snow on the ground, it may be difficult to see the difference between old, deep snow and a thin layer of new snow. This may be clarified by the use of meteorological data. The sun angle may also disturb the interpretation due to special effects of shadows.

Clouds are another disturbing factor because they appear in the imagery with the same grey tones as the snowcover. Separation of clouds from snow and ice can be done visually due to cloud shadows and the special shape of clouds. An automatic differentiation does not exist today and will probably be difficult to develop with the sensors available.

A test was made to determine how much of the snowcover on the mountain plateau Hardangervidda in southwestern Norway was in shadow when the whole area was covered with snow. The image 2024-10034 obtained on February 15, 1975, had a sun elevation of 14 degrees. The area is relatively flat, and less than five percent of the area was then covered by shadows.

The snowmelt from this area starts approximately in the middle of May each year, and the use of satellite data will be most interesting in June and July, when the sun elevation has increased to 45 to 50 degrees. Thus, shadows are not considered a problem unless we approach areas of more broken topography which also exist in Norway.

## NOAA-VHRR/TIROS-AVHRR IMAGES

After preliminary work with Landsat imagery, attention was focused on NOAA-VHRR imagery. In the spring of 1978, a National Partnership Project (NPP) was initiated between the Norwegian National Committee for Hydrology (IHP) and IBM to develop methods for snow mapping using Landsat, NOAA, and TIROS digital data.

The work has been performed using the IBM/ERMAN-2 interactive system connected to an IBM 370/158 computer. The imagery can be fully manipulated and displayed on a color monitor. Final results are presented as tabular values and plotted maps.

The NOAA/TIROS images can be obtained almost every day, a fact which is most important for Scandinavia, where complete or partial cloud cover is common. When working digitally the pixel (picture element) size is satisfactory, except for small watersheds (Figure 7). It was found that the use of photographically enhanced NOAA imagery did not satisfy the requirements for snow mapping. If data are used digitally, it is not satisfactory to classify each 900 m x 900 m pixel as either snow-free or snow-covered because more information on snowcover for each pixel is available.

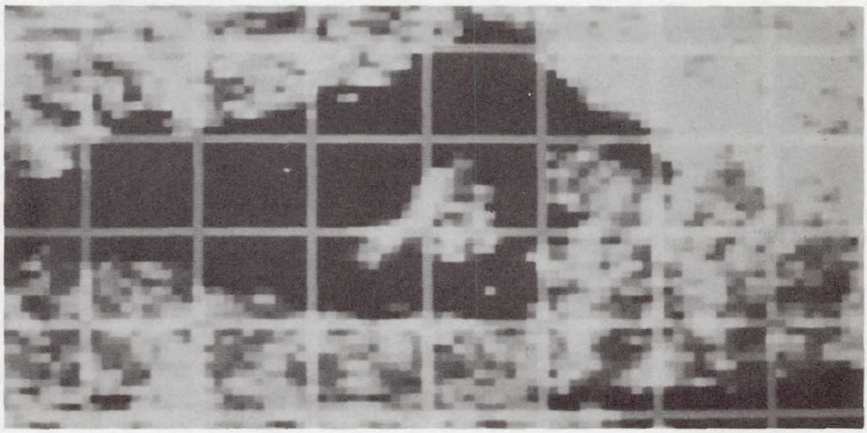

Figure 7 The same Landsat image as shown in Figure 5b with the 900 x 900 m resolution grid of NOAA or TIROS superimposed. This resolution seems to be well suited for larger areas.

To solve this problem, we might consider a square on the ground 900 x 900 m in size, covered by dark soil and some small bushes, which is normal for the high-mountain basins. If this area is gradually covered by 1/10, 2/10, 3/10, etc., of snow, the reflectance from the area will also increase up to a value which, finally, corresponds to a complete snowcover. The reflectance of the area will therefore change from that of soil to that of snow, depending on the snow/soil ratio (Figure 8).

Such intermediate values are very useful because they can be utilized to estimate the snowcover more precisely. Data are used to indicate the percent snowcover within each pixel, and the results can be presented as plotted maps and in a tabular form. This method was used in a semioperational mode for the first time in 1977.

The average size of the larger catchment areas in Norway are on the order of 1,000 $km^2$. Digital enhancement of VHRR imagery was therefore required to make the data useful for snow mapping. The following procedure is now being tested for determining the areal extent of snowcover:

1. A digital description of each catchment area (coordinates) is stored in the computer and registered to UTM projection.
2. VHRR-VISIBLE data are read from magnetic tape. A subset is made of the area of interest. Geometric correction and registration to UTM projection are performed using well-distributed ground control points.
3. Training fields are selected in snow-free areas and in areas with full snowcover (2 to 4 of each kind). Each field contains 20 to 40 pixel. The mean response for the two types of fields are computed. The response interval between the two values is divided in classes: 0-20, 20-40, 40-60, etc., percent snowcover, assuming a linear relationship.
4. Each catchment area is termed a test field, and a classification is made for each test field using the registered data.
5. The result is a printout showing the distribution of snow within each catchment area and the total snowcover for each area in a tabular form.
6. This result is compared with a curve giving the relationship between areal snowcover in square kilometers and subsequent runoff. The information is transferred to the user.

The spectral reflectance value of soil/vegetation for VHRR data has been approximately 10, and for full snowcover approximately 100. This will give an interval of 90 steps which is 35 percent of the full 1 to 255 value range.

The NOAA/TIROS receiving stations in Lannion, France, and Tromsoe, Norway, have provided digital VHRR data for the project. A day-pass image is now available at the computer within 20 hours. The results should reach the user the following day.

The second phase of the NPP project is to investigate further the relationship between areal extent of snowcover and subsequent runoff. Information obtained from Landsat at an earlier stage as well as filed NOAA-VHRR data are now used for this purpose.

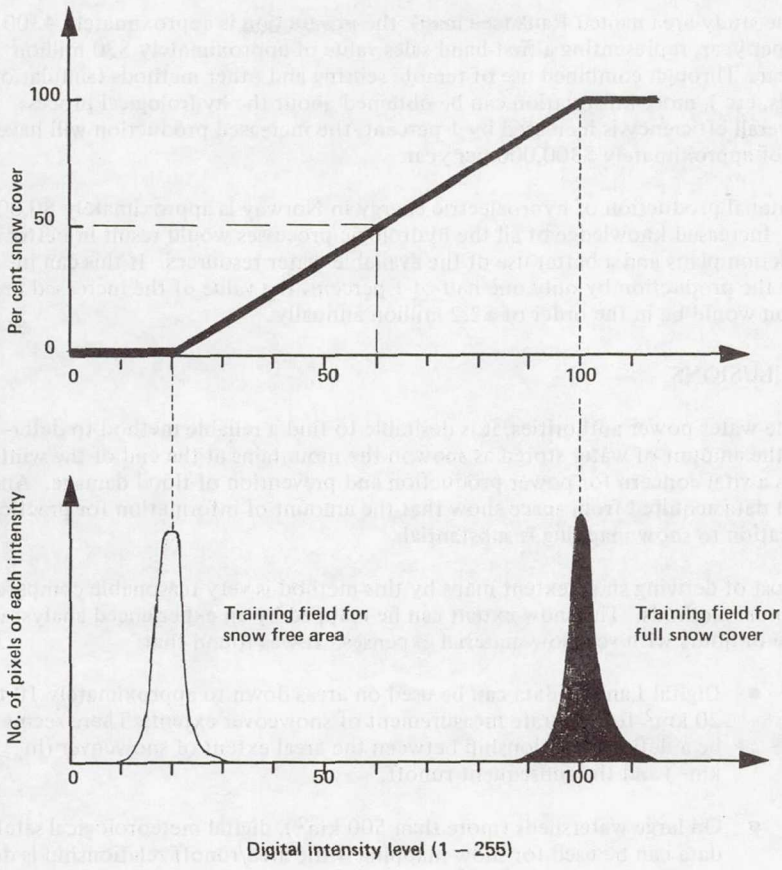


Figure 8 The lower part is the histogram for pixel intensities for training fields. The curves are well separated. At the top, the relationship between intensity level and pixel percent snowcover is indicated. In this example, a pixel with intensity level 60 has a 50 percent snowcover.

The system described is now being adapted for TIROS AVHRR data. The quality of the new TIROS data is impressive and the 0.55–0.68 $\mu$m visible band will be used for the snow mapping during the summer of 1979.

## COST-EFFECTIVE BENEFIT

Determining the economic value of data acquired from space is difficult, but some examples will illustrate the benefits. The mean annual production of electricity at the Røssåga power plant in north Norway is 2470 GWh (2470 million kWh). If the use of space-acquired data could prevent the loss of 1 GWh and instead route it through the turbines, the increased energy production would then represent a first-hand value of approximately $10,000, but the final value will be even higher.

For the study area named Rana (see map), the production is approximately 4300 GWh per year, representing a first-hand sales value of approximately $30 million per year. Through combined use of remote sensing and other methods (simulation models, etc.), more information can be obtained about the hydrological process. If the overall efficiency is increased by 1 percent, the increased production will have a value of approximately $300,000 per year.

The annual production of hydroelectric energy in Norway is approximately 80,000 GWh. Increased knowledge of all the hydrologic processes would result in better production plans and a better use of the available water resources. If this can increase the production by only one-half of 1 percent, the value of the increased production would be in the order of $2.2 million annually.

## CONCLUSIONS

For the water power authorities, it is desirable to find a reliable method to determine the amount of water stored as snow in the mountains at the end of the winter. This is a vital concern for power production and prevention of flood damage. Analysis of data acquired from space show that the amount of information for practical application to snow mapping is substantial.

The cost of deriving snow extent maps by this method is very reasonable compared to manual methods. The snow extent can be mapped by an experienced analyst in a couple of hours with very low material expenses. It was found that:

- Digital Landsat data can be used on areas down to approximately 10 to 20 $km^2$ for accurate measurement of snowcover extent. There seems to be a definite relationship between the areal extent of snowcover (in $km^2$) and the subsequent runoff.

- On large watersheds (more than 500 $km^2$), digital meteorological satellite data can be used for snow mapping if the area/runoff relationship is determined by the use of observations from previous years.

- A close relationship was found between snow-covered area and subsequent runoff for different parts of the country. Information obtained for a group of areas can be transferred to a new area. This will make it possible to use the method for a new area where little information is available. The areas should be located in the same general type of climate and terrain and should have the same runoff characteristics.

- The relationship developed (see above) is quantitative, and the result is an important parameter in hydrologic runoff models. It is a great advantage that the data can be easily obtained and are easy to handle. The importance of such methods increases with the increased cost of energy.

It is difficult to determine the economic value of data acquired from space for hydrological purposes in Norway. A better knowledge of the hydrologic conditions will, however, result in better production plans. An increased energy production of only one-half of 1 percent will have a great economic value.

REFERENCES

Barnes, J. C., and Bowley, C. J., 1974, Handbook of Techniques for Satellite Snow Mapping, Final Report, NAS5-21803, NASA, Goddard Space Flight Center, Greenbelt, MD, 95 pp.

Bartolucci, L. A., Hoffer, R. M., and Luther, S. G., 1975, Operational Applications of Satellite Snowcover Observations. Paper No. 21 at a workshop held in South Lake Tahoe, Calif., Aug. 18-20, 1975.

Dahl, J. B., and Odegaard, H. A., 1970, "Areal Measurements of Water Equivalent of Snow Deposits by means of Natural Radioactivity in the Ground." Conference on Isotope Hydrology 1970 in Vienna, Austria. IAHA - SM - 129/12, p. 191-210.

Hoffer, R. M., 1975, Computer-Aided Analysis of Skylab Scanner Data for Land Use Mapping, Forestry and Water Resource Applications. Proceedings of the Eleventh International Symposium on Space Technology and Science, Tokyo 1975, p. 935-941.

Leaf, C. F., 1967, "Areal Extent of Snow Cover in Relation to Streamflow in Central Colorado." Proceedings of the International Hydrology Symposium, Fort Collins, p. 157-164.

Odegaard, H. A., 1974, "The Application of ERTS Imagery to Mapping Snow Cover in Norway." ERTS-1 Contract NASA F-418, Final Report. May 1974, 15 p.

Odegaard, H. A., and Ostrem, G., 1977, "Application of Landsat Imagery for Snow Mapping in Norway." Contract NASA 29020, Final Report February 1977, 61 p.

Rango, A., Salomonson, V. V., and Foster, J. L., 1975, "Seasonal Streamflow Estimation Employing Satellite Snowcover Observations." Preprint X-913-75-26, NASA/Goddard Space Flight Center, 34 p.

Rango, A., Salomonson, V. V., and Foster, J. L., 1977, "Seasonal Streamflow Estimation in the Himalayan Region employing Meteorological Satellite Snow Cover Observations," Water Resources Research, 13, (2), 265-281.

Salomonson, V. V., and Rango, A., 1974, "ERTS-1 Applications in Hydrology and Water Resources," Journal American Water Works Association, 66 (3), 168-172.

Strong, A. E., McClaim, E. P., and McGinnis, D. F., 1971, "Detection of Thawing Snow and Ice Packs through the Combined Use of Visible and Near-Infrared Measurements from Earth Satellites," Monthly Weather Review, Vol. 99, No. 11, p. 828-830.

Tangborn, W. V., 1977, "Application of a New Hydrometeorological Streamflow Prediction Model," Proceedings of the 45th Annual Western Snow Conference, Albuquerque, NM, pp. 35-43.

Wiesnet, D. R., 1974, "The Role of Satellites in Snow and Ice Measurements." NOAA Technical Memorandum NESS 58, U.S. Department of Commerce, Washington, D.C., August 1974, 12 p.

Wiesnet, D. R., and McGinnis, D. F., 1973, "Snow-Extent Mapping and Lake Ice Studies using ERTS-1 MSS together with NOAA-2 VHRR," Third Earth Resources Technology Satellite-1, Symposium, December 10-14, 1973. Goddard Space Flight Center, Washington, D.C. Vol. 1, Section B, p. 995-1009.

# SATELLITE SNOWCOVER AND RUNOFF MONITORING IN CENTRAL ARIZONA

Herbert H. Schumann, U.S. Geological Survey, Phoenix, Arizona,
Edib Kirdar, Salt River Project, Phoenix, Arizona, and
William L. Warskow, Salt River Project, Phoenix, Arizona

## ABSTRACT

The operation of multipurpose reservoirs in semiarid central Arizona requires timely and dependable snowmelt information. Conventional ground surveys and aerial observations have been used in an attempt to monitor the rapidly changing moisture conditions in the Salt-Verde watershed. Since 1974, timely satellite imagery has provided repetitive snowcover observations to assist the managers of the Salt River Project in the operation of their reservoir system.

Results of studies in central Arizona indicate that multispectral Landsat imagery permits rapid and accurate mapping of snowcover distributions in small- to medium-sized watersheds. Low-resolution (1 kilometer or 0.6 mile) meteorological satellite imagery provides the synoptic daily observations necessary to monitor the large and rapid changes in snowcover. Satellite and microwave telemetry systems are used to furnish near-real time data from streamflow gages and snow-monitoring sites.

Seasonal runoff predictions by conventional index models and a modified hydrometeorological model (HM) were compared. Significant reductions in the standard error for seasonal runoff predictions (March-May) were obtained using the HM model. Short-term runoff predictions using snowcover depletion models were also tested. Statistically significant correlations between short-term snowcover depletion rates and runoff rates were determined for selected periods.

## INTRODUCTION

Snowfall provides an important renewable source of water for irrigation, hydroelectric-power generation, and municipal and industrial uses in the Western United States. In semiarid central Arizona the efficient operation of multipurpose reservoirs for both water conservation and the reduction in peak floodflows

requires timely and dependable information on the rapidly changing rates of snowmelt and runoff (Kirdar et al., 1977).

The area of the Salt-Verde watershed is about 34,000 km$^2$ (13,000 mi$^2$) and ranges from about 400 to 3,900 m (1,325 to 12,670 ft) above mean sea level (Fig. 1). The annual

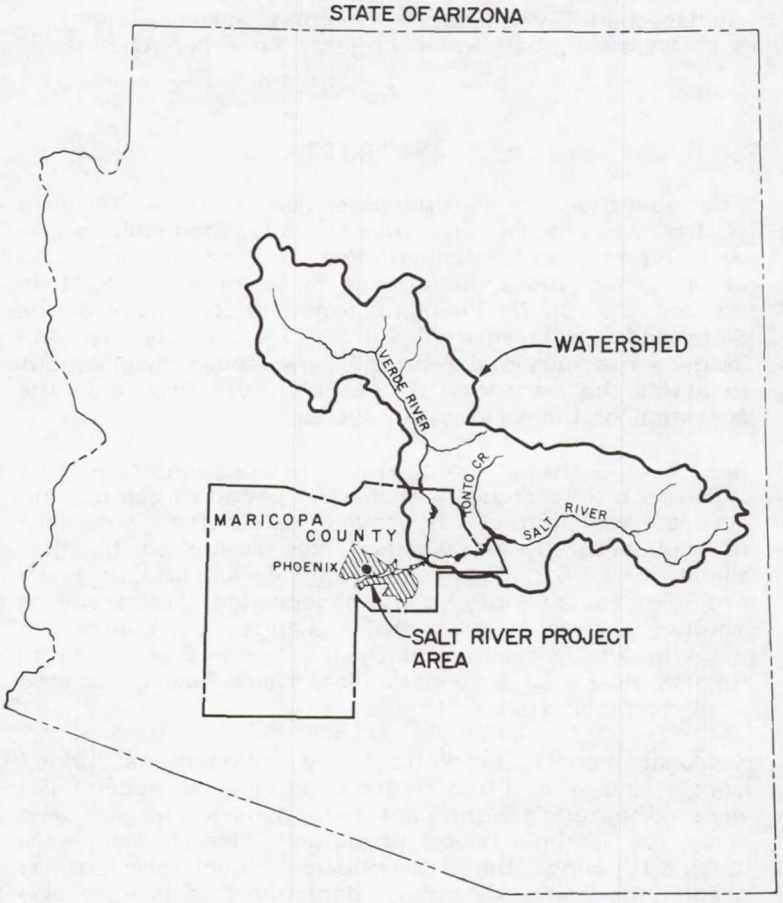


Fig. 1—Salt-Verde watershed

precipitation ranges from less than 250 mm (10 in.) to more than 640 mm (25 in.). (See Green and Sellers, 1964.) About half the annual precipitation comes from winter storms that produce about 75 percent of the mean annual runoff (Kirdar et al., 1977). The extremely variable runoff of the Salt and Verde Rivers is stored in six reservoirs near Phoenix; the reservoirs have a combined storage capacity of about 2,500 hm$^3$ (2 million acre-ft). The reservoirs provide water for municipal, industrial, and

irrigation use in the 101,000-hm$^2$ (250,000-acre) Salt River Project area, which includes most of metropolitan Phoenix (Fig. 1). In addition, the reservoirs also furnish hydroelectric power and limited flood protection to the Phoenix area.

Runoff from the Salt-Verde watershed is characterized by frequent and extreme variations. For example, the second smallest annual runoff volumes since 1913 occurred in 1977, and the second largest runoff volumes occurred in 1978. These extremes have produced significant economic impacts. For example, the floods in March 1978 in Maricopa County resulted in the loss of four lives and more than $33 million in property damage (U.S. Army Corps of Engineers, 1979).

Historically, snowcover conditions in the Salt-Verde watershed were evaluated by ground surveys and more recently by repetitive aerial reconnaissance flights. Near-real time information on streamflow rates is provided by a network of observers that report by telephone to the Salt River Project in Phoenix. Since 1974, the U.S. Geological Survey and the Salt River Project in cooperation with the National Aeronautics and Space Administration (NASA) have evaluated repetitive aerial and satellite snowcover observations and tested the satellite data collection systems for telemetry of hydrometeorological data in central Arizona.

The Salt-Verde watershed is one of four major test sites included in the NASA-sponsored Applications Systems Verification and Transfer (ASVT) Project. The purpose of the project is to develop applications of satellite observations for snowcover mapping and to predict snowmelt-derived streamflow volumes (Schumann, 1975). The purpose of this paper is to summarize the results of the evaluations and to describe the techniques developed for snowcover mapping and for making runoff predictions.

## AERIAL SNOWCOVER OBSERVATIONS

Since 1965, light aircraft have been used to make low-level reconnaissance flights over the Salt-Verde watershed to map snowcover distributions and to estimate snow depths and runoff conditions (Warskow et al., 1975). The quality of the snowpack information thus obtained is a direct function of the experience of the observer and the conditions of the flight.

Techniques for using low-cost 35-mm oblique photographs of aerial snow markers from 300 m (980 ft) above the terrain were developed and tested to obtain snow-depth information. The photographs provide a permanent record of snow depths that can be evaluated in the office as opposed to making hazardous low-level—less than 50 m or 160 ft—visual observations of the aerial snow markers (Schumann, 1975).

The availability of frequent satellite snowcover observations has greatly reduced the necessity for routine aerial reconnaissance flights over the Salt-Verde watershed. Significant savings have resulted, and the time that flight crews must be exposed to hazardous low-level flights over mountainous terrain has been greatly reduced. However, aerial observations will continue to provide valuable information on snowcover distributions and snow depths during periods of cloud cover that preclude effective satellite snowcover observations.

## SATELLITE SNOWCOVER OBSERVATIONS

Snow could be detected in eastern Canada in some of the images taken by the first weather satellite—TIROS-I—as early as April 1960 (Schneider et al., 1976). In March 1969 photographic imagery taken by the Apollo 9 astronauts indicated the general feasibility of using satellite snowcover observations to provide the synoptic coverage needed for mapping snowcover distributions over the Salt-Verde watershed; however, aerial observations showed that frequent repetitive coverage was required to monitor rapid changes in snowcover.

### Landsat System

The experimental Landsat satellite system consists of satellites placed in nearly circular, sun-synchronous, polar orbits at altitudes of about 925 km (575 mi). Multispectral scanners (MSS) aboard the satellites provide high-resolution imagery (80-m or 260-ft ground resolution) that covers 185- by 185-km (115- by 115-mi) areas of the surface of the Earth in the visible and near-infrared parts (from 0.5 to 1.1 μm) of the spectrum (National Aeronautics and Space Administration, 1976). Two Landsat satellites can provide coverage of any ground point every 9 days. The Landsat imaging system is shown diagrammatically in Figure 2. The Landsat MSS imagery can be considered virtually orthographic when used for direct mapping at a scale of 1:1,000,000—the scale that is commonly used for snowcover mapping in Arizona (Fig. 3).

Visual interpretation of 1:1,000,000 Landsat MSS band 5 (0.6 to 0.7 μm) imagery allows rapid and direct mapping of snowcover distributions using conventional photointerpretation techniques. The snowline is traced onto a transparent overlay that contains the watershed outline and major drainages, and the areal extent of the snowcover is determined using a manual planimeter or a suitable grid. Although this technique allows inexpensive measurement of snowcover distributions, the degree of precision is dependent on the skill and experience of the interpreter.

Color-additive viewing of multispectral Landsat imagery enhances the contrast between snowcovered areas and bare rock

and greatly facilitates snowcover mapping in densely forested areas. Snowcover measurements can be made from color-composite images using the transparent overlay technique described by Schumann (1978).

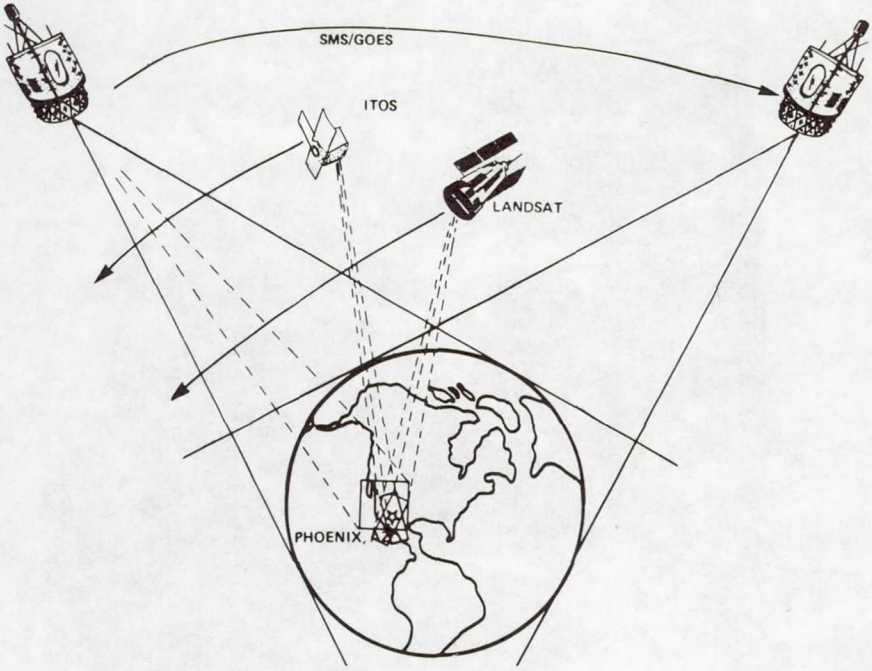


Fig. 2—Satellite imaging systems

The use of electronic density-slicing equipment and appropriate watershed masks allows the rapid determination of the percentage of snowcovered area over small to intermediate watersheds. The density slicer makes a television scan of a masked transparency copy of the black and white satellite image, the enhanced image is displayed on a color television monitor, and the percentage of snowcovered area is measured by means of the electronic planimeter (Schumann, 1978).

The Landsat MSS imagery is available in digital form on computer-compatible tapes (CCTs). Several systems have been developed to produce snow maps from computer-processed digital imagery (Salomonson and Rango, 1975). The systems can provide snow maps of high precision at slow to moderate speed.

The main limitation of using Landsat imagery for snowcover mapping in central Arizona is that only one observation is available every 9 days for a part of the Salt-Verde watershed. Six Landsat images taken on 3 consecutive days are required to

cover the entire watershed (Fig. 3). Winter cloud cover over the mountains often prevents effective Landsat snowcover observations for long periods of time.

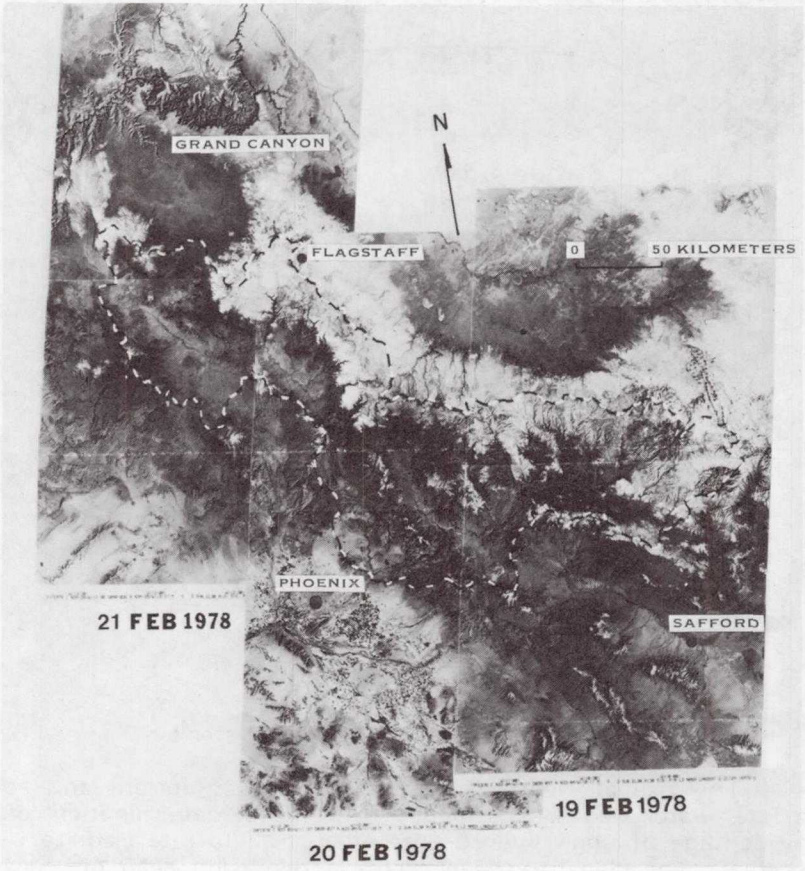


Fig. 3—Landsat image mosaic of the Salt-Verde watershed

The use of photographic copies of Landsat imagery and simple overlays permits direct mapping of snowcover distributions at a low cost. Although the multispectral character of Landsat imagery permits the use of a variety of image-enhancement techniques that facilitate snowcover mapping in densely forested areas, these techniques require expensive specialized equipment. Computer processing of digital Landsat imagery is slow and expensive compared with other methods of image processing.

## Improved TIROS Operational Satellite System (ITOS)

The National Environmental Satellite Service (NESS) has used the Improved TIROS Operational Satellite (ITOS) series of

improved Television Infrared Observational Satellite (TIROS) operational satellites (NOAA series) to produce satellite-derived areal snowcover maps of selected river basins including the Salt-Verde watershed (Schneider et al., 1976). The satellites operate in sun-synchronous polar orbits about 1,500 km (930 mi) above the Earth. Very high resolution radiometers (VHRRs) aboard the satellites provide daily coverage of the Western United States in the visible spectrum (0.6 to 0.7 μm) and twice-daily coverage in the thermal infrared (10.5 to 12.5 μm) part of the spectrum (McGinnis, 1975). The imaging system is shown diagrammatically in Figure 2.

The VHRR imagery provides horizon-to-horizon coverage, has a spatial resolution of about 1 km (0.6 mi) at the subpoint, and has a nominal scale of about 1:10,000,000 (Fig. 4). The

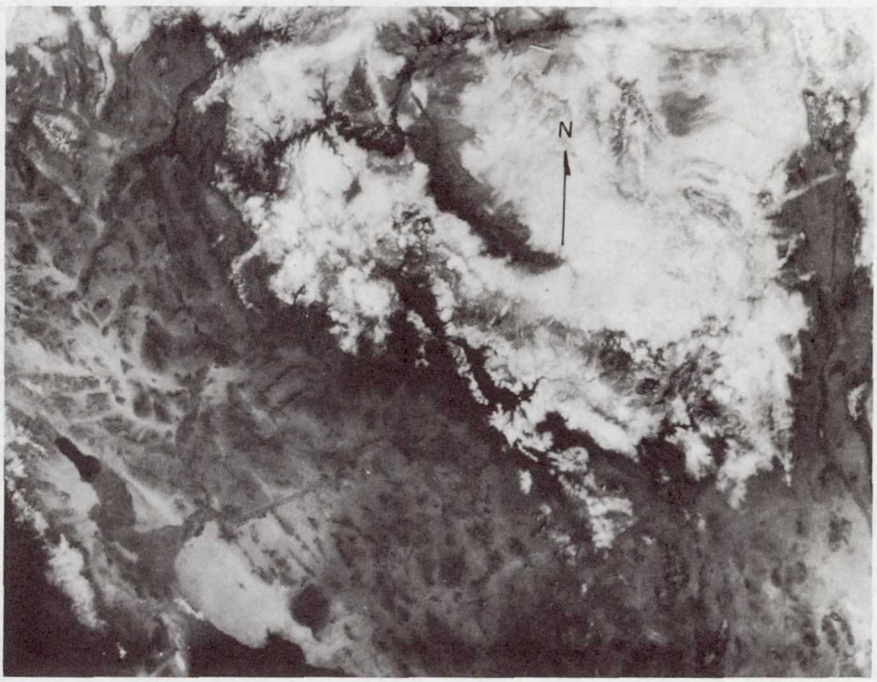


Fig. 4—Enlarged NOAA VHRR image taken in the visible part of the spectrum, March 15, 1978

imagery provides a highly distorted panoramic view of the surface of the Earth that requires geometric correction before it can be related to planimetric basin maps. Specialized optical equipment is used to enlarge and stretch the VHRR imagery and to project the corrected image onto small-scale basin maps. The snowline as visually interpreted on the corrected image is then

traced onto an overlay of the basin map, and the percentage of snowcovered area is then determined either by manual or electronic-planimeter methods.

SMS/GOES Satellite System

The synchronous meteorological satellites (SMS) now in geostationary orbit are prototypes for an operational satellite series designated "Geostationary Operational Environmental Satellites (GOES)." The satellites are in geostationary orbits at about 35,000 km (22,000 mi) above the Earth—their position with respect to the Earth remains fixed. The subpoint of the eastern satellite is at longitude 75° W. over the equator; the subpoint of the western satellite is at longitude 135° W. (Breaker and McMillan, 1975).

The SMS/GOES satellites acquire Earth imagery in the visible (0.55 to 0.75 μm) and thermal infrared (10.5 to 12.6 μm) parts of the spectrum by means of spin scan radiometers (VISSRs). Although the VISSR sensors can image almost the entire Earth (full disk) per scanning cycle, sectors of limited and specified geographical areas are extracted for detailed study (Fig. 5). The sectorized SMS/GOES visible imagery has a maximum spatial resolution of 1 km (0.6 mi) at nadir and is routinely available every 30 minutes (Breaker and McMillan, 1975). The SMS/GOES imaging system is shown diagrammatically in Figure 2.

The VISSR imagery produces a distorted view of the surface of the Earth that changes in scale and resolution north and south of the equator; however, the distortion tends to be fairly constant. Specialized optical equipment can be used to correct the VISSR imagery and to project it onto planimetric basin maps. The position of the snowline can then be plotted, and snowcover measurements can be obtained either by manual or electronic-planimeter methods.

Advantages and Limitations of Meteorological Satellite Imagery

The main advantage of using imagery acquired by the NOAA and SMS/GOES satellites for snowcover mapping in central Arizona is that the systems provide daily observations of the entire Salt-Verde watershed. Daily synoptic observations are required to monitor the large changes in snowcovered area that occur during periods of rapid snowmelt. A comparison of imagery taken simultaneously in the visible and infrared parts of the spectrum can sometimes be helpful in differentiating between clouds and snowcover.

The main disadvantages of using imagery taken by the NOAA and SMS/GOES meteorological satellites for snowcover mapping are the low resolution and geometric distortion of the imagery. The geometric distortions in the VHRR imagery are

highly variable, but the distortions in the VISSR imagery tend to be more constant. Research now being conducted by NESS indicates that the necessary geometric corrections, image enhancements, and snowcover measurements may be accomplished by computer processing of the VISSR digital data (R. S. Gird, National Environmental Satellite Service, written commun., 1978). A review of current SMS/GOES imagery for Arizona prior to aerial snow-reconnaissance flights has provided valuable information that improved not only the efficiency of the missions but the safety of the flights relative to the effects of incoming storms.

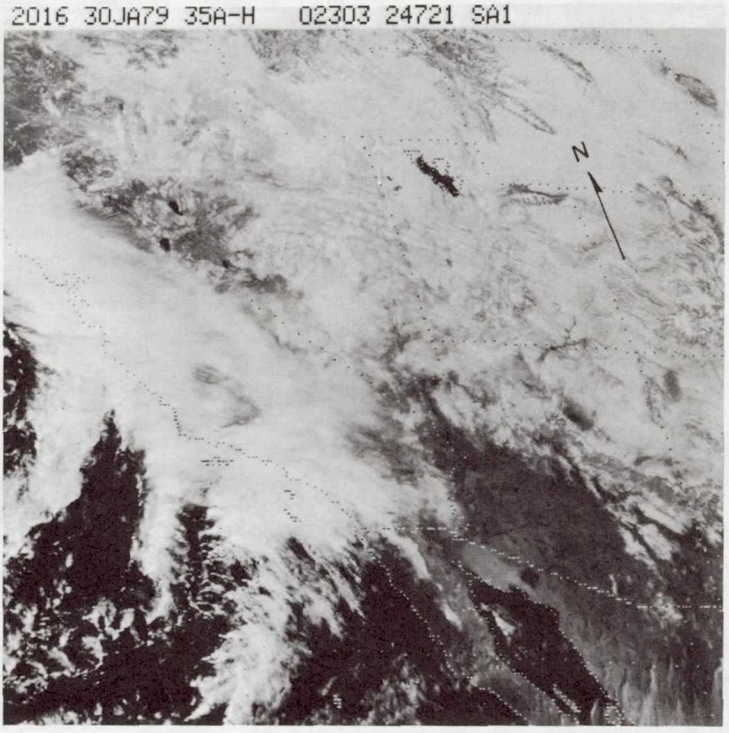


Fig. 5—SMS/GOES VISSR image taken in the visible part of the spectrum

## TELEMETRY OF HYDROMETEOROLOGICAL DATA

Rapid changes in winter streamflow rates in response to rainfall and snowmelt present serious water-management problems in central Arizona. Telemetry systems are used to relay hydrometeorological data from selected sites in the Salt-Verde watershed to assist in the operation of multipurpose reservoirs and to provide flood-warning information. The systems include microwave telemetry, two satellite telemetry systems, and a meteor-burst communication system.

## Microwave Telemetry System

The Salt River Project operates a conventional microwave telemetry system to monitor streamflow rates at seven key gaging stations above the reservoirs. The system can be interrogated, and the desired data can be obtained in real time. The main disadvantage of this type of system is the high cost of equipment and maintenance.

## Landsat Data Collection System

During 1972-76, the experimental Landsat data collection system (DCS) was successfully tested to relay hydrometeorological data from selected streamflow-gaging stations and snow-monitoring sites (Schumann, 1975). On several occasions, the system provided valuable information to managers of the Salt River Project for use in making reservoir-management decisions during periods of large and rapidly changing runoff.

The Landsat DCS uses battery-powered data collection platforms (DCPs) to relay hydrometeorological data from remote sites via the Landsat satellites to one or more of the ground-receiving sites in California, Maryland, and Alaska (Fig. 6). The Landsat

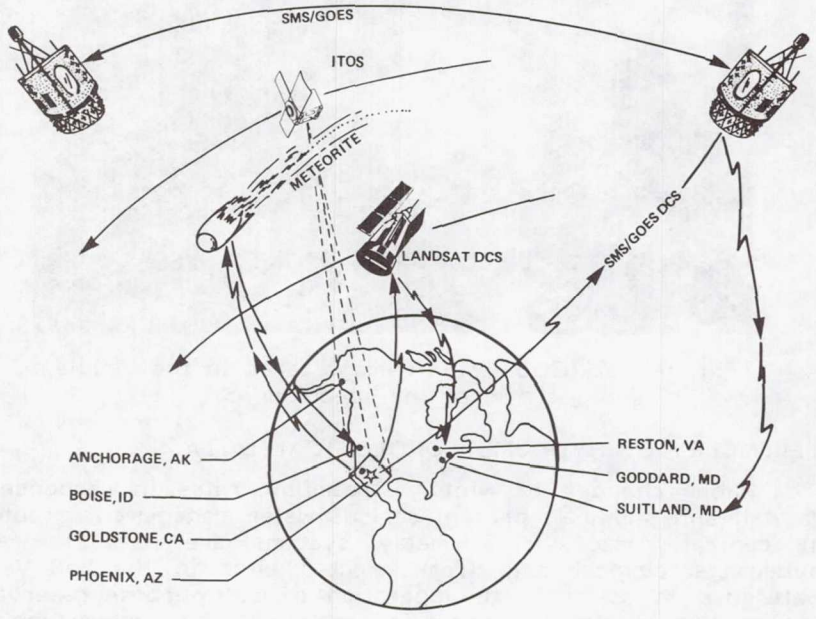


Fig. 6—Satellite telemetry systems

DCPs transmit as many as 64 bits of data every 90 or 180 seconds and relay data from anywhere in North America during at least two orbits per day—one at about 9:30 in the morning and one at about 9:30 in the evening. When the satellite is in mutual view of a transmitting DCP and one of the ground-receiving sites, the satellite relays the transmission in real time to the ground-receiving site (National Aeronautics and Space Administration, 1976).

The Landsat DCPs proved to be reliable under a wide range of environmental conditions and were simple to operate. The main disadvantages of using the Landsat DCS to relay hydrometeorological data are the small amount of information relayed per transmission (64 bits) and the small number of transmissions received each day.

SMS/GOES Data Collection System

The operational SMS/GOES DCS telemeters large volumes of hydrometeorological data from remote sites at low cost. The SMS/GOES DCPs are operated in a self-timed mode—units transmit every 3 hours—and are microprocessor controlled. Since 1977, data from four streamflow-gaging stations and one snow-monitoring site in central Arizona have been collected at 15-minute intervals and stored in the DCP memory unit (832-bit capacity) for relay every 3 hours to the western satellite. When powered by batteries that are recharged by solar panels, the DCPs can operate unattended for long periods of time (LaBarge Incorporated, 1977).

Data transmitted by the DCPs are relayed in real time by the SMS/GOES satellites to the NOAA ground-receiving site at Wallops Island, Virginia, and are sent to the World Weather Building in Suitland, Maryland (Fig. 6). The data are then relayed to the National Center of the U.S. Geological Survey in Reston, Virginia, where the data are routinely processed into engineering units and sent to Arizona on a weekly basis via a high-speed computer terminal. Unprocessed SMS/GOES DCS data also are available from the NOAA computer center in Suitland, Maryland, in near-real time—less than 1 minute after transmission to the satellite—through the use of low-speed computer terminals. The value of near-real time satellite telemetry was dramatically demonstrated during the storms of March 1978, December 1978, and January 1979 in central Arizona. Streamflow data relayed by the system were used by personnel of the Salt River Project to monitor runoff into the Salt River and to make water-management decisions.

Snotel System

The Snotel system implemented by the Soil Conservation Service (SCS) uses a meteor-burst telemetry technique to relay

hydrometeorological data from snow-monitoring sites in the Salt-Verde watershed (Fig. 6). (See Barton and Burke, 1977.) Snow-water equivalents and other data relayed from the sites and snowcovered area measurements from satellite snowcover observations may permit improved estimates of the volume of water stored in the snowpack.

## SNOWCOVER DEPLETION AND RUNOFF

The rate at which snowcover is depleted from the watershed can be considered as an index of the runoff generated by snowmelt. In the Salt-Verde watershed snow above an altitude of about 2,100 m (7,000 ft) does not melt until March, April, or May. A thin snowcover below an altitude of about 2,100 m (7,000 ft) is ephemeral and is subject to rapid melting induced by sharp increases in temperature or by rain on the snow (Warskow et al., 1975). Rain falling on snow often produces rapid increases in runoff and creates a large flood potential in the Salt River Valley when reservoirs are filled to near capacity (Warskow et al., 1975).

### Statistical Analyses

Snowcovered area measurements and corresponding mean daily runoff values for the Salt and Verde Rivers are shown in Figures 7 and 8. A comparison of the measurements suggests that periods of reduction in snowcovered area often correspond to periods of changes in runoff rates. Because winter cloud cover often limits satellite snowcover observations to periods following major storms, most observed periods of reduction in snowcovered area correspond to periods of decreasing runoff rates. An example of increasing runoff rates during a period of reduction in snowcovered area occurred in late February 1978 (Figs. 7 and 8).

A linear regression analysis was used to determine the relation between snowcovered area and the corresponding runoff rates for 28 events on the Salt River and 22 events on the Verde River during 1974-78. The percentage of snowcovered area was considered as the independent variable, and the corresponding mean daily runoff was considered as the dependent variable. The simple linear regression equation developed for each event is

$$R = bS + a, \qquad (1)$$

where R is the mean daily runoff in cubic feet per second, b is the regression coefficient or the slope of the regression line, S is the snowcovered area in percent, and a is the intercept along the ordinate (Ezekiel and Fox, 1959).

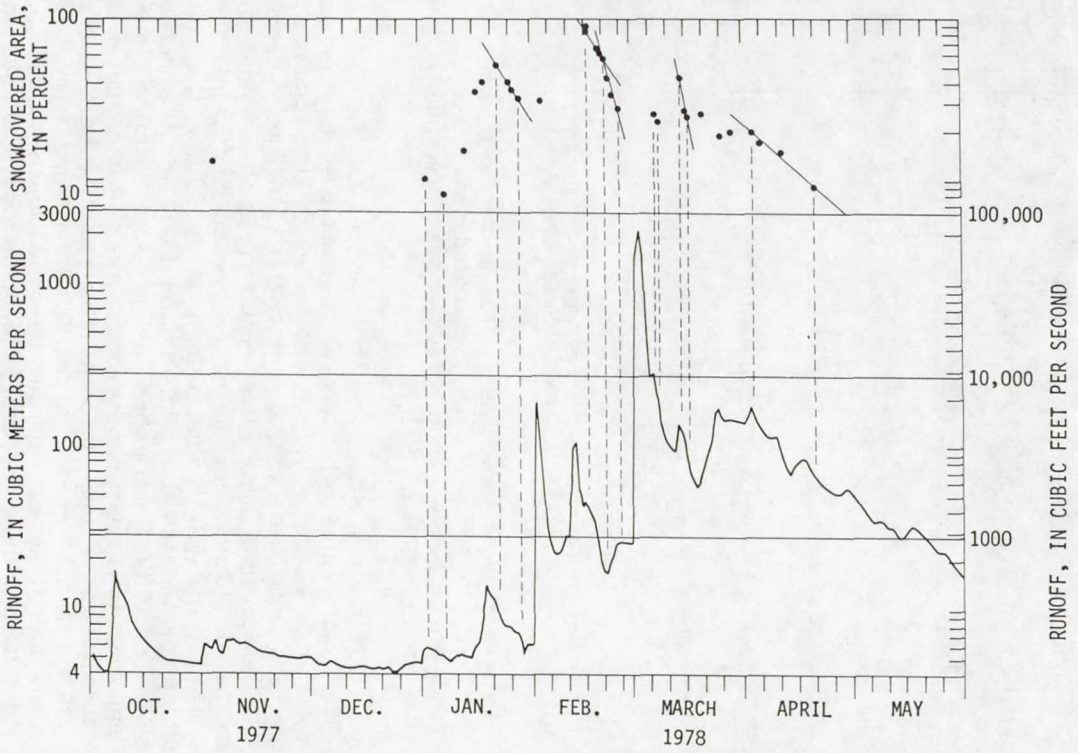


Fig. 7—Percentage of snowcovered area and runoff from the Salt River part of the watershed above the Salt River near Roosevelt gaging station, 1977-78

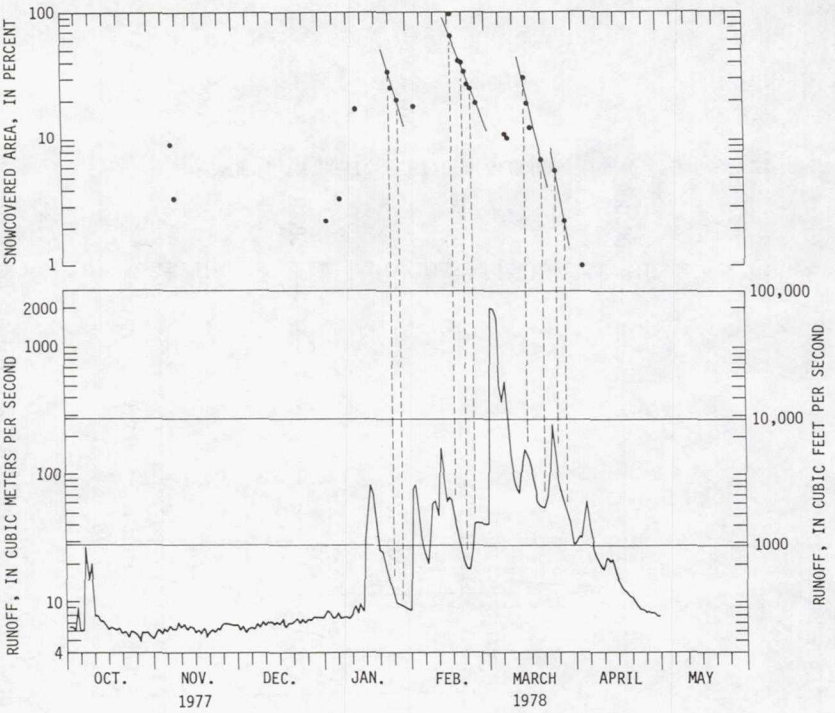


Fig. 8—Percentage of snowcovered area and runoff from the Verde River part of the watershed above the Verde River below Tangle Creek above Horseshoe Dam gaging station, 1977-78

Early in the winter runoff season—October 1 to February 15—runoff rates often are at or near base-flow levels in the Salt and Verde Rivers, and most of the snowmelt replenishes soil moisture and ground-water storage. Large changes in snowcovered area often result in small changes in runoff rates. Absolute values of the regression coefficients for winter runoff for 1974-78 ranged from 0.48 to 36 for the Salt River part of the watershed and from 0.66 to 12 for the Verde River part of the watershed. In late winter and spring—February 15 to May 15—small changes in snowcovered area can correspond to small or large changes in runoff rates. Absolute values of the regression coefficients ranged from 0.79 to 416 for the Salt River part of the watershed and from 0.88 to 233 for the Verde River part of the watershed. Values in excess of 200 were observed only in late spring—April through May.

Coefficients of determination (Ezekiel and Fox, 1959) ranged from 0.69 to 0.99+ and averaged 0.91 for the Salt River data; the coefficients ranged from 0.62 to 0.99+ and averaged 0.90 for

the Verde River data. Confidence levels ranged from 60+ to 99+ percent for both sets of data, and most were more than 85 percent. Although only a small number of measurements—3 to 7—were available for each event, the data suggest a strong relation between changes in snowcovered area and short-term changes in mean daily runoff for the Salt-Verde watershed.

Snowcovered area measurements often fall along a straight line when the logarithms of snowcovered area are plotted against time in days (Figs. 7 and 8). The same relation was observed in the Salt and Verde parts of the watershed during the 1974-75, 1975-76, and 1976-77 winter runoff seasons for which frequent sequential satellite snowcover observations were available from NESS. The relation can be expressed by the linear equation

$$\log S = bt + a, \qquad (2)$$

where S is snowcovered area in percent, t is time in days after the initial snowcover measurement, and b and a are regression constants. As few as two consecutive snowcover measurements can be used to determine a first approximation of the rate of depletion of snowcovered area and to make short-term predictions of the percentage of snowcovered area (S') a few days in the future.

## Short-Term Runoff Predictions

Equation 1 may be used with predicted values of snowcovered area from equation 2 to predict mean daily runoff (R'). The volume of short-term runoff can be calculated by summation of the estimates of mean daily runoff using the equation

$$V = (R'_1 + R'_2 + R'_3 + \ldots + R'_n)\ (1.98), \qquad (3)$$

where V is the volume of runoff in acre-feet, R' is the predicted mean daily runoff in cubic feet per second, and 1.98 is a constant. The short-term runoff predictions will be reasonably accurate if additional precipitation or large changes in air temperature do not occur. If a subsequent observation of snowcovered area differs significantly from the projected value, a new relation must be developed before additional runoff predictions can be made.

## Seasonal Runoff Predictions

In the Salt River Project area seasonal runoff predictions are estimated to produce average annual benefits of more than $11 million to users of runoff for the irrigation of cropland (Elliott, 1977). Seasonal runoff predictions require careful consideration of many hydrologic parameters, such as antecedent precipitation and runoff amounts, soil moisture and ground-water

storage conditions, and the volume and distribution of water stored in the snowpack. The probability of postprediction precipitation and energy exchange, which may affect snowmelt and evapotranspiration rates, also should be considered.

Operational runoff predictions are made by personnel of the SCS and Salt River Project using conventional index forecast models (Warskow et al., 1975). The models provide reasonably accurate predictions for years of low to average runoff volumes; however, the models rely strongly on averages and have greatly underestimated the large runoff volumes in recent years.

A concern for the apparent large changes in basin storage early in the winter runoff season led to the testing of the hydrometeorological model (HM) developed by the U.S. Geological Survey in an attempt to improve runoff predictions in the Salt-Verde watershed. The model implicitly incorporates snow, soil moisture, and ground-water storage as part of basin storage (Tangborn, 1977). Seasonal runoff predictions for the March-May runoff periods for 1960-75 were developed using monthly precipitation and runoff values. A comparison of the HM predictions with the SCS model predictions indicates a reduction in the overall standard error of estimate of 42 percent for the Salt River, 46 percent for the Verde River, and 29 percent for Tonto Creek.

Further modification of the HM was necessary to develop short-term runoff predictions. The HM was modified to use daily precipitation and runoff values and to make runoff predictions of less than a month duration. The modifications resulted in an even greater improvement in the accuracy of seasonal runoff predictions (Fig. 9). The modified HM was installed on the Salt River Project computer early in 1978 for operational testing.

In spring 1978 and spring 1979 the Salt River Project used the HM to make seasonal and short-term runoff predictions. Additional modification of the HM to include air-temperature data resulted in a 22-percent improvement in the short-term runoff predictions for the Black River near Fort Apache in the upper part of the Salt River watershed (Tangborn, written commun., 1978). Additional research is needed to allow the effective use of snowcovered area measurements in future seasonal runoff predictions. Repetitive satellite snowcover observations concurrent with hydrometeorological data relayed in near-real time from snow-monitoring and streamflow-gaging sites should facilitate the research.

## CONCLUSIONS

The availability of frequent satellite snowcover observations has greatly reduced the necessity for routine aerial reconnaissance flights over the Salt-Verde watershed. Significant savings

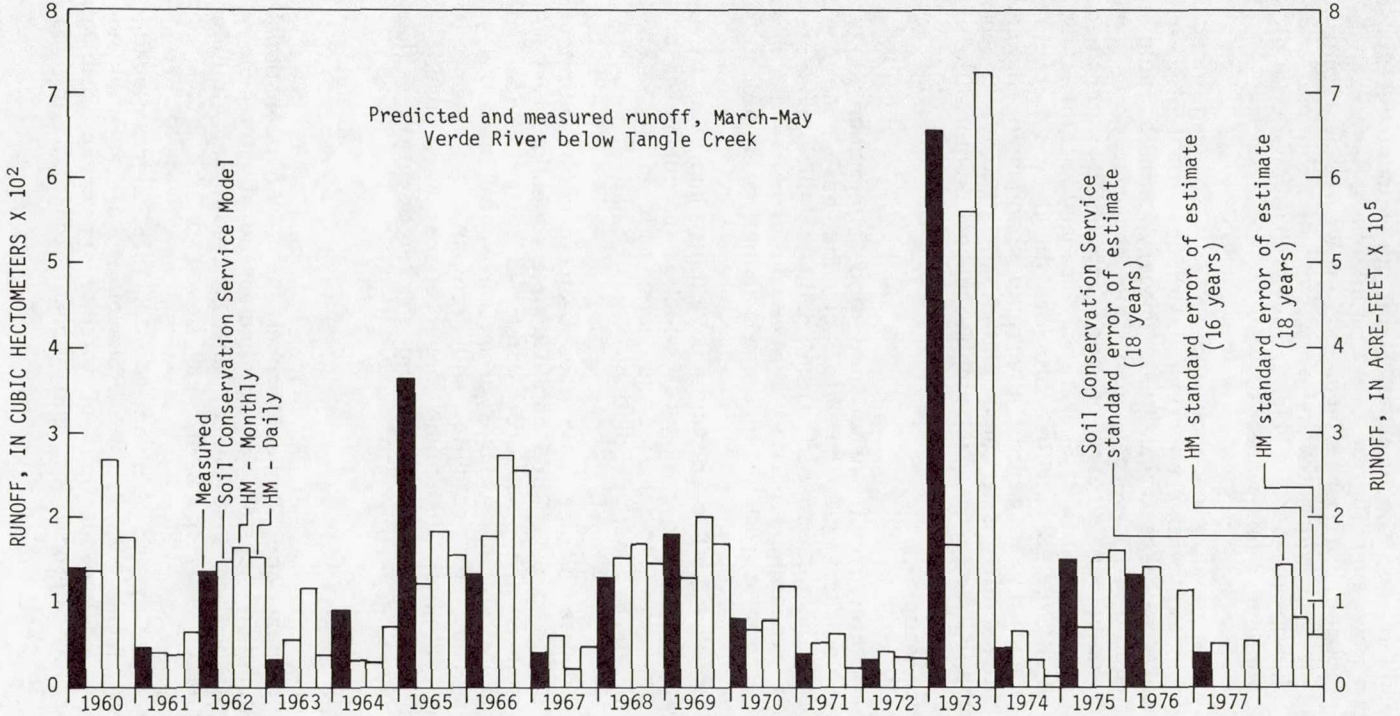


Fig. 9—Seasonal runoff predictions, Verde River below Tangle Creek

have resulted, and the time that flight crews must be exposed to hazardous low-level flights over mountainous terrain has been greatly reduced. Aerial observations, however, will continue to provide valuable information on snowcover distributions and snow depths during periods of cloud cover that preclude effective satellite snowcover observations.

Satellite imagery provides the synoptic coverage needed for mapping large snowcovered areas. Although the high-resolution experimental multispectral Landsat imagery permits rapid snowcover mapping at low cost, only one observation is available every 9 days for a part of the Salt-Verde watershed. In contrast, low-resolution operational imagery acquired by the ITOS and SMS/GOES satellites provides the daily synoptic observations necessary to monitor the rapid changes in snowcovered area in the entire Salt-Verde watershed. However, geometric distortions in meteorological satellite imagery require the use of specialized optical equipment or digital-image processing for snowcover mapping.

Short-term runoff predictions and information on basin-storage conditions can be made on the basis of snowcover depletion rates determined from daily satellite observations. Additional research is needed to allow the effective use of snowcovered area measurements in seasonal runoff predictions.

Seasonal runoff predictions have been improved by use of the modified hydrometeorological model in recent years of large runoff volumes. The model also was modified successfully to make short-term runoff predictions.

Hydrometeorological data have been successfully relayed by the Landsat and SMS/GOES satellite data collection systems from remote sites on the Salt-Verde watershed under a wide range of environmental conditions. Hydrometeorological data relayed in near-real time by satellite and conventional telemetry and frequent satellite snowcover observations were used as an integral part of an early warning system during the floods of spring 1978 and spring 1979.

REFERENCES CITED

Barton, Manes, and Burke, Michael, 1977, An operational data acquisition system using meteor-burst technology, in Western Snow Conference, 45th Proceedings: Albuquerque, N. Mex., 1977, p. 82-87.

Breaker, L. C., and McMillan, M. C., 1975, Sierra Nevada snow melt from SMS-2, in Proceedings of a workshop on operational applications of satellite snowcover observations: National Aeronautics and Space Administration SP-391, p. 187-197.

Elliott, S. J., 1977, Value of water supply forecasts to irrigated agriculture, in Western Snow Conference, 45th Proceedings: Albuquerque, N. Mex., 1977, p. 63-67.

Ezekiel, Mordecai, and Fox, K. A., 1959, Methods of correlation and regression analysis: New York, John Wiley, 548 p.

Green, C. R., and Sellers, W. D., eds., 1964, Arizona climate: Tucson, University of Arizona Press, 503 p.

Kirdar, Edib, Schumann, H. H., and Warskow, W. L., 1977, The application of aerial and satellite snow-mapping techniques for multi-purpose reservoir system operations in Arizona, in Western Snow Conference, 45th Proceedings: Albuquerque, N. Mex., 1977, p. 95-101.

LaBarge Incorporated, 1977, Instruction manual for the convertible data collection platform (CDCP) and related equipment: Tulsa, Okla., 163 p.

McGinnis, D. F., Jr., 1975, A progress report on estimating snow depth using VHRR data from NOAA environmental satellites, in Proceedings of a workshop on operational applications of satellite snowcover observations: National Aeronautics and Space Administration SP-391, p. 313-324.

National Aeronautics and Space Administration, 1976, Landsat data users handbook: Greenbelt, Md., Document 76SDS4258, 149 p.

Salomonson, V. V., and Rango, Albert, 1975, Summary of the operational applications of satellite snowcover observations, August 20, 1975, in Proceedings of a workshop on operational applications of satellite snowcover observations: National Aeronautics and Space Administration SP-391, p. 421-426.

Schneider, S. R., Wiesnet, D. R., and McMillan, M. C., 1976, River basin snow mapping at the National Environmental Satellite Service: National Oceanic and Atmospheric Administration Technical Memorandum NESS 83, 19 p.

Schumann, H. H., 1975, Operational applications of satellite snowcover observations and Landsat data collection systems operations in central Arizona, in Proceedings of a workshop on operational applications of satellite snowcover observations: National Aeronautics and Space Administration SP-391, p. 13-28.

_____ 1978, Satellite snow-cover observations in Arizona, in Fall technical meeting of the American Society of Photogrammetry, 1978 Proceedings, Albuquerque, N. Mex.: p. 480-489.

Tangborn, W. V., 1977, Application of a new hydrometeorological streamflow prediction model, in Western Snow Conference, 45th Proceedings: Albuquerque, N. Mex., 1977, p. 35-42.

U.S. Army Corps of Engineers, 1979, Flood damage report 28 February-6 March 1978 on the storm and floods in Maricopa County, Arizona: U.S. Army Engineers District, Los Angeles, 75 p.

Warskow, W. L., Wilson, T. T., and Kirdar, Edib, 1975, Application of hydrometeorological data obtained from remote sensing techniques for multipurpose reservoir operations, in Proceedings of a workshop on operational applications of satellite snowcover observations: National Aeronautics and Space Administration SP-391, p. 29-38.

# USE OF SATELLITE DATA IN RUNOFF FORECASTING IN THE HEAVILY FORESTED, CLOUD-COVERED PACIFIC NORTHWEST

John P. Dillard, Bonneville Power Administration, Portland, Oregon; Charles E. Orwig, National Weather Service, River Forecast Center, Portland, Oregon

ABSTRACT

Data are reviewed for five basins in the Pacific Northwest and are analyzed for up to a 6-year period ending July 1978, and in all cases cover a low, average, and high snow cover/runoff year.

Tree cover and terrain are sufficiently dense and rugged to have caused problems. Cloud cover is also a perennial problem in these springtime runoff analyses. Data periods of up to 30 days are obscured by clouds.

The interpretation of snowlines from satellite data has been compared with conventional ground truth data and tested in operational streamflow forecasting models. When the satellite snow-covered area data are incorporated in the Streamflow Synthesis and Reservoir Regulation (SSARR) model, there is a definite but minor improvement. However, this improvement is not statistically significant. Satellite snow-covered area data are being used operationally for streamflow forecasting here in the Pacific Northwest via the SSARR model.

## INTRODUCTION

The Portland River Forecast Center has relied, for a number of years, upon infrequent aerial flights to update the snow-covered area (SCA) parameter in the Streamflow Synthesis and Reservoir Regulation (SSARR) snowmelt model. In recent years, estimates of snow cover have been made from the satellite imagery and the Forecast Center has been using them in the operational model in conjunction with the aerial flight data. The advantage of the satellite estimates of snow cover is that they are available at more frequent intervals than flight data.

The Pacific Northwest was one of four Application Systems Verification and Transfer (ASVT) areas chosen by the National Aeronautics and Space Administration (NASA) to test methods to incorporate satellite-derived snow cover observations into the prediction of snowmelt-derived streamflow. The five test sites chosen in the Pacific Northwest were: the Upper Snake basin above Palisades Dam,

the Boise basin above Lucky Peak Dam, the North Fork Clearwater basin above Dworshak Dam, the Kootenai basin above Libby Dam, and the South Fork Flathead basin above Hungry Horse Dam. These basins give diversity in location, elevation, aspect, slope, size, and tree cover.

## DATA REDUCTION AND VERIFICATION

Data for all five of these basins were collected and analyzed for the 4-year period 1975-1978. This period included two average snow-cover years, a near-maximum year (1975), and an extreme drought year (1977). In addition, some data were collected in 1973 and 1974 for the Upper Snake and the Boise basins.

Landsat data were collected and reduced by a subcontractor using an interactive console and single-band radiance tresholding, and in-house using an optical zoom transfer scope. NOAA satellite data were collected and analyzed for snow-covered area using a zoom transfer scope by either National Oceanic and Atmospheric Administration/National Environmental Satellite Service (NOAA/NESS) or Bonneville Power Administration (BPA). Using NOAA imagery with good contrast, there was good agreement between the same image analyzed by both NOAA/NESS and BPA personnel. Cross-checks were also made between the Landsat and the NOAA data. There was excellent agreement when the operator was familiar with the basin, but there were also instances where, due to unfamiliarity with the basin, the satellite data had to be completely reanalyzed. This was the case in 1975 for the Dworshak, Libby, and Hungry Horse basins.

Aerial flights are one of the ground truths available to verify the satellite SCA data. When flights are made, only the continuous snowline is plotted. Discontinuous patches are thin, contribute little to runoff, and are, therefore, not included. Conversely, the satellite imagery integrates patches into the overall snowline. Thus, the satellite SCA data are generally higher than the aerial flight data. When the 50 percent snowline (50 percent of patchy snow) is plotted, there is perfect agreement between the aerial flight and satellite data.

The other ground truth available is the SSARR streamflow model. At the end of each flood season, a streamflow reconstruction or "reconstitution run" was made for each basin with the SSARR model. In these reconstitutions, daily indexed values of temperature and precipitation and also the total actual seasonal runoff are supplied to the model. The streamflows are initialized at target points in the basin with actual values, and the initial basin snow-covered area is supplied the model. Thereafter, throughout the time frame of the flood season study, actual observed daily values of temperature and precipitation (but not streamflow) are given to the program; and the SSARR model melts the snowpack, handles the overland and subsurface portions of runoff, and provides a channel routing to generate the daily streamflows at target locations. No intermediate adjustments for snow-covered area are made to these reconstitution runs. When compared with the observed hydrograph, a reconstitution run provides a visual check on the model's perfor-

mance, and therefore, gives credance to the SCA curve generated by the model. In general, the satellite SCA data were equal to, or slightly greater than, the SSARR generated snow cover curve.

## DATA REDUCTION PROBLEMS

### Forest Cover and Shadow

In the Upper Snake and the Boise basins there were no problems interpreting the snowline from satellite imagery. In the Dworshak, Libby, and Hungry Horse basins tree cover, steep slopes, and sun angle/shadow caused problems in determining the snowline from the satellite imagery. In these three basins the mountain crests are above the timberline and are bare rock, making it easy to spot snow. Moving down the slopes into the timber it is increasingly difficult to determine the snowline, especially if the forest cover is dense. This caused only sporadic problems in the Dworshak basin, but was a major problem in the Libby and Hungry Horse basins. Figures 1-5 are a series of Landsat images for the Hungry Horse basin illustrating the forest canopy, slope, and shadow problems. To the left of the basin is Flathead Lake. Immediately to the right is the Middle Fork of the Flathead River, and beyond that the Continental Divide. The South Fork of the Flathead flows northwest out of the basin, and Hungry Horse Reservoir is at the top of the picture just before the river leaves the basin.

For clarity, figures 1 through 5 (and the appropriate discussion for each figure) are shown separately on the next 5 pages.

In figure 1 (7 Mar 76) the little clearcut areas surrounding Hungry Horse Reservoir are snow covered, portions of the reservoir are snow covered, and the area east of the Rockies is snow covered. Note that the north-facing slopes show as black and appear to be snow free even though several small valleys in these areas have snow. Lakes and valleys in the headwaters are snow covered. The SCA is 95 percent.

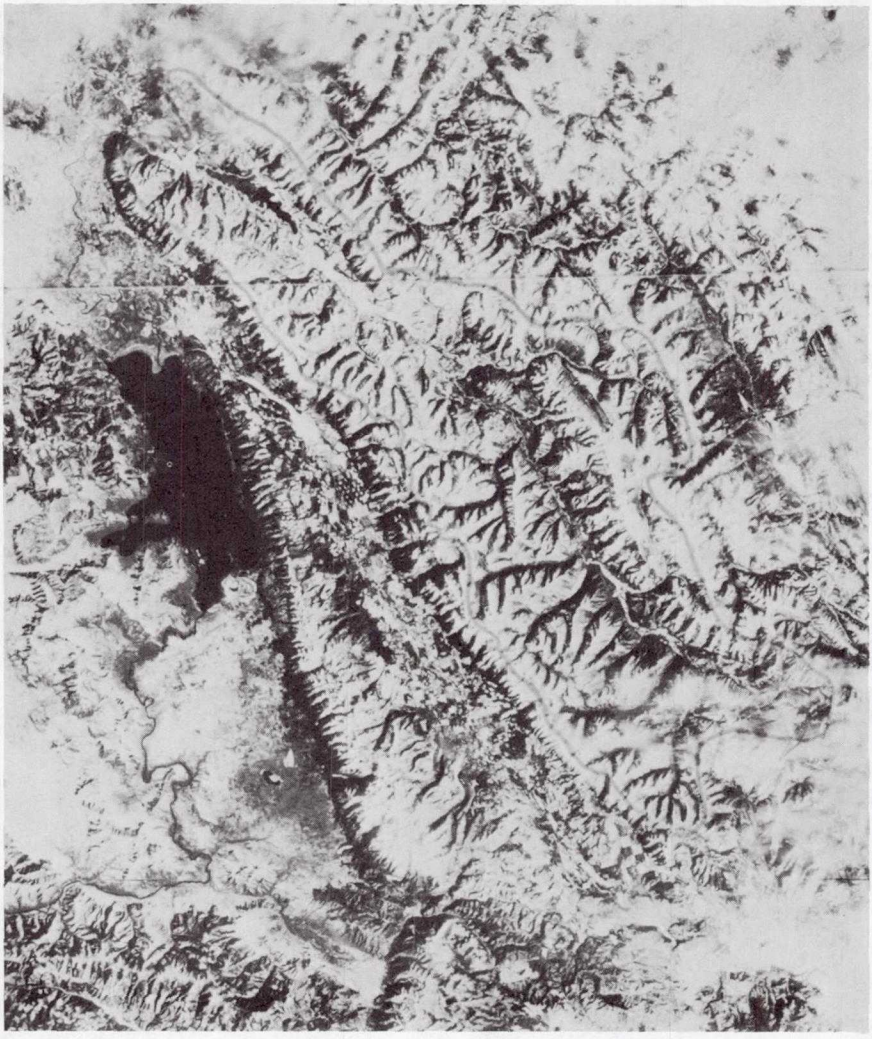

Figure 1: Hungry Horse Basin, 7 Mar 76, ERTS Imagery, MSS 5.

In figure 2 (3 Apr 76) the situation is much the same on north-facing slopes. Outside the basin, the valley around Flathead Lake has opened up. Within the basin, some additional areas have melted in the lower (northern) portion of the main valley. SCA is 87 percent.

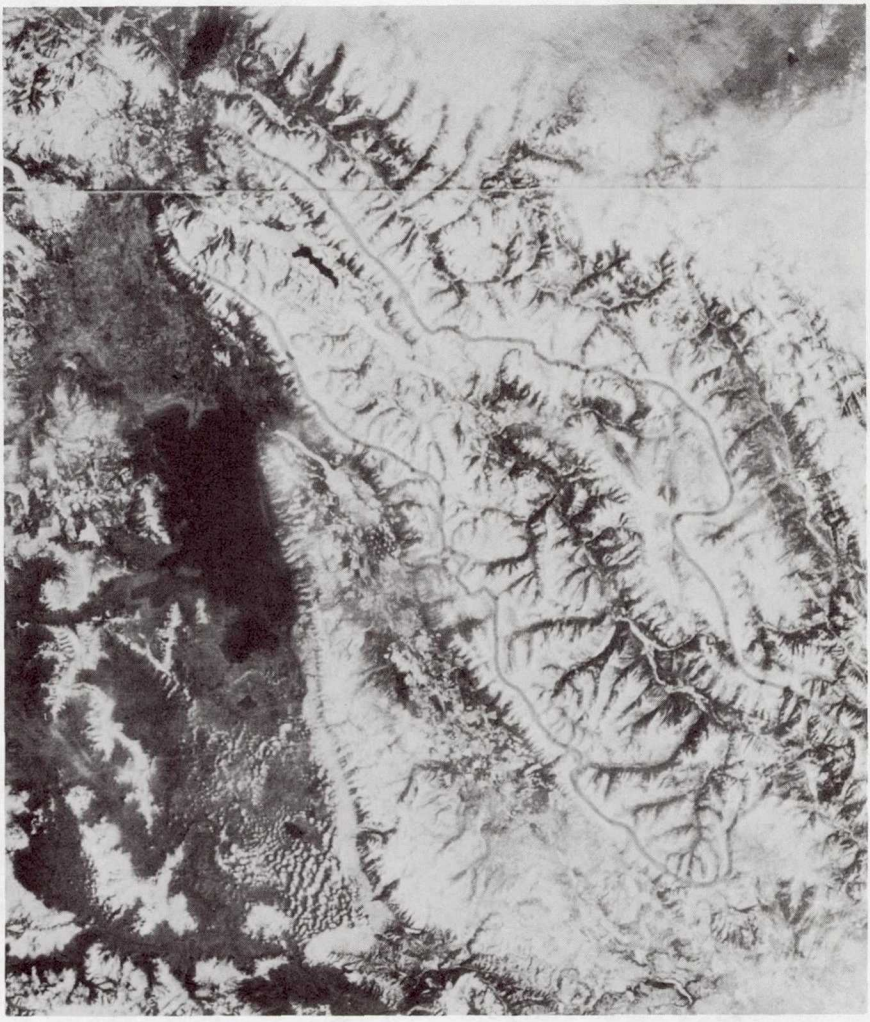

Figure 2: Hungry Horse Basin, 3 Apr 76, ERTS Imagery, MSS 5.

In figure 3 (12 Apr 76) areas outside the basin east of the Rockies and in the Flathead Lake area are completely snow free. Within the basin, melting has continued up the main valley and some melting has started on the south slopes of the side creeks. Within the side branches or small valleys, the low-lying snow intermittently visible on 7 March 76 has disappeared. Snow still shows in the clearcut areas. SCA is 74 percent.

Figure 3: Hungry Horse Basin, 12 Apr 76, ERTS Imagery, MSS 5.

In figure 4 (30 Apr 76) melting has continued on the south-facing slopes and in some clearcut areas near Hungry Horse Reservoir. New snow has fallen at the higher elevations and also east of the Rockies. SCA is 70 percent.

Figure 4: Hungry Horse Basin, 30 Apr 76, ERTS Imagery, MSS 5.

In figure 5 (18 May 76) melting has been rapid. The clearcuts are snow free, the main valley is completely barren, north and south slopes show equal in the photo. Note the rivers. All the rivers within and outside the basin that flow into Flathead Lake appear white from the muddy silt load. The Flathead River flowing south out of Flathead Lake is flowing clear and appears as grey. SCA in the Hungry Horse basin is 48 percent.

Figure 5: Hungry Horse Basin, 18 May 76, ERTS Imagery, MSS 5.

The Libby basin is steeper, more densely forested, and is more difficult to snow map than Hungry Horse. NOAA/NESS personnel do not feel confident mapping the Libby basin until the snow-covered area has dropped to below 50 percent.

### Bare Rock

In both the Libby and Hungry Horse basins the crests of the mountain ranges are bare rock. This rock is a light or whitish grey that can be confused with snow late in the season. For this reason, snow mapping is discontinued when the SCA drops to 10 or 15 percent.

### Cloud Cover

An ever present problem is that of cloud cover. Portions of the Columbia River basin are often obscured by clouds during the spring season. Utilizing Landsat data, the best possible coverage would be every 9 days. Because the snowline changes rapidly during the spring snowmelt season, a 9-day spacing between satellite images is less than ideal. In actuality, cloud cover reduced this coverage to as infrequent as 54 days, and in 1974 in the Upper Snake basin only one usable Landsat image was obtained. This was unfortunate because 1974 in the Upper Snake basin was a near-maxiumum snow cover year.

To be usable operationally, SCA data should be no older than about 48 hours. The average mail lag to receive Landsat "quick-look" imagery was 5 days. To alleviate the problem of having adequate satellite-derived SCA data, and receiving it in a timely manner, Landsat data was dropped and NOAA satellite data was used exclusively for operational purposes.

Even using NOAA data there were extended periods each year when one or more of the basins were obscured by clouds. These periods could be 34 or 36 days, and in 1977 for the Upper Snake was 43 days. Although these periods could be extensive, there has never been a case of only one image per melt season as with the Landsat data.

It should be noted that this cloud cover would also, in some cases, preclude the collection of aerial snow-flight data. Because cloud cover makes the collection of satellite data unreliable, the satellite-gathered SCA data cannot be used exclusively for operational purposes at this time. Nonetheless, NOAA satellite estimates of snow-covered area will be available more frequently then aerial flights and will have direct usefulness in the forecast model.

## SSARR OPERATIONAL FORECAST MODEL

It is appropriate at this point to discuss some of the operational procedures used in the SSARR model during the spring snowmelt season. At the beginning of each season, usually late March or early April, the model is initialized. Values for the model parameters such as snow-covered areas, seasonal volume, soil moisture, initial melt rate, and baseflow infiltration are estimated from all available information. The model is run daily and model

parameters are adjusted until the forecast and observed hydrographs match within a certain tolerance. Reliable estimates of basin snow-covered area are extremely useful during this initial adjustment period.

## SSARR Adjustment Routine

Some mention needs to be made of the SSARR model adjustment routine, since the watershed adjustment factor, to a large degree, pinpoints those basins which are not computing properly. Routinely during the spring snowmelt period, the model is backed up 2 days and runs with observed temperature and precipitation data for that 2-day period.

The model begins with an observed flow and a set of initial conditions and iterates to hit an observed flow 2 days later, within a certain tolerance. In the iteration routine the moisture input (snowmelt plus rain runoff) to the model is multiplied by a factor ranging between 0.5 and 2.0 until the current flow is matched within the specified tolerance. The final adjustment factor for each watershed is listed for each run. Those factors are entered daily on the hydrograph (see figure 6) and a history of an individual basin's performance is developed.

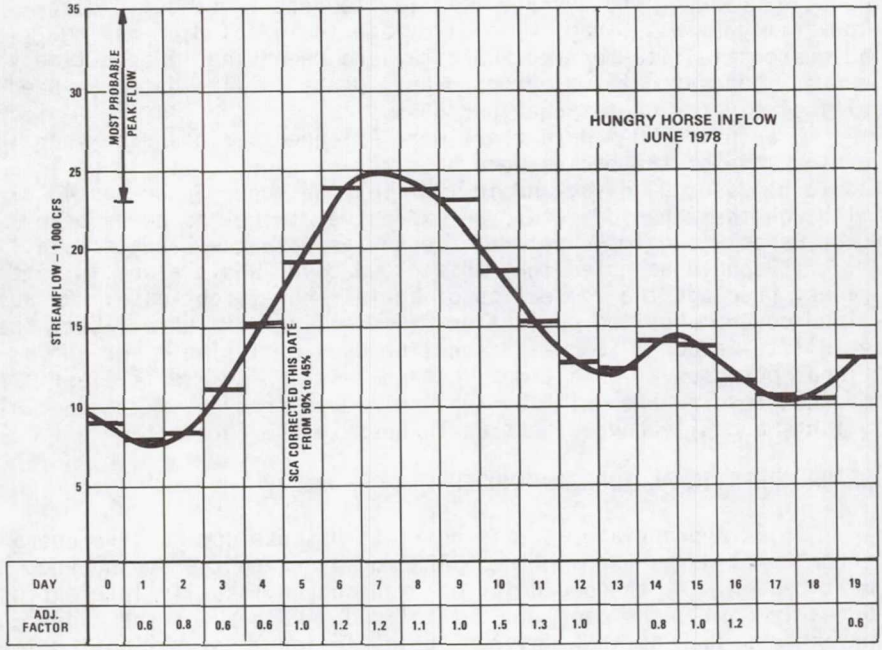


Figure 6.

A series of adjustment factors less than 1.0 or greater than 1.0 indicate that the parameters for that basin have some bias and need to be inspected. Snow-covered area is one of the parameter values that might be changed to improve the performance of an individual basin. An additional aspect of this adjustment routine needs to be considered here. Often, the watershed adjustment factors may be near 1.0, indicating that the basin parameters are in proper adjustment. A satellite snow-covered area report may be received which shows a snowline different than that carried in the model. In general, when this occurs only a token adjustment is made in the model unless some compensating parameter changes can be made to continue the good fit for that particular watershed. Conversely, when the SCA carried by the model and a satellite report are disparate, and the basin adjustment factors indicate that a change to the satellite snow-covered estimate would improve the model's fit, the satellite estimate would be used to directly update the basin parameter.

SSARR Volume and Peak Check

Another form of checking an individual watershed's operation is also utilized. One of the basic inputs to the model is the total volume of runoff from rain and snowmelt that is expected for a particular period (i.e., April-July for much of the Snake River area) for a particular basin. The SSARR model is routinely run for a 60- or 90-day period using several historical temperature sequences to test the validity of the parameter values.

Two main aspects of a watershed's fit can be checked in this manner. First, the ability of a watershed to generate the total forecast volume in the proper period can be ascertained. The two primary parameters that can be adjusted to improve the volume fit are initial soil moisture and initial snow-covered area. The importance of the snow-covered area parameter increases as one advances into the main snowmelt period. Secondly, a series of volume-peak relations (see figure 7) are available. When the seasonal volume is available from the water supply forecasts, estimates can be made of the expected peak flow for an individual basin. Here again the SSARR model can be run 60-90 days into the future and each basin can be checked to see if the individual basin is generating a peak within the expected range. The model parameters which are most effective in adjusting the peak flow for a basin are snow-covered area and melt rate. Thus, it can be seen that the snow-covered area parameter is highly important in assessing the proper performance of the SSARR model.

SSARR Reconstitutions

Let us now discuss some of the reconstitutions run for the 1975-78 water years. In each case, the initial parameters were set at the beginning of the reconstitution, observed temperature and precipitation were input, and the model then run without intervention through the whole snowmelt season. Comparisions can then

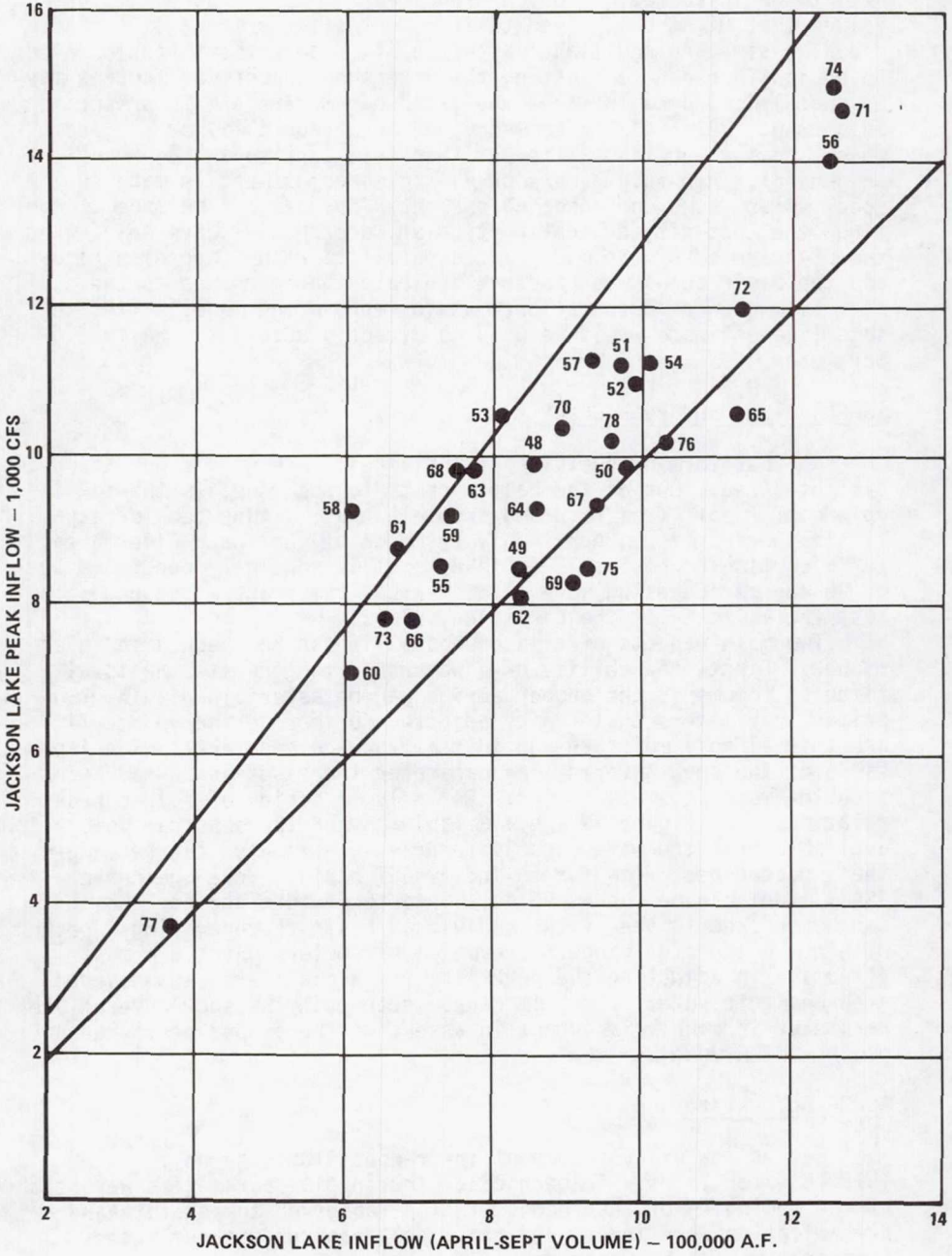


Figure 7. Jackson Lake Inflow Peak to Volume Relationship

be made between the model snow-covered area parameters, aerial snow-flight data, and the snow-covered area from the NOAA satellite. Figure 8 is a sample reconstitution plot which shows the interrelation of the SSARR model, snow flight, and NOAA satellite SCA data.

The early season snow-cover estimates from NOAA data exceeded the SSARR model snow-cover estimates for Snake above Palisades, 1977 (see figure 8); Boise above Lucky Peak, 1975 (figure 9), 1976 (figure 10), and 1977 (figure 11); and Clearwater above Dworshak, 1976 (figure 12) and 1977 (figure 13). In all of these cases the reconstitution fit early in the melt season was good, and using the satellite SCA estimate would not have improved the model performance. Using the NOAA data early in the season in 1977 would have caused overcomputing of runoffs in a year when runoff was at a record low. This was particularly true in the Lucky Peak and Dworshak basins. The probable cause of these overestimates was the large areas of thin snow cover which contributed little to runoff in this low year.

In the Hungry Horse and Libby basins there was a disparity of estimates in the opposite direction. In the early melt season for both Libby and Hungry Horse, NOAA satellite estimates of snow cover were lower than the model estimates, with the model reconstitutions fitting well in the early season. The heavy forestation in these two basins obscures some of the snow and easily causes underestimation of the snow-covered area.

Satellite SCA estimates also improve reconstitutions. The reconstitution for the Snake above Palisades in 1976 (figure 14) is a case where the early season reconstitution was not a good fit, and using the NOAA satellite SCA estimate would have improved the streamflow reconstitution. Also, the 1976 reconstitution for the Libby basin (figure 15) would have been improved using the satellite data. During the peak of the season the model tended to overcompute, and using the NOAA snow-cover data would have improved the reconstitution. At the end of the season the SSARR model was undercomputing, and using the satellite SCA estimates would have improved the model fit.

## SSARR Winter Forecast Runs

Heretofore, discussion has only been about the spring snowmelt season and the usage of satellite estimates of springtime snow cover. The estimates of snow-covered area from satellites are also important during the fall and winter season. In some ways the importance of satellite winter snow cover estimates may even be greater since no winter snow flights are made and the only information on snow cover otherwise available is from scattered point value reports from the various watersheds. Equal in consideration is the fact that for many basins the snowline can be highly variable during the winter period.

During a heavy runoff event, the actual snow-covered area can make a marked difference in the runoff that results (see figure 16). It can be seen that when rapid warming accompanied by heavy rain occurs, the resulting runoff will be markedly different depending

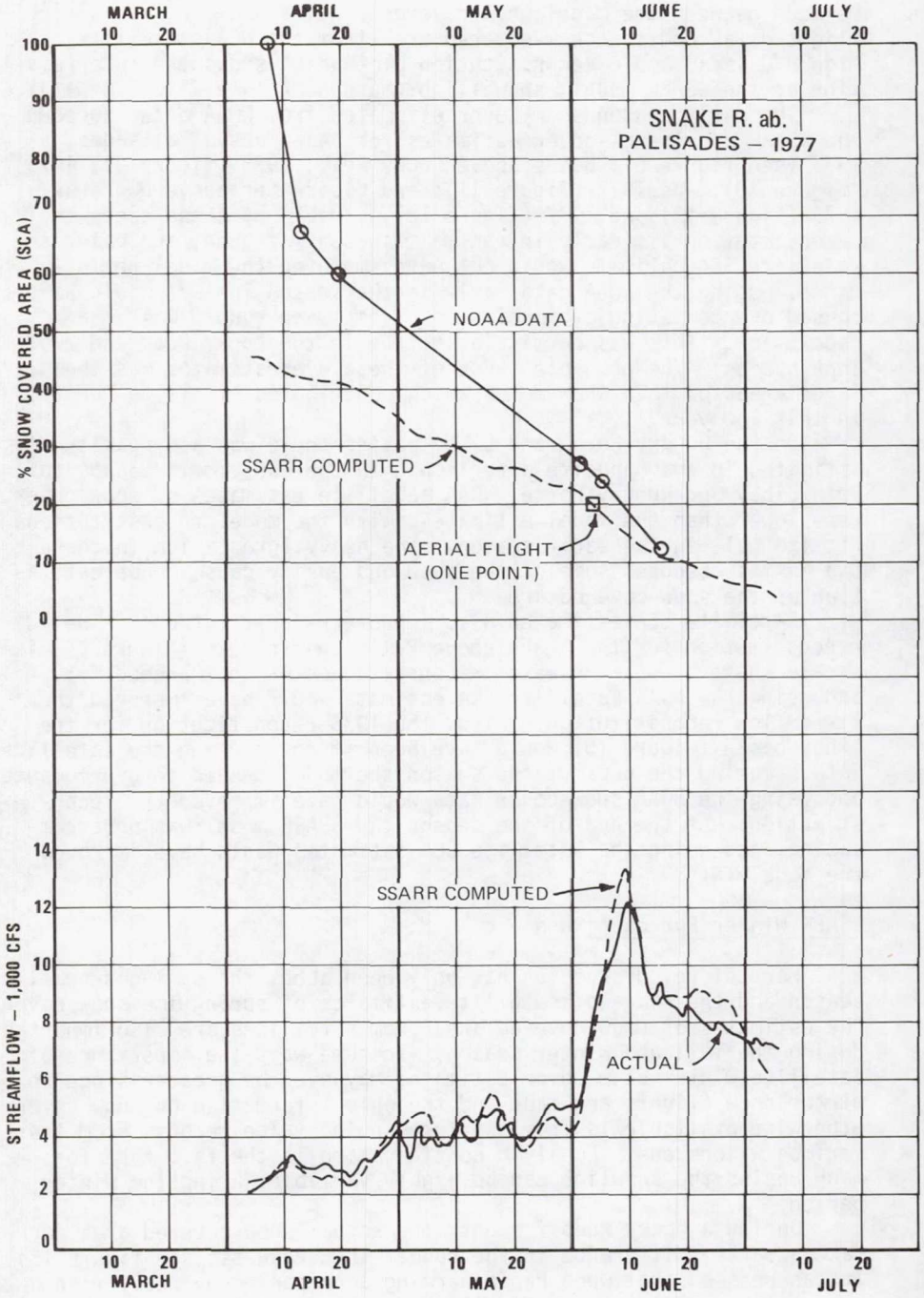


Figure 8. Snake River above Palisades - 1977

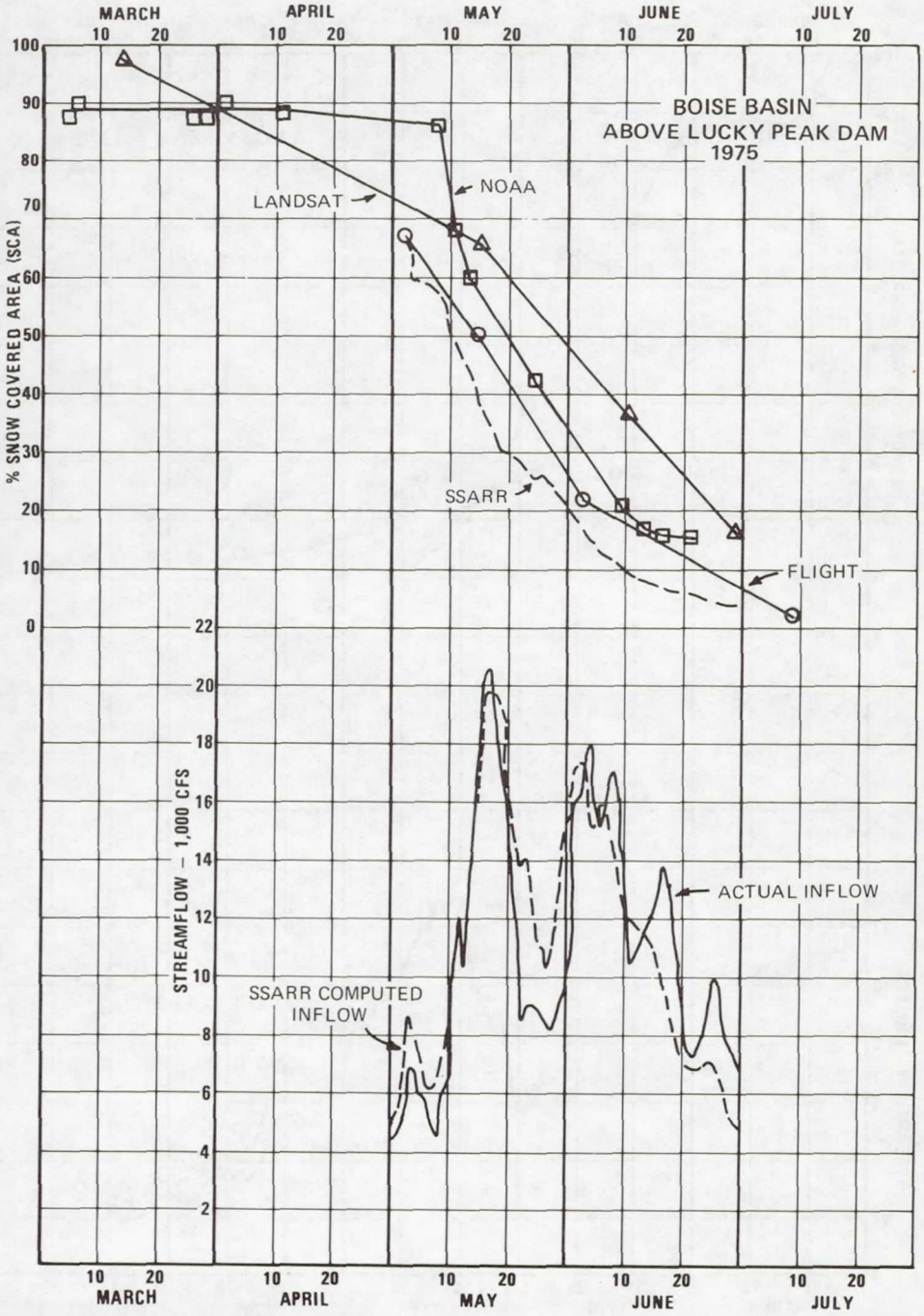


Figure 9. Boise Basin above Lucky Peak Dam - 1975

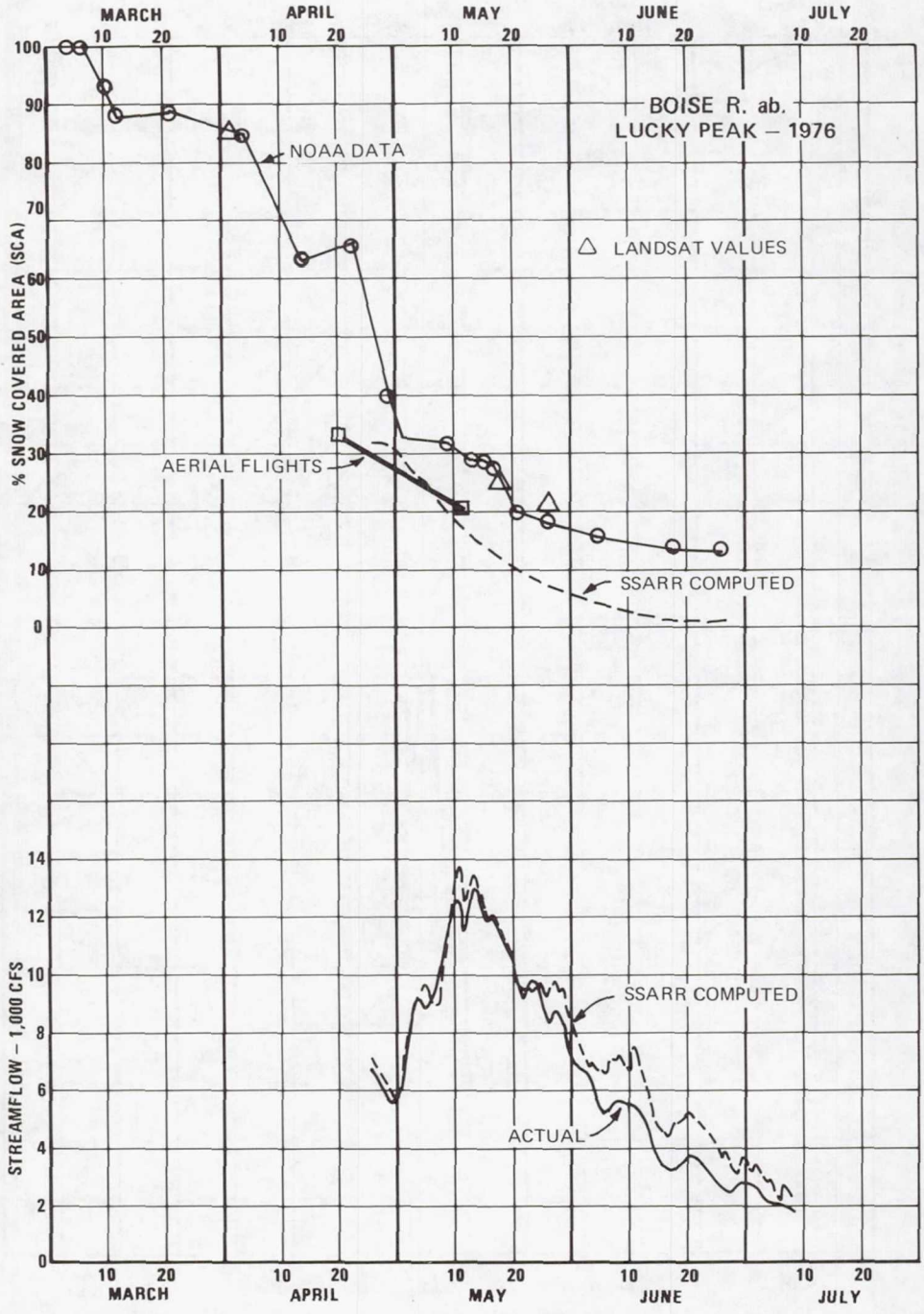


Figure 10. Boise River above Lucky Peak - 1976

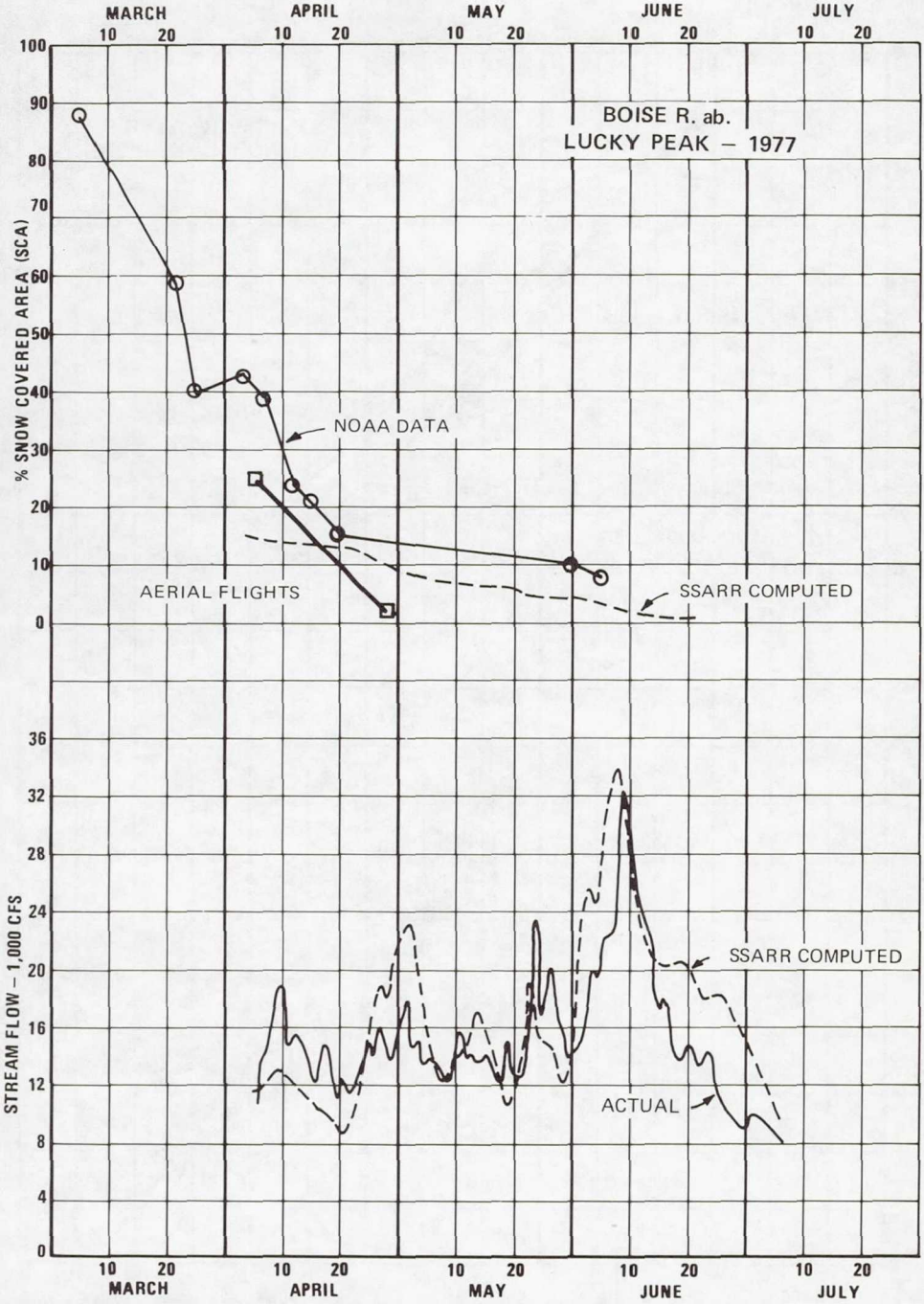


Figure 11. Boise River above Lucky Peak - 1977

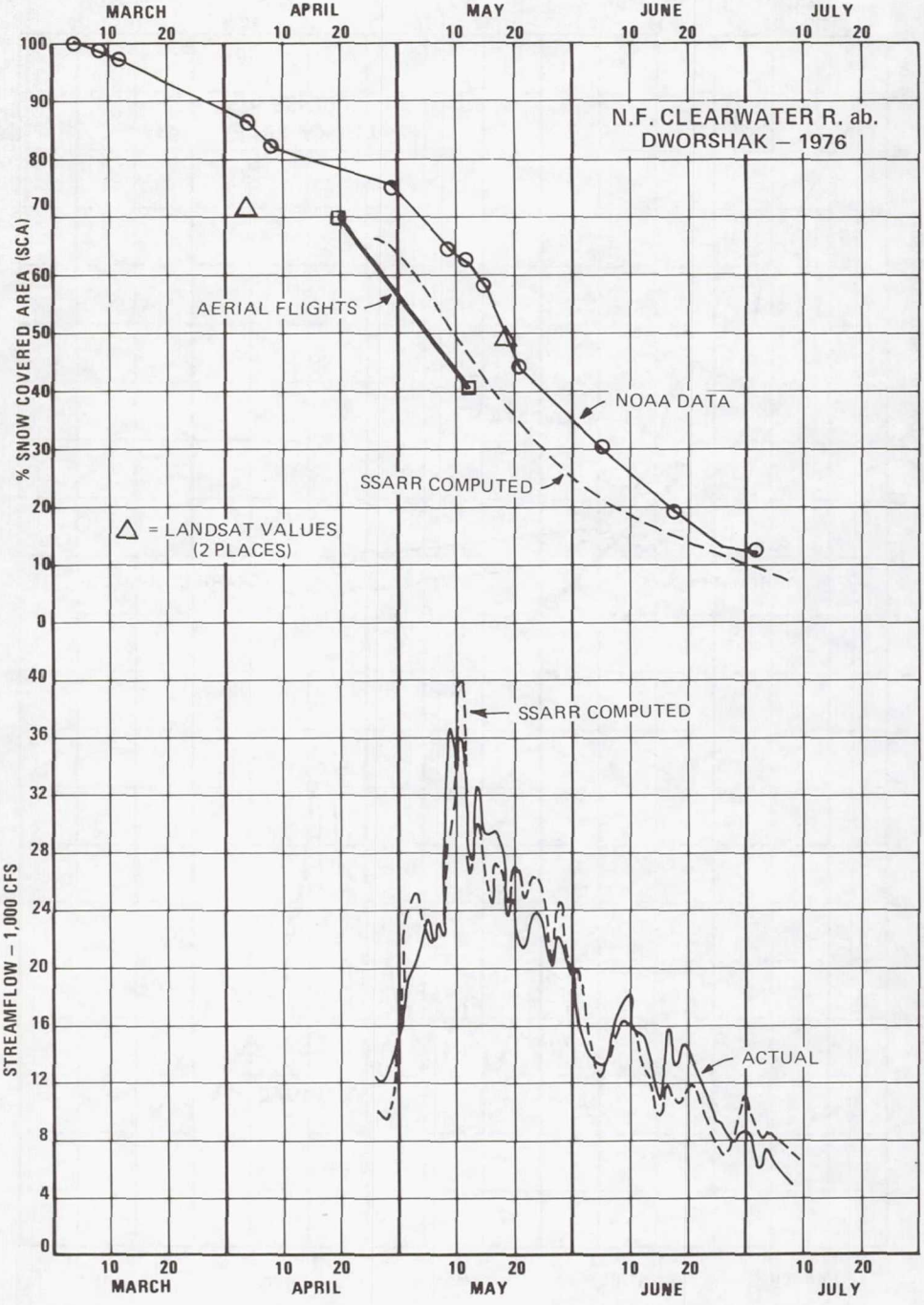


Figure 12. North Fork Clearwater above Dworshak - 1976

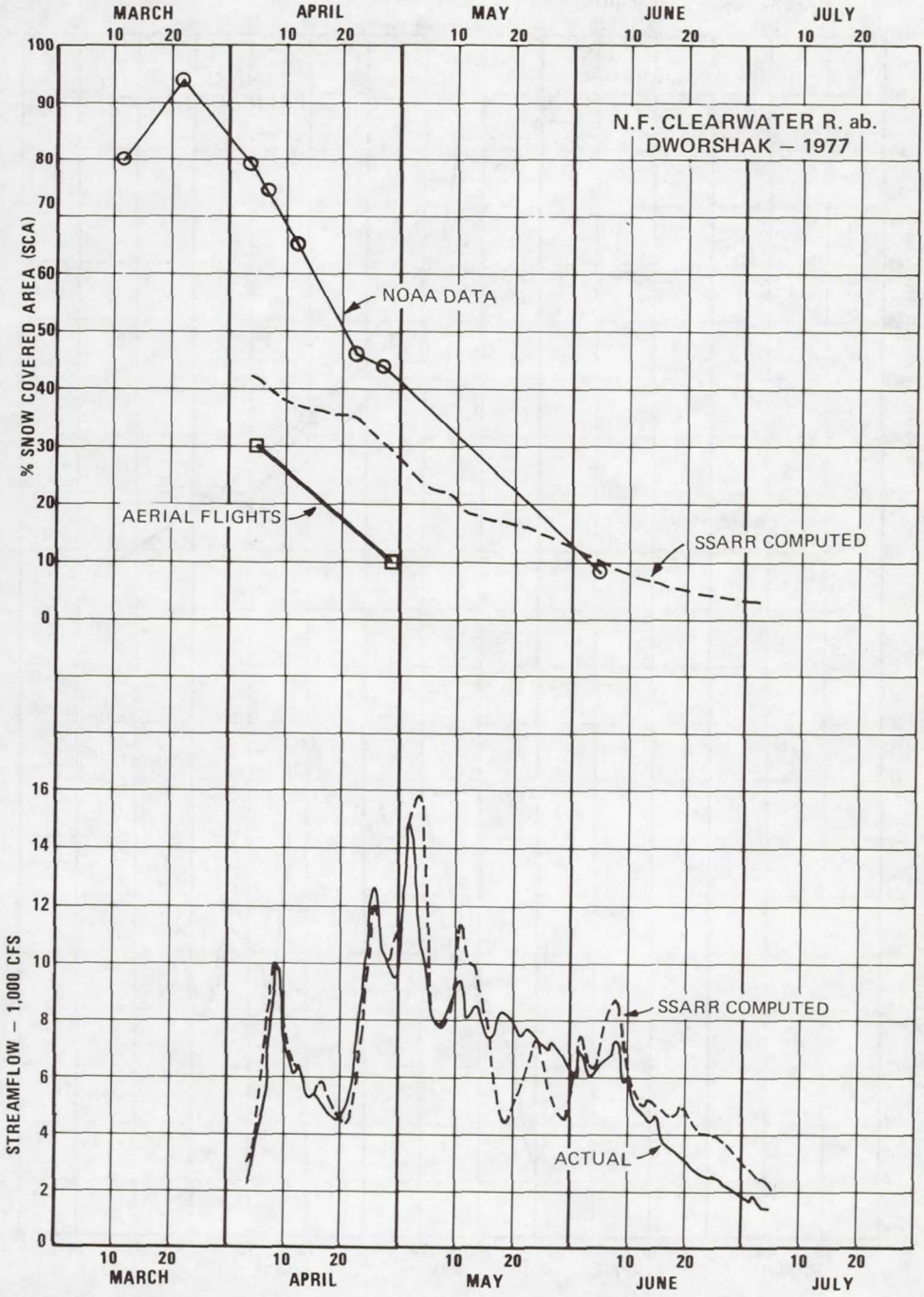


Figure 13. North Fork Clearwater above Dworshak - 1977

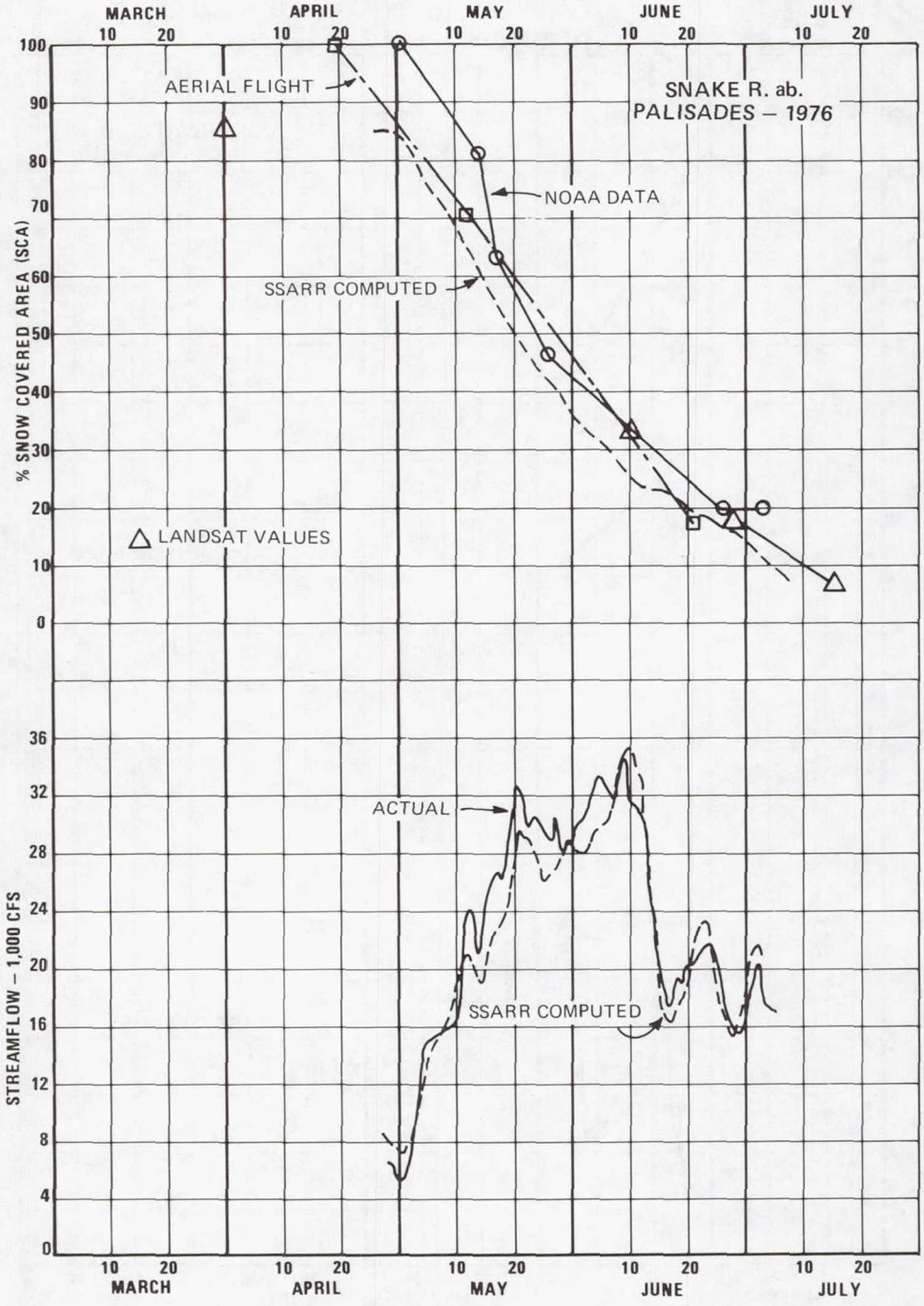


Figure 14. Snake River above Palisades - 1976

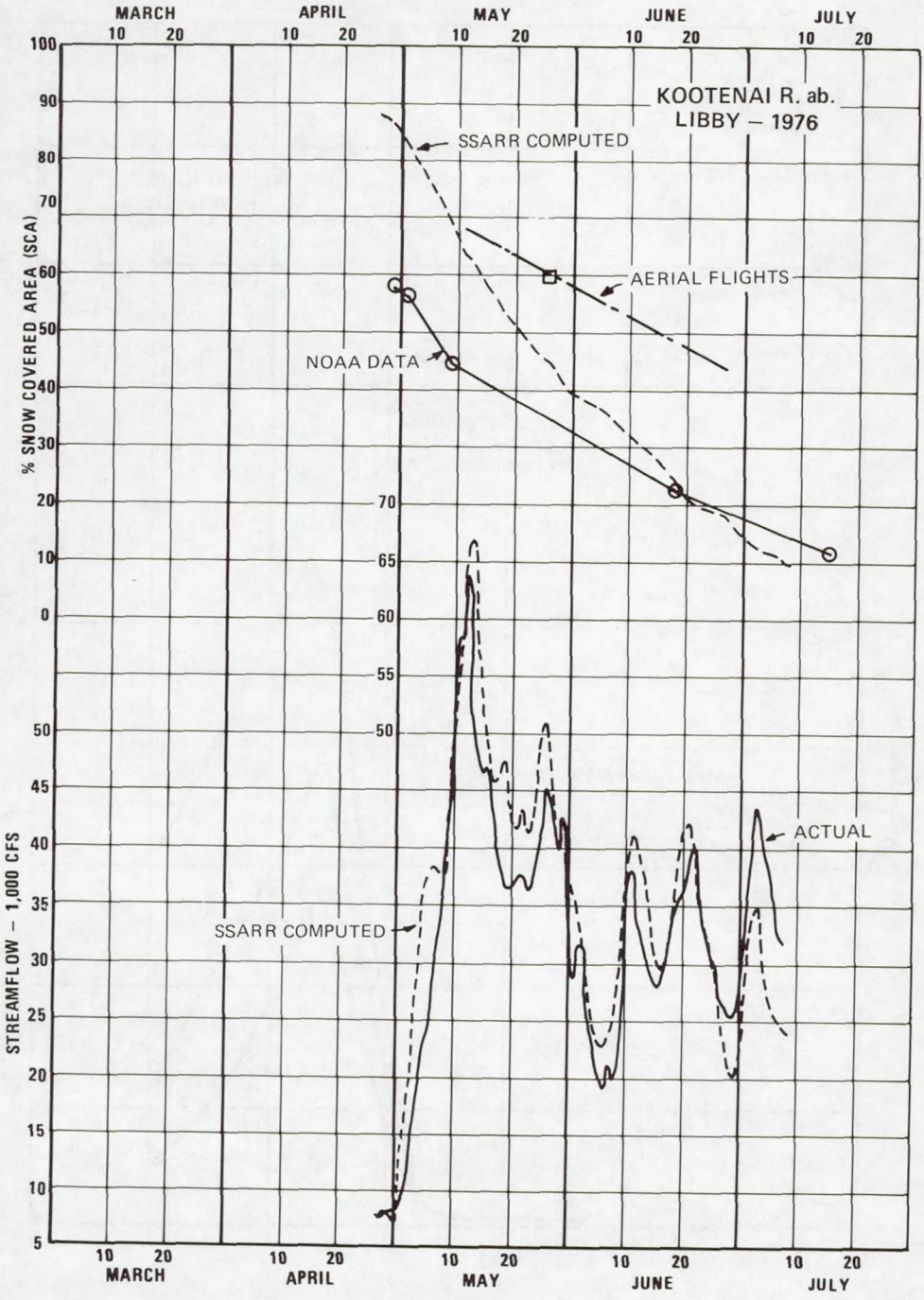


Figure 15. Kootenai River above Libby - 1976

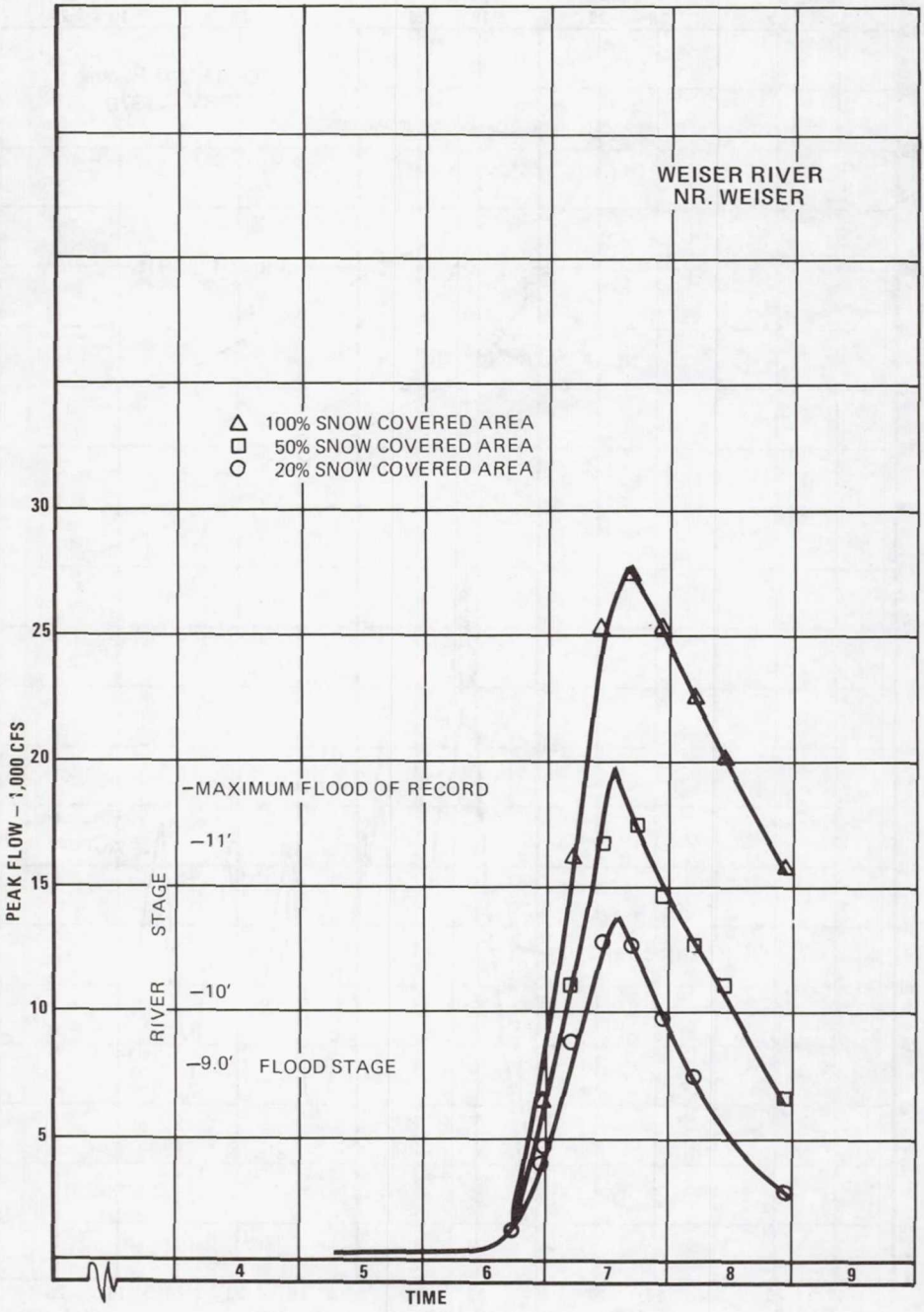


Figure 16. Weiser River near Weiser

upon the basin's initial snow-covered area. The example shown is for the Weiser River basin in central Idaho. In the one case a 5,000-foot snowline (20 percent snow-covered area) results in a rise slightly above flood stage which would cause only minor flood problems. In the extreme case with a 2,000-foot snowline and 100 percent of the basin snow covered a flood of record would occur.

## SSARR Operational Forecast Improvement

A test was made with 1978 satellite SCA data in the Boise basin to see what improvement could be made to the SSARR's daily streamflow forecasts. In this test, a dummy basin was set up in the model identical to the standard basin in all respects and for all data, except that satellite estimates of SCA were used exclusively in the dummy basin, and all available SCA data (including some satellite estimates) were used in the standard basin. These forecasting runs were made three to five times a week from April through June for a total of 49 forecasting runs. Comparisons were made for the 3-, 5-, 7-, and 14-day forecasts.

The chi-square test indicates that the dummy basin outperformed the standard basin forecasts for the 3-, 5-, and 7-day forecasts, but worsened the 14-day forecast. Both the dummy and standard basin forecasts degraded from the 14-day to the 7-day forecast, and then improved steadily as they progressed to a 3-day forecast. Based upon absolute average values, the dummy basin increased the standard basin's 14-day forecast error by 2.0 percent, but was able to decrease the forecast errors for the 7-, 5-, and 3-day forecasts by 2.7 percent, 9.6 percent, and 5.1 percent, respectively.

Of these various forecasts, the 3- and 5-day forecasts have forecasted values of temperature and precipitation. Instead of forecasted values of temperature and precipitation, the 7-day forecasts had only normal values, and the 14-day forecasts had a seasonally dependent "wow" imposed upon temperature and precipitation to account for other variables such as melt rate. Thus, the 7-day forecast is not as accurate as the 3- and 5-day forecast and the 14-day is purposely high or low to be used as a "what if" operational planning tool. Based upon this, the degradation from the 14- to the 7-day forecast is not surprising.

The dummy basin was able to reduce the forecast error of the standard basin's 5-day forecast by 9.6 percent. This is an absolute average error reduction of 190 cfs. The average computed inflow of the 49 values corresponding to the 5-day forecast is 7,291 cfs. The Geological Survey would give, at best, an accuracy to this measurement of ± 5 percent or 365 cfs. Thus, since the error reduction of 190 cfs is less than the overall accuracy of 365 cfs, the improvement gained by the exclusive use of satellite SCA data, unfortunately, is not statistically significant.

## CONCLUSIONS

Satellite-derived SCA data can be used to augment aerial snow-flight data, and vice versa. The satellite data provides many more additional SCA estimates than could be gathered from ground truth data alone. The satellite data improves forecasts, but not a statistically significant amount and, therefore, should not be used exclusively. Because of persistent cloud cover, forecasting routines should not be totally dependent upon the satellite data. The satellite data is an invaluable tool in fall and winter streamflow forecasting. Based upon the reconstitution runs, satellite-derived SCA data can be used to augment aerial snow-flight data in the Upper Snake, Boise, Dworshak, and Hungry Horse basins. The satellite data does not compare well with aerial snow-flight data in the Libby basin.

It can clearly be seen that the satellite-derived SCA data have utility in the operational forecast scheme during all periods of the year. At times the satellite data can make a critical difference in the forecasted streamflow hydrograph. Portland's Cooperative River Forecast Center has been subjectively using the satellite SCA data in conjunction with available ground truth data in its operational forecasts and will continue to do so. The River Forecast Center looks forward to an expansion of satellite snow-cover data, and also to possible use of other satellite-derived information such as soil moisture.

# LANDSAT DERIVED SNOWCOVER AS AN INPUT VARIABLE FOR SNOWMELT RUNOFF FORECASTING IN SOUTH CENTRAL COLORADO

B.A. Shafer, Soil Conservation Service, Denver, Colorado
C.F. Leaf, Consulting Hydrologist, Sterling, Colorado

## ABSTRACT

Landsat imagery for the period 1973-78 was used to calculate snow covered area on six drainages in Colorado. Snow covered area was used as a predictor variable to forecast both short-term and seasonal snowmelt runoff volumes. Operational snowcover estimation techniques were compared. The Leaf-Brink Subalpine Water Balance simulation model was adapted to use snow covered area as an input parameter to predict residual volume runoff. Areal snowcover was also used in a statistical model to forecast runoff and is compared to current water equivalent index methods of forecasting. Results indicate that Landsat derived snowcover is highly correlated with seasonal streamflow volumes. Snowcover extent is an important variable for forecast purposes once the main snowmelt season begins but is of limited value before that time.

## INTRODUCTION

Knowledge of areal extent of snowpack coverage has long been a desire of snow hydrologists for both seasonal volume prediction and flood forecasting. Until recently this desire has been largely unfulfilled due to the expense and time needed to acquire and process aerial photo coverage. Since the early 1970's satellites have made available relatively high resolution imagery on a repetitive basis from which snow covered area could be determined.

Leaf (1971) and Rango, et al. (1975) demonstrated applications of snowcover estimates in forecasting seasonal snowmelt runoff. Use of satellite derived snowcover, however, was not widespread in any major ongoing forecast program. The National Aeronautics and Space Administration (NASA) in 1974 undertook the task of demonstrating the feasibility of using remotely sensed snowcover from satellites in operational streamflow forecasting programs.

As part of their Applications Systems Verification and Transfer (ASVT) program NASA funded four demonstration projects in the Western United States to study the ways in which Landsat derived snow maps could be constructed and incorporated into existing schemes for forecasting snowmelt runoff. Further, evaluations were to be conducted in each study site to ascertain the potential improvement in forecast accuracy that could be ascribed to use of

snowcover data. The four demonstration study centers chosen were in Arizona, California, Colorado, and the Northwestern United States. This study effort within the ASVT program was called the Operational Application of Satellite Snowcover Observations (OASSO).

In Colorado three agencies were responsible for carrying out the intent of the ASVT program. The USDA Soil Conservation Service (SCS) was given lead responsibility, with assistance provided by the U.S. Bureau of Reclamation and the State of Colorado Division of Water Resources (State Engineer).

The study approach in Colorado consisted of four steps: (1) identify specific drainage basins and acquire the Landsat imagery to cover them; (2) examine various techniques of mapping the snowcover and determine which method is most useful in an operational mode; (3) develop a methodology for including snow covered area in a forecast of snowmelt runoff; and, (4) evaluate the adequacy of the forecasting techniques that employed snowcover.

## STUDY AREA

The Rio Grande Basin in Colorado was chosen as the primary drainage for study and the Upper Arkansas River as a secondary study basin. Within the Rio Grande Basin five watersheds were singled out for detailed analysis. In all, six watersheds encompassing some 9,335 $km^2$ (3,604 $mi^2$) were analyzed in the study, which corresponded to streamflow gaging stations currently forecasted by the Soil Conservation Service. They include the Arkansas River near Wellsville, Rio Grande above Del Norte, South Fork Rio Grande at South Fork, Alamosa River above Terrace Reservoir, Conejos River near Mogote, Culebra Creek at San Luis (Figure 1). The last five watersheds are in the Rio Grande Basin and flow into the San Luis Valley where they comprise the mainstem of the Rio Grande.

Both the Rio Grande and the Arkansas basins represent river systems whose primary source of water is snowmelt. The San Luis Valley is a virtual desert that could produce little in terms of agriculture were it not for the snowfed streams that enter it. Mean annual precipitation on the valley floor which averages 2,460 m (7,500 ft) elevation is only 17.8 cm (7 in) while the headwaters at elevations to 4,267 m (14,000 ft) averages 114 cm (45 in) annually. Over 80 percent of the annual flow of the Rio Grande is attributable to the snowpack contribution.

The Arkansas basin is similar to the Rio Grande. Valley floor elevations are between 2,438 m (8,000 ft) and 2,743 m (9,000 ft) and rise to heights of 4,389 m (14,400 ft). Mean annual precipitation ranges from 25 cm (10 in) on the valley floor to 102 cm (40 in) in the highest reaches of the basin. The mountain snowpack produces about 75 percent of the annual flow.

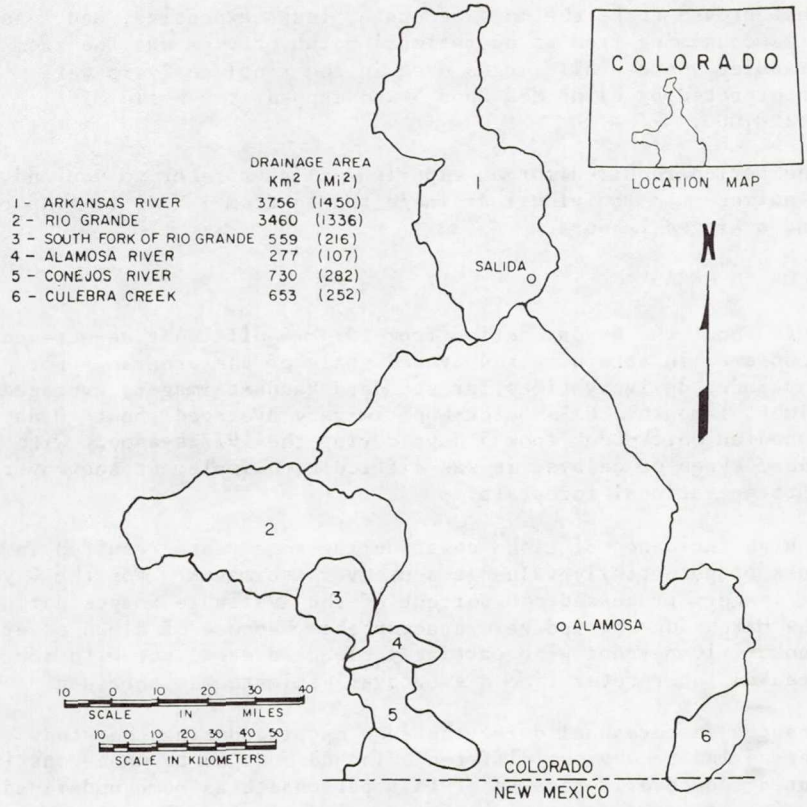


Fig. 1. Location of Colorado ASVT study drainages.

Accurate forecasts of streamflow in both the Rio Grande and in the Arkansas basins are essential for several reasons. Agricultural interests relying upon the snowmelt waters for irrigation require planning information on their prospective water supply to effectively manage their operations. Second, waters of both streams are regulated and distributed according to interstate compact agreements between Colorado and downstream states. Administration of the compact ageements in an equitable and timely manner depends upon reliable estimates of streamflow both before and during the runoff season.

## DETERMINATION OF SNOW COVERED AREA

During the period of the study six methods of mapping snowcover were investigated on one or all watersheds. They included zoom transfer scope, density slicing, color additive viewer, computer assisted classification, grid sampling, and NOAA/NESS basin snowcover maps prepared by Mr. Stanley Schneider. Each of these methods had some advantages and disadvantages. However, the technique

that proved to be the most accurate, least expensive, and least time consuming from an operational point of view was the zoom transfer scope. All images used in the final analysis were interpreted by using MSS Band 5 and mapped at a scale of 1:250,000.

The period required for an experienced interpreter to map and planimeter an individual drainage ranged from 1 hour to 4 hours and averaged 2 hours.

## PROBLEM AREAS

Throughout the 6-year period from 1973-78 difficulties were encountered in attaining the avowed goals of the program. For instance, delivery times for standard Landsat imagery averaged almost 1 month. NASA Quick-Look imagery averaged about 10 days. Canadian Quick-Look took 5 days during the 1977 season. With these types of delays, it was difficult to implement snowcover into operational forecasts.

A high incidence of cloud cover during some years resulted in the loss of potentially valuable snowcover estimates. For the 6 years of imagery processed, 40 percent of the available images during the March-June period were unacceptable because of cloud cover. Another 10 percent were partially cloud covered, but with increased interpreter time a snowcover estimate was obtained.

Changes in personnel doing the snow mapping during the study period led to obvious difference in judgment as to what constituted snowcover. Because of this personal bias some undefined degree of error creeps into the areal estimates of snow. Four of the six watersheds were completely remapped by one individual to reduce this source of error. Accuracy in mapping snowcover is certainly desirable albeit difficult to measure. More important than accuracy, however, is consistency. Without consistent interpretation from one observer to another, any technique is bound to yield questionable results. To obtain the level of consistency felt necessary for a meaningful analysis, only two interpreters performed final mapping in the Colorado study.

## SNOWCOVER IN FORECASTING

All usable images in the March-June meltout period were used to produce the snowcover depletion curves in Figures 2 through 7. These curves depict the gradual loss of watershed snowcover during the primary melt season. Although the curves were developed from only 6 years of data, they represent a fairly wide spectrum of hydrologic conditions. A frequency analysis of streamflow and snow course data reveal that the drought conditions that prevailed during the 1977 season have a recurrence interval of 100 years. The 1973 and 1975 seasons were relatively high and had a recurrence interval of 10 years.

Examination of the snowcover depletion curves shows a melt sequence that is similar from one year to the next, resulting in roughly parallel curves. The displacement of the curves with time in different years is directly related to the amount of water stored in the snowpack. In low snowpack years, melting begins and ends earlier, resulting in reduced runoff. In high snowpack years, the onset of melt is initially retarded owing to the depth of the snowpack and the increased energy requirement necessary to bring the pack to isothermal conditions. Meltout and the corresponding runoff are prolonged accordingly. Snow areal extent during the main melt period is a good measure of the water stored in the snowpack and the volume of runoff likely to be produced. This relationship appears to be valid except when large scale late season storms significantly alter the watershed mean areal water equivalent. Such an event occurred on May 8, 1978. Figure 6 shows the effects of the storm in the form of displacing the snowcover depletion curve in time from where it would normally have been. Events of a lesser magnitude have little effect, as evidenced by the same storm on the Arkansas River (Figure 2), which did not change appreciably the watershed mean areal water equivalent.

The relationship of snowcover estimates between adjacent and nearby watersheds was explored in the hope of reducing the amount of interpreter time needed to map each drainage separately. Snowcover correlations for 23 common image dates were computed among all watersheds in the study area and are shown in Table 1. Table 1 reveals that an excellent to moderate relationship exists between snowcover estimates on the various drainages. The analysis shows a distinct probability that satisfactory estimates of snowcover on adjacent watersheds can be obtained if necessary but will be subject to a varying degree of precision. The necessity might be occasioned by cloud cover obscuring a watershed, missing images, or the press of time in making forecasts of streamflow.

| Basin | Arkansas | Rio Grande | South Fork | Alamosa | Conejos | Culebra |
|---|---|---|---|---|---|---|
| Arkansas | 1.0 | .90 | .89 | .85 | .94 | .92 |
| Rio Grande | | 1.0 | .97 | .90 | .96 | .88 |
| South Fork | | | 1.0 | .94 | .98 | .92 |
| Alamosa | | | | 1.0 | .95 | .89 |
| Conejos | | | | | 1.0 | .95 |
| Culebra | | | | | | 1.0 |

TABLE 1. INTERBASIN CORRELATION OF SNOWCOVER USING 23 COMMON IMAGE DATES

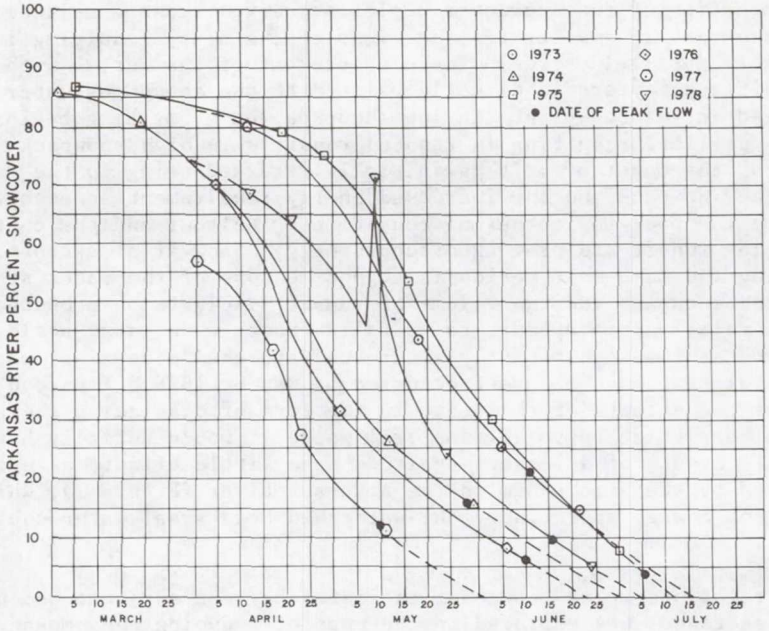


Fig. 2 Snowcover depletion curves for Arkansas River

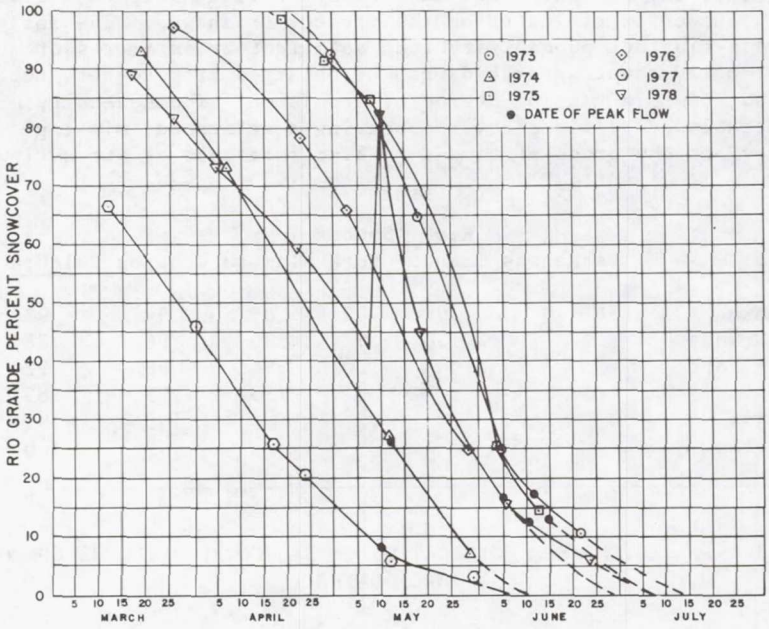


Fig. 3. Snowcover depletion curves for Rio Grande

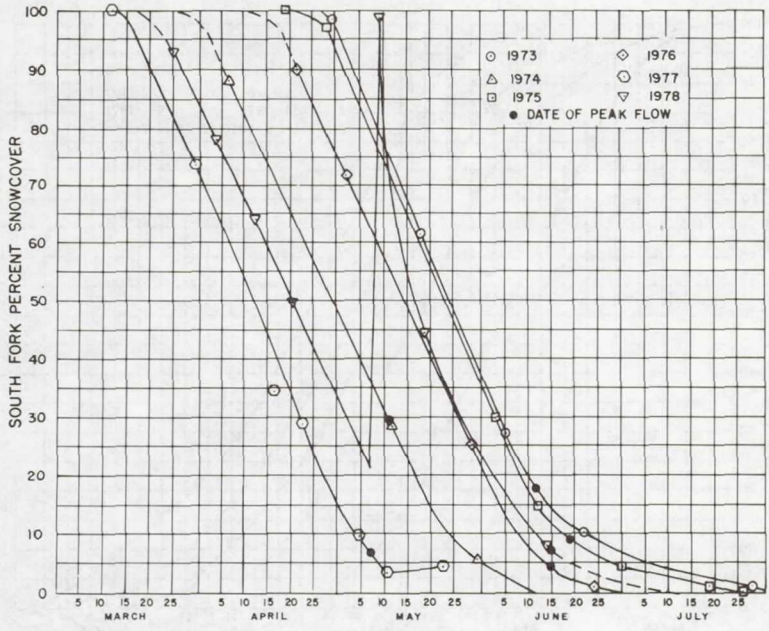


Fig. 4. Snowcover depletion curves for South Fork Rio Grande

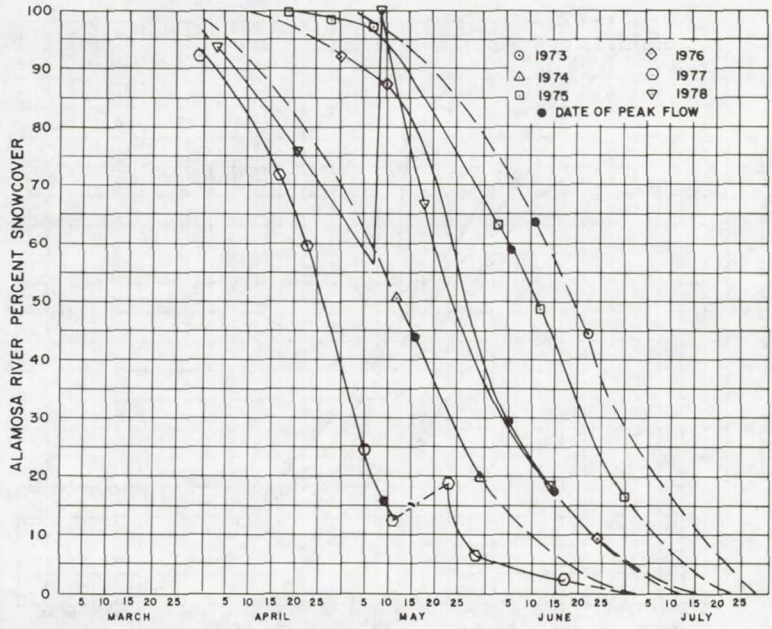


Fig. 5. Snowcover depletion curves for Alamosa River

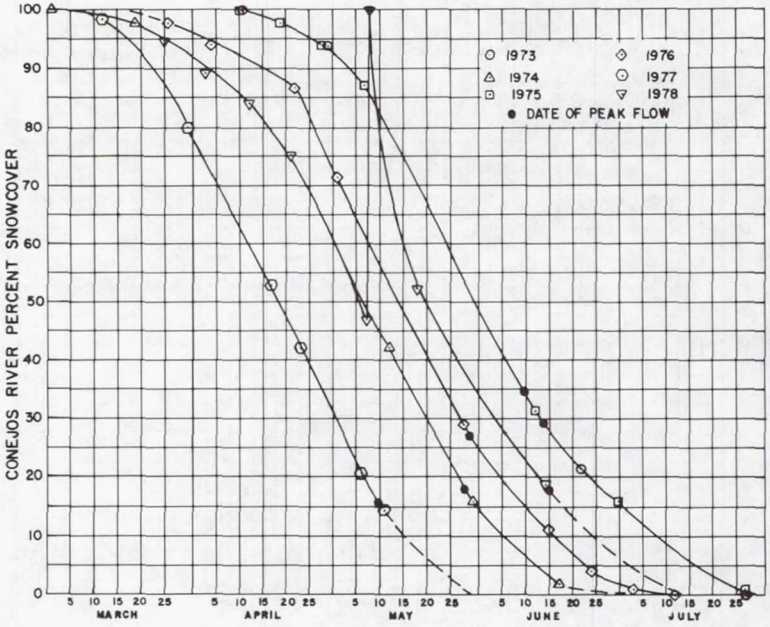


Fig. 6. Snowcover depletion curves for Conejos River

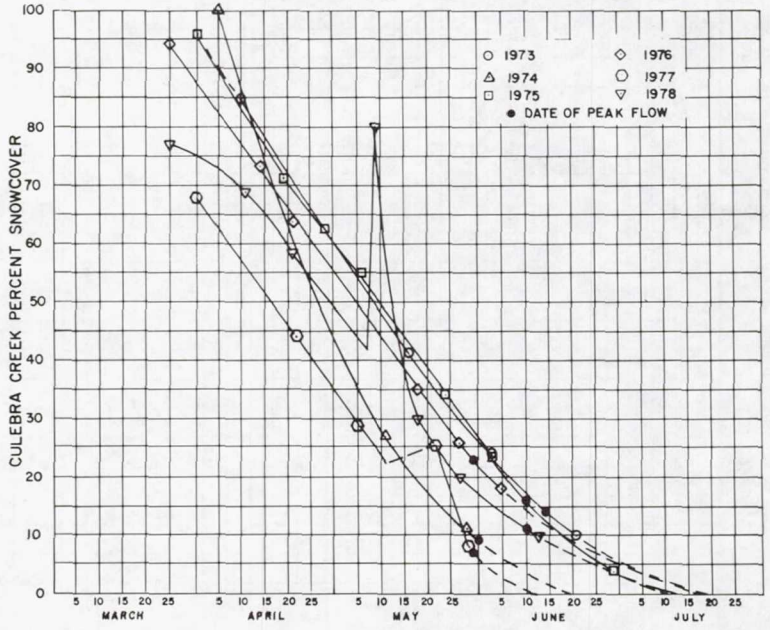


Fig. 7. Snowcover depletion curves for Culebra Creek

A statistical approach was taken to evaluate the relationship of basin snowcover to seasonal streamflow production. A simple linear regression analysis was performed between watershed snowcover on April 1, May 1, and June 1 and April-September streamflow. Snowcover values were derived from snowcover depletion curves. Table 2 summarizes the results. A high degree of correlation is apparent on all basins except Culebra Creek. A possible explanation for this exception may lie in the fact that only 40 percent of the watershed is in the main water producing zone above 3,048 m (10,000 ft), compared with between 65 and 80 percent for all other watersheds in the study. It is also the only watershed studied in the Sangre de Cristo Mountain Range. Streams in this range of mountains exhibit characteristically high coefficients of variation owing to the reduced snowmelt contribution to seasonal runoff. Their flow can be substantially influenced by the occurrence of summer convective storms.

| Basin | Number of Observations | April 1 | May 1 | June 1 |
|---|---|---|---|---|
| Arkansas near Wellsville | 6 | .96** | .87* | .89* |
| Rio Grande near Del Norte | 6 | .86* | .98** | .95** |
| South Fork at South Fork | 6 | .79 | .97** | .92** |
| Alamosa River above Terrace Reservoir | 6 | .85* | .95** | .98** |
| Conejos River near Mogote | 6 | .89* | .97** | .96** |
| Culebra Creek at San Luis | 6 | .24 | .67 | .65 |

*Significant at the 5% level.
**Significant at the 1% level.

TABLE 2. CORRELATION BETWEEN BASIN SNOWCOVER AND APRIL-SEPTEMBER VOLUME RUNOFF

In an effort to increase the sample size, snowcover on May 1 for Conejos, Alamosa and South Fork watersheds were pooled and a correlation was run against their respective April-September flows normalized to their 1963-77 averages (Figure 8). A moderately high correlation coefficient of 0.92 and a coefficient of determination of 0.85 with a standard error of 18.5 percent resulted.

Although a strong positive correlation is evidenced by the data in Table 2 and in Figure 8, it is instructive to compare them with the performance of forecast techniques using only snow course data and with techniques using both snowcover and snow course data. Snowcover and snow courses serve to index watershed moisture stored in the form of snow; both account for much the same proportion in streamflow variance and are therefore highly intercorrelated. One possible method of assessing their relative contribution in explaining the variance in runoff would be to

perform a linear multiple regression analysis with a number of snow courses and snowcover as predictor variables. Unfortunately, the length of record in this study was so short as to preclude this type of analysis.

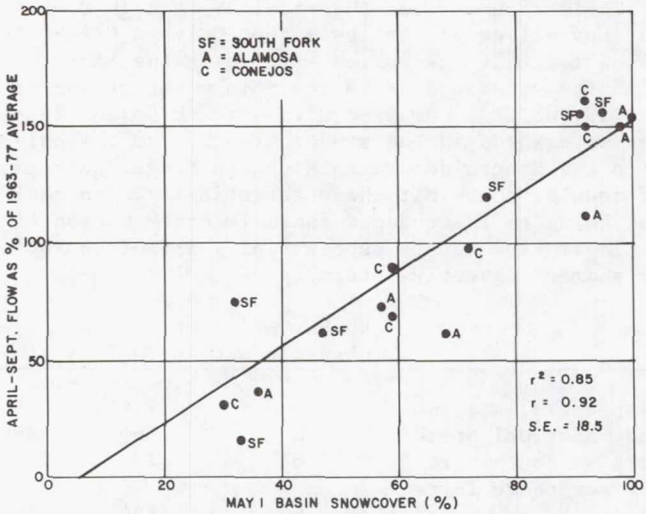


Fig. 8. Pooled linear regression analysis between snowcover on May 1 and normalized April-September streamflow.

An alternative approach was therefore devised that would indicate the improvement in forecast accuracy that might be obtained by incorporating snowcover into operational forecast techniques. A simple linear regression was calculated between a weighted snow course index consisting of snow course variables currently used to forecast each drainage on May 1 and April-September flow normalized to the 1963-77 average. A second regression was computed relating the product of the snow index and the fractional amount of snowcover on May 1 to the normalized runoff. Both of these analyses were compared to the regression analysis relating May 1 snowcover and streamflow tabulated in Table 2. Table 3 presents the results of this investigation.

In four of the six drainages addition of snow covered area to the forecast procedure improved the accuracy over snow course data alone; in one it decreased accuracy, and in one it remained unchanged. This tends to support the argument that use of snowcover can lead to better forecasts. However, care must be exercised in drawing conclusions from such a small sample.

The magnitude of snowmelt peaks is also known to be related to watershed snowpack. The date of occurrence of the maximum daily snowmelt peak is plotted on the snowcover depletion curves of Figures 2 through 7. Percent snowcover on the date of the peak

| Drainage | No. of OBS. | Variable: Weighted Snow Course Index May 1 | Variable: Landsat Snow Cover May 1 | Variable: Combined Snow Index and Snowcover May 1 |
|---|---|---|---|---|
| Arkansas | 6 | 0.985** | 0.834 | 0.895* |
| Rio Grande | 6 | 0.974** | 0.979** | 0.998** |
| South Fork | 6 | 0.907* | 0.972** | 0.981** |
| Alamosa | 6 | 0.941** | 0.946** | 0.998** |
| Conejos | 6 | 0.979** | 0.976** | 0.999** |
| Culebra | 6 | 0.881* | 0.670 | 0.874* |

*Significant at 5% level.
**Significant at 1% level.

TABLE 3. SIMPLE CORRELATION COEFFICIENTS BETWEEN INDICATED VARIABLES AND APRIL-SEPTEMBER FLOW NORMALIZED TO 1963-77 AVERAGE.

flow was correlated with the discharge. Table 4 summarizes the results of this analysis. A high correlation is observed between peak discharge and watershed snowcover. Correlations range from 0.81 on Culebra Creek to 0.96 on the Alamosa River. This relationship is of sufficient accuracy to be considered useful in making forecasts of peak flows. Making a forecast of the date when the peak will occur is much less precise. A review of the snowcover depletion curves shows that with few exceptions the peaks generally occurred in a range of about 15 percent in the last third of the melt period.

| Basin | Number of Observations | Correlation Coefficient |
|---|---|---|
| Arkansas near Wellsville | 6 | .88* |
| Rio Grande near Del Norte | 6 | .99** |
| South Fork at South Fork | 6 | .94** |
| Alamosa Creek above terrace | 6 | .96** |
| Conejos River near Nogote | 6 | .93** |
| Culebra Creek at San Luis | 6 | .81* |

*Significant at the 5% level.
**Significant at the 1% level.

TABLE 4. CORRELATION BETWEEN BASIN SNOWCOVER ON MAY 1 AND MAXIMUM DAILY SNOWMELT PEAK

## Computerized Short-Term Streamflow Forecasting

Statistical and graphical methods are reliable tools for making seasonal forecasts. However, extensions of these early-spring forecasts to a short-term basis using such methods is difficult, because precipitation and meteorological conditions during the ensuing melt season can vary widely from year to year. Because short-term forecasts that respond to varying hydrometeorological conditions are becoming increasingly important in water resource management, several procedures have been developed for making such forecasts. For example, one method used by the National Weather Service is the "Extended Streamflow Prediction (ESM)" model (Twedt, *et al.*, 1977).

In Colorado, the Subalpine Water Balance model developed by Leaf and Brink (1973a, 1973b) is being used for making and updating residual streamflow forecasts. Updating of this model during the snow accumulation season is accomplished by means of the SCS Snow Telemetry (SNOTEL) system. During the snowmelt season, when snowcover on the watershed is less than 100 percent, forecasts are revised on the basis of the percent snowcover and associated residual water equivalent.

### SUBALPINE WATER BALANCE MODEL FORECASTING PROCEDURE

The Subalpine Water Balance model was developed by the USDA Forest Service to simulate daily streamflow. This model simulates winter snow accumulation, shortwave and longwave radiation balance, snowpack condition, snowmelt and subsequent runoff on as many as 25 watershed subunits. Each subunit is described by relatively uniform slope, aspect, and forest cover. The simulated water balances on each subunit are compiled into a "composite overview" of an entire drainage basin.

Detailed flow chart descriptions and hydrologic theory have been published (Leaf and Brink 1973a, 1973b). Operational computerized streamflow forecasting procedures using the Subalpine Water Balance model are keyed to real-time telemetered snowpack (SNOTEL) data and satellite imagery. Landsat and SNOTEL data are used to update the model at any time by means of "control curves" for a given drainage basin which relate:

1. Satellite snowcover data to residual water equivalent on the basin and

2. SCS SNOTEL data to area water equivalent on the basin.

With these relationships, simulated residual volume streamflow forecasts can be revised as necessary to reflect the current meteorological conditions and the amount of snow.

MODEL CALIBRATION

During the study period, the Subalpine Water Balance model was calibrated to several index watersheds in the Rio Grande and Arkansas River basins as follows:

1. Rio Grande Basin
   a. Conejos River near Mogote
   b. Culebra Creek near Chama
   c. Rio Grande River above Wagonwheel Gap
   d. South Fork at South Fork

2. Arkansas Basin
   a. Arkansas River above Salida

All are key headwater tributaries that characterize the hydrologic regimes of the two basins. Table 5 summarizes pertinent geographic characteristics of each.

| Watersheds | Drainage Area ($km^2$) | Mean Elev. (m m.s.l.) | Aspect | No. Subunits[1/] |
|---|---|---|---|---|
| Conejos River | 730 | 3,200 | SE | 20 |
| Culebra Creek | 189 | 3,185 | W | 12 |
| Upper Rio Grande | 2,090 | 3,475 | E | 10 |
| South Fork | 559 | 3,124 | NE | 4 |
| Arkansas | 3,155 | 3,125 | SSE | 11 |

[1/] Includes all forested and open areas.

TABLE 5. GEOGRAPHIC CHARACTERISTICS OF COLORADO ASVT INDEX WATERSHEDS

Areas of the index watersheds vary from 189 $km^2$ (73 $mi^2$) (Culebra Creek) to 3,155 $km^2$ (1,218 $mi^2$) (Upper Arkansas), and the number of subunits used to characterize a given watershed varied from 4 (South Fork) to 20 (Conejos River). This range of size and level of detail has indicated that the model performs well on both large and small watersheds.

Figure 9 shows observed vs. simulated runoff on a water-year basis for the Conejos River for 1958-71. Having fixed model parameters for 1958-71, four subsequent years (1972-75) were then used for validation. These results are shown in Table 6.

Observed vs. simulated runoff from the South Fork are plotted in Figure 10. The calibration period on this basin was 1973-77.

FORECASTING SYSTEM DESIGN

The way in which the Subalpine Water Balance model is used to update streamflow forecasts is schematically illustrated in Figure 11. The primary model response is area snowpack water equivalent, and this variable is plotted as a function of time in Figure 11. Typically, the snowpack builds to a "peak" in late spring. To the left of this peak is the winter snow accumulation season (100 percent snowcover) and to the right is the snowmelt runoff (snowcover depletion) season.

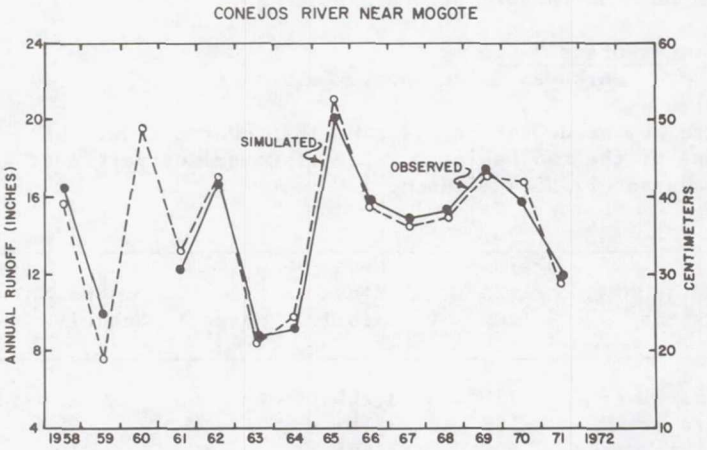


Fig. 9. Simulated vs. observed annual runoff, Conejos River 1958-71

| Year | October 1 - September 30 Runoff in cm(in) | |
|---|---|---|
| | Simulated | Observed |
| 1972 | 21.8 (8.6) | 20.3 (8.0) |
| 1973 | 51.0 (20.1) | 55.4 (21.8) |
| 1974 | 27.7 (10.9) | 24.1 (9.5) |
| 1975 | 46.7 (18.4) | 46.2 (18.2) |

TABLE 6. OBSERVED VS. SIMULATED STREAMFLOW, CONEJOS RIVER, 1972-75.

Control Functions

As seen in Figure 11, primary control of the hydrologic model during the winter months is from SNOTEL, whereas during snowmelt runoff, control of the model derives from Landsat. If field data obtained from these two systems indicate that the model is over or under predicting the snowpack, measures can be taken through use

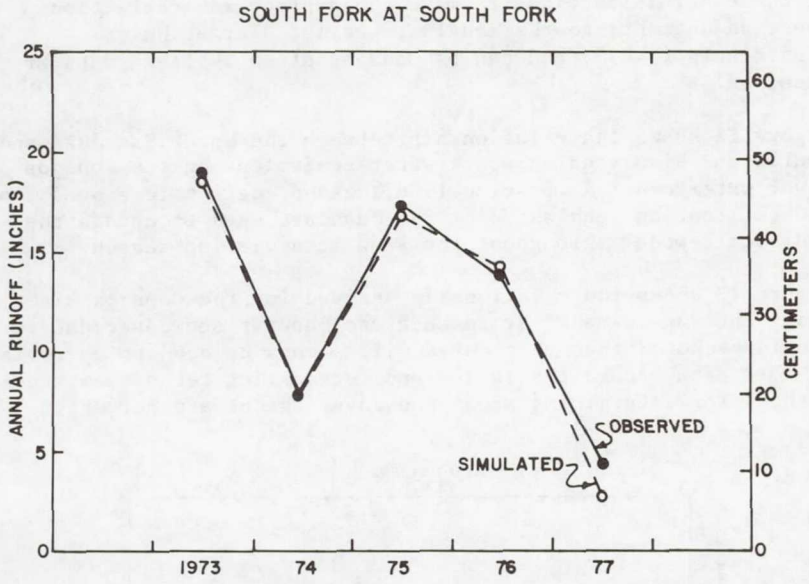


Fig. 10. Simulated vs. observed annual runoff, South Fork 1973-77

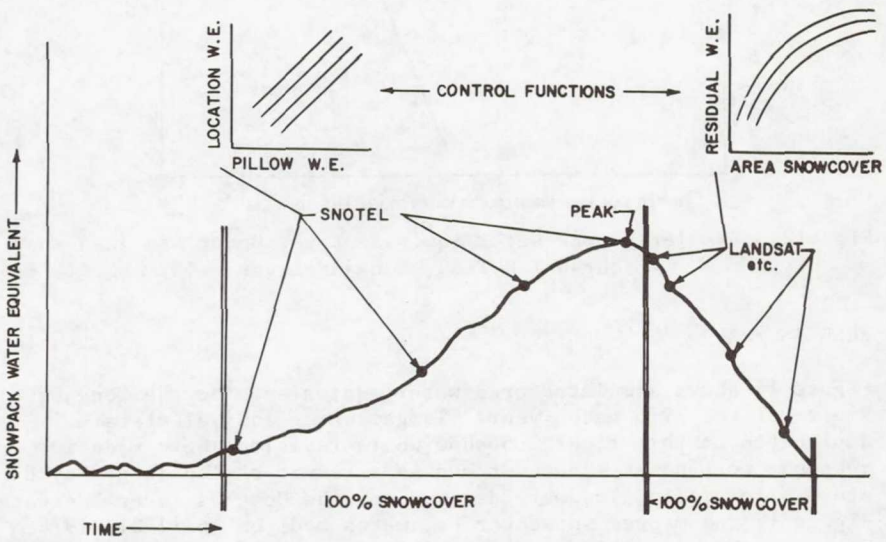


Fig. 11. Colorado ASVT short-term forecasting model configuration

of the control functions to make the appropriate correction. These adjustments to the model are called "Target Water Equivalents (TWE)", and can be made as often as field data are received.

Figure 12 shows the relationship between the Upper San Juan snow course and simulated snowpack water equivalent on the Conejos River watershed. As previously discussed, data telemetered from a SNOTEL location such as Upper San Juan are used to update the hydrologic model throughout the snow accumulation season.

Figure 13 shows the relationship derived for the Conejos River by using the Subalpine Water Balance and Landsat snowcover data. It should be noted that this curve will always be subject to revision as more data become available, and forecasting techniques and methods for determining areal snowcover extent are perfected.

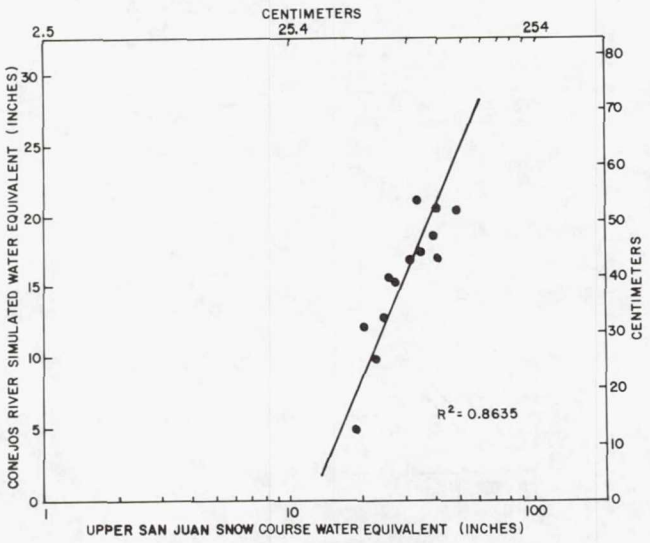


Fig. 12. Simulated peak water equivalent vs. Upper San Juan snow course (SNOTEL), Conejos River

RESULTS

Figure 14 shows simulated area water equivalent for the Conejos River for the 1978 water year. Target water equivalents are designated on this figure to show where revisions were made in response to Landsat snowcover and as a result of the large May 8 storm. Initially, TWE were derived for the Conejos River based on Figure 12 and mapped snowcover estimates made on April 21, 1978. However, the year 1978 was unusual in that peak area water equivalent on the Conejos was substantially less than indicated by

Figure 12. Thus, initial TWE were revised downward to approximately 25.4 cm (10 in) as opposed to 35.5 cm (14 in) based on the amount of snow accumulation at the Upper San Juan SNOTEL site.

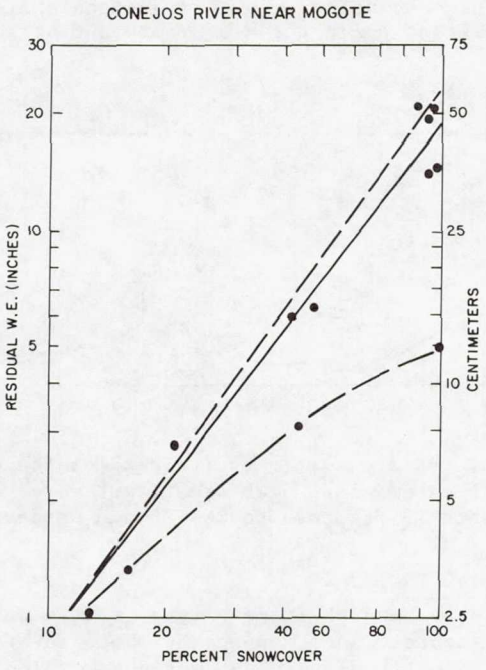


Fig. 13. Preliminary relationship showing residual water equivalent as a function of snowcover on the Conejos River. The lower curve was derived from the 1978 snowmelt season.

On April 21, snowcover extent was 75 percent which corresponded to less than 10.2 cm (4 in) of area water equivalent for 1978 (Figure 13). As seen in Figure 14, relatively minor but significant increases in snowpack were made through use of the TWE. Soon after the first adjustment, SNOTEL indicated that Upper San Juan snowcover gained 13.5 cm (5.3 in) of water equivalent between April 30 and May 10. Also, data from Landsat on May 8 showed that snowcover on the Conejos River was 100 percent. In response to this information, TWE were adjusted upward.

Total runoff for the 1978 water year was 30.5 cm (12 in) as compared to a simulated 31 cm (12.2 in) based for the most part on the original estimates of snowpack water equivalent. Subsequent corrections using the TWE capabilities in the model increased the initial residual streamflow estimates perhaps 2.5 cm (1 in). The increase in snowpack on the Conejos, as the result of the May upslope storm, was satisfactorily simulated by the model without appreciable corrections using TWE.

## SUMMARY AND CONCLUSIONS

Use of snow areal extent measurements in snowmelt runoff prediction shows promise but with the short period which the study encompassed it is difficult to assess its long range impact. However, a number of conclusions can be drawn concerning the use of snowcover in forecasting in the Rio Grande and Arkansas basins.

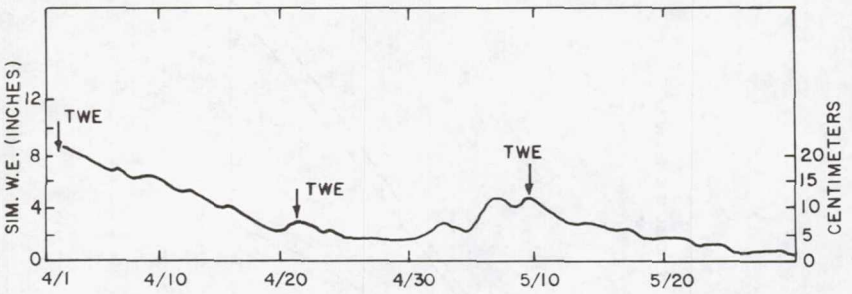


Fig. 14. Simulated area water equivalent for the Conejos River for the 1978 water year. TWE are target water equivalent adjustments in response to SNOTEL and Landsat data.

Currently available Landsat imagery is of sufficient quality and resolution for accurate snow mapping by photo interpretative means. Delay in image delivery, occurrence of cloud cover, and a nine-day interval between satellite coverage diminish to a significant extent the amount of reliance one can place in using snowcover as a forecast parameter.

Two methods of using snow covered area in forecasting have been explored and have proven successful. A statistical regression model relates snowcover to seasonal volume flow directly. A computerized simulation model provides short-term and seasonal forecasts using snowcover as an input variable. Results indicate about a ten percent reduction in average forecast error can be realized through use of satellite derived snowcover in forecast procedures.

A significant drawback to using snow covered area exclusively to make streamflow predictions is the lack of applicability prior to commencement of the main snowpack recession which normally occurs after May 1. Water management decisions frequently need to be made late in March and in April, necessitating streamflow forecasts before snowpack depletion gets well underway. For this reason, present forecast methods utilizing snow course and precipitation data will continue to be used. Use of snow covered area in hydrologic models and statistical prediction techniques in late

spring will be valuable as an independent method of checking the standard forecasts now being produced.

As successive years of satellite imagery are accumulated covering a wider range of hydrologic and climatic conditions forecasts can be expected to improve through the use of snow mapping. Satellite snow mapping together with improvements in remote hydrometeorological data collection systems will enable more frequent and accurate forecasts because of increased knowledge of what is happening in the major water producing zone above valley floors.

## References


Leaf, C.F. (1971) Areal snowcover and disposition of snowmelt runoff in Central Colorado, USDA Forest Service, Research Paper RM-66, Fort Collins, Colorado, 19 pp.

Leaf, C.F. and G.E. Brink (1973a) Computer simulation of snowmelt within Colorado subalpine watershed, USDA Forest Service, Research Paper RM-99, Fort Collins, Colorado, 22 pp.

Leaf, C.F. and G.E. Brink (1973b) Hydrologic simulation model of Colorado subalpine forest, USDA Forest Service, Research Paper RM-107, Fort Collins, Colorado, 23 pp.

Rango, A., V.V. Salmonson, and J.L. Foster (1975) Seasonal streamflow estimation employing satellite snowcover observation, X-913-75-26, Goddard Space Flight Center, Greenbelt, Maryland, 34 pp.

Twedt, Thomas M., J. C. Schaake, Jr., and E. L. Peck (1977) National Weather Service extended streamflow prediction, Proc. Western Snow Conference, pp. 52-57.

**Page intentionally left blank**

# A GRAPHICAL METHOD OF STREAM RUNOFF PREDICTION FROM LANDSAT DERIVED SNOWCOVER DATA FOR WATERSHEDS IN THE UPPER RIO GRANDE BASIN OF COLORADO

George F. Moravec and Jeris A. Danielson, Division of Water Resources, Colorado Department of Natural Resources, Denver Colorado

ABSTRACT

Graphical methods of stream runoff prediction are empirical in nature and demonstrate general relationships among selected parameters affecting snowmelt and runoff. Two watersheds examined in the Upper Rio Grande Basin of Colorado exhibit a unique relationship among snowcover depletion, time and runoff. Snowcover data derived from Landsat has shown that for six years of record snow line regression followed similar patterns. A family of curves were developed for the drainage basins by plotting snow areal extent with time for each Landsat pass. Each year of data produced a curve which was displaced from the others by a near logarithmic relationship based on total annual streamflow. This relationship was used to predict the lowest streamflow on record for the watersheds in 1977. Application of the graphical method to the Upper Arkansas River basin was not successful and revealed definite limitations in the method. The graphical method demonstrates the direct use of satellite snowcover data in stream runoff forecasting. In addition, a method using indexed base lines was developed to estimate snowcover for a watershed from marginal images due to cloud cover. The accuracy of estimates is dependent upon watershed characteristics, index line frequency, and the number of index lines visible for a given image.

## INTRODUCTION

In 1974, the U. S. Department of Agriculture, Soil Conservation Service Snow Survey and the Colorado Division of Water Resources began a cooperative study through NASA's Applications Systems Verification and Transfer (ASVT) program on Operational Applications of Satellite Snowcover Observations. The objective of the study was to determine the usefulness of satellite derived snowcover mapping to prediction of watershed seasonal volume

of runoff and streamflow resulting from snowmelt. At the beginning of the program there was no proven method for using satellite derived snowcover information to predict annual or seasonal volume of runoff or streamflow. As an early attempt to evaluate the significant relationships between snow areal extent and runoff, a simplified graphical approach was investigated as well as a review of previous work in the area of snow hydrology. Annual, seasonal and short term runoff forecasts are an important part of stream administration throughout the state of Colorado.

## Study Area

The upper Rio Grande drainage of Colorado was chosen as the primary study area and the Upper Arkansas River as a secondary basin (Figure 1). Within the Rio Grande drainage basin, five watersheds were identified for study, two of which were selected to test graphical methods of annual runoff prediction from snowmelt. These two basins are the Conejos River drainage and South Fork of the Rio Grande drainage. The Upper Arkansas River basin was included in the study to determine the limits of graphical prediction applications. The Conejos and South Fork basins are hydrologically similar in some respects but have certain physiographic characteristics which are significantly different. Hydrologic similarities are reflected by the repeated snowline recession patterns year after year, similar area-altitude distribution and altitude range. Physiographic differences are evident when the basins are compared. The South Fork of the Rio Grande basin is more or less symmetrical, with its length and width nearly equal, and its orientation is to the north. The Conejos, on the other hand, is an elongated, curved basin of irregular form oriented primarily east-west. Both the Conejos River and South Fork are moderate size basins, 734.4 $km^2$ (282 $mi^2$) and 562.5 $km^2$ (216 $mi^2$) respectively, while the Arkansas is a large basin, 3,171.9 $km^2$ (1,218 $mi^2$). Elevations for the Conejos River and South Fork of the Rio Grande drainages range from 2,460 m (7,500 ft) to over 3,963 m (13,000 ft) while elevations for the Arkansas River drainage range from 2,195 m (7,200 ft) to over 4,267 m (14,000 ft). Precipitation ranges from 17.8 cm (7 in.) on the floor of the San Luis Valley to 114 cm (45 in.) at the head of the watersheds. Nearly 80 percent of the water in the Rio Grande comes from snowmelt.

## The Graphical Method of Runoff Prediction

The graphical approach to solving problems and isolating significant variables in cause and effect relationships is probably

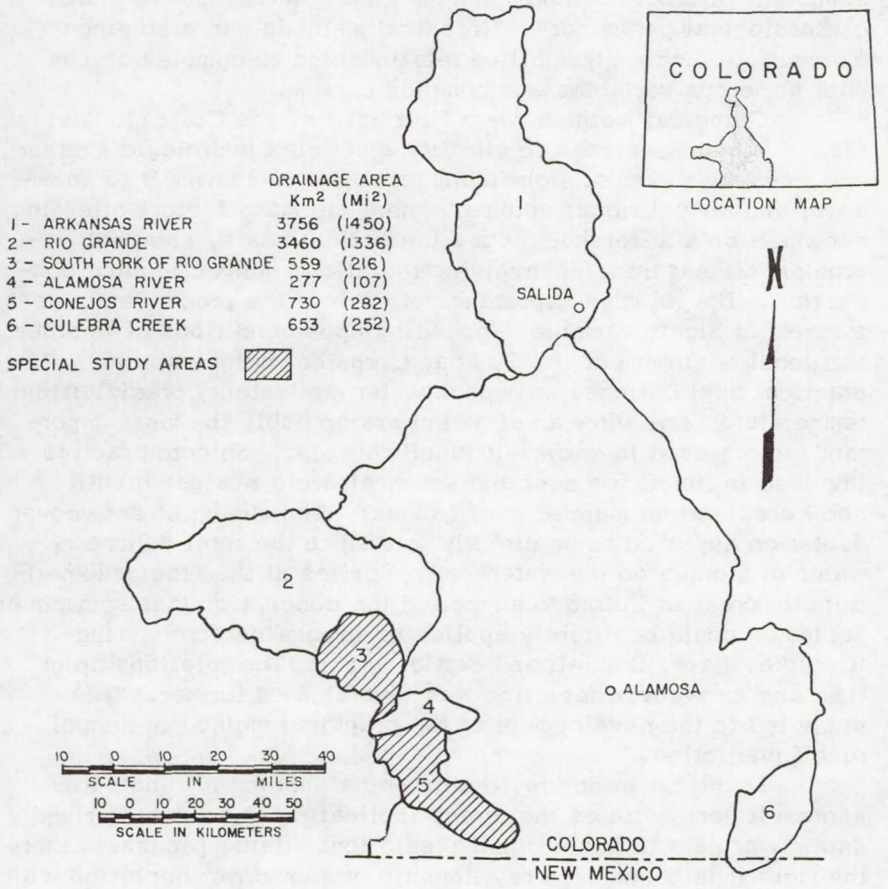


Figure 1. Index map of the study area.

one of the oldest techniques in the scientific method. The results are quite often empirical in nature particularly in a highly complex system such as snow hydrology. Graphical methods as applied to snow hydrology are mentioned in some detail in the U. S. Army Corps of Engineers' manual of Snow Hydrology (1956). Standard seasonal and annual forecast methods may range from multiple linear regression analysis using snow courses as indices to the complex hydrologic simulation model using numerous basin and climatological parameters. Graphical methods can also range from simple single straightline relationships to complex graphs with numerous variables and complex curves.

Graphical methods were first used by the Colorado Division of Water Resources to simplify a complex hydrologic system and to relate the most significant variables of snowmelt to snowcover and annual runoff volume. There are many factors affecting snowmelt on a watershed. On a theoretical basis, snowmelt is a problem of heat transfer involving radiation, convection and conduction. The relative importance of each of the processes of heat transfer is highly variable, depending upon conditions of weather and local environment (U. S. Army Corps of Engineers, 1960). In practical applications, snowpack water equivalent, precipitation, temperature, and snow areal extent are probably the most important factors used in snowmelt runoff forecast. Selected factors involved in runoff forecast and snowmelt were evaluated with snow areal extent mapped from Landsat. The timing of snowcover depletion appeared to be directly related to the total volume of water in storage on the watershed. Studies at the Frasier Experimental Forest in Colorado supported the conclusion that snowcover depletion could be directly applied to streamflow forecasting (Garstka, Love, Goodell and Bertle, 1958). The relationship of time and snowcover depletion was investigated further. This study led to the development of the graphical method of annual runoff prediction.

Empirical in nature, the graphical method of runoff from snowmelt demonstrates the direct application of Landsat derived snowcover data to basin runoff prediction. Using Landsat imagery, the method is based on a relationship of snowcover depletion with time. The method consists of two graphs. The first is a comparison of time and percent of snow areal extent remaining for a given basin (Figure 2). The second graph is a semi-logarithmic plot of annual runoff volume for the basin and linear displacement of annual snow area depletion curves measured from the first graph (Figure 3). Annual runoff volume is read directly from the second graph in cubic meters (ac-ft).

The first graph (Figure 2) is a family of similar curves comparing time to the percentage of snowcover remaining on a

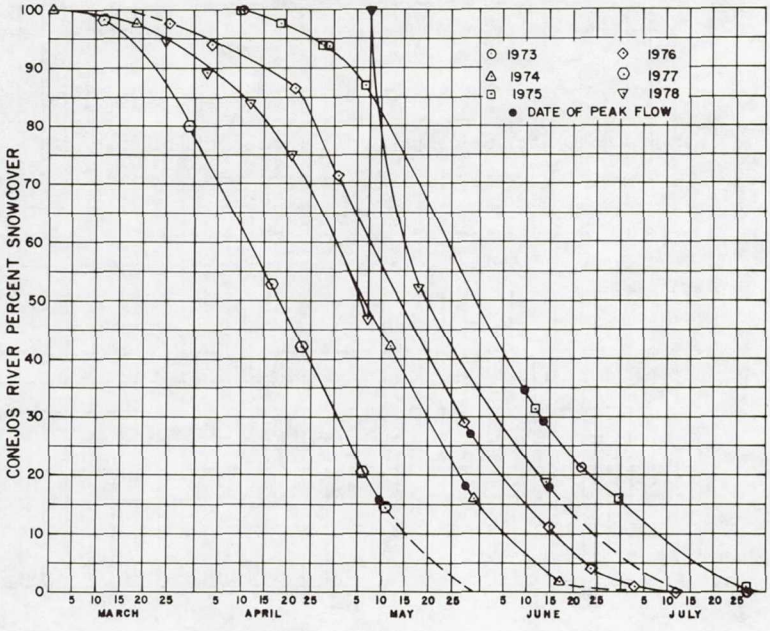


Figure 2. Time vs. percent of snowcover remaining for the Conejos River watershed.

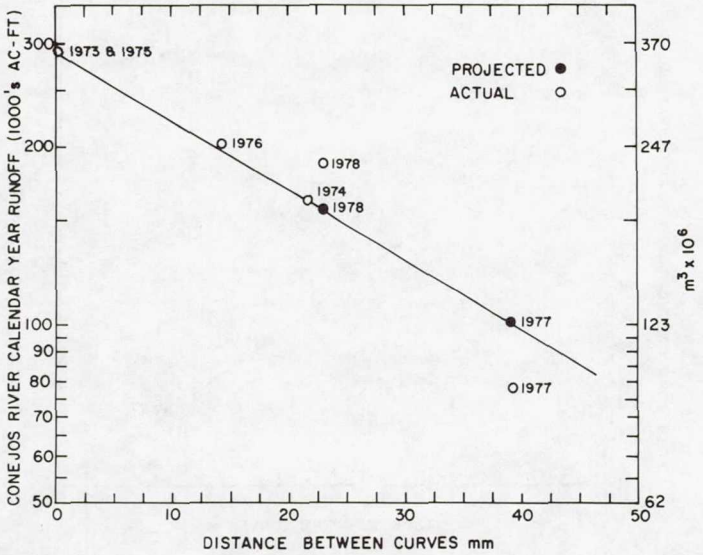


Figure 3. Annual runoff volume vs. snowcover depletion curve linear displacement for Conejos River watershed.

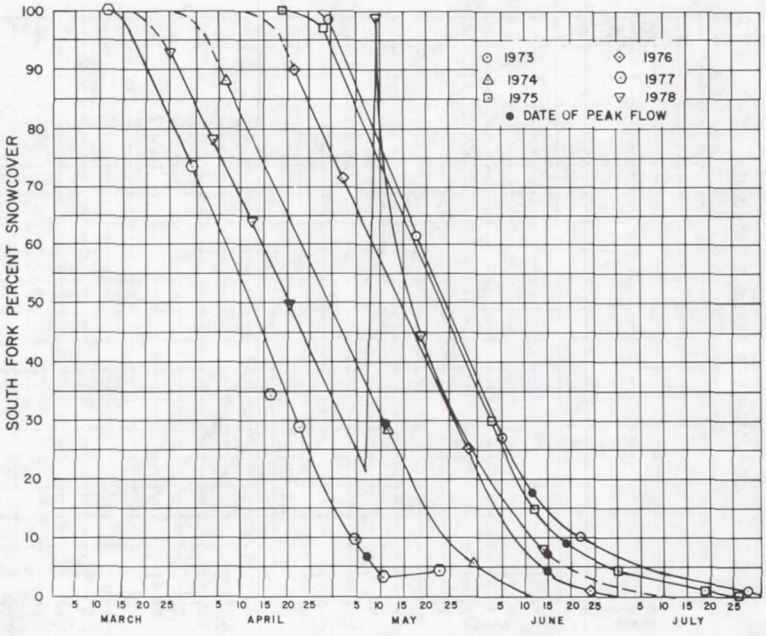


Figure 4. Time vs. percent of snowcover remaining for the South Fork watershed.

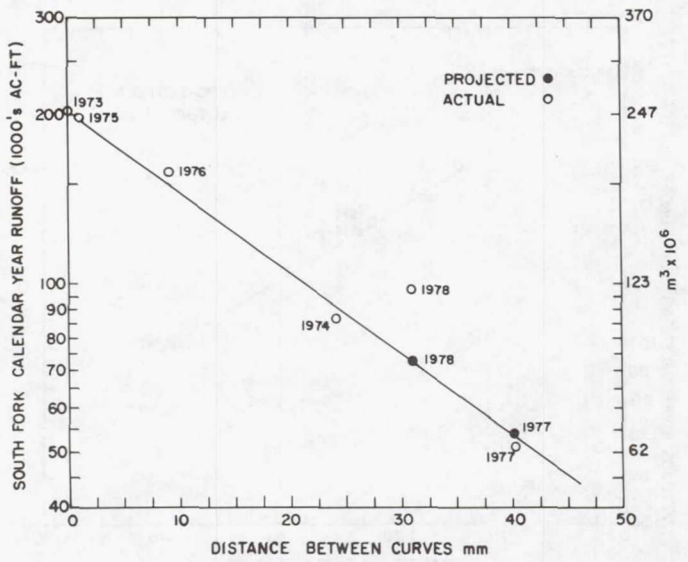


Figure 5. Annual runoff volume vs. snowcover depletion curve linear displacement for the South Fork watershed.

given watershed. Each curve represents a snowmelt runoff season and they are displaced relative to one another according to total annual streamflow volume. Every drainage basin studied appears to have a unique set of curves, so that a new set of curves must be constructed for each basin. The curves are plotted on standard 10 squares to the inch graph paper with time on the x-axis and the percentage of snowcover remaining as the y-axis. Snowcover remaining data taken from an image is plotted relative to the time of the Landsat pass. As the snow season progresses, each new data point is plotted until a straightline segment can be positively identified. This usually occurs when snow area remaining on the basin is around 80 to 90 percent. Once this straightline segment has been identified, the displacement between the new curve and a reference curve can be measured. The reference curve may be the maximum volume runoff curve or some convenient curve common to the family of curves. Displacement is relative; therefore, any convenient measurement system can be used (milimeters are used in this study as a standard unit). Each curve is unique and reflects climatological variations for each season. In the Conejos and South Fork basins, the straightline segments common to all of the curves are not necessarily parallel although they approximate parallel lines. The straightline segments of the different curves are a best fit of the data points as these points are not absolute values of snow areal extent. Also, these data points reflect image error and interpretation error which are significant and to a greater extent random.

The displacement of the family of curves (time vs. percent of snow areal extent remaining) has been found to be a near logarithmic relationship with total annual volume of runoff. The displacement when plotted on semi-logarithmic paper with total annual runoff volume in $m^3$ (ac-ft) results in a near straight line (Figure 3). Annual runoff volume can be found for a new snowcover depletion curve by plotting the curve's displacement directly on the semi-log paper. This relationship exists for two of the study basins tested, the Conejos River and South Fork of the Rio Grande.

## Results

This method evolved over a period of time from Landsat derived snowcover data for the Conejos River and South Fork of the Rio Grande. The method was used to make quasi-operational annual runoff volume forecasts for the Conejos River and South Fork of the Rio Grande in 1977 and 1978. The 1977 forecasts were successful in predicting the lowest annual runoff on record for both rivers. Annual runoff volume for the Conejos River was found to be approximately $113.3 \times 10^5$ $m^3$ (100,000 ac-ft). Actual annual

runoff was 883.7 x $10^4$ $m^3$ (78,000 ac-ft). The prediction was in error by 249.3 x $10^4$ $m^3$ (22,000 ac-ft) or 28 percent; however, average annual runoff volume for the river is 275.3 x $10^5$ $m^3$ (243,000 ac-ft). If we compare the 249.3 x $10^4$ $m^3$ (22,000 ac-ft) to the average annual runoff volume, error appears to be relatively small, or about nine percent. The lowest runoff recorded was 117.8 x $10^{-5}$ $m^3$ (104,000 ac-ft) in 1934. This prediction was made before April 5, 1977, prior to the snowmelt runoff season. The 1977 predicted annual runoff volume for South Fork was 609.5 x $10^4$ $m^3$ (53,800 ac-ft) (Figures 4 and 5). Actual annual runoff volume was 586 x $10^4$ $m^3$ (51,721 ac-ft), a difference of 240.3 x $10^3$ $m^3$ (2,121 ac-ft) representing an error of four percent. The average annual runoff volume for South Fork is 190.3 x $10^5$ $m^3$ (168,000 ac-ft) for 26 years of record. When the difference between actual and forecast annual runoff volume is compared to average annual runoff volume, the relative error is approximately one percent. The lowest flow recorded was 846.3 x $10^4$ $m^3$ (74,700 ac-ft) in 1940.

The 1978 annual runoff volume predictions were less successful because of a late massive snow storm, May 8, 1978, that left up to 5.08 cm (2 in.) of water equivalent snow on the basins. A prediction of 196.4 x $10^6$ $m^3$ (161,000 ac-ft) was derived for the Conejos before the May 8, 1978, snow storm, and 878.2 x $10^5$ $m^3$ (72,000 ac-ft) for the South Fork. The effects of this storm on total runoff cannot be fully assessed because of lack of adequate recording instrumentation. However, the Conejos watershed may have received as much as 366.9 x $10^5$ $m^3$ (30,000 ac-ft) of water. If 50% of this water reached the stream as runoff and the estimate revised, the new estimate would have been 214.6 x $10^6$ $m^3$ (176,000 ac-ft). Actual annual runoff for the Conejos was 214.6 x $10^6$ $m^3$ (175,920 ac-ft). The uncorrected estimate for the Conejos was approximately 182.9 x $10^5$ $m^3$ (15,000 ac-ft) or 8.5 percent in error, and the corrected estimate was in error by less than one percent.

The May 8, 1978, storm may have added as much as 281.0 x $10^5$ $m^3$ (23,000 ac-ft) of water on the South Fork watershed; and if 50 percent, 140.3 x $10^5$ $m^3$ (11,500 ac-ft), of this water reached the stream as runoff, the revised estimate would have been 101.8 x $10^6$ $m^3$ (83,500 ac-ft). The approximate annual flow for South Fork was 118.3 x $10^6$ $m^3$ (97,000 ac-ft). The uncorrected estimate was in error 304.8 x $10^5$ $m^3$ (25,000 ac-ft) or 26 percent, and the corrected estimate was in error by 164.6 x $10^5$ $m^3$ (13,500 ac-ft) or 14 percent.

It is obvious that major snow storms of the May 8, 1978, magnitude must be considered in any snowmelt runoff prediction. How much weight should be given to such a storm must be

determined at the time of occurrence. Before an effective method of revising forecast can be developed, additional study and better instrumentation are needed.

The graphical method was also applied to the Arkansas River drainage basin of Colorado above the Salida, Colorado, stream gage. The basin differs significantly from the Conejos and South Fork of the Rio Grande in size, snow conditions and watershed characteristics. The Arkansas drainage basin covers an area of 3,155 $km^2$ (1,218 $mi^2$) compared to the Conejos and South Fork which are less than 777 $km^2$ (300 $mi^2$) each. Elevations for the Arkansas range from 2,194.5 m (7,200 ft) to over 4,267 m (14,000 ft) with a larger percentage of the basin at lower elevations. Snow conditions are significantly affected by the high range of mountains along the Continental Divide on the west side of the valley. This range of mountains exceeds 4,267 m (14,000 ft) and its eastern slopes are the principal catchment areas for the Arkansas River. The valley floor and a large part of the east side of the valley are in a precipitation shadow and near desert conditions prevail.

Landsat snow areal extent data produced by the USDA Soil Conservation Service Snow Survey was plotted relative to the times of satellite passes in an effort to construct a family of snowcover depletion curves (Figure 6). The data points did not produce a systematic family of curves with the same relationship of total annual runoff as found in the other basins studied and the curve for the 1978 snowmelt season was out of sequence. The relationship between curve displacement and total annual runoff did not approach a near logarithmic function (Figure 7).

There are a number of possible explanations for the negative results. The most probable cause is due to significant differences in watershed characteristics and climatic factors previously mentioned. The Arkansas River basin has proven to be a difficult basin to predict using statistical as well as simulation models. This can be attributed to a number of factors: (1) the snowpack contribution to runoff is less than in the other basins, (2) complex water distribution systems exist in the basin bringing water from the west side of the Continental Divide, (3) spring and summer precipitation can substantially affect runoff predictions in any given year (Bernard Shafer, USDA SCS Snow Survey, personal communications).

## Problem Areas

Successful application of the graphical method is dependent upon consistent snow mapping data. When different image interpretation techniques are used, significant variations in snow

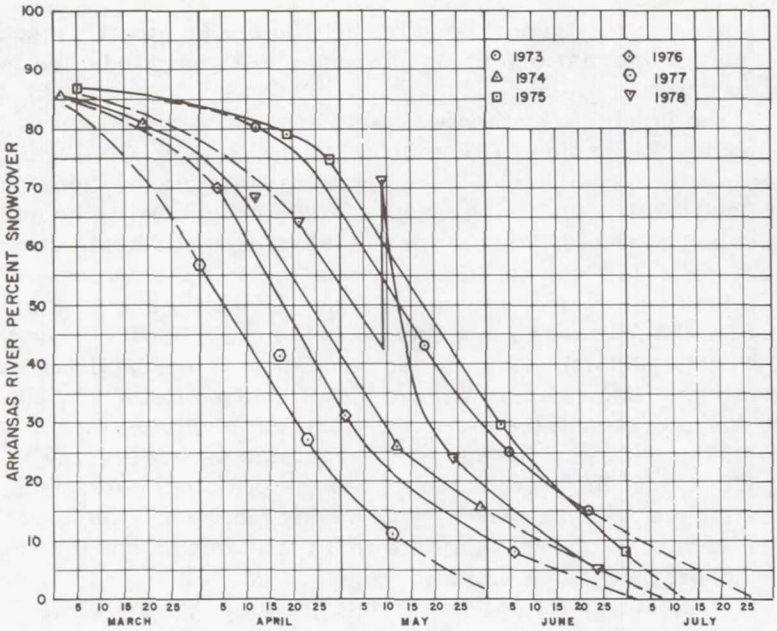


Figure 6. Time vs. percent of snowcover remaining for the Upper Arkansas River watershed.

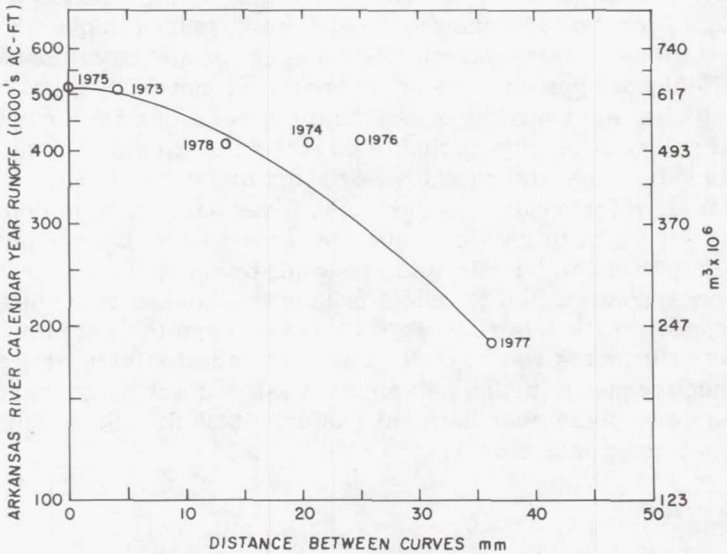


Figure 7. Annual runoff volume vs. snowcover depletion curve linear displacement for the Upper Arkansas River watershed.

areal extent mapping are found. Differences of a few percent will significantly affect plotting of snowcover depletion curves and affect the resulting displacement between curves.

Predictions based on graphical method are dependent upon snowcover depletion which is a function of total water content of the snowpack, temperature and precipitation. For a larger than average runoff year, snowcover recession will begin later than in a low water year. As a result, a runoff prediction may not be possible until fairly late in the season and after watershed management decisions must be made.

Cloud cover at the time of satellite passes has resulted in approximately 40 percent of the images being unusable or marginal. As many images as possible must be used to accurately plot snowcover depletion curves because the loss of a critical point can delay development of the curve. The Colorado Division of Water Resources has developed a method of indexed baselines for estimating snow areal extent on a basin from marginal Landsat images due to cloud cover. The method uses a network of indexed baselines that are optically superimposed over an image through a Zoom Transfer Scope (Figure 8). Where intersections of a baseline and the snowline can be recognized, the index line is measured and referenced to a table of index snowcover for that basin. The more index lines measured, the more accurate will be the overall snowcover estimate. Past results have shown that index baseline estimates are within five percent of standard Landsat snow mapping methods. For an operational forecast system to be useful, Landsat images must be received and processed without delay. A near real time processing of images is essential for short term forecast.

## Conclusion

In conclusion, the graphical method of annual runoff volume prediction represents a simplified relationship of snowcover depletion with time and runoff. The graphical procedure for predicting annual flow using Landsat snowcover data is relatively inexpensive and fairly reliable, particularly in regions lacking historical precipitation and snow course records. The method can be used as an independent means of checking other forecast techniques. Graphical methods appear to have definite limitations in application to large basins, in accounting for abnormal weather conditions, and variable watershed characteristics. It is possible to update early forecasts by using standard hydrologic methods of estimating runoff from late precipitation events. Additional empirical relationships other than those tested in this study may exist in snow hydrology that relate snowcover depletion

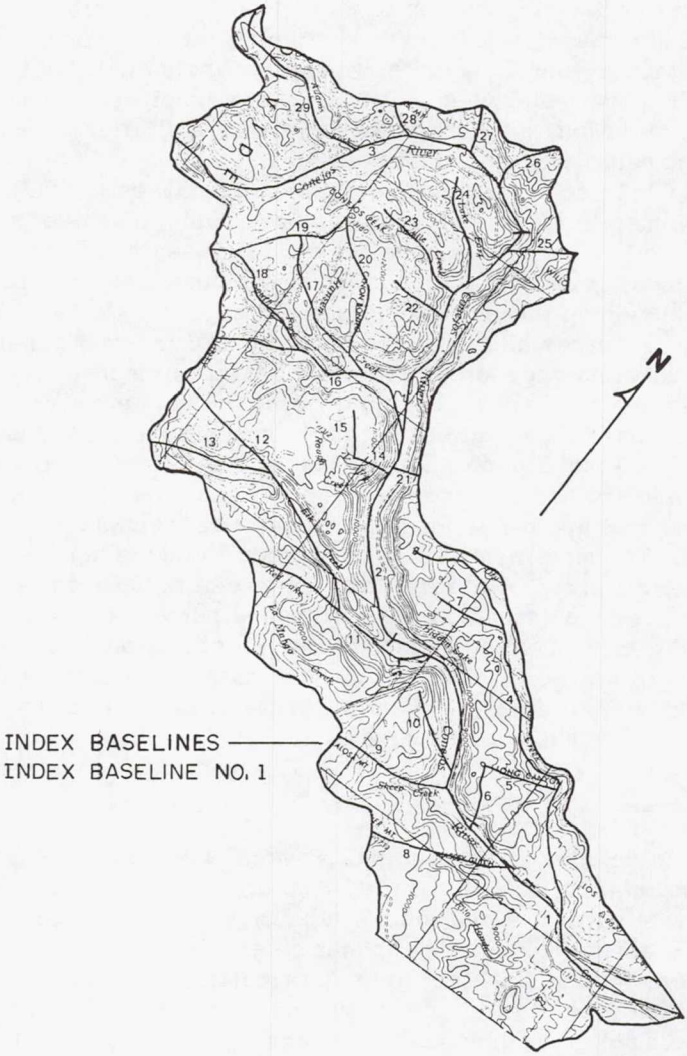


Figure 8. Index baseline network for the Conejos River watershed.

to watershed runoff. Graphical methods presented in this study are limited in scope; however, they may find wider applications as additional basins are studied. Each drainage basin appears to be unique and the graphical method must be applied independently. The successful application of graphical procedures is dependent upon consistent snowcover information on a repeated basis, a function well served by Landsat.

## REFERENCES


Garstka, W. U., Love, L. D., Goodell, B. C., and F. A. Bertle, 1958: Factor Affecting Snowmelt and Streamflow, Report on the 1946-53 Cooperative Snow Investigations at the Frasier Experimental Forest, Colorado, U. S. Bureau of Reclamation, Denver, Colorado, and U. S. Forest Service, Fort Collins, Colorado.

U. S. Army Corps of Engineers, 1956: Snow Hydrology, Summary of Reports of the Snow Investigations, North Pacific Div., Corps of Engineers, U. S. Army, Portland, Oregon.

_____, 1960: Runoff from Snowmelt, Manual EM 1110-2-1406, Corps of Engineers, U. S. Army.

**Page intentionally left blank**

# APPLICATION OF SNOWCOVERED AREA TO RUNOFF FORECASTING IN SELECTED BASINS OF THE SIERRA NEVADA, CALIFORNIA

A. J. Brown, California Department of Water Resources, Sacramento
J. F. Hannaford, R. L. Hall, Sierra Hydrotech, Placerville, CA

ABSTRACT

The California Applications Systems Verification and Transfer (ASVT) project, one of four ASVT's sponsored by NASA in the western United States, established two study areas covering the range of conditions found in California. These study areas were used to map SCA in near real-time mode; to compare satellite derived SCA with conventional snow data; and to operationally test the effects of incorporating SCA into the state's forecasts of snowmelt runoff. Results obtained during the four years of the ASVT indicate a potential improvement in the forecast accuracy by introducing SCA for those watersheds having a limited amount of representative real-time data during the period of snowmelt. Cloud cover and timely receipt of imagery were the major limitations to the usefulness of SCA.

## INTRODUCTION

The National Aeronautics and Space Administration (NASA) has been sponsoring research and investigation into utility of satellite imagery in water supply and other hydrologic forecasting in the western United States in the form of Applications Systems Verification and Transfer (ASVT) projects. NASA has contracted with the California Department of Water Resources (DWR) to investigate the operational application of snowcovered area from satellite imagery to DWR's hydrologic forecasting responsibilities, primarily in water supply forecasting in the Sierra Nevada. DWR subcontracted with Sierra Hydrotech, a consulting firm in Placerville, California, for technical assistance in determining snowcovered area (SCA) from satellite imagery, and in investigating applications of SCA to hydrology.

The objective of this paper is to report on the results and conclusions arrived at during the four years of the California ASVT project.

## Background

The Sierra Nevada and the southern portion of the Cascade Range supply California's fertile San Joaquin and Sacramento Valleys with water for agricultural, municipal, and industrial use. The average water-year runoff of Sierra streams tributary to the San Joaquin Valley and Tulare Lake Basin is approximately 11 million cubic dekametres (9 million acre-feet), while the average water-year runoff of Sierra and Southern Cascade streams tributary to the Sacramento Valley is approximately 19 million $dam^3$ (15 million ac-ft). In southern Sierra streams where elevations range up to about 4 300 metres (14,000 feet), as much as 75 percent of the average annual runoff occurs during the April-July snowmelt season. In the northern Sierra streams where elevations are much lower, only about 40 to 50 percent of the average annual runoff occurs during the snowmelt season.

The high degree of development and use of water in California's Central Valley has required development of forecast techniques for predicting volume and time-distribution of snowmelt runoff for water management purposes. Water management problems in certain areas require continual surveillance of streamflow and updating of forecasts during the runoff season to provide for management decisions as the season progresses. Forecast technology has advanced to the degree that application of new data types may possibly generate only limited improvement in forecast accuracy, particularly early in the season when forecast error is highly dependent upon the precipitation which occurs after the date of forecast. Development of new data types, such as snowcover from satellite imagery, will not eliminate the necessity or advisability of collecting data on precipitation, snowpack water content, and rates of snowpack accumulation and melt in the foreseeable future.

## Objectives

The basic objective of the California ASVT was to explore within an operational time frame the application of SCA obtained from satellite imagery in the State's snowmelt runoff forecasting procedures. Three specific tasks or areas of investigation were defined.

1. Data Interpretation. This task involved mapping SCA and equivalent snow lines from historic satellite and aircraft observations; and in a near real-time operational mode when the satellite imagery was available within 72 hours of satellite passage.

2. Data Analysis. This task involved developing and applying techniques to estimate SCA and to check the data. It further involved comparing imagery from various conventional and satellite sources to refine interpretative

techniques and to determine compatibility to SCA derived from satellite imagery with aircraft observations and other pertinent snowcover information.

3. Data Application. This task involved incorporating SCA operationally into volumetric projections of water year and snowmelt season (April-July) runoff, and investigating the use of SCA to refine and update a continuing analysis of the rates and remaining volume of snowmelt runoff during the progress of snowmelt.

Area of Investigation

The geographical area of this investigation is California's Sierra Nevada. The study area selected by DWR was composed of a northern and a southern project area. The northern project area included 24 watersheds and subwatersheds in or adjacent to the Sacramento River above Shasta Dam and the Feather River above Oroville Dam. The southern project area included 14 watersheds and subwatersheds in or adjacent to the San Joaquin, Kings, Kaweah, Tule, and Kern River Basins. The southern project area represented the relatively high elevation "high Sierra" region and the northern project area was characterized by lower elevations and more transient areas of snowcover. (Note that the Sacramento River Basin technically lies to the north of the Sierra in the Cascade Range.) Figure 1 shows the locations of these basins.

INTERPRETATION OF HISTORIC SCA DATA

Techniques described by Barnes and Bowley, 1974, were adapted to interpretative problems encountered in the Sierra project areas. Problems related to reflectivity of the bare, light colored granite rocks were critical in the southern Sierra, while problems related to timber cover, extensive cloud cover, and long shadows were most critical in the north. During the initial phases of the project, historical imagery obtained from NASA was interpreted for the 38 watersheds and subwatersheds within and adjacent to the Sierra project areas. Watersheds vary in size from 100 square kilometres (40 square miles) to 16 600 $km^2$ (6,400 $mi^2$). Determining SCA simultaneously from a relatively large number of basins and subbasins in each study area permitted crosschecking between adjacent and nearby basins, thus providing a means of estimating snowcover conditions even when portions of a given project area were obscured by clouds.

By 1978, preanalysis and editing of interpreted data indicated that sufficient historic information has been obtained from most of the subwatersheds for investigative purposes. As a consequence, analysis of many subbasins was discontinued and the program for acquisition, reduction and interpretation of satellite imagery was expanded to meet the future operational needs of DWR. NASA provided historic Landsat data so that 22 major watersheds in

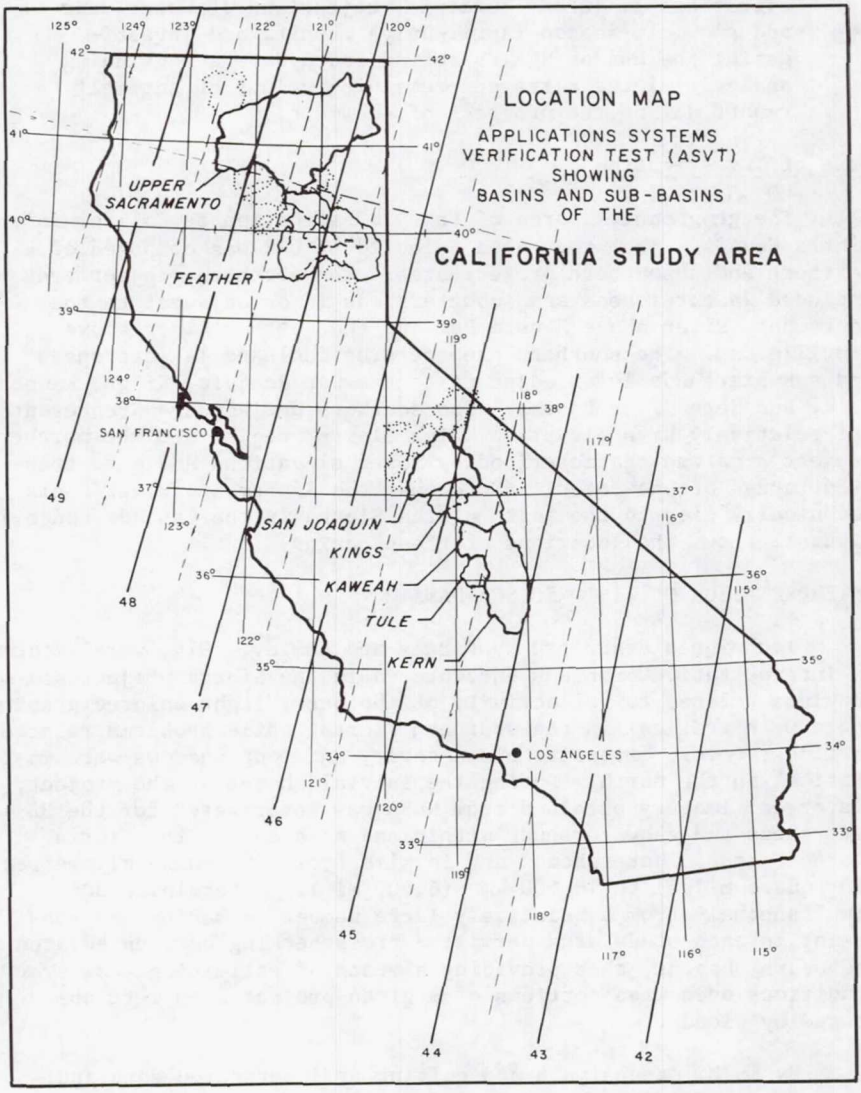


Figure 1. California Study Area

the Sierra Nevada, Cascade Range, and Coast Range could be interpreted to provide a data base for development of forecasting procedures in all the major snowmelt runoff areas of California. See Figure 2.

Historic data were initially reduced from Landsat images by both overlay and Zoom Transfer Scope (ZTS). Comparison of results indicated that reduction of Landsat images at a scale of 1:500,000 using the ZTS gives more consistent results, but takes considerably more time than a 1:1,000,000 direct overlay. NOAA images were also reduced by ZTS to fill the period between Landsat images.

In the reduction of Landsat imagery, the following items have been noted:

1. Transparencies of the Landsat imagery appear to be more consistent and more easily interpreted on the ZTS than the prints.

2. Direct overlay onto 1:1,000,000 prints takes about one-third the time of 1:500,000 ZTS analysis using transparencies, but the consistency of results observed using the transparencies has reduced the time required for data analysis.

3. Landsat imagery received well after the fact on transparencies is decidedly better and more easily interpreted than the near real-time data from Quick Look, or imagery from other sources such as NOAA.

For purposes of this investigation, an image set was defined as an image or group of images representing a nominal time of observation. NOAA images which cover much of the western United States in a single image have only one image per image set. A single NOAA image set includes all of California, but data were interpreted from two enlarged prints, each covering a portion of the Sierra. Landsat image sets may have included up to eleven images taken over a period of six days to cover the snowmelt streams of the State. The image set for a given basin or area represents all images required to describe that area on a given nominal date of observation.

Interpreted data representing a basin day includes the snow-covered area and effective snow line of a given basin or subbasin for a given image set. The overlap of images on succeeding passes provides an opportunity to obtain observational data when storm activity and clouds may obscure a single pass. Some data sets have been reinterpreted as techniques were improved. A significant portion of the imagery received but not interpreted was either obscured by cloud cover, had no remaining snow, or was outside the time period of investigation.

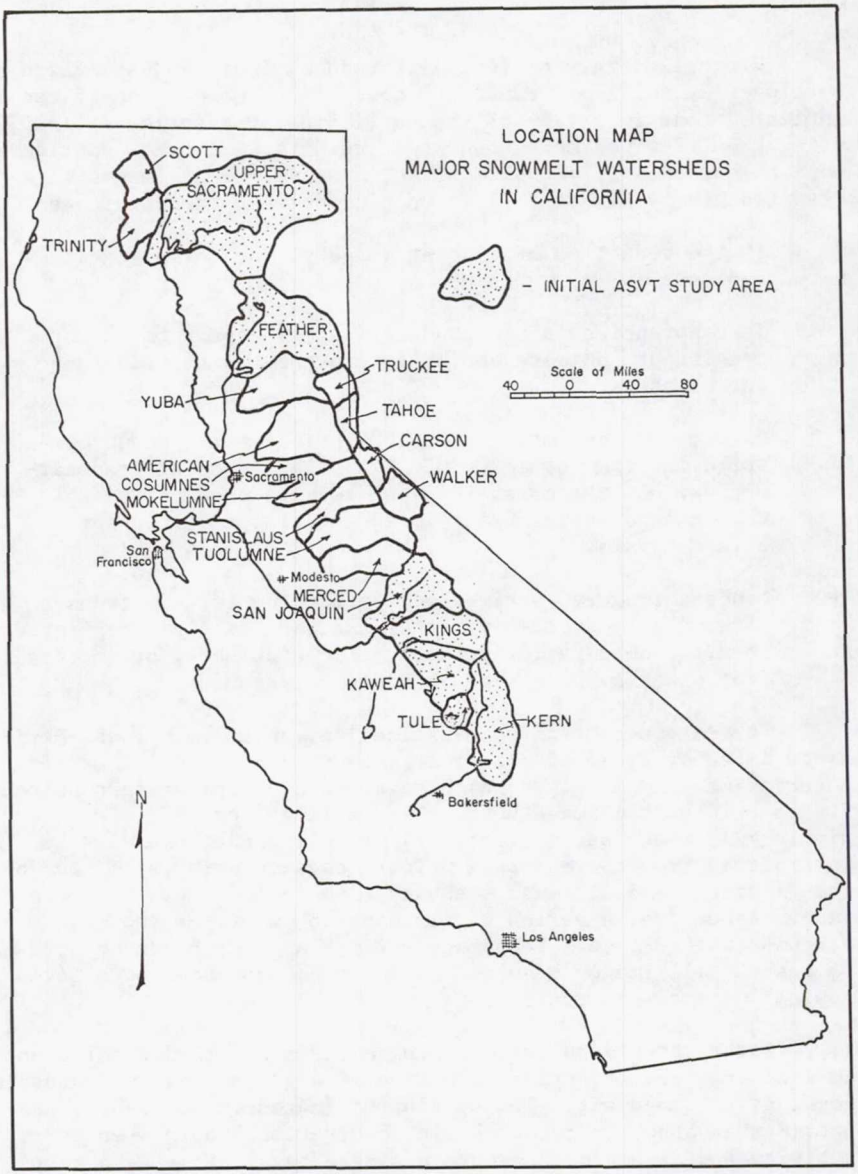


Figure 2. Major Snowmelt Watersheds in California

## INTERPRETATION OF OPERATIONAL SCA DATA

Canadian Quick Look imagery from Landsat was obtained directly from Integrated Satellite Information Services (ISIS), a Canadian readout station and service, during the snowpack accumulation and melt periods of 1976 through 1979 for use in operational forecasting. Additionally, Quick Look Landsat imagery was obtained from NASA.

One of the major operational problems during the 1978 and 1979 snowmelt seasons was securing timely imagery when runoff forecasts were required. Perhaps the greatest delay during 1978 was caused by the mail service. Canadian Quick Look imagery was postmarked in a timely fashion after observation, but mail delivery was much slower than in past seasons. Quick Look from NASA usually, but not always, arrived after the Canadian Quick Look. The average time was about five to six days as compared to the 72 hours originally hoped for. During 1979, data handling problems early in the season made it impossible to obtain near real-time data. NOAA and GOES imagery were used for supplemental data or when real-time data from Landsat was not available. Timeliness of data delivery cannot be overstressed with regard to operational forecasts.

## DATA ANALYSIS

Evaluation of results indicated that SCA can be practically determined from Landsat using the Zoom Transfer Scope for watersheds as small as 100 $km^2$ (40 $mi^2$), and snowpack depletion may be determined within reasonable limits of accuracy even as the area of snowpack becomes fragmented. Cross-basin plots were developed for the various major basins and subbasins, making it possible to estimate SCA on watersheds that were partly or completely cloud covered from data available on adjacent basins or subbasins.

Interpretative techniques improved with the increase in experience of the interpreter. A considerable amount of time was spent in checking and reanalyzing early (1973-1976) data sets to provide a data base for all watersheds that was homogeneous throughout the entire six-year period of available satellite imagery. This process included the important step of editing and preanalysis of the data, which involved deciding whether the data being obtained represented the data needed.

### Comparison of Satellite and Aircraft Observations

During the heavy snow season of 1952, the U. S. Army Corps of Engineers (Sacramento) initiated observations of snowcovered area from low flying aircraft in the southern Sierra Nevada in connection with the operation of reservoirs during the period of snowmelt. Initial work was done in the Kings River Basin for operation of Pine Flat Reservoir. Observations extended to the

Kern River in 1954, and eventually included the Kaweah and Tule River Basins. Observations were taken more or less routinely during the period of major snowmelt. The program continued for about 20 years until 1973.

During 1978, the Corps resumed aircraft observations in the southern Sierra as the result of the unusually heavy snowpack conditions and potential for spill of snowmelt runoff from reservoirs. Although the Corps was furnished data from the satellite observations throughout the ASVT program, the data generally arrived in Sacramento too late to meet the Corps' requirements for forecasting, necessitating resumption of the aircraft observations for that heavy runoff year. Information on SCA for estimation of both rate and volume of snowmelt runoff was obtained from aircraft and satellite. In many cases, aircraft observations varied considerably from the satellite observations. Figure 3(a) delineates the snowcovered area in the Kings River Basin during the 1973 season as derived from Landsat imagery, NOAA imagery, and aircraft observations. Figure 3(b) delineates snowcovered area during 1978 season, including the Canadian Quick Look imagery. Data in 1973 and 1978 for the Kern River Basin appears in Figures 4(a) and 4(b), and similar results were noted on other watersheds.

It will be noted that in general, the aircraft observations in 1978 appeared to show less snowcover than satellite observations as of a given date. Some precipitation occurred about mid-June 1978 which included light snowfall at higher elevations, and was probably very apparent to observers at that time. The Corps of Engineers attributes the difference between aircraft observations and Satellite SCA to the following possible causes:

1. Aircraft observers deleted patches of snow that were below the major unbroken snowpack. Historical aircraft observations, however, may not be entirely consistent in this respect.

2. Aircraft observers tried to delete areas with fresh light snowpack which did not represent the major winter accumulation. These areas might show up as snowcovered area on the satellite imagery, but an observer close to the ground could identify the freshly fallen snow on bare ground and eliminate it from the observation.

3. Aircraft observers and methods changed at various times.

During analysis, it was arbitrarily decided to make a correction to all aircraft observed data by increasing the aircraft observations by eight percent on the Kings River and 14 percent on the Kern River. Obviously, there is no means for otherwise testing or adjusting aircraft observations prior to the availability of satellite imagery.

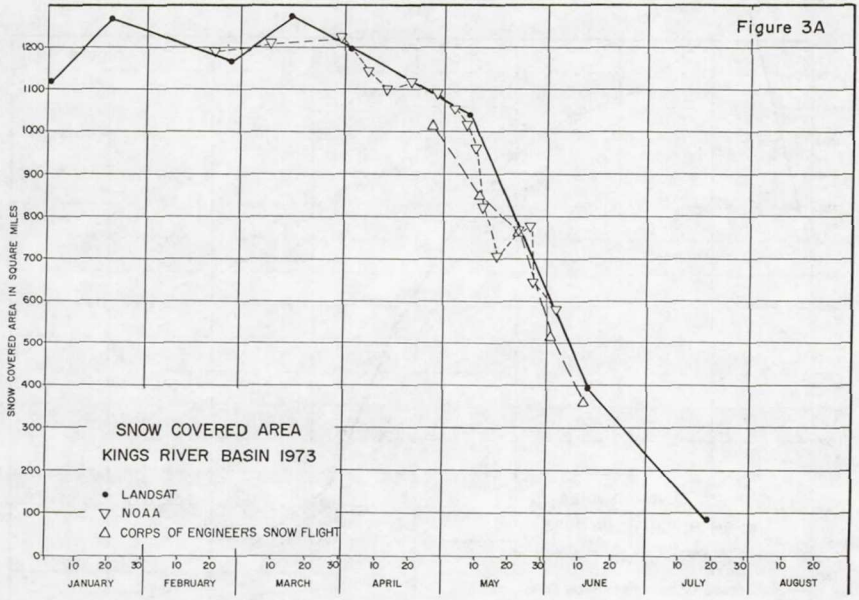


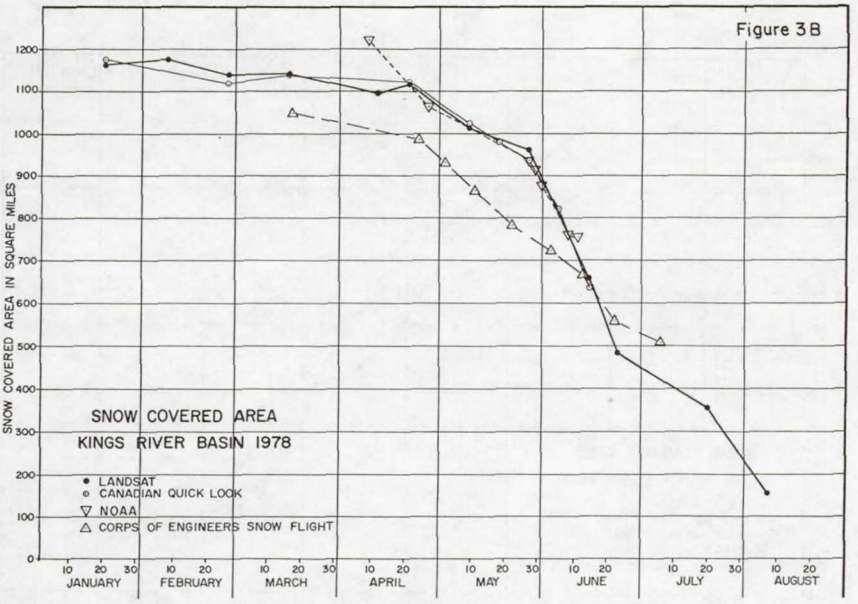


Figure 3. Snowcovered Areas


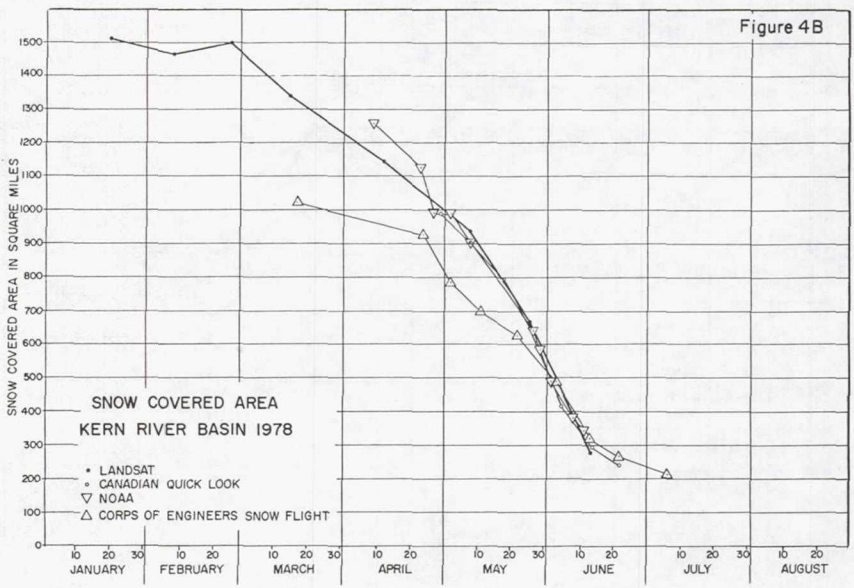


Figure 4. Snowcovered Areas

## DATA APPLICATION

Although utilization of snowcovered area as a supplemental parameter in seasonal runoff predictions seems logical and has been shown by various investigators to be useful (Rango, et al, 1979), the duration of satellite data is too short for conclusive testing of SCA in most conventional approaches to water supply forecasting. In order to expeditiously investigate the potential value of satellite SCA data in runoff prediction, long-term aircraft observations of SCA were used as a parameter in testing operational forecasting procedures for the Kings and Kern River watersheds in the southern Sierra Nevada.

### Test Basins

The Kings and Kern Rivers are adjacent watersheds (Figure 2) in the southern Sierra, ranging in elevation from about 300 metres (1,000 feet) in the foothill areas to over 4 300 metres (14,000 feet) along the Sierra crest, which is the eastern boundary for both watersheds. The Kings River has an east-west orientation with high subbasin divides and subbasin drainage in deep canyons. The Kern River has a north-south orientation with the Sierra crest along the eastern drainage boundary and the similarly high Great Western Divide along the western boundary of the basin. The Kern River is characterized by plateau areas with broad meadow areas and timbered slopes, although the North Fork heads in the steep rocky areas near the Kings-Kern divide and flows in the deep canyons for most of its length to Lake Isabella. About 74 percent of the Kings River annual runoff of about 2 million $dam^3$ (1.6 million ac-ft) occurs during the April-July snowmelt period. About 67 percent of the average Kern River annual runoff of 773,000 $dam^3$ (627,000 ac-ft) occurs during the April-July snowmelt.

### Test Procedures

In a preliminary analysis, a multiple regression technique was utilized to relate runoff subsequent to the date of forecast to causitive parameters. The analysis was intended to develop and demonstrate a procedure for updating water supply forecasts during the period of snowmelt to reflect observed conditions of precipitation, runoff, and change in SCA with the intention of reducing the residual error in the remaining flow subsequent to date of forecast.

The analysis was predicated on the operational requirement for accurate updating of water supply forecasts throughout the period of snowmelt runoff. Forecasts prepared by DWR have historically been for April-July snowmelt period. Updating has been primarily on the basis of precipitation observed subsequent to the April 1 forecast. Only a limited amount of data is available from the high mountain watersheds on a continuing basis during the period of snowmelt. Observed precipitation, runoff, and depletion

of SCA as the melt season progresses provide parameters on a near real-time basis to reflect the progress of melt in the watersheds. This investigation developed and demonstrated usable techniques for updating the conventional DWR forecast procedures during the progress of snowmelt.

The updating procedures used the same data as the conventional DWR procedures, which includes high and low elevation snow indexes (based on snow water content measurements), October-March precipitation index, precipitation during the period of snowmelt, and previous year's April-July runoff. In addition, the updating procedures included the runoff from April 1 through date of forecast, and SCA as of the date of forecast.

Figure 5 illustrates the variation in standard error, expressed as a percentage of April-July runoff, for forecast updates, and depicts the effective reduction in forecast error as the melt season progresses. Updating procedures without SCA are shown as a dashed line, while updating procedures utilizing SCA are shown as a solid line. On the Kings River, standard error increased slightly between April 1 and May 1, probably as a result of additional forecast parameters (observed runoff and SCA) used subsequent to April 1 which increased the degrees of freedom lost. After May 1, standard error declined appreciably until on June 15 it was approximately 70 percent of the error on April. The addition of SCA as a parameter on the Kings River appeared to offer little significant improvement in procedural error during the melt season. On the Kern River, standard error declined as the season progressed, but inclusion of SCA as a parameter appeared to make a substantial decrease in volumetric error of remaining runoff as the season progressed.

The analysis indicated that use of SCA as a parameter in forecasting snowmelt runoff may result in significant improvement of forecasting procedures under certain circumstances. It may be hypothesized that watershed characteristics, as well as availability of data representative of the watershed, may be factors related to response of forecast procedures to SCA. Historically, forecast errors on the Kern River have been substantially larger (percentage-wise) than those on the Kings River. Inclusion of SCA during the period of snowpack depletion allowed forecast accuracy on the two watersheds to be brought more in line with each other than was possible with conventional parameters alone. This suggests that SCA provides information pertinent to updating forecasts under some circumstances which may not be readily available from other basic data investigated here.

During the 1978 season, a forecast procedure using SCA was developed for the Kaweah River Basin which is adjacent to both the Kings and Kern River Basins. This procedure was developed specifically for operational use during the unusual 1978 snowmelt season.

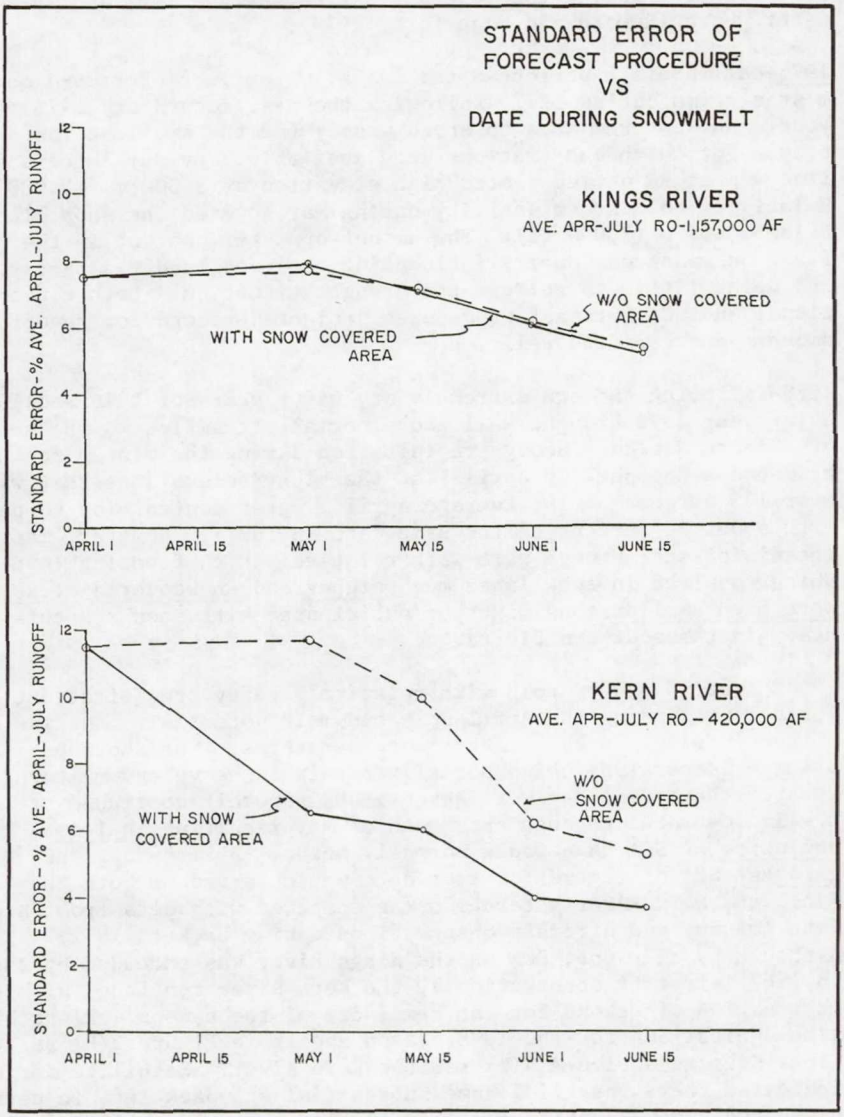


Figure 5. Standard Error of Forecast Procedure vs. Date During Snowmelt

Operational Forecasting

Water supply forecasts utilizing SCA as a forecast parameter were prepared during the snowmelt period for the 1977 and 1978 water years (Howard and Hannaford, 1979).

1977-California experienced the driest water year of record on most streams during 1977, following the near record dry 1976 water year. Snowcovered area observed was by far the smallest for any season for which observations were available. By May 1 the snow line was at an unprecedented high elevation of 3 000 m (10,000 ft). Relatively cold storm activity during May lowered the snow line to below 2 100 m (7,000 ft). The amount of water content in the fresh snowpack was small, influencing observed runoff slightly, and doing little to relieve the drought situation. Both conventional and SCA forecast procedures projected record low runoff amounts and verified well.

1978-Following the two extremely dry water years of 1976 and 1977, water year 1978 brought well above normal streamflow to the southern Sierra Nevada. Heavy precipitation during the winter months produced a snowpack by April 1 at the higher elevations that was over 175 percent of the average April 1 water content (as compared with about 20 percent of the same date in 1977). However, many of the winter storms were warm with relatively high freezing levels which resulted in snow lines much higher and snowcovered areas were much smaller than might be anticipated with snowpack this heavy in the southern Sierra.

April was very cold with relatively heavy precipitation, further increasing the April-July snowmelt potential. May was dry with only slightly below average temperatures. The short periods of high temperature which normally result in heavy snowmelt runoff towards the end of May were absent, and snowmelt continued at relatively low rates through the month of May resulting in less depletion of SCA than would normally occur. By mid-May, the greatest SCA of record for that date was observed on both the Kings and Kern River watersheds (as compared with data from satellite imagery and aircraft observations dating back to 1952). Although by mid-June, SCA on the Kings River was exceeded by that in 1967 (aircraft observations), the Kern River continued with the maximum SCA of record for the remainder of the season. Plots of time against SCA for the 1978 season appear in Figure 3(b) for the Kings River and Figure 4(b) for the Kern River. Satellite imagery indicated there was still some substantial snowpack left in certain protected high elevation portions of the watersheds well into August and some isolated snowfields persisted throughout the summer.

Because SCA on April 1 was well below that which might normally be anticipated with the relatively large snowpack water content at the higher elevations, water supply forecasts for the Kings and Kern Rivers using SCA as a parameter were substantially

lower than those from other sources. By May 1, forecasts were raised as a result of heavy precipitation during April, but forecasts utilizing SCA were still substantially below the forecasts utilizing the conventional procedure. Subsequent updates gave similar results.

Forecasts utilizing SCA verified well, while conventional procedures tended to overforecast. The record large SCA after May 1 gave some assurance that flow which had not materialized prior to that date was still available in the form of snowpack within the watersheds. The forecasts utilizing SCA were conveyed to operating agencies in the southern Sierra as part of the NASA program. The major operational problem during the 1978 snowmelt season, as discussed under SCA Data Interpretation, was in securing imagery at the time forecasts were required.

## CONCLUSIONS

The areal extent of snowcover as derived from satellite imagery does appear to have some potential for improving the timeliness and frequency of hydrologic forecasts in California's ASVT test areas. The greatest potential for water supply forecasting is probably in improving forecast accuracy and in expanding forecast services during the period of snowmelt. Problems of transient snow line and uncertainties in future weather are the main reasons that SCA appears to offer little in water supply forecast accuracy improvement during the period of snowpack accumulation.

During snowmelt, both rate and volume of snowmelt runoff can be related to receding SCA as well as other parameters. Based on the period of analysis of approximately 25 years, including both aircraft and satellite observations, SCA appears to offer considerable improvement in accuracy of forecast updates under certain conditions. The improvement in accuracy appears to be greatest from watersheds with a limited amount of representative data available from the watershed on a real-time basis during the period of melt. Also, SCA may have some potential in making forecast procedures more responsive to conditions involving unusual distribution of snowpack throughout the watershed.

Use of SCA, from an operational standpoint, can become restricted when there is considerable cloud cover over the mountainous region for extended periods of time. At these times, neither the Landsat nor the daily NOAA imagery may be available. The experience of the interpreter is extremely valuable in estimating SCA during partial cloud cover from observed SCA on portions of the observed basins and adjacent basins. This skill may be critical to the operational use of SCA. Delivery of imagery from the source to the interpreter also may pose a critical problem. Operational experience during the past two seasons suggests that much more rapid dissemination of observed satellite imagery will

be required before completely effective use can be made of SCA in DWR forecast responsibilities.

SCA as a forecast parameter does not obviate the need for other accurate data from conventional sources to define water supply and anticipated runoff. SCA does, however, provide one more piece of supplemental information needed to increase the reliability of forecast updates during the period of snowmelt runoff. DWR plans to continue the interpretation of satellite imagery associated with water supply forecasting on California's snowmelt streams.

REFERENCES

Barnes, J. C. and Bowley, C. J., "Handbook of Techniques for Satellite Snowcover Mapping", December 1974.

Rango, Albert, et al, Snowcovered Area Utilization in Runoff Forecasts, Journal of the Hydraulics Division, ASCE, January 1979.

Howard, C. H. and Hannaford, J. F., "Operational and Technical Considerations Regarding Recent Forecast Seasons in California", WSC, April 1979, Sparks, Nevada.

# APPLICATION OF SATELLITE IMAGERY TO HYDROLOGIC MODELING SNOWMELT RUNOFF IN THE SOUTHERN SIERRA NEVADA

J. F. Hannaford & R. L. Hall, Sierra Hydrotech, Placerville, Ca.

## ABSTRACT

Snowcovered area was examined as a parameter for estimating rate of snowmelt runoff as input to an operational hydrologic model. SCA and surface air temperature provided a very effective means for simulating daily snowmelt runoff for the Kings River.

## INTRODUCTION

### General

The purpose of this investigation has been to explore the application of satellite imagery to hydrologic modeling of snowmelt runoff in the southern Sierra Nevada. The investigation has been conducted under the sponsorship of the National Aeronautics and Space Administration in conjunction with the California Applications Systems Verification and Transfer Project.

### Objectives

The major objective of this investigation has been to develop and test application of areal extent of snowcover to hydrologic simulation of daily snowmelt runoff on the Kings River basin in California's southern Sierra Nevada. The California Department of Water Resources (CDWR) currently operates a hydrologic model to simulate daily runoff on the Kings River basin for operational purposes. Although previous investigation leading to the Kings River model suggested that areal extent of snowcover influences rate as well as remaining volume of snowmelt, techniques had not been developed to incorporate this parameter in the operational model, since at that time, only intermittent observations of snowcovered area by low flying aircraft were available.

This investigation was intended to (1) explore techniques for application of snowcovered area (SCA) to the existing Kings

River hydrologic model, (2) develop and describe SCA-snowmelt relationships in a manner to make the technique readily transferable to other similar watersheds, and (3) develop techniques for interpolating and extrapolating SCA for operational use on a daily basis from satellite observations as well as precipitation and temperature data. This investigation by Sierra Hydrotech has been considered complimentary to "Operational Applications of Satellite Snowcover Observations in California" currently being conducted by the California Cooperative Snow Survey Branch, (CDWR) and sponsored by NASA.

## BACKGROUND

### General

Water originating from snowmelt in California's southern Sierra Nevada has high value for municipal and agricultural application. Detailed information on the volume and rate of snowmelt runoff through operational hydrologic forecasts is important in water management decision making. For half a century, measurements of snowpack water content have been made on a monthly basis in these watersheds for the purpose of estimating volume of runoff, and for over 20 years, aircraft observations of the areal extent of snowpack were made. Satellite observation of areal extent of snowcover have been interpreted for each snowmelt season since 1973.

### Study Area Description

The Kings River is a southern Sierra Nevada watershed (Figure 1) that discharges into the Central Valley near Fresno, California. The basin ranges in elevation from below 300 m in the foothill areas to over 4300 m along the Sierra Nevada crest, which is the eastern boundary ot the watershed. The Kings River has an east-west orientation with high subbasin divides and subbasin drainage in deep canyons. The average elevation of the April 1 snow line is about 1900 m, although late winter and early spring storms may cause a temporary drop, or "transient" snow line, lasting sometimes only a few days. The distribution of area with elevation is relatively uniform within the area of major melt contribution between 1900 m and 3600 m elevation.

The 4000 $km^2$ Kings River basin has an average annual runoff of 1,568,000 acre-feet ($1934 \times 10^6 m^2$) which represents 480 mm of runoff, 75 percent of which occurs during the April-July snowmelt period. Snowpack accumulation increases with

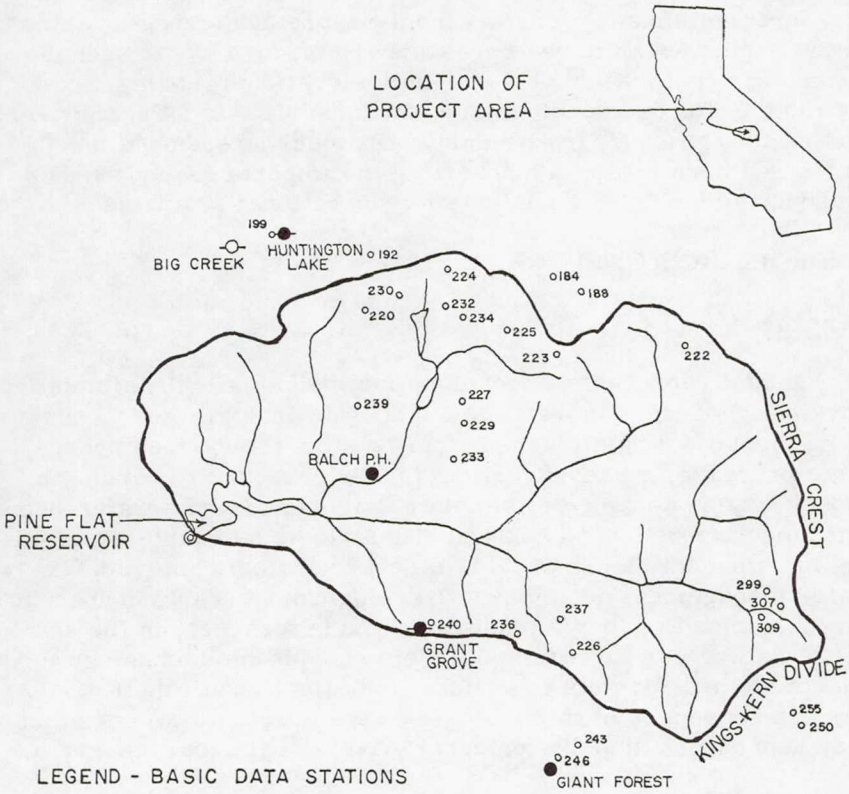


FIGURE 1

PROJECT AREA

KINGS RIVER

HYDROLOGIC MODEL

elevation to about 2800 m and is fairly consistent at about 800 mm of water above that elevation, although local topography may affect accumulation to some extent. Average annual precipitation at the 2800 m elevation is about 900 mm. Winter precipitation measurements made along the frontal slope at the western side of the basin appear to be representative of, or at least proportional to, precipitation at the higher elevations, making these data useful for hydrologic analysis within the basin. Precipitation and resulting runoff are extremely variable from season to season in the southern Sierra, emphasizing the importance and need for an adequate hydrologic analysis for operational requirements.

## HYDROLOGIC MODELING

### General

A model represents a technique for mathematically simulating physical processes or relationships. A hydrologic model consists of mathematical relationships representing the various hydrologic processes occurring within the watershed. A hydrologic model may be designed to simulate daily flow from a watershed utilizing various hydrologic and climatologic parameters, resulting in output which can provide timely hydrologic analysis for water management decisions. Hydrologic models are not specific forecasts nor are they intended to provide forecasts in the same sense as weather forecasts. Models provide the technology to enable the hydrologists to evaluate the effect upon runoff of various sequences of climatologic or meteorologic events which may represent either historical or hypothetical occurrences.

### Description of Existing Model

Digital hydrologic models have been developed and used as water management tools in the southern Sierra Nevada since the snowmelt season of 1969, when a hydrologic model was developed for simulation of daily runoff during the snowmelt season for the Kings River basin.[1/2/] The Kings River hydrologic model, and a similar model for the San Joaquin River, are operated weekly during each snowmelt season by CDWR.

The existing Kings River hydrologic model[1/] evolved through development of several submodels representing various runoff processes as illustrated in Figure 2. The general mathematical characteristics of each submodel were developed and fit to approximately 25 years of observed data. The Kings River hydrologic model consists of five basic submodels of varying

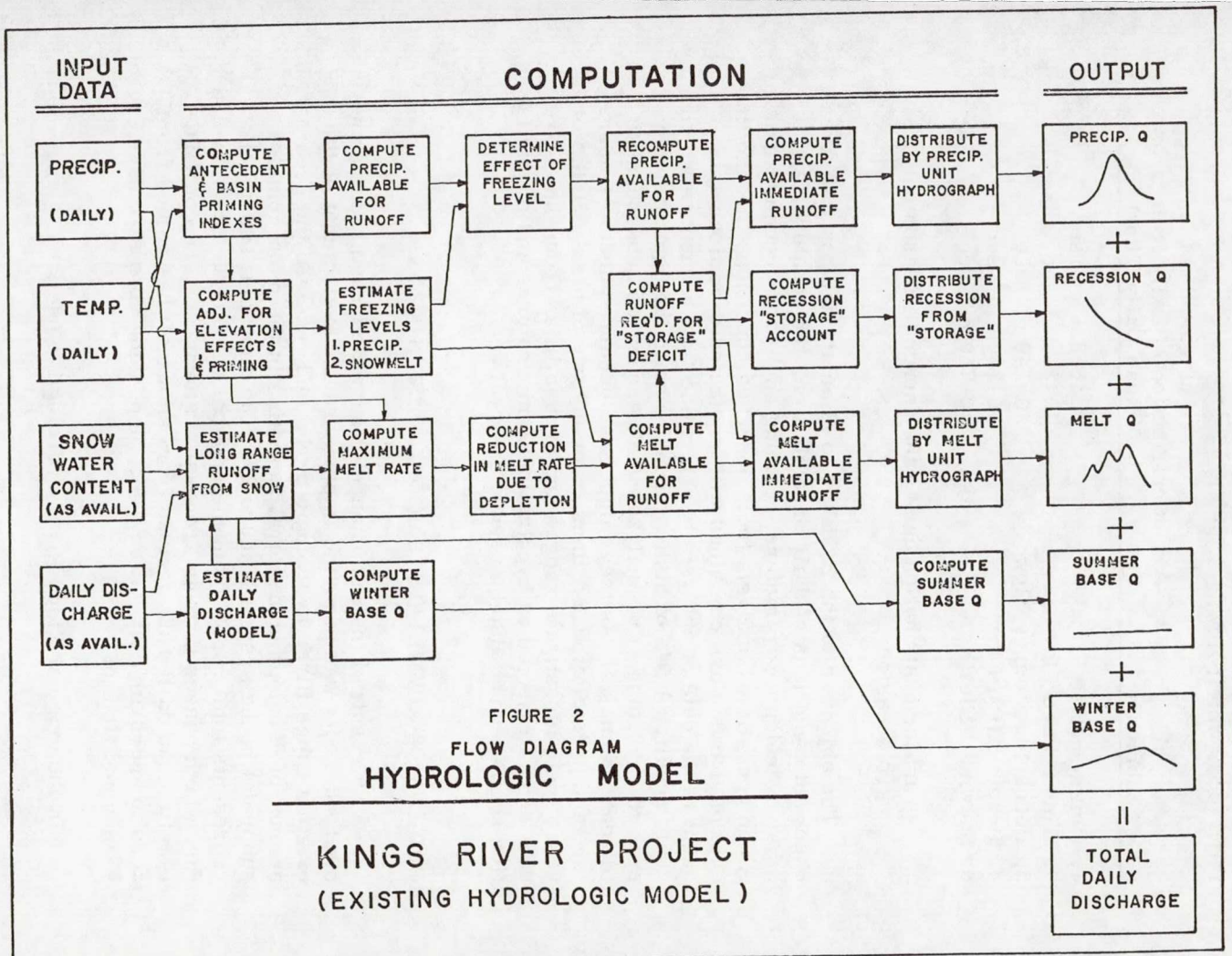


FIGURE 2

FLOW DIAGRAM

**HYDROLOGIC MODEL**

KINGS RIVER PROJECT

(EXISTING HYDROLOGIC MODEL)

complexity and influence on the overall hydrograph. The submodel of primary concern in the present investigation is that related to snowmelt flow.

| Submodel | Magnitude of Contribution of Daily Hydrograph (Mean Daily Flow) |
|---|---|
| 1. Summer Base Flow | 2.8-8.5 $m^3$/sec |
| 2. Winter Base Flow | 0-25 $m^3$/sec |
| 3. Recession Storage Flow | 0-140 $m^3$/sec |
| 4. Precipitation Flow* | 0-1400 $m^3$/sec |
| 5. Snowmelt Flow | 0-750 $m^3$/sec |

*A major contribution during the snowmelt season only on rare occasions

The objective of the model is to simulate daily runoff given observed conditions of daily precipitation, temperature, and other hydrologic parameters including snowpack accumulation. As an operational analysis tool, observed conditions through the date of analysis are combined with projected conditions subsequent to the date of analysis to determine flow sequences which could result. A file of historic conditions in the computer permits the hydrologist to analyze runoff sequences subsequent to the date of analysis as they might have occurred under temperature and precipitation regimes from any one of nearly 30 historic years or to investigate ranges and probabilities from the entire data set. Projected or hypothetical temperatures and precipitation regimes may also be used if desired.

## ORIGINAL SNOWMELT SUBMODEL DESCRIPTION

As a result of the importance of snowmelt runoff, the snowmelt submodel was of prime importance in development of the original Kings River hydrologic model and received the greatest amount of developmental work, resulting in the most complex submodel in the system (Figure 2). The snowmelt submodel represents total runoff from the snowpack, both surface flow and flow which passes through "recession storage". The contribution to mean daily flow derived from snowmelt has varied from zero to approximately 750 $m^3$/sec, depending upon size of season and time of year.

In the original Kings River hydrologic model, daily snowmelt

volume was based upon total quantity of snowpack, degree of snowpack priming, volume of remaining snowmelt runoff, and mean daily air temperature as an index to the effect of available energy on snowpack. A portion of the daily melt was passed through recession storage and the remainder was distributed by a four-day unit hydrograph. The original snowmelt model proved to be very effective under most conditions, in spite of its very empirical nature.

The final report on the original model stated that both snowpack volume and SCA are related to melt rate. However, the SCA relationship was not defined in that investigation. It should be pointed out that relationships between the remaining volume and rate of snowmelt runoff may still prove useful in operational analysis of runoff subsequent to the last date of satellite observation.

## SCA SNOWMELT SUBMODEL - DEVELOPMENT AND DESCRIPTION

### General Approach

The objective of this investigation was to develop techniques using SCA as a parameter to estimate the rate of snowmelt contribution as input to the Kings River hydrologic model. Although previous investigation leading to the Kings River model suggested that areal extent of snowcover influenced rate of snowmelt runoff, the technique had not been developed to incorporate this parameter in the operational model. Utilization of SCA required a relationship between the rate of snowmelt contribution to the runoff hydrograph and temperature, SCA, and related parameters which would permit simulation of daily snowmelt runoff from the hydrologic model. The original snowmelt submodel was completely removed from the hydrologic model and replaced by the SCA submodel, since the basic techniques used in the two submodels differed conceptually.

The SCA snowmelt submodel is based upon the following premises:

. . . The technique was to be capable of transference to other similar watersheds given the comparable characteristics of those watersheds. It was hypothesized that the greatest degree of transference could be achieved through development of the snowmelt submodel by elevation bands or zones within the watershed, basing the

melt procedures upon similar and differing characteristics of the zones as well as relative levels of energy input.

. . . Melt in any elevation zone in the basin can be related to air temperature within that zone.

. . . Melt of snowpack may occur at any point or elevation zone in the watershed (assuming air temperatures are above freezing in that zone), but runoff will occur from the snowpack in a given elevation zone only after the snowpack in that zone becomes fully "primed". For purposes of the snowmelt submodel, the effective "elevation of prime" represents that elevation above which no snowmelt is available to the snowmelt hydrograph.

. . . The rate at which snowmelt is made available to the snowmelt hydrograph is proportional to the area of fully primed snowpack within each elevation zone below the "elevation of prime" as well as the temperature within each zone.

Basic Data - Elevation Zones and Temperatures

Figures 3 and 4 show various types of basic data used as input to the SCA snowmelt submodel and the Kings River hydrologic model. The following comments refer specifically to basic data as related to the SCA snowmelt submodel.

In the development phase, SCA was interpreted from satellite imagery by 150 m (500 foot) elevation bands or zones. It should be pointed out that the developmental model using elevation zones of snowpack is not particularly well suited to operational forecasting as the reduction of satellite imagery by 150 m elevation zones is a time consuming process. This approach is better left to the research and developmental stages of analysis, while a more simplified approach to data reduction is more applicable to operational analysis during the forecast season. Fortunately, in the Kings River watershed, the basinwide SCA seems to provide an adequate index to be used in future operational work, while analysis by zones provides for a means of transference of techniques to other areas and watersheds.

Temperature used in analysis is mean daily surface air temperature derived from three stations in or adjacent to the watershed and adjusted to an approximate elevation of 2100 m for

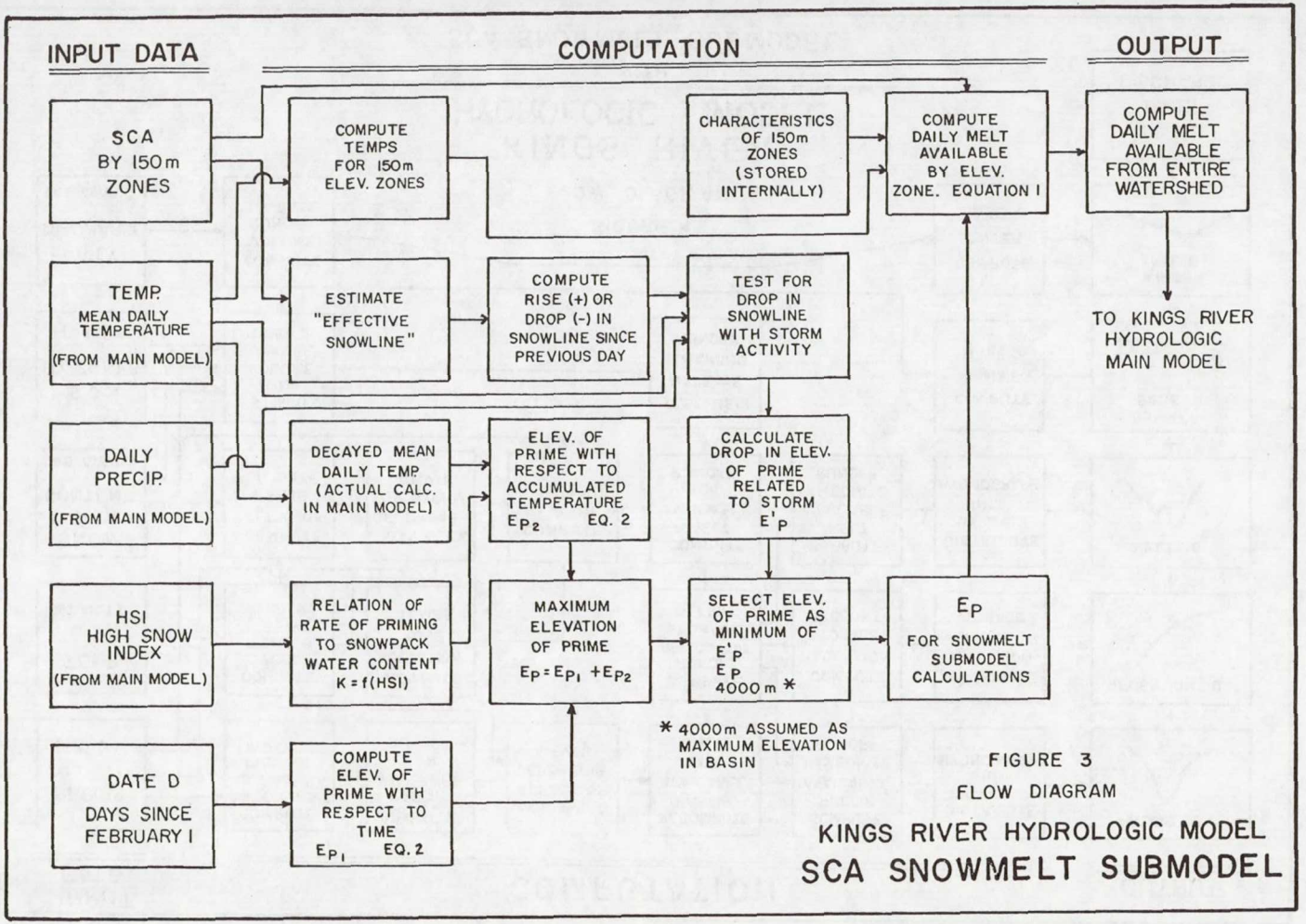


FIGURE 3

FLOW DIAGRAM

KINGS RIVER HYDROLOGIC MODEL

SCA SNOWMELT SUBMODEL

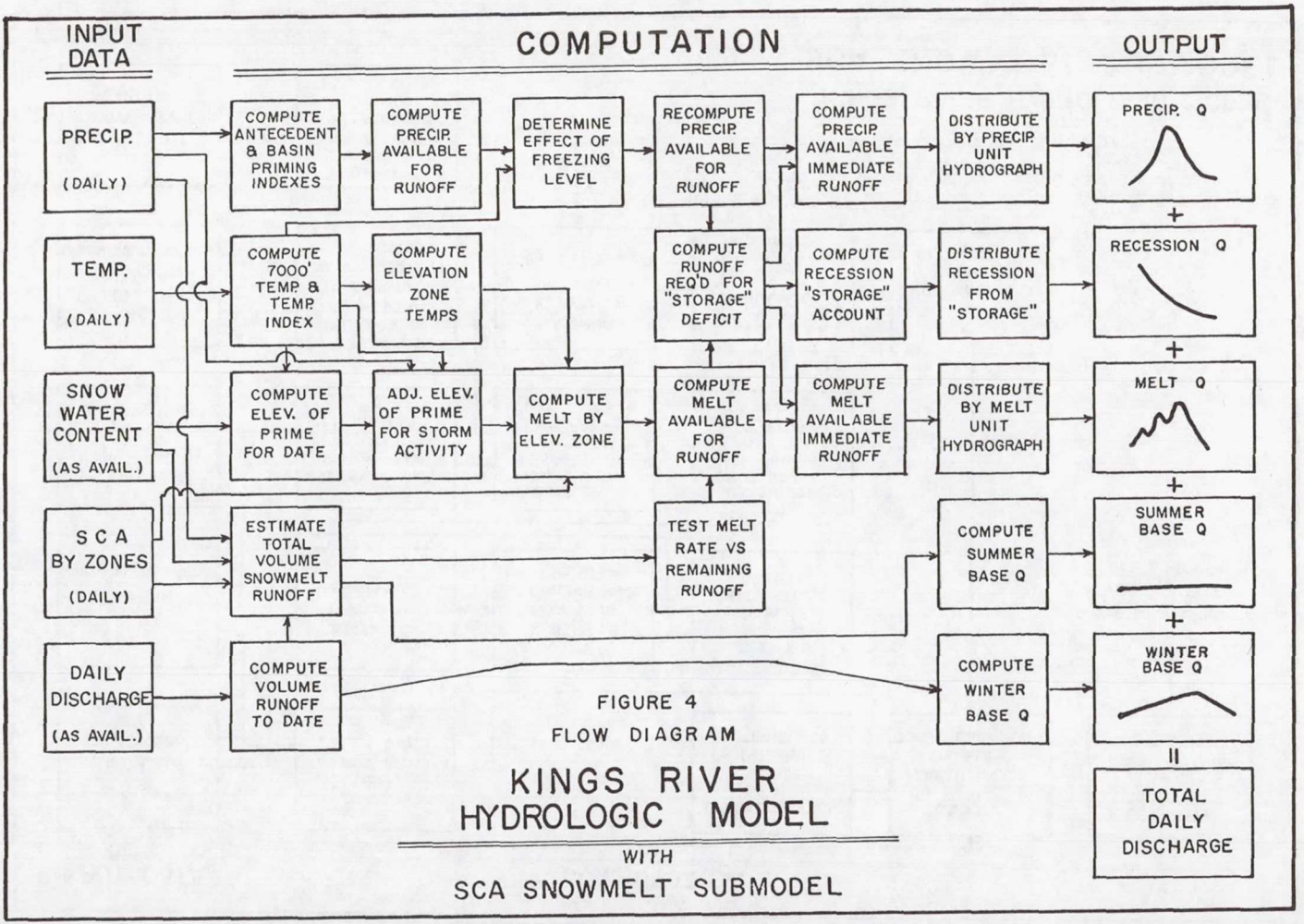


FIGURE 4

FLOW DIAGRAM

# KINGS RIVER HYDROLOGIC MODEL

WITH

SCA SNOWMELT SUBMODEL

analysis purposes. Air temperature is one of the few measurements related to the input of energy to the watershed which has been recorded systematically over the years. Fortunately, temperature appears to provide a good integration of the effect of available energy upon the snowpack under most conditions, both during accumulation and melt of the snowpack. Temperature within each elevation zone was based on the mean daily model temperature computed with a lapse rate of 6.4°C/km. Analysis indicated that a base temperature of -1°C appeared to give the most satisfactory results. Melt was computed on the basis of the difference between the mean daily temperature (adjusted by lapse rate) and -1°C.

Melt by Zones

The snowmelt submodel was first developed for that portion of the season after which the entire watershed was considered to be primed and producing melt. This simplified the process of developing and calibrating techniques to calculate melt by elevation zones. The same basic technique is utilized throughout the entire snowmelt season, but during the period of priming, only a portion of the SCA in the watershed has the ability to produce water contributing to the runoff hydrograph.

Operation of the existing model uses input data in conventional units and output for operational analysis is also in similar units. The SCA snowmelt submodel was similarly developed in the conventional system. However, the following equations are shown in SI units. Melt volume for each elevation zone is computed by the following equation according to the flow chart in Figure 3.

Equation 1 $$QMELT_z = C_q C_z A_z P_z T_z$$

Where: $QMELT_z$ = daily melt volume from given elevation zone "z" expressed as a mean daily flow rate, $m^3/sec$

$C_q$ = coefficient to describe relationship between area, temperature and melt. The value of $C_q$ was about 0.024

$C_z$ = coefficient to adjust for the efficiency within the elevation zone. Values were near 1.0, probably dependent upon loss characteristics of the zone

$A_z$ = area within elevation zone in square kilometers

$P_z$ = percentage of the zone subject to melt on a given day limited by SCA in zone and "elevation of prime" as described in the following section

$T_z$ = effective temperature above base within elevation zone "z", $^{o}C$.

The summation of QMELT from all zones is the output from the SCA snowmelt submodel and the required input for the Kings River hydrologic model. A value of QMELT for any elevation zone was calculated as zero (1) if there was no SCA within the zone, and (2) if the temperature for the zone was less than $-1^{o}C$, or (3) if the effective elevation of prime was lower limit of the zone. Although analysis suggests that the relationship between temperature and melt is not linear, it appears to be sufficiently linear throughout the range of temperature where significant melt occurs that the assumption of the linear relationship is not detrimental. One degree C change in temperature with this relationship represents about 2 mm of QMELT as input to the basic hydrologic model. This figure does not appear at all inconsistent with observed depletion of snowpack of 50 mm per day with observed mean daily air temperature (corrected for elevation) in the order of $20^{o}C$.

Melt During Prime

Analysis of melt volume and melt rate during the period of snowpack priming is complicated by the fact that the snowpack is not fully primed throughout the watershed, and therefore the watershed is not capable of producing runoff from the entire SCA, no matter what the temperature. It has been assumed for purposes of the model that the watershed produces no snowmelt runoff above the "elevation of prime" and all of the runoff required to meet the observed hydrograph of snowmelt runoff comes from the area of the watershed which is snowcovered below the effective "elevation of prime". It was assumed that a given set of temperature and SCA conditions would produce snowmelt volume equivalent to that derived from the relationship in section "Melt by Zones", and that any reduction or difference between the calculated and observed melt was attributable to the fact that no runoff occurred above an "elevation of prime", regardless of temperature.

To systematically develop relationships to describe the "elevation of prime", the basinwide melt was calculated from the relationship in section "Melt by Zones". Next, the volume of daily melt required to reproduce the observed hydrograph was estimated. The difference between the calculated and "observed" melt volumes was then used to determine the elevation above which no snowmelt could occur if the "observed" runoff hydrograph were to be realized from "calculated" melt. This elevation was defined for purposes of the SCA snowmelt model as the effective "elevation of prime". The elevation of prime was then defined in terms of other measured or calculated parameters considered related to the priming process. Many combinations of parameters were tested to establish a relationship between "elevation of prime" and the following factors.

. . . Temperature -- A decayed accumulative temperature (0.96 daily decay factor) was based upon the accumulation of degree days above freezing at 2100 m from January 1. This factor represented a measure of the accumulation of energy to which the snowpack might be subjected as reflected by air temperature.

. . . Date -- The date of the season also appears to reflect some measure of energy introduced to the snowpack that would be somewhat independent of temperature.

. . . Snowpack Water Content -- April 1 snow pack water content (expressed in percentage of average April 1 water content), updated for subsequent precipitation, was used to describe the amount of snowpack which must be primed before runoff would occur. The greater the water content of the snowpack, the slower the elevation of prime would rise.

The basic equation for computation of elevation of prime for the Kings River SCA snowmelt submodel took the following form:

Equation 2 $$E_p = 945K((1.009)^D + .00987(T1 - \frac{55.5}{K}))$$

Where: $E_p$ = the elevation of prime in metres

D = number of days since February 1

T1 = decayed accumulated temperature ($^oC$ days at 2100 m) since January 1 with a decay factor of 0.96

K = a variable affecting the elevation of prime as related to snowpack water content (HSI). K decreases with increasing HSI

HSI = high snow index expressed as a percentage of average April 1 water content, adjusted for subsequent precipitation.

The resulting elevation of prime represents the maximum elevation to which the watershed is fully primed and capable of producing snowmelt (for purposes of model computation) as of the given date. A flow diagram for calculation of the elevation of prime appears in Figure 3.

Generally during the spring snowmelt period, the elevation of prime will continue to increase as the season progresses. However, spring storms may deposit new snowpack at lower elevations. Usually this pack is transient and may melt in a few days with little increase in rate or volume of runoff. Snowmelt is often retarded below what might be expected with the increased area of snowpack until the freshly fallen snow has become primed. Occasionally, heavy precipitation may occur and some substantial increase in water supply and rate of runoff may be noted from the new snowpack. This hydrologic process has been modeled to force the elevation of prime to drop when the snow line drops, and then increase at a rate dependent upon temperature until it equals the calculated elevation of prime in the basic equation. If the snow line drops, the elevation of prime is required to drop a like amount. On each subsequent day, the elevation of prime rises at a rate equal to the rise in snow line plus an additional rise related to the 2100 m temperature.

Compute Snowmelt and Runoff Hydrograph

A flow diagram for the Kings River hydrologic model with the SCA snowmelt submodel is shown in Figure 4. Daily calculation of melt to eventually appear as surface runoff from calculation of individual elevation zone melt volumes (figure 3) results in the volume of daily snowmelt available for distribution as runoff in the main model. A portion of the volume of melt is directed through "recession storage", dependent upon the current level in storage which, from a hydrologic standpoint, would represent how wet the basin had been. After addition of a portion of the daily volume of melt to recession storage, recession storage is depleted at approximately six percent of total volume per day to form the recession flow. Recession storage has the capability of

smoothing a portion of the snowmelt by distributing it over many days as it is released from this temporary model storage. The remaining volume of snowmelt is distributed by a four-day unit hydrograph to produce the temperature related fluctuations noted in the observed runoff hydrograph.

Daily computed volumes of runoff distributed from recession storage and direct snowmelt runoff distributed by unit hydrograph are added to winter base flow, summer base flow, and precipitation flow derived from other submodels in the Kings River hydrologic model. The net result is a simulation of total mean daily discharge. During the period of maximum snowmelt runoff in seasons with average snowpack water content, the snowmelt submodel (including water distributed through recession storage) may account for 95 percent or more of the total mean daily flow. Winter base, summer base, and precipitation flow submodels account for the remainder.

## Results

As of the present time, testing of the SCA snowmelt submodel for the Kings River hydrologic model has not been completed. The results of preliminary testing and analysis have, however, been encouraging. Simulated mean daily runoff for the Kings River computed as output from the model has been plotted for 1973, 1974, 1975 and 1976, in Figures 5 through 8. Plots are in conventional units representing actual input and output from the model. Plots represent mean daily discharge in cubic feet per second against time, April 1 through the end of snowmelt. Shown for comparison are the discharges calculated from the model, unimpaired discharges observed, observed air temperature corrected to 2100 m, observed effective snowline, and calculated elevation of prime.

Calculation of daily discharges using the SCA snowmelt submodel appears to give results which are entirely acceptable in analysis. In addition, the conceptual model appears to be more consistent with known hydrologic relationships than the formerly used snowmelt submodel. This fact may give assurance in extrapolating the techniques into extreme conditions as well as representing an academically esthetic improvement over the original model. At this time, no testing has been done on other watersheds, but it is believed that the conceptual model will have a high degree of transferability.

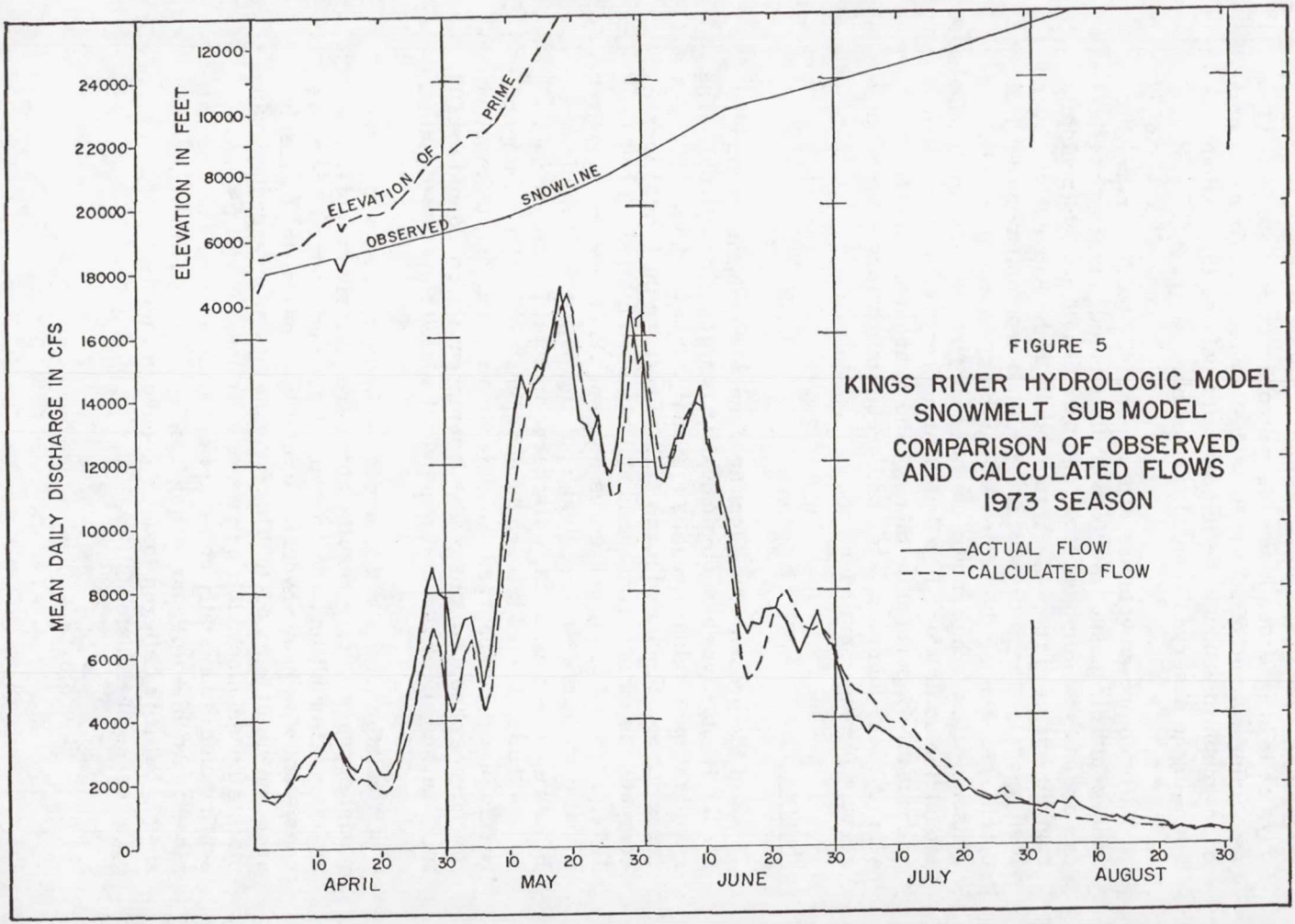


FIGURE 5

KINGS RIVER HYDROLOGIC MODEL
SNOWMELT SUB MODEL
COMPARISON OF OBSERVED
AND CALCULATED FLOWS
1973 SEASON

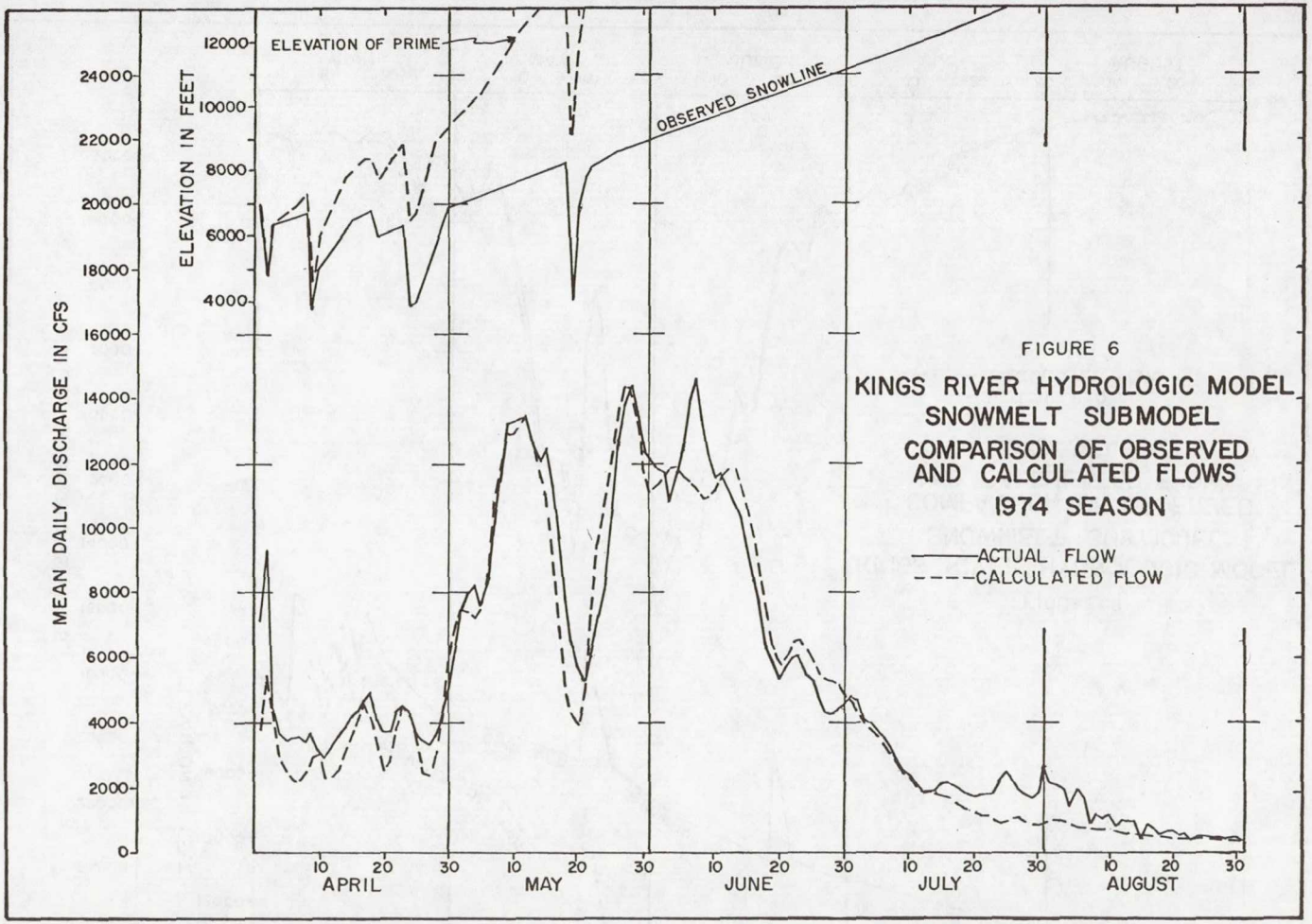


FIGURE 6

KINGS RIVER HYDROLOGIC MODEL
SNOWMELT SUBMODEL
COMPARISON OF OBSERVED AND CALCULATED FLOWS
1974 SEASON

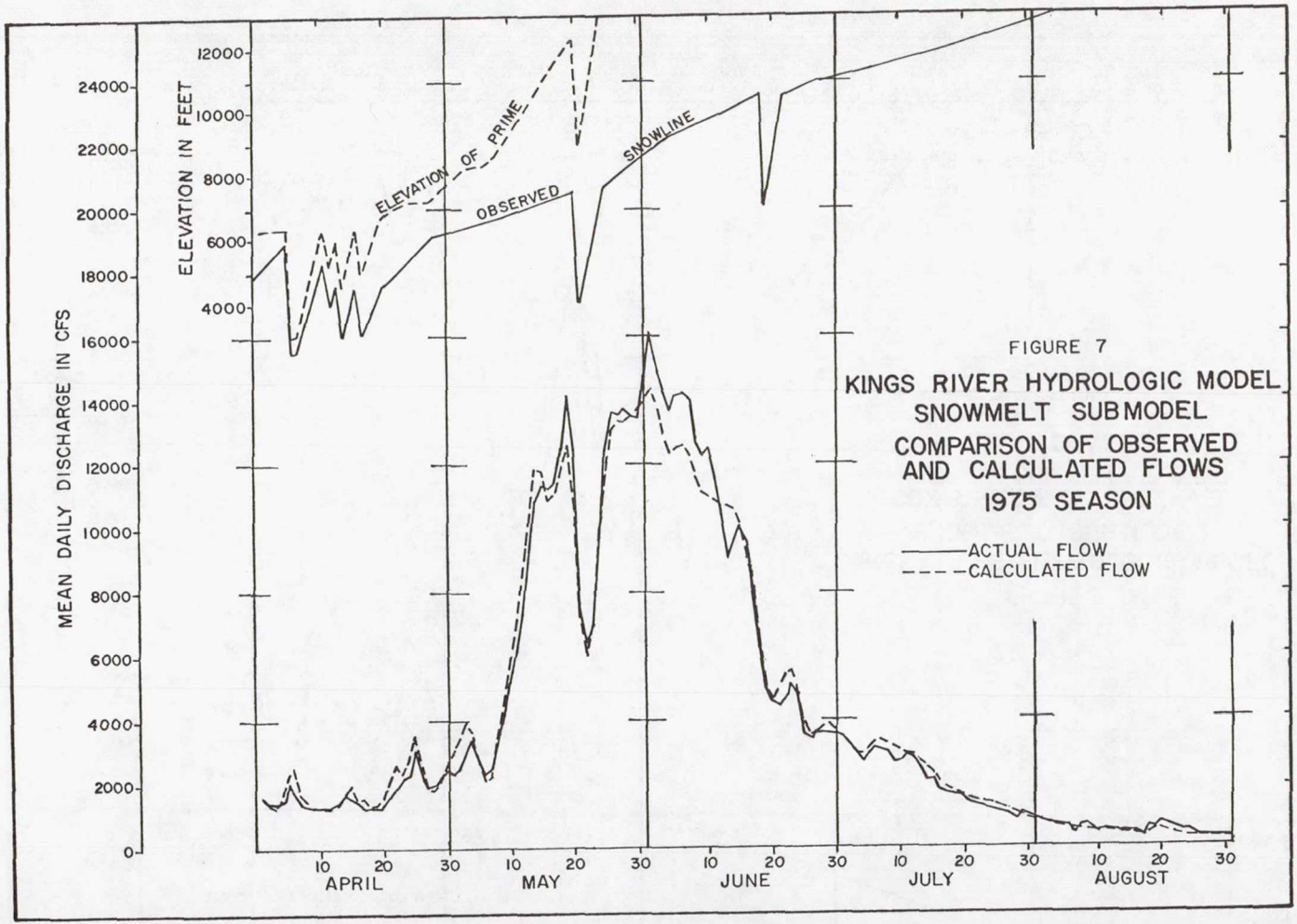
MEAN DAILY DISCHARGE IN CFS
ELEVATION IN FEET
ELEVATION OF PRIME
SNOWLINE
OBSERVED
APRIL
MAY
JUNE
JULY
AUGUST
FIGURE 7
KINGS RIVER HYDROLOGIC MODEL
SNOWMELT SUB MODEL
COMPARISON OF OBSERVED
AND CALCULATED FLOWS
1975 SEASON
ACTUAL FLOW
CALCULATED FLOW

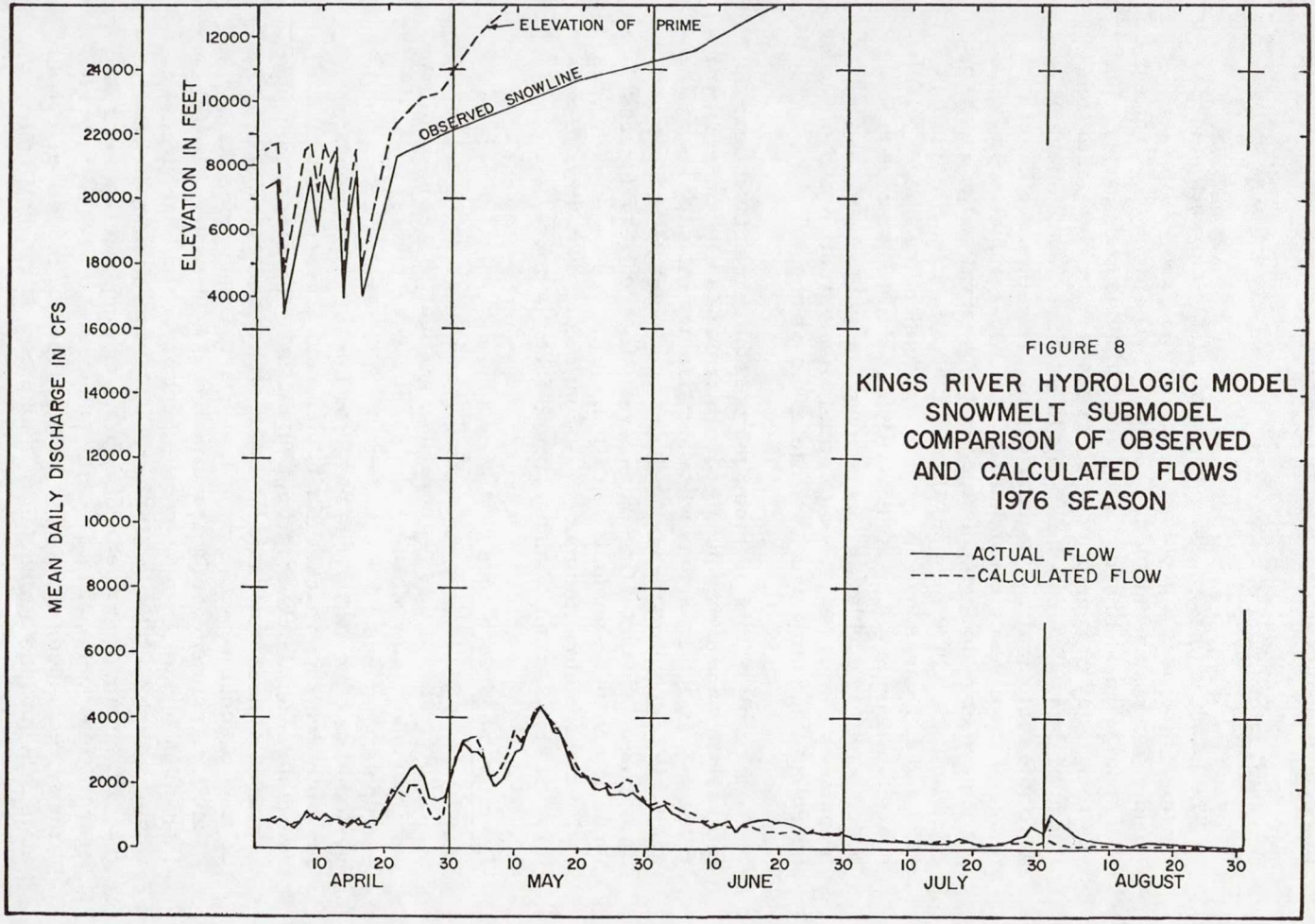


FIGURE 8

KINGS RIVER HYDROLOGIC MODEL
SNOWMELT SUBMODEL
COMPARISON OF OBSERVED
AND CALCULATED FLOWS
1976 SEASON

## INTERPOLATION AND EXTRAPOLATION OF SCA

### Availability of Imagery

The Landsat imagery is currently available only on a nine-day cycle. This poses a problem, since one image set obliterated by cloud cover may result in an 18-day period between observations that make Landsat imagery very difficult to use effectively. In addition, delay in receipt of imagery also adversely affects timeliness of data. The more difficult to interpret NOAA imagery is available historically on a daily cycle. Timeliness of satellite imagery has already caused difficulty in operational work, making it necessary to interpolate between observations and extrapolate into the future for operational analysis. Results for the 1977 and 1978 seasons have shown how misleading images widely spaced in time may be. Availability and timeliness of data may pose a critical problem in operational analysis, even though techniques can be developed to simulate snowmelt runoff through hydrologic modeling with satellite observations.

As a result of this problem, the possibility was investigated of interpolating and extrapolating results from satellite imagery with respect to time for periods when satisfactory imagery is not available. Modeling techniques are very sensitive to SCA, and an error in extrapolating data beyond the "date of forecast" tends to create an unstable situation. If the recession of SCA is estimated too slow, the model will continue to overestimate runoff until areal extent of snowcover is forcibly corrected.

### Description of Technique

The objective of this phase of the investigation was to (1) allow for interpolation of SCA between observations and (2) permit extrapolation beyond the last date of satellite observation for the period of at least two weeks based on intervening temperature, precipitation, snowpack water content and characteristics, and available satellite observations. Results in the Kings River basin appeared entirely adequate for interpolation and extrapolation for up to two weeks beyond date of last observation during the period of melt. Tests suggest that estimates of SCA could be extrapolated even further than two weeks, but undoubtedly accuracy would decline with time. It should be borne in mind, however, that if the primary value of SCA in water supply forecasting or hydrologic modeling is to describe unusual or unprecedented conditions, techniques which may be developed to "model" or extrapolate SCA into the future using other parameters may not

adequately reflect those unusual conditions.

Data have been collected for the Wind River Range in Wyoming to further test methods for extrapolating SCA. This testing is incomplete at the present time, but to date, many similarities have been noted between conditions in the Wind River and in the southern Sierra Nevada, in spite of the completely different climatologic and hydrologic regimes noted in the two areas.

## SUMMARY AND CONCLUSION

From a technical standpoint, results of the investigation were entirely acceptable in terms of simulating mean daily discharge and reproducing the snowmelt hydrograph. The ability to simulate rate of snowmelt runoff utilizing areal extent of snowcover from satellite imagery as a parameter in hydrologic modeling was demonstrated. The presence of cloud cover, missing data, delayed data or other problems have made information on snowcover unavailable for operational forecasting for considerable periods of time even in the southern Sierra which is normally reasonably clear during the period of snowmelt. This problem appears to be one of the major operational problems in the use of SCA. Areal extent of snowcover or elevation of snow line may be extrapolated with adequate accuracy for water supply forecasting and some hydrologic modeling for extended periods of time.

Applicability of information on SCA from satellite imagery to hydrologic modeling in the Kings River basin was demonstrated, and additional work should be done in this area, not only on the Kings River, but on other watersheds. It is hoped that there is enough local interest in this work to sponsor operational use of SCA in hydrologic modeling in the southern Sierra Nevada within the next few years.

References

1. "Hydrologic Model Research and Application -- Kings and San Joaquin River Basins", Final Report, December 1971, Sierra Hydrotech.

2. Hannaford, J.F., Bush, R.H., Barsch, R.E. "The Development and Application of a Hydrologic Model as an Operational Tool", Proceedings 38th Annual Meeting, Western Snow Conference, April 21-23, 1970.

3. Linsley, R.K. "A Simple Procedure for the Day to Day Forecasting of Runoff from Snowmelt", Transaction American Geophysical Union, Vol. 24, Part 3, pps. 62-67, 1943.

4. Hannaford, J.F., Howard, C.H. "Upper Air Data as a Parameter in Estimating Snowmelt Runoff", Proceedings 43rd Annual Meeting, Western Snow Conference, April 23-25, 1975.

# DISCHARGE FORECASTS IN MOUNTAIN BASINS BASED ON SATELLITE SNOW COVER MAPPING

J. Martinec and A. Rango, Federal Institute for Snow and Avalanche Research, Weissfluhjoch/Davos, Switzerland and Goddard Space Flight Center, Greenbelt, Maryland, U.S.A.

## ABSTRACT

Depletion curves of the areal extent of snow cover are shown to be basic information in a snowmelt-runoff model. Originally developed in European mountain basins, the procedure is now applied to simulate the runoff in the Rocky Mountains with the use of the Landsat imagery and air temperature data. The method requires a proper assessment of the recession coefficient of discharge in a given basin. It is adaptable to operational short-term forecasts of discharge and to evaluation of seasonal runoff volumes.

## INTRODUCTION

It has long been recognized that the areal extent of snow cover in a basin is an important factor for determining the amount of snowmelt runoff produced in the spring. Attempts to measure the snow-covered area from the ground using oblique photography or visual observations have not been acceptable, especially in large basins, because of a lack of basin-wide measurements including those for hidden slopes and a poor observing perspective. As a result, aircraft have been employed to provide an improved observing capability for snow-covered area mapping. Because most flights are conducted at low altitudes, in cases where complete basin coverage is required, much of the photography is still necessarily oblique which causes significant locational problems and limits the approach to general snow cover estimates. An alternative approach using low altitude aircraft flights makes use of a previously drafted watershed base map and a snow cover observer (Warskow, Wilson, and Kirdar, 1975). In this method the observer records the visual location of the snowline on the base map as the flight passes over pre-selected ground areas. At the same time he may make estimates of snow depth and melting condition of the snowpack based on the appearance of ground features. After returning from a flight the data are processed and a snow-covered area map is produced.

Because earth-oriented vertical photographs taken from low altitudes cover only a relatively small area, they are limited to snow-covered area determinations on correspondingly small watersheds or index areas for larger basins. Snow-cover mapping with 1:6,000 scale aerial photography was found to produce useful data for snowmelt runoff simulation in the Colorado Rocky Mountains (Leaf, 1969; Haeffner and Barnes, 1972). As the aircraft altitude is increased, larger areas come into the field of view of the cameras and snow cover over increasingly large watersheds can be mapped. It has been shown by Martinec (1972) that photography from 8.5 km altitude could be used to repetitively map the snow cover of the 43.3 $km^2$ Dischma basin near Davos, Switzerland. The snow cover data thus

obtained was used in simulation of daily snowmelt runoff for the Dischma basin. When larger watersheds are encountered, however, more expensive and time consuming use of several photographs is necessary. Even from the altitude of the NASA U-2 aircraft (18.3 km), mosaicking of five photographs is required to cover the 228 km$^2$ Dinwoody Creek watershed in the Wind River Mountains (a part of the Rocky Mountains) of Wyoming, U.S.A. (Rango, 1977).

Figure 1 shows an orthophoto of the Dischma basin. In this typical alpine valley with rugged terrain, the snow cover consists of many scattered patches. In order to determine the areal extent of the snow as a percent of the total area, a computerized procedure was adopted which consists of counting the snow-covered

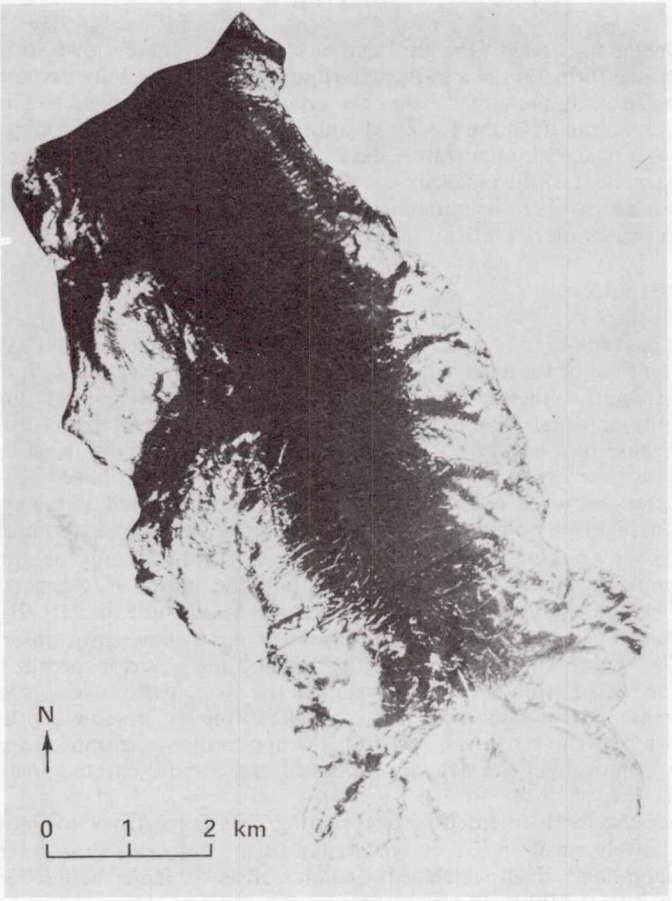


Fig. 1—Orthophotograph showing the snow cover in the Dischma basin (Swiss Alps) on 8 June 1976.

and snow-free points. Because about 215,000 points are counted within the watershed boundary, the effective resolution is about 15 m.

Figure 2 shows a simultaneous Landsat image which has been produced (Urfer, 1978) by digital classification of each pixel as snow-covered, partially snow-covered, or snow-free, respectively. The resolution of Landsat is entirely adequate for hydrological evaluations even in a basin of this relatively small size. For larger basins the use of Landsat eliminates the troublesome task of mosaicking several aerial photographs. Conversely, the periodic monitoring of the seasonal snow cover in the Alps is frequently disturbed by clouds.

## SNOW-COVER DEPLETION CURVES

The areal extent of snow cover constitutes basic information for the day-to-day computation of snowmelt runoff. The snow-covered area cannot reliably indicate the water volume stored in the snowpack, however, as illustrated by Figure 3. Although the snow coverage was similar on both dates, the water equivalent measured in a representative site was about 800 mm on June 22, 1970, and only about 410 mm on May 16, 1969. The snow coverage should probably be related to the ratio of the current snow depth, $H_{s\ actual}$, to the maximum snow depth of the

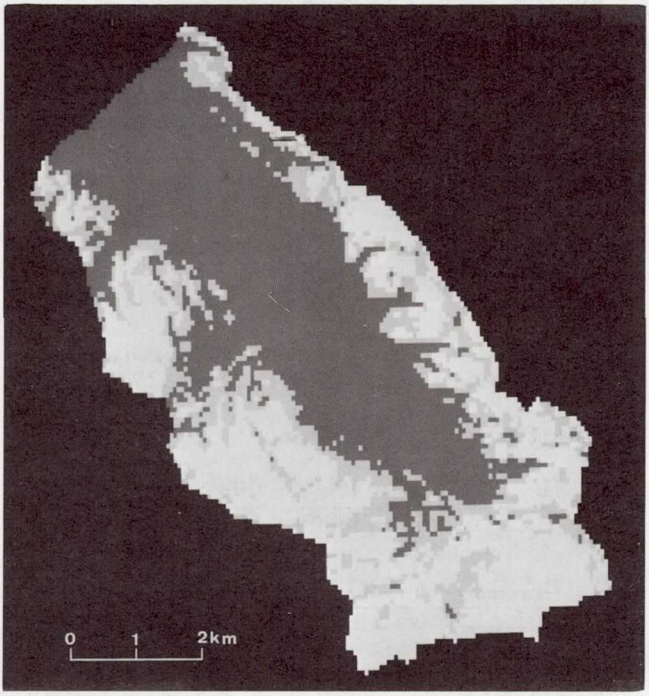


Fig. 2—Satellite image of the Dischma basin on 8 June 1976 with digitally classified snow cover evaluated from Landsat 2 data (reproduced by courtesy of the Department of Geography, University of Zurich, Switzerland).

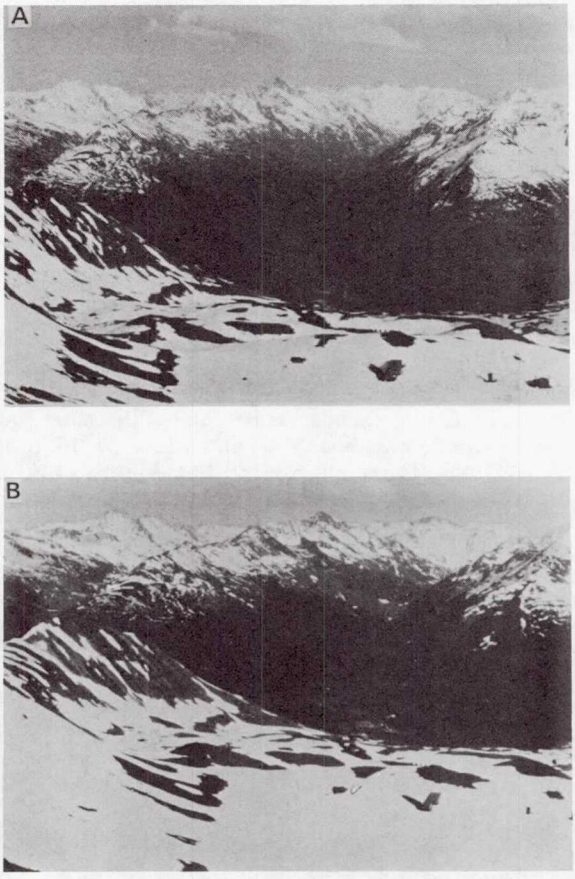


Fig. 3—Terrestrial photos of the Dischma basin and the vicinity, A) 16 May 1969, B) 22 June 1970.

respective winter season, $H_{s\,max}$. In this case,

$$\frac{H_{s\,actual}\,(\text{May 16, 1969})}{H_{s\,max}\,(\text{April 18, 1969})} = \frac{109\text{ cm}}{208\text{ cm}} = 0.524$$

$$\frac{H_{s\,actual}\,(\text{June 22, 1970})}{H_{s\,max}\,(\text{May 2, 1970})} = \frac{158\text{ cm}}{321\text{ cm}} = 0.492$$

Thus similar areal extents of the snow cover as shown in Figure 3 correspond to similar snow-depth ratios.

For seasonal discharge forecasts, it would be useful to replace snow depths by water equivalents. It remains to be seen whether such interpretations of the snow coverage can produce reasonably consistent relations. In any case, a short-lived

snow cover caused by occasional snow storms during the snowmelt season should be disregarded in these evaluations.

An example of depletion curves of the snow coverage in the Dischma basin is shown in Figure 4. In addition to the entire watershed, separate curves have been plotted for the three elevation bands A(1668-2100 m), B(2100-2600 m), and C(2600-3146 m), respectively. In Figure 5, depletion curves in the Dinwoody basin for four elevation bands (A:1981-2438 m, B:2438-2896 m, C:2896-3353 m, and D:3353-4202 m) show a different pattern of the snow cover retreat. The gradually rising snow line can be better defined than in Dischma, enabling photo interpretation and planimetering to be used with much greater ease.

## RUNOFF CHARACTERISTICS IN MOUNTAIN BASINS

During a snowmelt season, the seasonal increase of temperature is accompanied by a gradual diminution of the snow-covered area. This situation is shown in Figure 6. If the meltwater volume is a product of the energy input (represented by degree-days) and of the snow-covered area, the maximum is reached when the snow coverage is already reduced and while temperatures are still rising. The highest temperatures cannot produce extreme snowmelt volumes since the snow-covered area has diminished in the meantime.

A different runoff pattern is obtained from a snow lysimeter with a surface area of 5 $m^2$. The snow coverage was 100% until the last few days. Consequently, the outflow from the lysimeter keeps rising and then abruptly ceases.

This example shows the importance of the snow cover monitoring for snowmelt-runoff computations. A realistic input thus obtained must be of course transformed into the output, that is to say into discharge from a mountain basin.

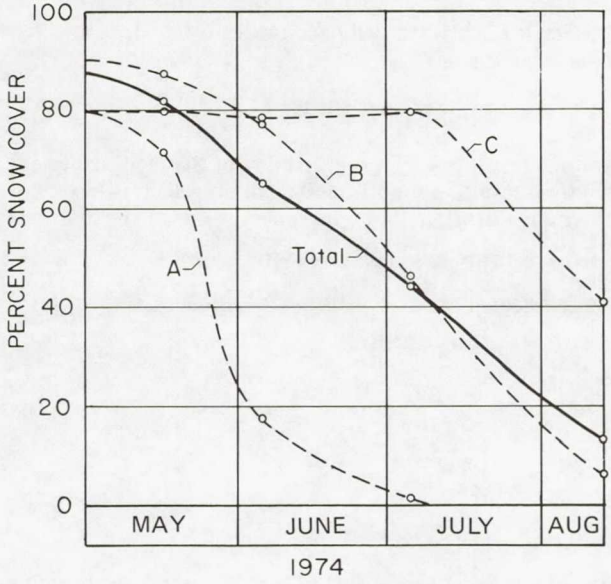


Fig. 4—Depletion curves of the snow coverage in the Dischma basin and in the zones A, B, C, 1974.

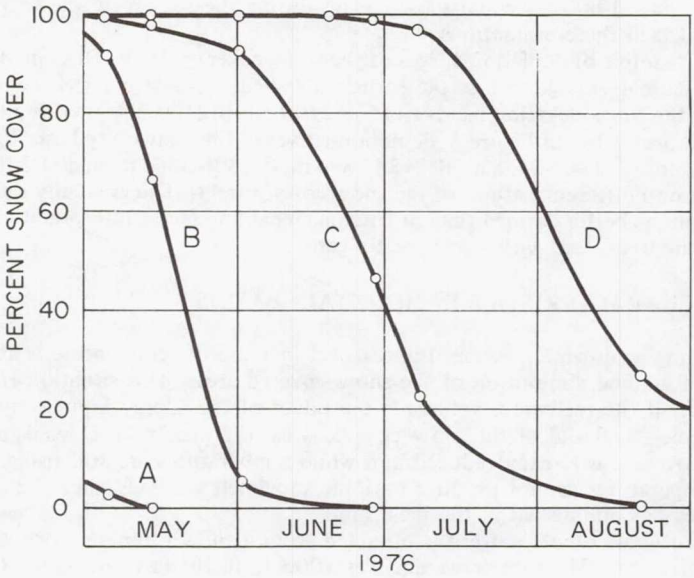


Fig. 5—Depletion curves of the snow coverage in the Dinwoody Creek basin (Rocky Mountains), zones A, B, C, D.

## SNOWMELT-RUNOFF MODEL

A simple relation between daily meltwater production and resulting runoff can be derived as follows:

$$M_1 = R_t = R_1 \frac{k^{\infty} - 1}{k - 1} \tag{1}$$

where $M_1$ is the snowmelt [cm] on the first day of the melting period,
$R_t$ is the total resulting runoff depth [cm] (neglecting losses),
$R_1$ is the runoff depth in 24 hours since the rise of the hydrograph [cm],
$k = \frac{R_m}{R_{m-1}}$ is the recession coefficient.
m refers to a sequence of days during recession.

Since $k < 1$, it follows that:

$$M_1 = R_t = R_1 \frac{1}{1 - k} \tag{2}$$

and

$$R_1 = M_1 (1 - k) \tag{3}$$

On the nth day,

$$R_n = M_n (1 - k) + R_{n-1} \cdot k \tag{4}$$

The superimposition of the immediate meltwater contribution on the extrapolated recession curve is illustrated in Figure 7.

Daily snowmelt depths are determined by the degree-day method:

$$M = a \cdot T \tag{5}$$

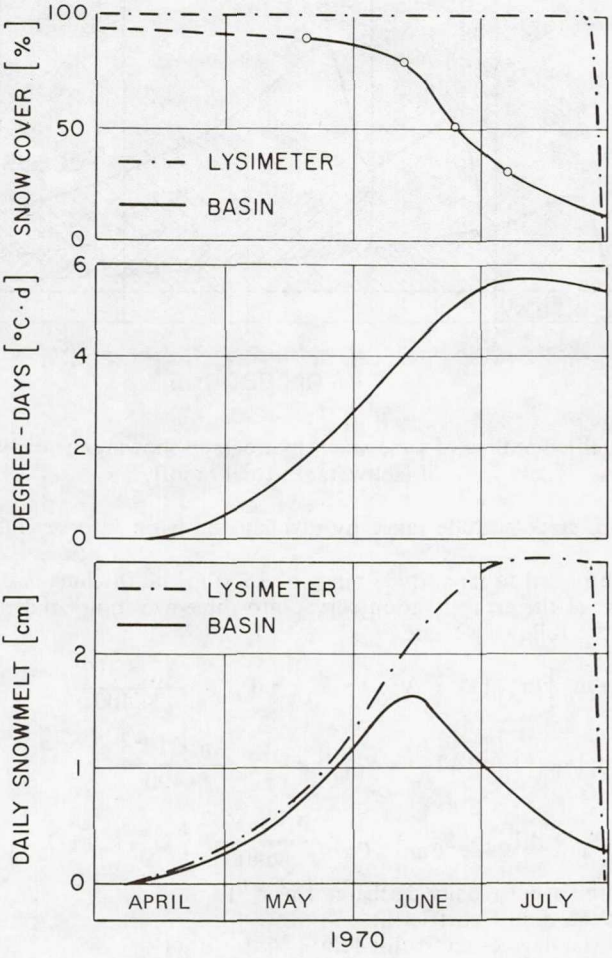


Fig. 6–Effect of depletion curves of snow coverage on runoff patterns in a basin and on a snow lysimeter.

where M is the daily snowmelt depth [cm],
a is the degree-day factor [cm · $°C^{-1}$ · $d^{-1}$],
T is the number of degree-days [°C · d]

This simple relation could be refined by taking into account the whole energy balance. However, if a snowmelt runoff model can perform well with temperature data only, there are better prospects of practical applications.

The so called "Martinec model" [Martinec, 1970] has been developed with the characteristics of snowmelt-runoff in mountain basins in mind, without attempting to achieve a universal validity. It is based on monitoring the areal extent of the snow cover and on a proper assessment of the recession coefficient. It can be

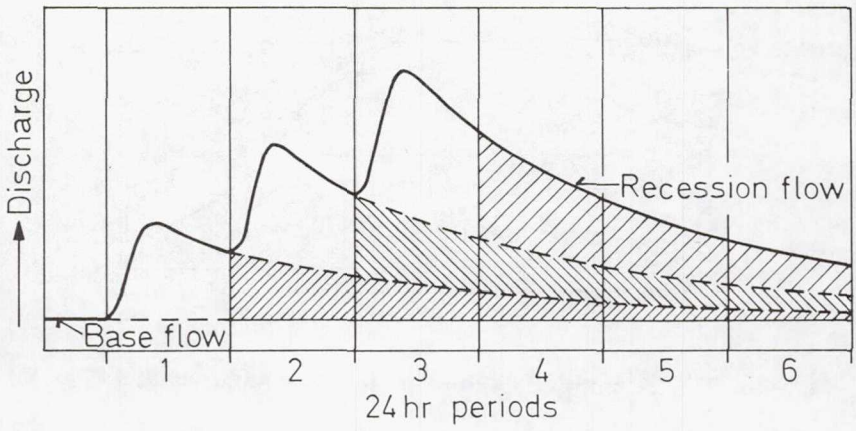


Fig. 7—Simplified outline of a snowmelt hydrograph showing the daily contribution of meltwater to total runoff.

adapted to a great altitude range by dividing the basin into several elevation zones.

With regard to its altitude range of 1500 m, the Dischma basin was divided, with the use of the area-elevation curve, into three elevation bands. The model then takes the following form:

$$Q_n = c_n \Big\{ [a_{An}(T_n + \Delta T_A) \cdot S_{An} + P_{An}] \frac{A_A \cdot 10^{-2}}{86400} + [a_{Bn}(T_n + \Delta T_B) \cdot S_{Bn} + P_{Bn}] \frac{A_B \cdot 10^{-2}}{86400} + [a_{Cn}(T_n + \Delta T_C) \cdot S_{Cn} + P_{Cn}] \frac{A_C \cdot 10^{-2}}{86400} \Big\} (1 - k_n) + Q_{n-1} \cdot k_n \quad (6)$$

where Q is the average daily discharge [$m^3 s^{-1}$]
$c_n$ is the runoff coefficient
$a_n$ is the degree-day factor [$cm \cdot °C^{-1} \cdot d^{-1}$]
$T_n$ is the measured number of degree-days [$°C \cdot d$]
$\Delta T$ is the correction by the temperature lapse rate [$°C \cdot d$]
S is the snow coverage (100% = 1.0)
$P_n$ is the precipitation contributing to runoff [cm]
A is the area [$m^2$]
$k_n$ is the recession coefficient
n is an index referring to the sequence of days
A, B, C as indices refer to the three elevation zones
$\frac{10^{-2}}{86400}$ converts $cm \cdot m^2$ per day to $m^3 s^{-1}$

The recession coefficient appears to be variable, depending on the current discharge by a function:

$$k = x \cdot Q^{-y} \quad (7)$$

The factors x, y must be determined for the given watershed. For example, each daily discharge $Q_n$ can be plotted against the subsequent discharge $Q_{n+1}$. From

the envelope of points indicating a decreasing runoff, it is possible to determine k for any desired Q and to evaluate x, y. If discharge data are not available, the size of the basin might be of assistance to estimate the relation between k and Q.

Since direct measurements of the degree-day factor are seldom available, an empirical relation [Martinec, 1960] may be of assistance:

$$a\ [\text{cm} \cdot {}^{\circ}\text{C}^{-1}\text{d}^{-1}] = 1.1\frac{\rho_s}{\rho_w} \qquad (8)$$

where $\rho_s$ and $\rho_w$ are the density of snow and water, respectively. This equation is not valid for ice.

The model can be tested by comparing the computed values with the measured discharge data.

## RESULTS OF THE RUNOFF SIMULATION

Figure 8 shows a comparison of day-to-day computations by equation (6) with the measured discharge in the Dischma basin. The numbers of degree-days were determined for 24 hour periods starting at 0600 hours. With regard to the time-lag, the corresponding discharge values refer to 24 hour periods starting at 1200 hours. The simulation started on 8 May by computing $k_{8.5} = 0.87$ from the

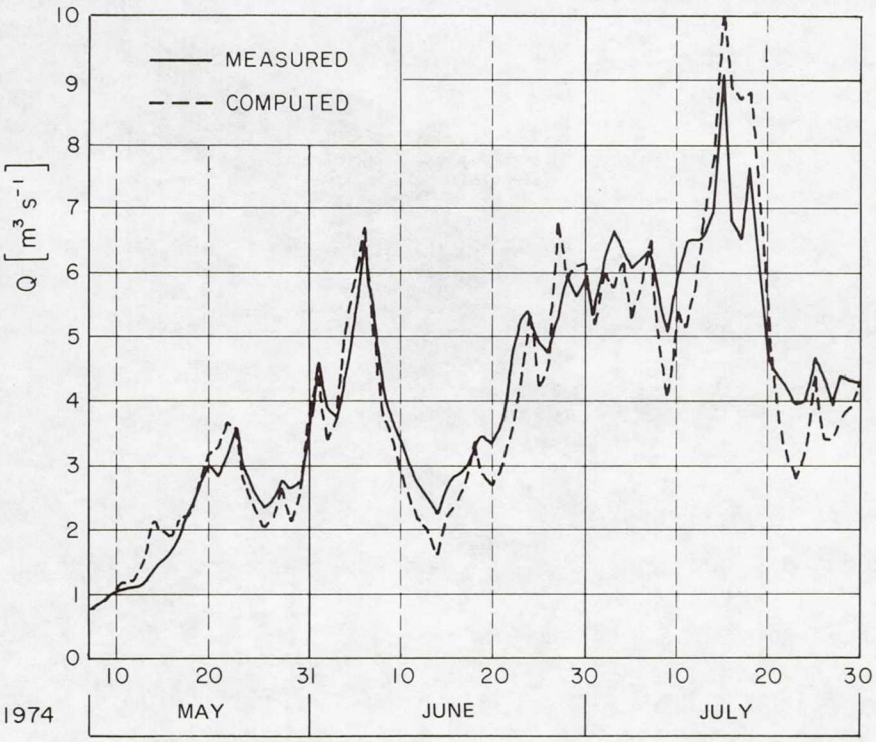


Fig. 8—Computed and measured runoff in the Dischma basin in the snowmelt season 1974.

measured $Q_{7.5} = 0.77\ m^3s^{-1}$ by equation (7) with x = 0.85, y = 0.086. From then on, only computed Q was used until 30 July to determine the next day's value of k. The degree-day ratios were obtained by equation (8) from snow density measurements and varied from 0.45 to 0.55. A uniform temperature lapse-rate of 0.65°C per 100 m altitude difference was used for extrapolations of degree-days to the hypsometric mean elevations of the zones A, B, and C. Uncertainties associated with this temperature extrapolation were reduced by an automatic meteorological station placed at the average altitude of the basin. The runoff coefficient c was estimated in the range of 0.9 to 1.0 for snow and by 0.7 for any additional rainfall. The snow coverage was periodically determined from orthophotographs and read off each day from the depletion curves (Figure 4).

Another application in the Dinwoody Creek basin in the Wind River Mountains tested the model in new, less favorable conditions differing from those of a well-equipped representative basin. Only temperature and precipitation data from a station 100 km outside the basin, as well as snow-cover images from Landsats 1 and 2 were available for computing the snowmelt runoff. An example of Dinwoody Creek snow cover as viewed from Landsat is shown in Figure 9.

In view of the altitude range of over 2000 m on the Dinwoody basin, the model formula was extended to four elevation bands. A time-lag of about 18 hours was estimated from discharge records. This value is at least partially explained by

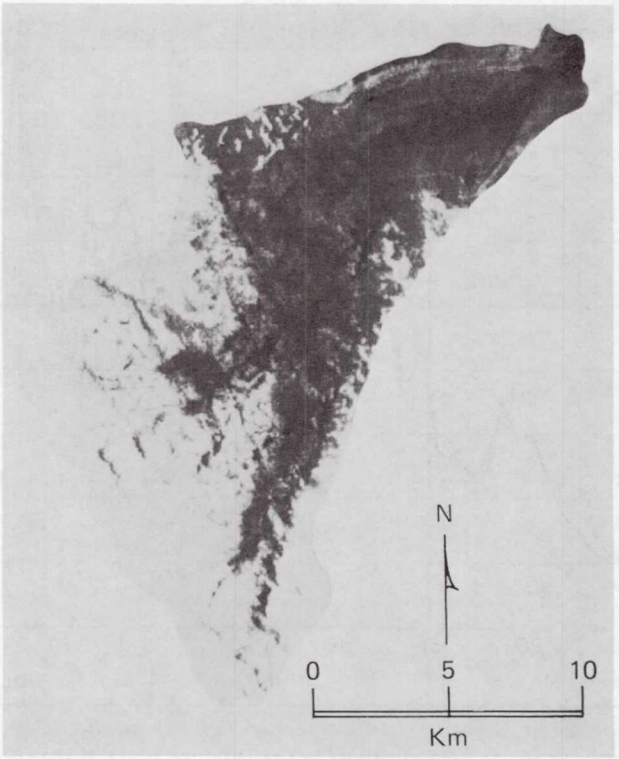


Fig. 9—Landsat image of the Dinwoody Creek basin on 28 June 1976.

the greater size of the basin as compared with the previous case. Equation (6) was thus rearranged as follows:

$$Q_{n+1} = c_n (I_{An} + I_{Bn} + I_{Cn} + I_{Dn}) (1 - k_{n+1}) + Q_n k_{n+1} \quad (9)$$

where the inputs I are again:

$$I_{Nn} = [a_{Nn} (T_n + \Delta T_N) \cdot S_{Nn} + P_{Nn}] \frac{A_N \cdot 10^{-2}}{86400} \quad (10)$$

By analyzing Dinwoody discharge data from 1973 to 1976, x = 0.884 and y = 0.0677 were derived for determining k by equation (7).

The simulation started on April 1, 1976 by computing $k_{2.4}$ from the measured $Q_{1.4}$ to compute $Q_{2.4}$. Afterwards, for the 6-month period, the computed Q was always used to determine the next k. No updating was thus carried out. In view of the length of the period, seasonal variations of losses and of the temperature lapse rate were taken into account on the basis of available information about the climate [Barry and Chorley, 1970]. The runoff coefficient was estimated in the range from 0.85 in April to 0.75 in July to 0.9 in September. The temperature lapse rate appeared to be higher than in the Alps. Values varying from 0.85°C per 100 m in April to 0.95°C per 100 m in July and 0.80°C per 100 m in September were used. In addition, regional differences between the meteorological station at Lander airport and the basin were accounted for by subtracting up to 2°C from the Lander data.

The degree-day factor was assessed in the range from 0.35 at the start to 0.6 at the end of the snowmelt season. The delay of the snow ripening in the high parts of the basin was taken into account by differentiating the degree-day ratios in the respective elevation zones. The snow coverage was determined each day from the depletion curves shown in Figure 5.

With all variables and parameters of the model thus measured or determined, tables have been prepared for the numerical and graphical evaluation according to Equations (9, 10). While S, k, T, P are changing each day, a, c, $\Delta T$ are adjusted stepwise in intervals of several weeks or months.

The comparison of the simulated runoff with discharge measurements of the U.S. Geological Survey illustrated in Figure 10 shows a reasonable agreement. A number of the deviations seem to have been caused by the insufficient precipitation data.

Adequate Landsat data from the year 1974 provided another opportunity for a snowmelt-runoff simulation in the Dinwoody Creek basin. Seasonal changes of of the temperature lapse rate, of the runoff coefficient, and of the degree-day factor were again varied as in 1976 for this basin. Judging from the depletion curves of 1974, the progress of the snowmelt season seemed to be accelerated by about 2 weeks in comparison with 1976. In an attempt to take this roughly into account, the seasonal course of the runoff coefficient, of the temperature lapse rate, and of the degree-day factor was generally shifted in a corresponding sense. Figure 11 shows again a good agreement between the simulated and measured runoff for 1974.

Since the measured discharge was never used for an updating, it seems possible to simulate discharge in ungaged sites by using Landsat images of the snow cover together with temperature and precipitation data.

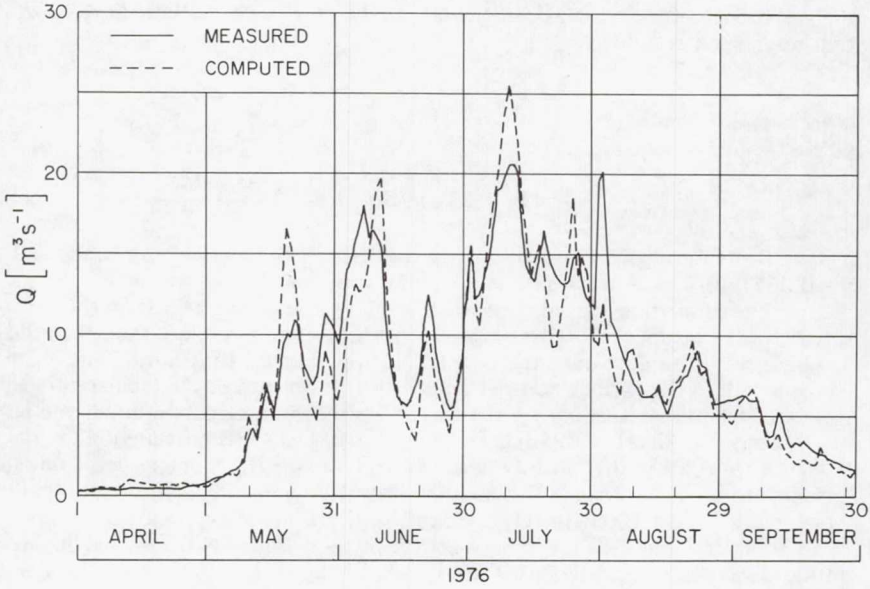


Fig. 10–Computed and measured runoff in the Dinwoody Creek basin in the summer half year 1976.

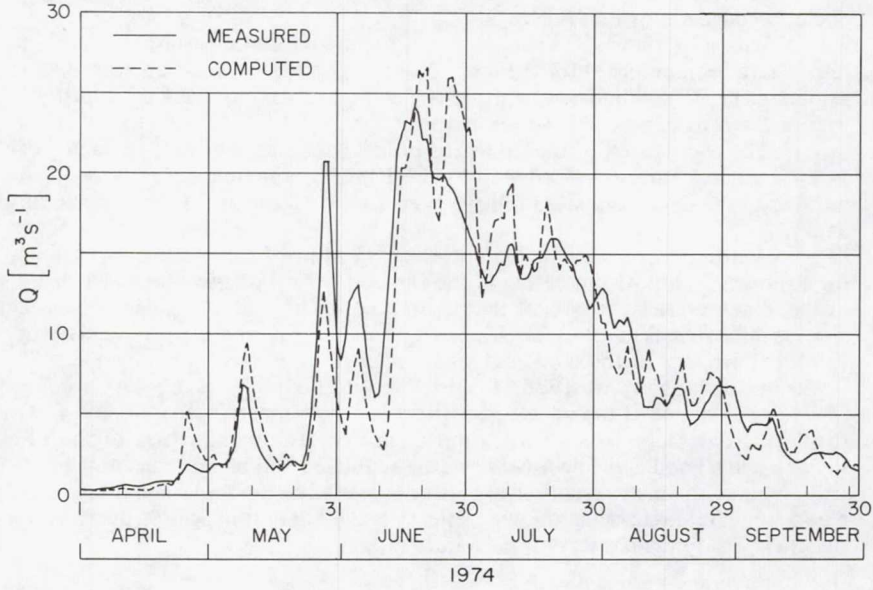


Fig. 11–Computed and measured runoff in the Dinwoody Creek basin in the summer half year 1974.

## APPLICATION TO OTHER AREAS; DISCHARGE FORECASTS

In order to be useful for operational hydrology, satellite snow-cover monitoring must satisfy certain requirements, primary of which are frequency of coverage, spatial resolution, and timeliness of data. Although the snowmelt model can provide daily runoff forecasts, it is not necessary to observe the snow cover on a daily basis. Rather, in the Wind River Mountains it appears that because of favorable cloud cover conditions during the snowmelt period, satellite coverage of once every nine days (as provided with the 80 m resolution data from the two Landsat vehicles) is nearly adequate for runoff forecasting purposes. When cloud cover frequency increases (as shown in Figure 12), however, more frequent satellite coverage is also required, perhaps as much as once every 1-3 days. In the future in extremely cloudy areas it may even be necessary to switch from visible to high resolution microwave sensors that can penetrate clouds. Timeliness of data is essentially an information management problem which can be solved as the required satellite systems become operational. It appears that a realistic goal for delivery of the snow-cover data for operational purposes is within 72 hours after data acquisition.

To facilitate a determination of where Landsat capabilities would be appropriate for snow-cover monitoring and daily runoff forecasts, cloud cover statistics for Landsat overpasses were generated for the Wind River Mountains of Wyoming (considered a marginally useable area) and then compared with statistics from other

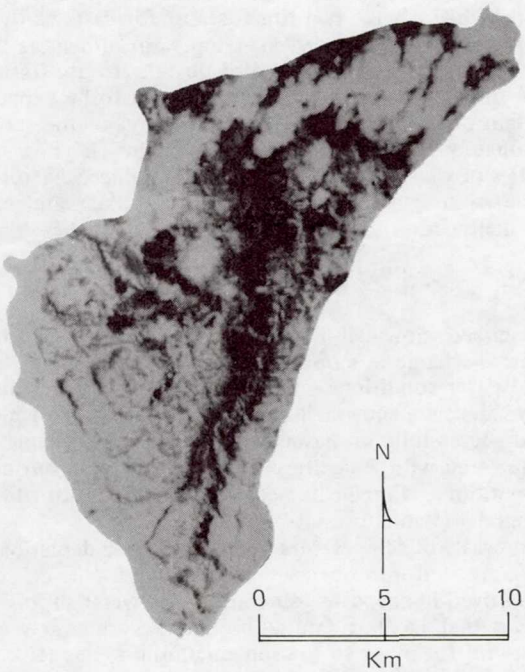


Fig. 12—Landsat image of the Dinwoody Creek basin showing snow cover with clouds on 10 June 1976.

important snowmelt runoff areas in the western United States. The cloud cover for each Landsat image obtained during the April – September snowmelt period was categorized as a percent (%) rounded off to the next highest increment of 10 for 1973–1978. Assuming that Landsat scenes with 40% or less cloud cover are useable for snow-cover delineation, approximately 73% of all Landsat passes over the Wind River Mountains during the snowmelt period will provide meaningful snow-cover information. This compares to 81% in the White Mountains of central Arizona, 91% in the southern Sierra Nevada Mountains of California, 81% in the San Juan Mountains of Colorado, and 55% in the northern Rocky Mountains of Montana. Based on these comparisons it appears that Landsat-type operational snow-cover data would be useful for snowmelt runoff simulations and perhaps forecasts in several important snowmelt runoff zones in the western United States, with the major difficulty being experienced in the northern Rocky Mountains and coastal ranges of the northwest United States where an increased frequency of cloudiness as well as heavy timber cover limits unobstructed Landsat views. More frequent coverage as well as cloud penetrating microwave capabilities will probably be necessary in this important snow zone of the northwest United States.

Cloud cover data for other mountain ranges around the world is incomplete and comparisons cannot be made. It is known, however, that significant cloud cover problems exist in the Alps that mandate improvements over the current Landsat system before snowmelt-runoff forecasts can be made.

Naturally, a runoff simulation from a past season for which all data are available is not a forecast. However, this simple model needs only temperatures and the snow coverage. While real time data or forecasts of the energy budget are difficult to obtain (Limpert, 1975), temperature forecasts for several days in advance are frequently available. It is also possible to use statistical temperature data to predict the maximum and minimum runoff to be expected in a given period with a certain probability. The depletion curves of the snow-covered areas can be approximately extrapolated and up-dated by each new satellite observation. The uncertainties of this extrapolation could be reduced by research into the relation of the snow-cover depletion curves to the initial water equivalent of the snowpack and melt-period temperatures.

## CONCLUSIONS

The described snowmelt-runoff model together with Landsat data can be used to simulate discharge in mountainous areas with a large elevation range and moderate cloud cover conditions (cloud cover of 40% or less during Landsat passes 70% of the time during a snowmelt season). So far the snowmelt-runoff model has been tested successfully on basins with areas not exceeding several hundred square kilometers and with a significant component of subsurface runoff. For different basin conditions, it might be necessary to emphasize additional factors in such a runoff model (Hannaford, 1977).

With forecasts of temperature and snow-cover depletions, the model simulations can be converted into operational discharge forecasts. The forecasts would be used for improved hydropower generation and water supply allocations.

It appears that Landsat data with once every nine day coverage would be operationally useful for input to the snowmelt-runoff model in mountainous portions of Wyoming, Colorado, the arid Southwest, and southern California in the United States. Cloud cover in the northern Rocky Mountains and the coastal ranges of the northwest United States markedly reduces the effectiveness of Landsat, however.

In regions where cloud cover frequency limits the usefulness of the current Landsat system, several alternative solutions should be considered for the future: evolution of an operational Landsat system with coverage available at least once every three days; the use of synchronous satellite data with a resolution of 1 km or less; operational aircraft coverage; or development of a high resolution microwave system for penetrating the clouds. Any of these systems should facilitate obtaining the important snow cover input data for use in snowmelt-runoff forecasts.

## ACKNOWLEDGMENTS

We would like to thank H. J. Etter, G. Klausegger, J. V. Niederhäusern, and E. Wengi, Federal Institute for Snow and Avalanche Research, James L. Foster, Goddard Space Flight Center, and Ralph Peterson, General Electric Company, Beltsville, Maryland, U.S.A. for performing essential data analysis for this project. Necessary data were supplied by the U.S. Geological Survey, U.S. Soil Conservation Service, and the National Oceanic and Atmospheric Administration. Special gratitude is extended to the Director of the Federal Institute for Snow and Avalanche Research, Prof. M. de Quervain, and to the Acting Director of Applications, Goddard Space Flight Center, Dr. L. Meredith for their continuing support of this international cooperation.

## REFERENCES

Barry, R. G., and R. J. Chorley, Atmosphere, Weather and Climate, Holt, Rinehart, and Winston, Inc., New York, 320 pp., 1970.

Haeffner, A. D., and A. H. Barnes, Photogrammetric determinations of snow cover extent from uncontrolled aerial photographs, American Society of Photogrammetry, Technical Session Proceedings, Columbus, Ohio, pp 319-340, October, 1972.

Hannaford, J. F., Investigation application of satellite imagery to hydrologic modeling snowmelt runoff in the southern Sierra Nevada, Phase 1 Final Report, NAS 5-22957, NASA, Goddard Space Flight Center, Greenbelt, Maryland, 48 pp., 1977.

Leaf, C. F., Aerial photographs for operational streamflow forecasting in the Colorado Rockies, Proceedings of the 37th Annual Western Snow Conference, Salt Lake City, Utah, pp. 19-28, 1969.

Limpert, F. A., Operational application of satellite snowcover observations – northwest United States, Proceedings of the Workshop on Operational Applications of Satellite Snowcover Observations, NASA SP-391, Washington, D.C., pp. 71-85, 1975.

Martinec, J., The degree-day factor for snowmelt-runoff forecasting, IAHS Publication No. 51, Surface Waters, pp. 468-477, 1960.

Martinec, J., Study of snowmelt-runoff process in two representative watersheds with different elevation range, IAHS Publication No. 96, Symposium of Wellington (N.Z.), pp. 29-39, 1970.

Martinec, J., Evaluation of air photos for snowmelt-runoff forecasts, Proceedings of the Banff Symposium – The Role of Snow and Ice in Hydrology, IAHS – AISH Publication No. 107, pp. 915-926, 1972.

Rango, A., Remote sensing: snow monitoring tool for today and tomorrow, Proceedings of the 45th Annual Western Snow Conference, Albuquerque, New Mexico, pp. 75-81, 1977.

Urfer, H. P., Routinemässige Schneekartierungen in hydrologischen Einzugsgebieten (Routine snow mapping in hydrologic basins), M. Sc. Thesis, Department of Geography, University of Zurich, 1978.

Warskow, W. L., T. T. Wilson, and E. Kirdar, The application of hydrometeorological data obtained by remote sensing techniques for multipurpose reservoir operations, Proceedings of the Workshop on Operational Applications of Satellite Snowcover Observations, NASA SP-391, Washington, D.C., pp. 29–37, 1975.

# COST/BENEFIT ANALYSIS FOR THE OPERATIONAL APPLICATIONS OF SATELLITE SNOWCOVER OBSERVATIONS (OASSO)

Peter A. Castruccio, Harry L. Loats, Jr., Donald Lloyd, Pixie A. B. Newman,
ECOsystems International, Inc., Gambrills, Maryland

ABSTRACT

Irrigation and hydropower benefits for the 11 western states by forecast improvement from satellite snowcover area were made based on data supplied by OASSO ASVT's.

## INTRODUCTION

It is almost a decade, dating from the early 1970's that satellite technology has been capable of providing relatively high quality images on a frequent enough basis to indicate to hydrologists that a possibility for gathering data on the snowpack area was practical. Both the techniques for mensurating the snowpack area and its application for improving seasonal runoff predictions have been demonstrated (Leaf, 1971; Rango, 1975; Barnes and Bowley, 1974). As a result, an Applications Systems Verification and Transfer (ASVT) program was established, whose major thrust was to extend these efforts to operational forecasting.

The operational employment of satellite snowcovered area measurement (SATSCAM) to runoff forecasting has been evaluated at four ASVT sites strategically located throughout the western United States. To supplement the ASVT technical evaluation, NASA initiated a study to determine the costs and benefits of operationally applying SATSCAM.

Previous benefit estimates due to improved information on the area of the snowpack have used parametric estimates of overall improvement and did not rely upon actual experience or expert evidence on the actual levels of improvement possible. These approaches have not included detailed treatments of the physical mechanisms "driving" the benefits; e.g., increased irrigation value of specific crops, cost differential between hydroenergy and thermal electric energy, etc. The present study was established to use the results and experiences gathered from operationally oriented ASVT personnel whose expertise, knowledge, and estimates form the basis for the benefit estimate presented herein. In this regard, a note of special thanks to all the ASVT personnel for their valuable assistance, consideration, and patience throughout this project.

### Benefits Derived from Improved Information

The major benefits of improved snowmelt runoff forecasting are naturally related to the major uses of water.

The major uses of water in the United States, ranked by importance in terms of gross value, are:

- Hydropower
- Irrigation
- Municipal and Industry
- Navigation
- Recreation, Land and Wildlife Management

The principal direct and indirect benefits for each use are given in Table 1.

In addition to the above, the benefits due to flood damage reduction must be added. The direct benefits are the reduction in losses to public and private property and the increases in net income arising from more extensive use of property. The indirect benefits to reduced flood damage result from the reductions of losses caused by the interruption to public and private activities. Major intangible benefits accrue to the prevention of the loss of human life and to positive effects on the general welfare and security of the populace.

Hydroelectric energy production is the largest user of water in the 11 western states and is potentially the largest benefactor of improved streamflow forecasting in terms of energy produced. Approximately 190 terawatt-hours of hydroelectric energy are produced annually in the 11 western states, requiring over 2 billion acre-feet of water. The annual dollar volume of hydroelectric energy sales at current prices is on the order of $6 billion.

Irrigation is second to hydropower in quantity of water used and potential physical benefit from improved knowledge of streamflow. Twenty-five percent ($12 billion) of all crops sold in the United States are produced on irrigated land. Irrigation accounts for approximately 40 percent of all the water withdrawn annually in the United States (with hydropower excluded since it does not withdraw water). Sixty percent of the irrigation water is consumed as evapotranspiration from crops and soil surfaces, making irrigation the largest consumptive user of water. The 11 western states contain approximately 23 million acres of irrigated land and account for approximately 58 percent of the nation's irrigation requirements or approximately 100 million acre-feet of water annually.

The next largest use of water is municipal and industrial water supply. As shown in Table 2 which reports recent annual withdrawals for various uses in the 11 western states, municipal and industrial uses required only 10 percent of the water required by irrigation and less than 1 percent of that required by hydropower. Consequently, the central focus of this study was directed at estimating the benefit of improved streamflow forecasting to hydropower production and to irrigated agriculture.

Estimation of the Upper Bound Value of Water for Hydroelectric

Table 3 summarizes the results of the computation of the value of snowpack runoff water for hydropower production. Baseline data (Colorado State University: Economic Value of Water, 1972) from 1968 shows that the average value of alternative energy was 6.8 mills/kWh at a capacity utilization factor of 48 percent. Data for

Table 1

Generic Benefits of Improved Information for Water Management and Utilization

| | HYDROENERGY | IRRIGATION | MUNICIPAL/INDUSTRIAL | NAVIGATION | RECREATION, FISH & WILDLIFE |
|---|---|---|---|---|---|
| DIRECT BENEFITS | • Cost savings due to optimal mix of hydroenergy and thermal energy.<br>• Value added by optimal production at upstream/downstream sites<br>• Improved power production scheduling hence improved overall plant efficiency | • Increase in net farm income due to lower production costs<br>• Increase in net farm income due to optimal crop selection<br>• Improvements in operational efficiency of in place irrigation projects. | • Improved surface water withdrawal scheduling hence improved overall waterworks efficiency.<br>• Cost saving by reduction of high cost ground water withdrawal. | • Reduction in cost of transport through improved scheduled releases of reservoirs water storage to improve or expand irrigable waterways.<br>• Increased value of transport services resulting from expanded demand for the improved service. | • Increased revenues from increased utilization of recreational lands and facilities.<br>• Increased populations of higher value fish and wildlife.<br>• Reduction of fish embolism through better control of reservoir releases. |
| INDIRECT BENEFITS | • Conservation of fossil energy supplies<br>• Conservation of labor | • Increases in net income to Ag. industry suppliers<br>• Reduction in food costs to populace<br>• Reduction in energy required to provide irrigation. | • Reduction of fire insurance rates.<br>• Cost savings to populace due to increased availability of water.<br>• Expansion of industry due to increased availability of water. | • Increased industrial and commercial activity.<br>• Increase utilization/value of land along waterway. | • Increased revenues from the sale of recreational equipment.<br>• Improved health of recreationally active populace. |
| INTANGIBLE BENEFITS | • Improved level of life due to cheaper energy production | • Improved community facilities and services<br>• Increased level of living. | • Improved standard of living within area. | • Enhanced strategic value of inland waterways. | • Esthetic value of improved waterways and wildlife habitat.<br>• Ecological value of improved waterways and wildlife habitat.<br>• Scientific value of improved water ecosystems. |

Table 2

Recent Withdrawals with State and Region[1]
(1,000 Acre/Feet)

| STATE | WITHDRAWL YEAR | IRRIGATION | M&I INCLUDING RURAL | MINERALS | THERMAL ELECTRIC | RECREATION FISH & WILDLIFE | OTHER | TOTAL |
|---|---|---|---|---|---|---|---|---|
| ARIZONA | 1965 | 7,096 | 349 | 102 | 7 | 169 | 78 | 7,942 |
| CALIFORNIA | 1965 | 29,020 | 4,131 | 118 | 8,220 | 652 | - | 38,897 |
| COLORADO | 1970 | 7,826 | 473 | 65 | 19 | 29 | 111 | 9,794 |
| IDAHO | 1966 | 17,668 | 739 | 27 | - | 245 | 49 | 25,505 |
| MONTANA | 1970 | 6,292 | 361 | 14 | 67 | - | 206 | 8,052 |
| NEVADA | 1969 | 3,301 | 245 | - | 63 | - | 10 | 4,718 |
| NEW MEXICO | 1970 | 3,206 | 205 | 84 | 66 | 45 | 52 | 3,919 |
| OREGON | 1975 | 7,624 | 1,581 | - | 23 | 36 | 17 | 10,878 |
| UTAH | 1965 | 4,803 | 415 | 95 | 7 | 616 | 951 | 7,348 |
| WASHINGTON | 1975 | 6,523 | 1,934 | - | - | - | 29 | 9,886 |
| WYOMING | 1968 | 7,358 | 134 | 85 | 13 | - | - | 7,977 |
| EVAPORATION | | - | - | - | - | - | - | 1,862 |
| SUMMARY | | 100,717 | 10,567 | 590 | 265 | 1,792 | 1,503 | 136,778 |

[1]Includes both surface and groundwater withdrawls
SOURCE: Westwide State Reports (unpublished)

Table 3

Upper Bound for the Value of Snow for Hydropower

| STATE | AVERAGE HYDROPOWER WATER USE (MAF) | AVERAGE HYDROPOWER GENERATION TERA-WATTS-HR. | VALUE OF WATER FOR HYDROPOWER $/AF | VALUE OF WATER FOR HYDROPOWER ($B) | AVERAGE SNOW FRACTION | CONTRIBUTION $B |
|---|---|---|---|---|---|---|
| WASHINGTON | 1,204.1 | 86.6 | 2.87 | 3.46 | 0.67 | 2.32 |
| OREGON | 617.0 | 30.0 | 2.87 | 1.77 | 0.67 | 1.18 |
| IDAHO | 112.6 | 8.4 | 2.87 | 0.33 | 0.66 | 0.22 |
| MONTANA | 82.6 | 7.5 | 2.87 | 0.24 | 0.70 | 0.17 |
| WYOMING | 18.3 | 1.3 | 2.18 | 0.04 | 0.73 | 0.03 |
| NEVADA | 15.9 | 2.0 | 6.85 | 0.12 | 0.65 | 0.07 |
| UTAH | 4.1 | 1.1 | 2.187 | 0.01 | 0.74 | 0.01 |
| COLORADO | 7.6 | 1.4 | 2.18 | 0.01 | 0.74 | 0.01 |
| CALIFORNIA | 132.3 | 40.7 | 6.85 | 0.90 | 0.73 | 0.66 |
| ARIZONA | 39.1 | 7.8 | 6.85 | 0.27 | 0.74 | 0.20 |
| NEW MEXICO | 1.0 | 0.1 | 2.18 | 0.003 | 0.71 | 0.002 |
| TOTAL OR (AVERAGE) | 2,234.6 | 186.0 | (3.20) | 7.15 | (0.68) | 4.86 |

1974 (FEA National Energy of Outlook, 1976) summarizing industry averages, shows that this value has risen by a factor of 1.32 to 9 mills/kWh primarily due to increase in the world price of oil. Applying the yearly growth rate of 9.5 percent indicated by the price indices of petroleum, yields a combined factor of 1.60 or a current value of energy of 10.9 mills/kWh at 48 percent capacity utilization. Equivalent adjustment was made for the value of energy at the average capacity utilization factor for each state. Short-run values of water for hydropower were computed using the following equation:

$$V_W = \frac{0.74\ eh\ y - 0.08\left(\frac{eh\ C}{f}\right)}{721.13} \qquad [1]$$

$V_W$ = Value of water used in $/cfs-yr.
e = Overall plant efficiency
h = Effective head (ft.) (pond elevation minus tailwater elevation)
y = Cost of electricity from cheapest alternative source mills/kWh
C = Annual capital cost of generation/kWh installed $
f = Annual capacity utilization factor

Data for the quantity of water used for hydropower was determined by trending from current levels, on a state-by-state basis. Average fractions of the total water supply from snowmelt were applied on a state basis to determine the upper bound value of hydropower inputed to snowmelt runoff.

The results shown in Table 3 indicate that the 11 western states use an average of 2,235 AF per year for hydropower. At an average alternate energy cost of $3.20/AF, the total value of the hydropower generated is $7.15B. This corresponds to a price of 3.8¢/kWh. Adjusting this value by the average snow fraction of 68 percent yields an upper bound value of $4.86B for the upper bound contribution of snow runoff to hydropower.

Estimate of the Upper Bound Benefit of Water Used for Irrigation

The value of water used for crop irrigation can be measured by the marginal value inputed to yield increases of existing crops resulting from the use of irrigation water, or from the use of higher value mixes of crops vis-a-vis non-irrigated areas.

The marginal value per acre-foot of water from Ruttan (The Economic Demand for Irrigated Acreage, 1965) amended by communication with Colorado ASVT personnel, and updated to 77 dollars, was computed as the ratio of the total marginal value of irrigated crops (acres x $/acre divided by total irrigation water used for each state).

Table 4 summarizes the computations for the upper bound value for snowmelt water to irrigation for the 11 western states. The tables indicate that the 11 western states use an average of 112 AF per year for irrigation purposes. At an average net marginal value of $163/acre, the total value of irrigation is $3.72 billion. Reducing this value by the fraction of water due to snow and that due to groundwater yields an upper bound value of $1.74 billion for the contribution of snowmelt water for irrigation purposes.

Table 4

Upper Bound Value of Snowmelt for Irrigation

| | ARIZONA | CALIFORNIA | COLORADO | IDAHO | MONTANA | NEVADA | NEW MEXICO | OREGON | UTAH | WASHINGTON | WYOMING | TOTAL AVERAGE |
|---|---|---|---|---|---|---|---|---|---|---|---|---|
| WATER USE FOR IRRIGATION (MAF) | 1.05 | 36.95 | 14.56 | 16.79 | 8.51 | 3.36 | 3.13 | 5.37 | 4.03 | 6.27 | 6.05 | 112.1 |
| IRRIGATED AREA (M ACRES) | 1.178 | 7.24 | 2.895 | 2.761 | 1.841 | 0.753 | 0.823 | 1.519 | 1.025 | 1.224 | 1.523 | 22.8 |
| AVERAGE CROP VALUE PER IRRIGATED ACRE ($/ACRE) | 820 | 766 | 304 | 248 | 130 | 213 | 389 | 260 | 190 | 516 | 199 | (453) |
| REVENUE ADJUSTMENT FACTOR (q) | 1.09 | 1.02 | .41 | .33 | .17 | .28 | .52 | .34 | .25 | .69 | .27 | (.36) |
| (268.9 x q) = MARGINAL $/ACRE | 294 | 275 | 109 | 89 | 46 | 76 | 139 | 93 | 68 | 185 | 71 | (163) |
| AVERAGE WATER USE PER ACRE (AF/ACRE) | .89 | 5.1 | 5.03 | 6.08 | 4.625 | 4.46 | 3.80 | 3.53 | 3.94 | 5.1 | 3.97 | (4.9) |
| MARGINAL $/AF | 330 | 53.9 | 22.6 | 14.64 | 10.64 | 17.04 | 36.58 | 26.34 | 17.26 | 26.27 | 17.88 | (33.2) |
| TOTAL VALUE OF WATER (M$) | 346.5 | 1992.0 | 329.06 | 245.8 | 90.5 | 57.25 | 114.5 | 141.4 | 69.55 | 227.4 | 108.17 | 3,722.13 |
| SNOW FRACTION | .74 | .73 | .74 | .67 | .70 | .65 | .71 | .67 | .74 | .67 | .73 | (.71) |
| % SURFACE WATER USE | 30 | 62 | 60 | 84 | 98 | 84 | .50 | 84 | 84 | 88 | 96 | (65) |
| (M $) VALUE OF SNOWMELT | 76.92 | 901.58 | 146.10 | 138.34 | 62.08 | 31.26 | 40.65 | 79.58 | 43.23 | 134.08 | 75.81 | 1,729.63 |

Note that the upper bound serves here only to show that the value of water for hydropower and irrigation is large and hence an important target for forecast improvement. Estimates for the value of SATSCAM for improving the forecast accuracy were developed by the procedures discussed in the remainder of the paper.

## The Economic Impact of Improved Runoff Forecasting

The less perfectly the future supply of water (quantity and timing) is known the less efficient are the water supply management activities. This is illustrated conceptually in Figure 1.

Curve A, the locus of benefits accruing to perfect forecast reflects optimal management of water dependent activities at each level of water supply. For example, the "value" from a perfectly managed volume of water $X_0$ is given by $Y_0$. Curve $B_1$, is the locus of the values accruing to water volumes lower than the forecasted quantity $X_0$. Curve $B_2$ is the analogous locus to over-forecasts.

To illustrate: if the volume $X_0$ is forecast, and the lesser volume X is obtained, the corresponding value is $Y_1$. Had X been forecasted correctly the benefit would have been $Y'_1$. The benefit loss is the difference between the X intercept of curves $B_1$ and A.

A physical explanation of the benefit loss is that in an attempt to maximize benefits, activities are planned which will utilize the forecasted quantity of water efficiently; if subsequently the supply of water actually obtained differs from that forecasted; efficiency suffers, and the results obtained are less than optimal. This conceptual model was applied to hydroenergy and irrigated uses.

## Hydroenergy Benefit Model

To a utility which contracts hydroenergy sales at prime rates, excess water results in benefit losses from sales below prime rates; deficit water results in losses because contracted demand must be satisfied by alternative generation at higher cost.

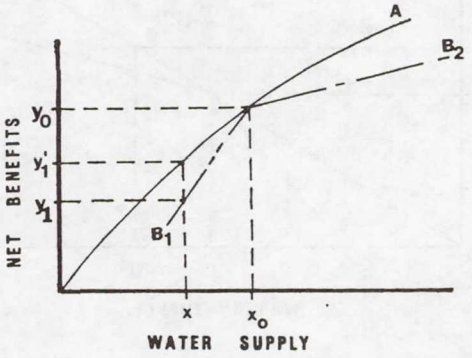


Figure 1. Conceptual Description of Benefits to Improved Forecasting

The curve of maximum potential revenue water supply, shown in Figure 2 as line A, is the locus of sales contracted at prime rates.

$$R = C\,Q_F\,G \qquad [2]$$

where:

$R$ = Value of water at average rate charged for hydroenergy

$Q_F$ = % of mean annual water supply forecasted

$G$ = Average annual generation in kWh per % of mean annual supply

$C$ = Average price charged for hydroenergy, \$/kWh

For a forecasted % of mean flow $Q_F$, the expected energy is $E_F = Q_F G$: the corresponding expected revenue is $R_F = C\,E_F$.

If the forecast is too low, the available water ($Q_1$) exceeds that expected by $\Delta Q_1 = Q_1 - Q_F$. The potential revenue at $Q_1 = R_1 > R_F$. However, the "perfect" utility can only sell the excess energy at a rate $C_1 < C$. Thus, the actual revenue will be $R_F + C_1\,\Delta Q_1\,G$, as per curve $B_1$ in Figure 2. The corresponding benefit loss ($L_B$) is:

$$L_B = (C - C_1)\,\Delta Q_1\,G \qquad [3]$$

If the forecast is too high, the available water ($Q_2$) is less than that expected by $\Delta Q_2 = Q_F - Q_2$. Total contracted sales cannot be met by hydroenergy production: the deficit must be supplied by higher cost alternate means of generation. The added cost defines the loss of benefit.

With reference to Figure 2, the potential revenue at $Q_2$ is $R_2$. The revenue achieved is computed by subtracting from $R_2$ the added cost of producing the deficit by alternate means:

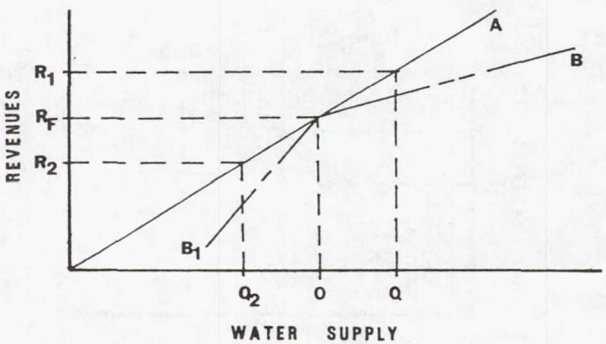


Figure 2. Conceptual Model of Sales Revenues under Stochastic Water Supply Conditions

$$B_2 = C\,Q_F\,G - (C_2 - C)\,\Delta Q_2\,G \qquad [4]$$

where:

$B_2$ = Hydroenergy revenue obtained when the forecasting supply of water is greater than the realized supply.

$C_2$ = Price charged for electric energy generated by alternate means.

The annual value of improved forecasting is the difference between the average annual loss of value under current accuracies and the average annual loss of value under the improved accuracies.

From available statistics the value of improved forecasting to hydroenergy marketing is calculated as:

$$V_{IF} = 0.67\sigma_{FE}\,G\,C^*\,\beta \qquad [5]$$

where:

$V_{IF}$ = Value of improved forecasting

$\sigma_{FE}$ = Standard deviation of forecast error

$G$ = Average annual generation

$C^*$ = Mean of the difference in prime and secondary hydropower tariffs and the difference in hydroelectric and steam-electric production costs

$\beta$ = Fractional improvement in forecast due to SATSCAM

The hydroenergy benefit model derived uses available empirical data consistent with planning and marketing operations currently practiced in the western states.

Irrigation Benefit Model

Existing methods of estimating irrigation benefits employ empirically based linear programming techniques. Such a technique for computing the benefits of improved streamflow forecasting to irrigation is the linear programming method developed by the SCS (Soil Conservation Service: An Evaluation of the Snow Survey and Water Supply Forecasting Program, February 1977), and tested for three key project areas in the western United States: the Salt River Project in Arizona, the Owyhee Project in Oregon-Idaho, and the Clarks Fork area in Montana.

SCS developed a crop-specific linear programming model for each site. Specific inputs included: the water requirements per acre of crop, the levels of irrigation, and existing limitations on regional crop acreages and availability of land. Model outputs are net revenues and optimal acreages for various levels of water availability.

SCS chose eight representative crops for each project area: it used 1973 prices derived from 1976 U.S. Water Resources Council data. The model estimates potential maximum benefits of improved forecast to irrigation.

The SCS model was modified and adapted by ECOsystems to produce a generalized irrigation benefit model which eliminated the need for specific linear programming at each site.

The SCS technique was generalized by normalizing the results of the SCS River Project simulation. The value of forecast improvement is the difference between the benefit loss calculated for the existing and improved forecast performance level. The benefit loss is given in Figure 3 as the difference of value obtained for a perfect forecast and that obtained for the actual quantities of water experienced. This benefit loss determination assumes optimum response by agricultural managers to water supply forecasts.

The total value of the crops produced at mean flow and with perfect forecast was normalized to the total number of irrigated acres for the Salt River Project for the base year 1973 chosen for the SCS simulation. The revenue was normalized by the revenue adjustment q, the ratio of the average revenue per irrigated acre for new sites under study to the revenue of Salt River in 1973 = $7.50/acre.

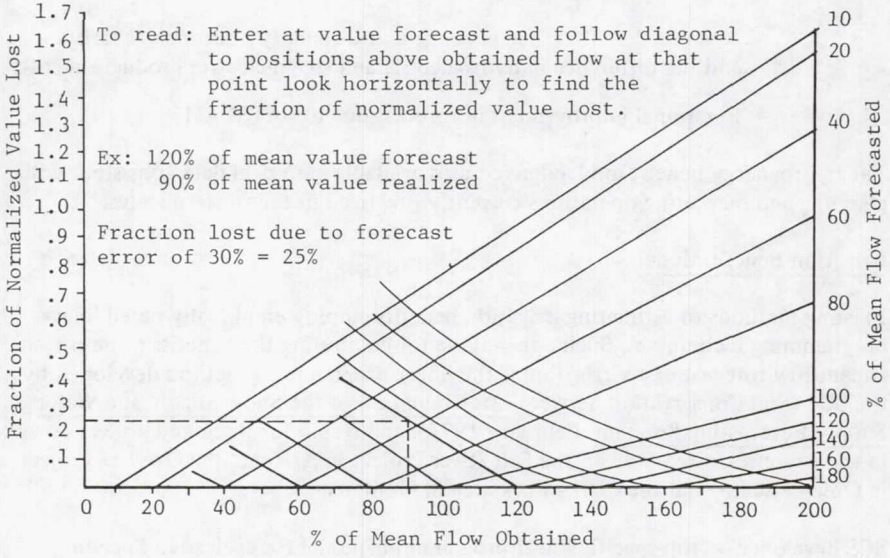


*Note value lost (expressed as a fraction of the value obtained zero error @ mean flow)

Figure 3. Graph for the Calculation of the Value Lost at the Salt River Project under Stochastic Water Supply Conditions

$$q = \frac{I}{B} \qquad [6]$$

where:

I = The average revenue per irrigated acre at new site

B = The average crop revenue per irrigated acre of the Salt River Project in 1973.

The value lost due to any level forecast error is computed from equation [7] using the relationship graphically presented in Figure 3.

$$V_L = \alpha q A k \qquad [7]$$

where:

$V_L$ = Value lost due to forecast error

$\alpha$ = Annual fraction of normalized value lost (obtained from Figure 3 for a given forecasted percent of mean flow and realized percent of mean flow)

q = Revenue adjustment factor

A = The irrigated acreage for the geographical and base year

k = Average added value due to irrigation; i.e., for the Salt River Project with a perfect forecast at mean flow as determined by the SCS model = 268.90.

## COMPUTERIZATION OF BENEFIT MODELS

Two computer models were developed for computing the benefit of improved forecast accuracy to irrigated agriculture and hydroelectric electric energy. Both models are interactive, requiring input information on the level of forecast improvement, existing forecast accuracy, and streamflow variability. The irrigation model additionally required the input of irrigated acreage and average value of crops per acre for each area. The hydroelectric energy benefit model required the input of average annual generation hydroelectric and steam-electric production expenses, and revenues received from primary and secondary energy sales for each subregion.

The irrigation model employs multiple regression relationships to weight the input parameters. Outputs are current benefits to improved forecasting for the irrigated acreage within each subregion and a single aggregate value of the total benefit for all the subregions considered. The hydroenergy model computes the current values of the benefit to improved forecast on a subregional basis and further summarizes the computations with a total value for all subregions.

Stochastic models were also developed and used to check the results of the models using simulated yearly streamflows.

## Data Base Development

Empirical data required for the exercise of the benefit models were obtained from numerous sources. The individual ASVT personnel and local hydrologic experts were of great assistance in the collection of accurate, up-to-date data.

Analysis of the benefit of SATSCAM to irrigation and hydroelectric energy required the development of three extensive data bases: one for the basic characterization of the subregions which are impacted by snow survey forecasting, the second to provide the data inputs for the irrigation simulation model, and the third to provide the data inputs for the hydroenergy simulation model. These data bases contain geographically specific information at as fine a level of granularity as is presently available consistent with the total area covered.

Irrigated acreage data were not available on a project-by-project basis but were collected on a subregion basis. Hydroelectric and steam-electric energy data were available on a project basis.

The Snow Survey Forest Unit of the Soil Conservation Service provided data on average streamflow, streamflow coefficient of variation, forecasts, and forecast accuracy for 361 primary snow survey forecast points covering the 11 western states. Twenty additional forecast points with the supporting data were obtained from the California Department of Water Resources.

Estimates of the irrigated acreage which could potentially benefit from SCAM were computed by adjusting the total irrigated acreage within each subregion by the fraction of surface water to total water used to irrigate those lands. These data were obtained from the USGS 1975 Water Use Survey (The summary form of this data is reported in Estimates of Water Use in the United States in 1975 U.S.G.S. Circular #765). Average annual crop value per acre were extrapolated from 1976 crop value/acre statistics calculated by the Bureau of Reclamation for each of its irrigation projects. These values were used to produce an area-weighted annual crop value/acre for each snow survey impacted subregion.

Electric energy data were acquired for the plants located within the 11 western states as listed by the Federal Energy Regulatory Commission (FERC) and the Energy Information Administration (EIA). These data, reorganized on a subregion basis, included: (1) 1978 average annual hydroelectric energy generation (MWH); (2) current estimates of hydroelectric production expenses (mills/kWh); (3) current estimates of steam-electric production expenses (mills/kWh); and (4) current estimates of the revenues obtained from the sale of prime and secondary energy. Production expenses initially based on 1976 figures, and energy sales revenues, initially based on 1975 figures, were adjusted for inflation.

## Benefit Computation Results

The estimated 6% relative forecast improvement from the Colorado ASVT personnel and the extensive data bases previously described were used in the computer benefit

models and resulted in a computed total average annual SATSCAM benefit of $38M for the irrigation and hydroenergy for the western United States: $28M/year for irrigation and $10M/year for hydroenergy.

Irrigated agriculture is the primary benefactor of SATSCAM receiving 74% of the benefit of $28M annually. Figure 4 depicts the regional benefits to irrigated agriculture and also shows the average per acre benefit received in these regions.

The Pacific Northwest region receives the largest portion of the agricultural benefit despite receiving the lowest per acre benefit of all the regions. This is a result of the relatively large crop acreage irrigated by the surface water in the Pacific Northwest region as compared to other regions compounded with the relatively lower values of crops planted.

The Lower Colorado region, which is relatively water scarce, receives the largest per acre benefit: $8.95/acre. The Lower Colorado has 1/100 of the acreage irrigated by surface water relative to the Pacific Northwest but generally plants high value irrigated crops.

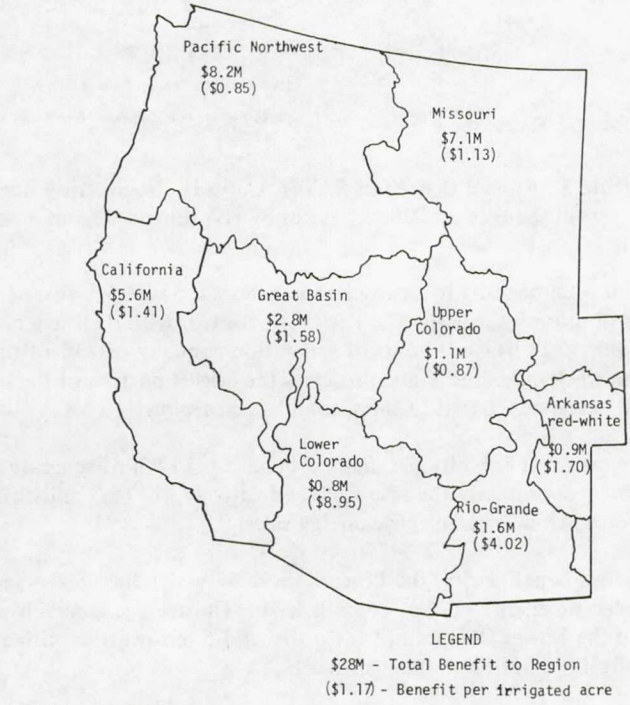


Figure 4. Annual Benefit of SATSCAM to Irrigated Agriculture in the Western United States by Hydrologic Region

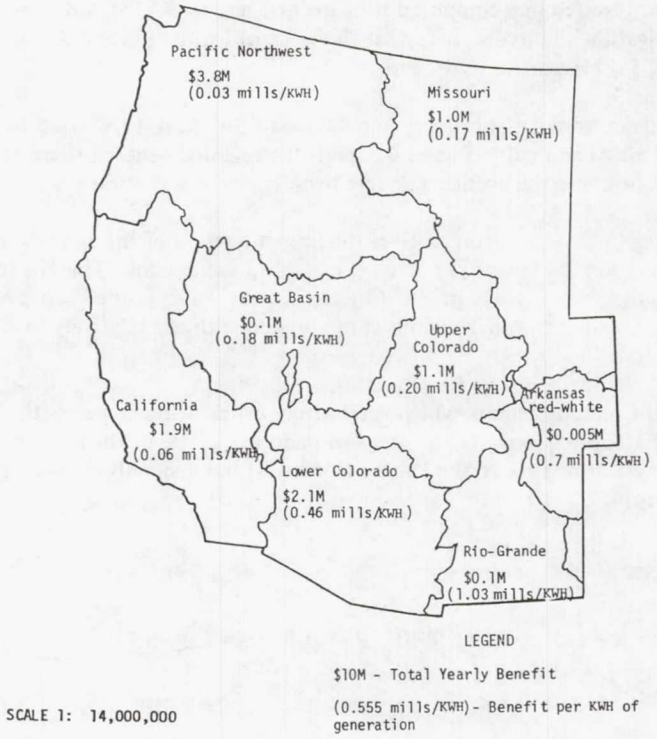


Figure 5. Annual Benefit of SATSCAM to Hydroelectric Energy in the Western United States by Hydrologic Region

The estimated total benefits to hydroelectric energy is $10M per year. Figure 5 depicts the distribution by region. The Pacific Northwest with its heavy concentration of hydropower (132 terrawatt-hours of generation annually or 73% of the total generation in the western United States) receives the largest portion of the benefit (38% of the total), nearly twice that of the second largest region.

The Pacific Northwest exhibits the smallest benefit per kWh of generation, 0.028 mills/kWh which is primarily the result of the relatively low (8.3 mills/kWh) return per kWh received from hydroelectric energy sales.

The next highest beneficiary is the Lower Colorado, which has an average revenue from hydroelectric energy sales of 26 mills/kWh. The average annual hydroelectric generation in the Lower Colorado of the order of 4.5 terrawatt-hr with a computed annual benefit of $2.1M (0.46 mills/kWh).

The Rio Grande region receives the highest benefit per kWh of generation at 1.03 mills/kWh, but exhibits the lowest total benefit of only $0.1M due to the small amount of annual hydroelectric generation on this region (0.096 terrawatt hr).

## SATSCAM IMPLEMENTATION COSTS

The cost associated with employing SATSCAM operationally consists of four components: satellite data products, image interpretation, data implementation, and equipment. Costs associated with satellite research and development and with operational SATSCAM "start up" in a forecasting scheme have been considered sunk for purposes of these estimates. An analysis of the cost of each of the non-sunk components was derived from data supplied by the Colorado ASVT site personnel.

The Colorado ASVT effort focused on six study watersheds covering a total area of 9295 $km^2$. Five Landsat frames were required to provide adequate basin coverage for each data. The forecast period during which SATSCAM was used extended from mid-March to mid-June. Eight observations (image dates) were used during this period. Using a Landsat per frame cost of $10, the total cost of image procurement was $400. Image interpretation for the six basins required 16 man-days per season and resulted in a total cost of $800. Implementing the data into the forecasting scheme required an additional 8 man-day/season of effort at a cost of $600. The total seasonal cost, exclusive of equipment, was 1,800 or $0.194/$km^2$.

The Colorado ASVT used a conventional zoom transfer scope (ZTS) for image analysis. Typical capital cost for the ZTS is $10K. The yearly capital equipment cost was computed assuming a utilization factor of 25% and amortizing the cost over 10 years at $250. The total cost associated with SATSCAM in the Colorado ASVT was $2,050 which equates to 0.22/$km^2$.

Extrapolating to the 2,238,890 km area impacted by snow-survey forecasting in the western United States, the total yearly cost of employing SATSCAM is approximately $493K.

## SUMMARY AND CONCLUSIONS

The results of the OASSO ASVT's have been used to estimate the benefits to the added information available from satellite snowcover area measurement. Estimates of the improvement in runoff prediction due to addition of SATSCAM have been made by the Colorado ASVT personnel. The improvement estimate is 6–10%.

This data was applied to subregions covering the western states snow area amended by information from the ASVT and other watershed experts to exclude areas which are not impacted by snowmelt runoff. Benefit models were developed for irrigation and hydroenergy uses. Results of the benefit estimate for these two major uses yielded a yearly aggregate benefit of $38M.

Cost estimates for the employment of SATSCAM based upon the Colorado ASVT results and expanded to the western states totalled $493K. The benefit/cost ratio thus formed is 77:1. Since only two major benefit contributors were used and since the forecast improvement estimate does not take into account future satellite capabilities these estimates are considered to be conservative.

The large magnitude of the benefit/cost ratio supports the utility and applicability of SATSCAM. Future development in the use of SATSCAM in computer models specifically tailored or adapted for snow input such as those developed by Leaf, Schuman and Tangborn, and Hannaford will most certainly increase the use and desirability of SATSCAM.

REFERENCES

Barnes, J. C. and C. J. Bowley, Handbook of Techniques for Satellite Snow Mapping, Final Report under Contract #NAS5-21805, 1974.

Colorado State University, Economic Value of Water, 1972.

FEA National Energy Outlook, 1976.

Leaf, C. F., Areal Snow Cover and Disposition of Snowmelt Runoff in Central Colorado, U.S.D.A. Forest Service Research Paper RM-66, 1971.

Rango, A., "Ed.", Proceedings of Workshop on Operational Applications of Satellite Snowcover Observations, August 18–22, 1975, South Lake Tahoe, CA.

Ruttan, V. W., The Economic Demand for Irrigated Acreage, 1966.

Soil Conservation Service, An Evaluation of the Snow Survey and Water Supply Forecasting Program, February 1977.

USGS, Estimates of Water Use in the United States in 1975, Circular #765.

# SNOW EXTENT MEASUREMENTS FROM GEOSTATIONARY SATELLITES USING AN INTERACTIVE COMPUTER SYSTEM

R. S. Gird, National Environmental Satellite Service, Washington, D.C.

## ABSTRACT

An interactive computer data access system (McIDAS) is used to measure the extent of snow fields in the Salt and the Verde River Basins in central Arizona from satellite images. This study was based on real-time visible image data of 1 Km resolution generated by the eastern GOES (Geostationary Operational Environmental Satellite) in orbit approximately 37,500 Km (20,000 nm) above the earth at $0^{o}$ latitude, $75^{o}$ longitude. This new method for preparing Snow Covered Areas (SCA) is compared to the current operational SCA techniques used by the National Environmental Satellite Service (NESS).

## INTRODUCTION

Environmental satellite data provides much of the needed information concerning snow cover. Accurate snow interpretation and mapping from environmental satellites has been demonstrated by Barnes and Bowley (1966, 1974); in 1973, the National Environmental Service (NESS) established a quasi-operational snow cover program (Schneider, et. al., 1976). Satellite-derived snow covered area (SCA) measurements for specific river basins within the United States have been provided since then by NESS to selected National Weather Service Forecast Centers for use in various hydrological models. Two of these operational basins, the Salt and Verde in Arizona, were selected for this study (figure 1).

This study used real-time data from the Geostationary Operational Environmental Satellite (GOES), analyzed by an interactive computer system to calculate SCA. Full resolution (1 Km) visible data from the eastern GOES satellite ($0^{o}$N, $75^{o}$W) was selected for this study; the GOES visible sensor detects radiation between 0.55-0.75 μm. A complete description of the GOES system is given by Bristor (1975). The University of Wisconsin's Man-computer Interactive Data Access System (McIDAS) used to make the SCA measurements is described by Smith (1975), and by Chatters and Suomi (1975).

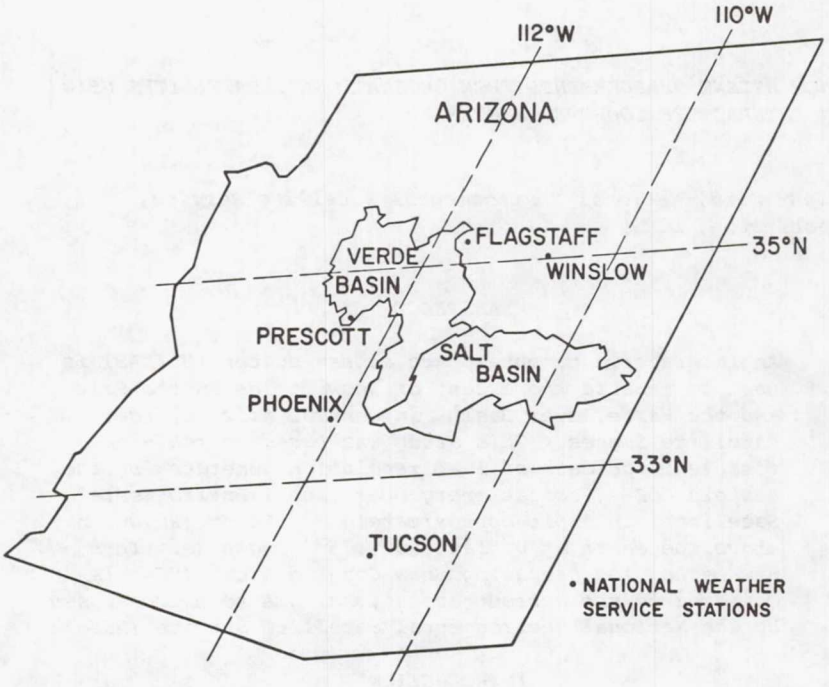


*Figure 1. Salt and Verde river basins, viewed from the eastern GOES satellite position.*

*The GOES and McIDAS combination provided many opportunities to improve and increase the flexibility of SCA. The GOES satellite provides real-time data and generates more than one image per day, so it was possible to select an optimum image for each specific basin, taking into account such factors as solar zenith angle and cloud cover. A recent study by Breaker and McMillan (1975), indicated that daily and perhaps hourly snow-melting rates could be obtained from GOES data film loops. In related reports, Schumann (1975), and Warskow, et al. (1975) indicated the need for such hourly snow-melting rates during periods of high run-off and minimum available reservoir storage capacity--rate calculations that are extremely important for desert cities like Phoenix, Arizona.*

*Throughout this paper, reference will be made to a Registered Image Sequence (RIS). This is a time series of GOES full resolution visible image sectors viewed on the McIDAS video component in chronological order and registered (navigated) to within ± 1 image pixel. For a complete description of the McIDAS navigation*

system see Phillips and Smith (1973). During a RIS, the land masses remain fixed, clouds may move, form and dissipate, while snow fields change shape and character in response to meteorological conditions. By studying a RIS that is compiled from real-time data, the McIDAS analyst can compute real-time hourly snow melting rates. The McIDAS software, under analyst control, can eliminate synoptic-scale clouds from a RIS to create a SCA from a composite image. The usefulness of cloud-free composite images for SCA has been established by McClain and Baker (1969), although they did not use real-time data. The cloud elimination technique used in this paper is described in a later section.

Finally, it should be noted that all SCA measurements are performed by the McIDAS computer directly from the satellite data; this reduces errors by reducing the number of transformations in the SCA measurement process.

## EXPERIMENTAL PROCEDURES

The Salt and Verde river basins used in this paper, were selected for the following reasons. The basins are routinely mapped by the NESS SCA program, so comparison of NESS versus GOES/McIDAS results would be straightforward. Second, these basins have many visible landmarks (Lake Roosevelt, Mormon Lake, and the Little Colorado River) which would be helpful in establishing the accuracy of the McIDAS navigation. (Navigation is required for any type of RIS analysis and can be used in the final SCA measurement.) Third, five National Weather Service Stations are located in or around the basins (figure 1), so conventional data (including weather radar reports) could be useful to examine closely the winter history of the basins. Finally, the basins are frequently cloud-free, even during the winter months, thereby making it possible to compile a long-term data set for SCA analysis.

This study was conducted in three phases: the set-up phase, the data collection phase, and the analysis phase. In the set-up phase, the basin perimeters were defined in terms of latitude and longitude points and stored within McIDAS. Second, a preliminary GOES image data set (early December) was collected in which both basins were free of cloud and snow cover. During the data collection phase, GOES image data was saved for those days on which a SCA measurement looked feasible. In the final analysis phase, SCA measurements were conducted using McIDAS.

### Set-up Phase

The first step in defining the basin perimeters was to obtain a map of the basin areas from the United States Geological Survey in Phoenix, Arizona. The map was a Phoenix Sectional Aeronautical Chart, scale 1:500,000. A number of latitude and longitude points were selected from the perimeter outlines--56 and 89 points for

*the Salt and Verde basins, respectively. These grid points were then punched onto computer cards and read into McIDAS. Once stored in McIDAS, the perimeter outlines could be displayed on the McIDAS video at any time by typing in a single command line via the keyboard. A denser network of points could have been used, but for this study it was not deemed necessary.*

*The second part of the set-up phase was the collection of the preliminary data set. These images were used to familiarize the McIDAS analyst with the basin geography (landmark features). Numerous landmarks were clearly visible within the area of interest; the most prominant are Lake Roosevelt, Mormon Lake, Mount Baldy, and the Little Colorado River. The preliminary data set was collected from December 7, 1976 to December 24, 1976; a local noon image, 1900 GMT, was selected as the primary data collection time for this study. During this 17-day period, nine images were collected but only three images satisfied the cloud and snow free requirements and were of acceptable quality (i.e., had no missing data lines). The three images were then navigated via McIDAS and assembled to form the initial RIS--the start of the "winter history" for both basins.*

*In the final part of the set-up phase, the accuracy of the computer-generated basin perimeters was checked. First, the basin perimeters and GOES satellite data were viewed simultaneously on the McIDAS video display. This product was compared to the aeronautical chart and obvious mistakes in the perimeter points were corrected. Second, the total area of the two basins was computed using the GOES data and McIDAS. The basin perimeters were traced using the McIDAS video cursor, controlled by a manual joy-stick; the McIDAS software then automatically calculated the number of satellite pixels enclosed by the cursor derived outline. The area results, expressed in terms of square kilometers differed by less than 2% (33,235 $Km^2$ vs. 32,686 $Km^2$) from the ground truth numbers provided by Schumann (1975).*

*Data Collection Phase*

*The data collection phase of this project took place between January 4, 1977, and February 1, 1977. During this phase all possible 1900 GMT cloud-free GOES images of the basins were collected using McIDAS. Daily checks of the synoptic weather conditions were conducted at 1400 GMT and updated at 1800 GMT, using the National Weather Service products collected by the University of Wisconsin - Madison, Department of Meteorology. If all conditions at 1800 GMT looked favorable, McIDAS ingested the 1900 GMT GOES visible data centered on Phoenix, Arizona. After ingest, the data was archived onto magnetic tape so the SCA analysis could be carried out at any later time (depending on McIDAS availability). During this 28-day period, a total of 14 images were collected and saved. Only five of the 14 images were completely cloud-free and were used for SCA; the remaining nine had*

*some degree of cloudiness, mostly thin cirrus, in the basins.*

*Analysis Phase*

*Prior to final SCA analysis, the image to be studied was incorporated into the already existing RIS in the following way. The first three images of the RIS were the three snow-free, cloud-free images from the preliminary data set. The fourth image of the RIS was the first image of the data-collection phase, and so on, until all five images from the data collection phase were incorporated into the RIS. It was quite easy to detect minor changes in the snow fields between two sequential images; this "historical" RIS was a valuable aid in maintaining a consistent SCA product throughout the project. A further discussion is presented in the Results section.*

*Once the specific image was incorporated chronologically into the RIS and compared to previous images and the trend of the snow field changes was established, the SCA analysis was conducted.*

*To make an accurate SCA, each GOES image had to be displayed as a four-fold expansion on the McIDAS video (16 CRT pixels for every satellite pixel). Because of this expansion, analysis of each basin had to be carried out in four sub-sectors. A second expanded image--"yesterday's" image relative to the five images of the data collection set--was displayed alternately on the McIDAS video to help detect very small changes in the snow fields. While these images alternated on the video, the cursor was used to outline the snow fields. Once a snow field within the sub-sector was outlined, a second tracing using the cursor was initiated. Completion of this second tracing automatically invoked the area calculation software of McIDAS, and the area calculation for the snow field within the sub-sector was displayed and printed out. The area calculation was expressed in terms of the number of satellite pixels and in $km^2$. Once the areas for all the snow fields were calculated for the sub-sector, another sub-sector was selected and appropriate steps repeated. After the analysis of all sub-sectors was completed, the snow field calculations for each basin were added together. Since the total area of the two basins was calculated from the preliminary data set, a SCA could be calculated for the two basins.*

*Cloud Subtraction Technique for SCA*

*A powerful feature of the McIDAS software is the Cloud Subtraction Routine (CSR). For a complete description of the Cloud Subtraction Routine see Mosher (1977). In order to produce meaningful results, the CSR must be performed on a RIS. Inside McIDAS, the CSR matches up to six images from the RIS, scanning the images and retaining only the darkest pixels at each location from the RIS images. The resulting composite image is thus composed of the darkest pixels from the RIS, in effect eliminating*

the lighter clouds moving over the darker land.

To demonstrate the usefulness of the CSR in doing SCA calculations, a RIS was compiled from 1830, 1900 and 1930 GMT images for February 6, 1977. In each of the three images, both basins were obscured by clouds and no SCA could have been prepared from any of the individual images. The CSR successfully eliminated the clouds from the three images and produced a composite image suitable for a SCA. The results of this technique will be discussed in the following section.

## EVALUATION OF RESULTS

### Comparison of Methods

The GOES/McIDAS SCA results show good agreement when compared with the NESS products (figure 2) during the first part of this study (January 10-15, 1977). The second part of this study (January 16-28, 1977) shows the GOES/McIDAS products to be approximately three to five percent less than the NESS polar-orbiting based products. A similar result has been previously observed by Schneider and McGinnis (1977). Another significant difference was noted. From January 13 to January 15, 1977, the NESS products showed an increase in the snow cover for the Verde basin, while the GOES/McIDAS product implied no change in the snow cover for approximately the same period. Additionally, a check of National Weather Service Radar Reports during this period indicated no precipitation had occurred within the Verde basin. Therefore, the increase in snow cover reported in the NESS analysis appears to be an error--the type of error that might be expected using the current manual techniques during periods of little or no change in the snow cover. The use of RIS could help eliminate this type of error, since small changes in the snow cover between any two days are easily detected when viewing the images within a RIS. The RIS thereby provides continuity for sequential SCA operations.

A comparison of SCA results for January 10, 1977 is shown in figure 3, indicating an apparent loss of detail in the snow cover outlines produced by GOES/McIDAS. This difference, however, is not real. It results from the transfer of the SCA analysis from the McIDAS video to the worksheet; the actual outlines generated by McIDAS and used for the SCA did contain more detail. The two products show good agreement with the minor exception of the snow-capped mountain peaks located in the southern part of the Verde basin. Old or new snow on mountain peaks shows up very clearly when the analysis image was compared to a snow-free image in the RIS.

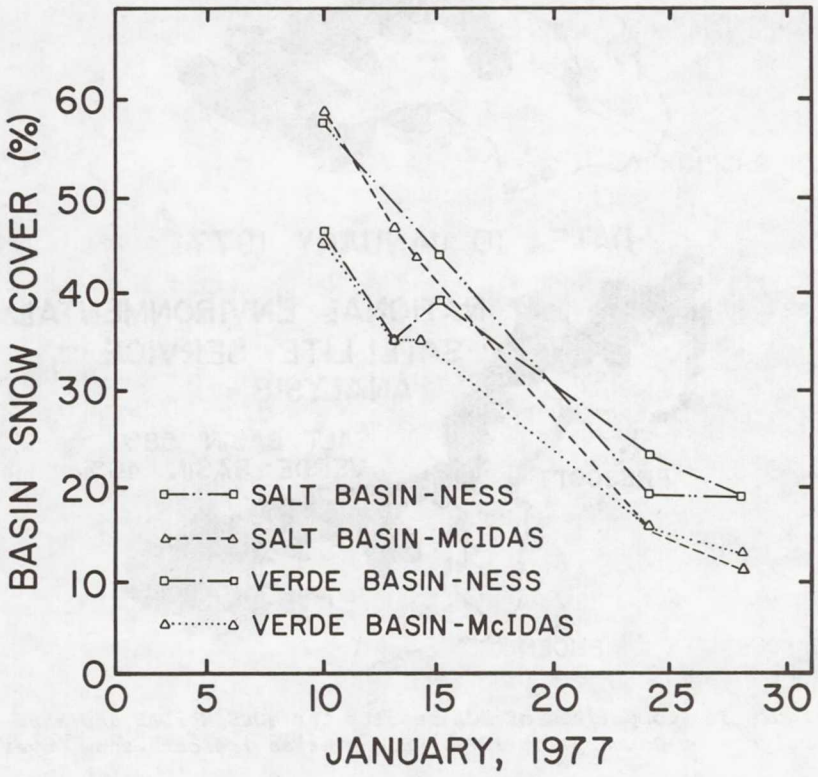


*Figure 2. Comparison of Snow Cover Area (SCA) measurements for the Salt and Verde river basins.*

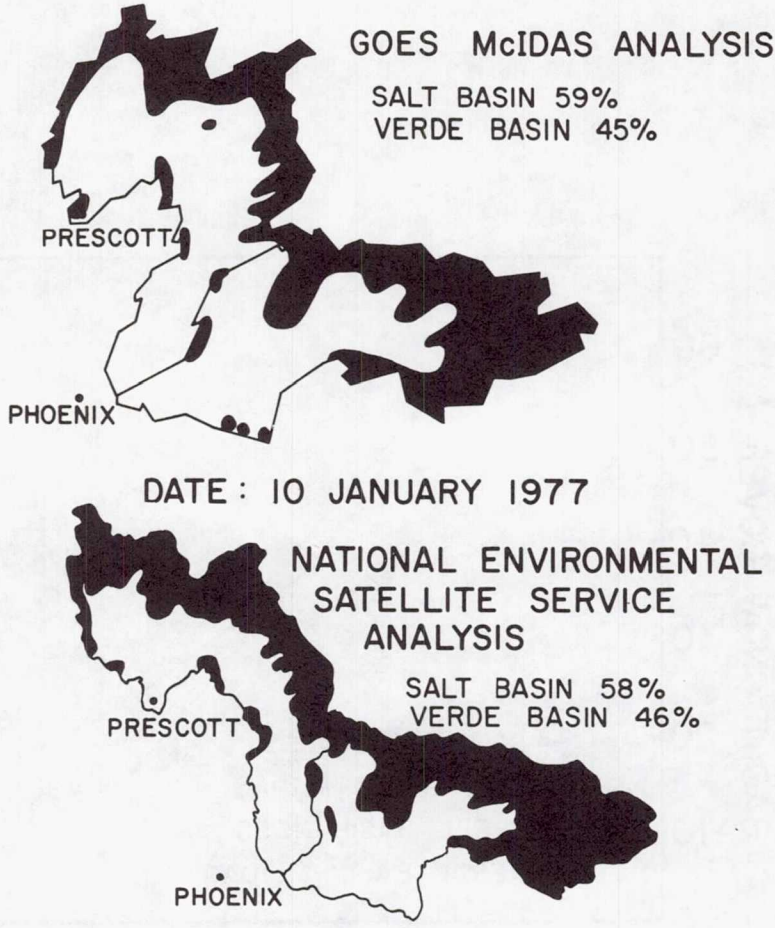


*Figure 3. Comparison of SCA results for GOES/McIDAS and NESS analysis on January 10, 1977. Black areas indicate snow cover.*

*Satellite Pixel vs Km$^2$ Results*

*A comparison of GOES/McIDAS-generated SCA results using both satellite pixels and km$^2$ areas was conducted. The results indicate only second-order differences between the two methods. The shape of the satellite pixel is approximately square for this basin location, although the pixel distortion does get worse the further away an Earth pixel is located from the GOES satellite subpoint (0°N, 75°W). The navigation software in McIDAS calculated the approximate dimensions in the area of the basins as 0.59 nm wide and 0.68 nm long. Although the units of area used to calculate SCA (satellite pixel or km$^2$) did not matter for these two basins, other basins analyzed by GOES/McIDAS would have to be*

*treated as individual cases when selecting the area units.*

*Cloud Subtraction Results*

*The SCA results generated by McIDAS from the cloud-free composite image agreed favorably with the NESS products. The GOES/McIDAS SCA for the Salt basin for February 6, 1977, indicated 11% snow cover; the NESS product for February 7, 1977, showed the Salt basin to be 17% snow covered. The clouds that were eliminated from the images were estimated to be of either the mid-level or high-level type, and they did produce significant shadows on the ground which were not eliminated from the composite image. Further investigation of the cloud elimination scheme is recommended.*

*Analysis Time*

*The time required to complete a SCA with the GOES/McIDAS system averaged 30 minutes per image throughout this study, but this time can fluctuate ± 15 minutes depending upon the complexity of the snow cover. New snow cover, which covers a larger, more uniform area, is easier to analyze than older, patchy snow cover. The GOES/McIDAS analysis time is approximately equal to the current manual NESS operation. The significant difference between methods is that a GOES/McIDAS analysis can be completed within an hour after image reception time, whereas the current manual NESS operation takes 24 hours or more to complete. It should be noted,however, that an improvement in analysis time was not an objective of this study.*

*Errors*

*The most significant source of error in the GOES/McIDAS scheme is the experience of the analyst in snow mapping, although experience and confidence increased rapidly (and errors declined) during this study. A second source of error was in the McIDAS tracing software routines. This software requires the storage of satellite pixels in order to define the snow cover outline. Because this storage array is limited, the McIDAS analyst had to rapidly trace the outlines in order to avoid overflowing the storage array. Faster tracing implies fewer satellite pixels to be stored. This limitation would be a serious problem when performing a SCA that required fine detail in the outlined basin. Since these tracing software routines are still considered developmental, corrections could be applied to the operational version. Another source of error (related to the tracing problem) was the extreme sensitivity to trace details as small as one or two pixels (isolated snow-capped mountain peaks); considerable practice was required.*

## CONCULSIONS AND RECOMMENDATIONS

This study indicates that the GOES/McIDAS SCA process can produce reliable, consistent snow mapping results. Further, interactive computer systems like McIDAS offer advantages over the present manual techniques. Improvements, however are needed in the McIDAS software. Additional software could be included to introduce semi-automatic tracing techniques; parts of the snow cover that extend up to the basin perimeters could be outlined automatically, since the basin perimeter is defined within the computer in terms of latitude and longitude. Total automation of SCA seems remote, however; accurate definition of snow cover still requires human interpretation.

On the basis of this study, it is recommended that snow cover mapping using the GOES/McIDAS method should be incorporated into the present snow mapping program of the National Environmental Satellite Service. Further investigations should examine the following topics: selection of a wider variety of snow basins for study; use of polar-orbiting satellite data with McIDAS for the mapping of northern basins; and the use of techniques such as elevation slicing and cloud elimination schemes to further improve SCA procedures.

## ACKNOWLEDGEMENTS

Special thanks to my advisor, Dr. Verner Suomi (Space Science and Engineering Center), for this direction and continual support. Thanks also to Tom Haig (Space Science and Engineering Center), Stan Schneider (National Environmental Satellite Service), and Herb Schumann (United States Geological Survey) for their excellent cooperation and information. Technical assistance and support was graciously provided by J. T. Young and Dee Cavallo (Space Science and Engineering Center), and by Gene Legg (National Environmental Satellite Service).

This work was supported under NASA Contract NAS5-21798.

## REFERENCES

Barnes, J. C., and C. J. Bowley, 1966: Snow Cover Distribution as Mapped from Satellite Photography, Final Report, Contract No. Cwb-11269, Allied Research Associated, Inc., Concord, MA, 180 pp.

Barnes, J. C., and C. J. Bowley, 1974: Handbook of Techniques for Satellite Snow Mapping, ERT Document No. 0407-A Environmental Research and Technology, Inc., Concord, MA, 95 pp.

*Breaker, B. C., and M. C. McMillan, 1975: Sierra Nevada Snow Melt from SMS-2, Operational Applications of Satellite Snow Cover Observations, South Lake Tahoe, CA, pp. 187-198.*

*Bristor, C. L., 1975: Central Processing and Analysis of Geo-Stationary Satellite Data, NOAA Technical Memorandum NESS 64, U.S. Department of Commerce, Washington, D.C., 155 pp.*

*Chatters, G. C., and V. E. Suomi, 1975: The Applications of McIDAS, IEEE Transactions on Geoscience Electronics, GE-13, pp. 137-146.*

*McClain, E. P., and D. R. Baker, 1969: Experimental Large-Scale Snow and Ice Mapping with Composite Minimum Brightness Charts, ESSA Technical Memorandum NESCTM 12, U.S. Department of Commerce, Washington, D.C.*

*Mosher, F. R., 1977: Composite Images Using Navigated SMS/GOES Data, Studies of Soundings and Image Measurements, Final Report of NAS5-21798, Space Science and Engineering Center, University of Wisconsin, Madison, WI.*

*Phillips, D., and E. Smith, 1973: Geosynchronous Satellite Navigation Model, Studies of the Atmosphere Using Aerospace Probes, NOAA Grant NG-26-72, Space Science and Engineering Center, University of Wisconsin, Madison, WI, pp. 253-271.*

*Schneider, S. R., D. R. Wiesnet and M. C. McMillan, 1976: River Basin Snow Mapping at the National Environmental Satellite Service, NOAA Technical Memorandum NESS 83, U.S. Department of Commerce, Washington, D.C., 19 pp.*

*Schneider, S. R., D. R. McGinnis, Jr., 1977: Spectral Differences between VHRR and VISSR Data and their Impact on Environmental Studies, Proceedings of the American Society of Photogrammetry, Washington, D.C., pp. 470-480.*

*Schumann, H. H., 1975: Operational Application of Satellite Snowcover Observations and LANDSAT Data Collection Systems Operations in Central Arizona, Operational Applications of Satellite Snowcover Observations, South Lake Tahoe, CA, pp. 13-28.*

*Smith, E. A., 1975: The McIDAS System, IEEE Transactions on Geoscience Electronics, GE-13, pp. 123-136.*

*Warskow, W. L., T. T. Wilson Jr., and K. Kirdar, 1975: The Application of Hydrometeorological Data Obtained by Remote Sensing Techniques for Multi-purpose Reservoir Operations, Operational Applications of Satellite Snowcover Observations, South Lake Tahoe, CA, pp. 29-37.*

**Page intentionally left blank**

# AN ALL-DIGITAL APPROACH TO SNOW MAPPING USING GEOSTATIONARY SATELLITE DATA

J. D. Tarpley, Stanley R. Schneider, Edwin J. Danaher, and Gordon I. Myers, National Environmental Satellite Service, Washington, D.C.

## ABSTRACT

This paper describes an all-digital snow-mapping technique that utilizes 4-km resolution visible data from a geostationary satellite, GOES-W. The study area includes nine contiguous river basins in the Sierra Nevada. The snow-mapping procedure uses a brightness threshold for each individual basin pixel to identify snow cover. The method allows for daily and seasonal changes in solar illumination angles and variations in the nature of ground cover across the basins.

## INTRODUCTION

Areal snowcover maps and calculations of percent snowcover are now operationally produced at the National Environmental Satellite Service (NESS). The data are disseminated to federal and state agencies for use in runoff forecasting and water resource planning. Selected river basins in the Sierra Nevada have been operationally monitored at NESS since early 1973. One hundred and seventy-eight (178) areal snow-cover determinations were made for the American River basin (above Folsom Dam) between January 1973 and June 1978 and transmitted to the National Weather Service/ River Forecast Center in Sacramento, California. At the request of the California State Department of Water Resources, the Sacramento river basin above Shasta Dam and the Feather above Oroville Dam were added to the NESS operational snow-mapping program in January 1977. In February 1978, the U.S. Soil Conservation Service Office in Reno, Nevada, requested that operational coverage be extended to three river basins on the eastern slopes of the Sierras, the Tahoe-Truckee, Carson, and Walker.

Snowcover analyses at NESS are presently done through photointerpretation of satellite images using optical rectification techniques and density slicers

(Schneider et al., 1976). This method of analysis is time-consuming and its accuracy is dependent upon the skill of the analyst. To meet user demand, it is important that a faster, more objective method for snow mapping be developed. The digital snow mapping experiment is directed toward this goal.

## THE STUDY AREA

The study area includes nine contiguous basins in the central and northern Sierra Nevada. This area is depicted under almost snow-free conditions in Figure 1, a 1-km resolution visible image taken from GOES-W on August 1, 1978. The basins have been outlined on the image using a Bausch and Lomb Zoom Transfer Scope (ZTS) and are labelled for orientation purposes. Six of the rivers (Sacramento, Feather, Yuba, American, Mokelumne, and Stanislaus) drain west from the Sierras and have basins covered with grassy lowlands grading into higher elevation coniferous forests. Light-colored granite is exposed at several locations above the timber line. Each of these western basins delineated on Figure 1 encompasses the drainage area above a dam and reservoir. The remaining three basins, the Carson, Tahoe-Truckee, and Walker, drain east from the Sierras and are covered by low elevation desert shrublands and salt flats interspersed with highlands covered by pine-juniper woodlands. The nine basins range in size from 1,590 $km^2$ (Mokelumne) to 16,630 $km^2$ (Sacramento above Shasta).

## DESCRIPTION OF THE SATELLITE AND SENSOR

Two geostationary meteorological satellites operated by NESS, the geostationary operational environmental satellites (GOES), view the Earth's disk through Visible and Infrared Spin-Scan Radiometer (VISSR) instruments. A description of this dual geostationary satellite system can be found in *Technical Memorandum NESS 64* (Bristor, 1975). The satellites, GOES-E and GOES-W, are fixed over the equator at 75°W and 135°W, respectively at an altitude of about 36,000 km. The VISSR instrument provides concurrent observations in the infrared spectrum (10.5 to 12.5 μm) and in the visible spectrum (0.55 to 0.75 μm). The visible data which are used in snow mapping are expressed as 6-bit count values measuring relative brightness.

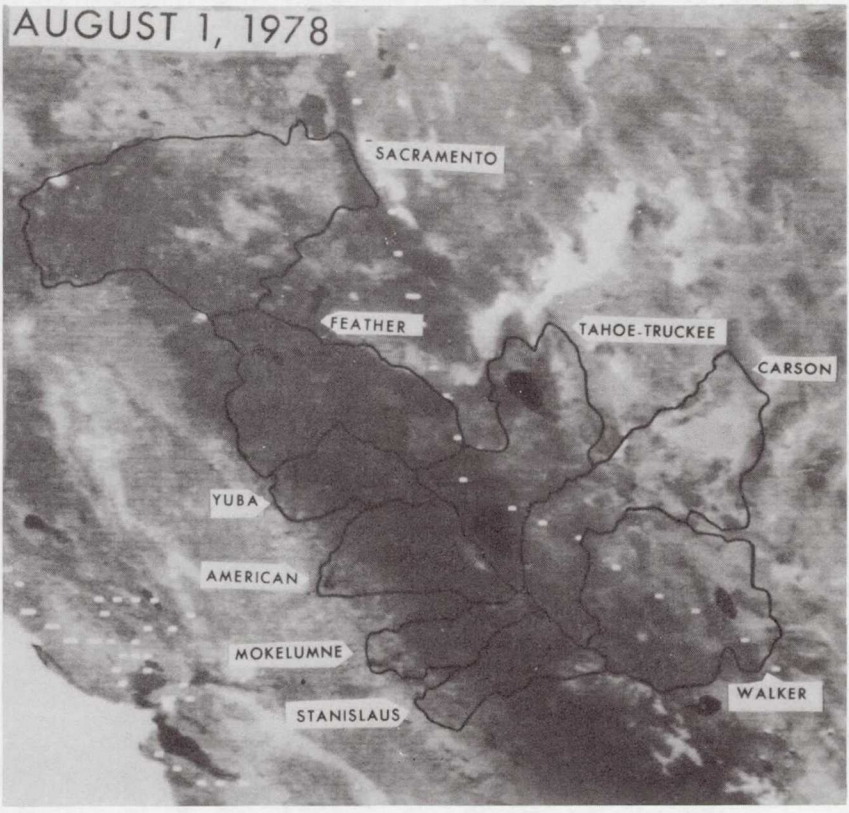


Fig. 1--GOES-W image of the Sierra Nevada test area

## THE VISSR DATA BASE

The digital VISSR data, at reduced resolution from the eastern and western satellites, are being processed into an experimental VISSR Data Base (VDB). Data may be obtained from each satellite at 30-minute intervals. About 18 minutes are required for the VISSR to produce the digital image or "picture" of the full disk. The western satellite data are normally acquired at 15 minutes and 45 minutes after the hour, while the eastern satellite data are acquired on the hour and half hour. Digital data from the full Earth disk are currently restricted to areas extending from 50°N to 50°S latitude and approximately 50° longitude east and west of the satellite subpoints.

The VDB is formed by processing data received in real time from the GOES and ingested onto computer disks, where the resolution of the visible channel is reduced from 1 km to 4 km. The VDB contains 12 selected 4-km visible pictures, six from each satellite. Data are maintained on the VDB for 24 hours before being overwritten with current data. The visible pictures from the western satellite are the source of data for the digital snow-mapping experiment described in this paper.

## PROCEDURE

The digital snow-mapping technique processes on a pixel-by-pixel basis an array of 4-km resolution GOES data containing the nine snow basins. For each pixel, a computer program performs the following operations:

1. Determines which river basin, if any, the pixel is in.
2. Calculates the clear brightness of the pixel, that is, its brightness in the absence of snow or clouds.
3. Checks whether or not the pixel brightness exceeds its clear brightness by more than a set theshold. If so, the pixel is classified as snow-covered. The snowcover in the basin is then determined as the percent of basin pixels that exceed their computed clear brightness by more than the threshold value.

### Construction of the Digital Mask

Determination of which pixels are located in a particular basin required creation of a digital mask. An example of a 129x129 array of 4-km GOES digital data can be seen in Figure 2. Basin outlines from standard hydrologic maps were converted to a GOES-W projection and drawn on the printout using a ZTS. A digital basin mask was then constructed by identifying each basin to the computer by line and pixel. The mask, shown in Figure 3, contains blanks in the pixel locations outside all river basins and an appropriate number from 1 to 9 indicating locations of the nine basins. Bodies of water in and adjacent to the basins (Lake Tahoe, Pyramid, Walker, Eagle, Almanor, and Mono) are indicated by the letter A for use as location landmarks. The mask is permanently stored on computer disk and can be used as long as GOES-W remains fixed at $0^{o}N$, $135^{o}W$. Movement of the satellite to another position would require construction of a new digital mask.

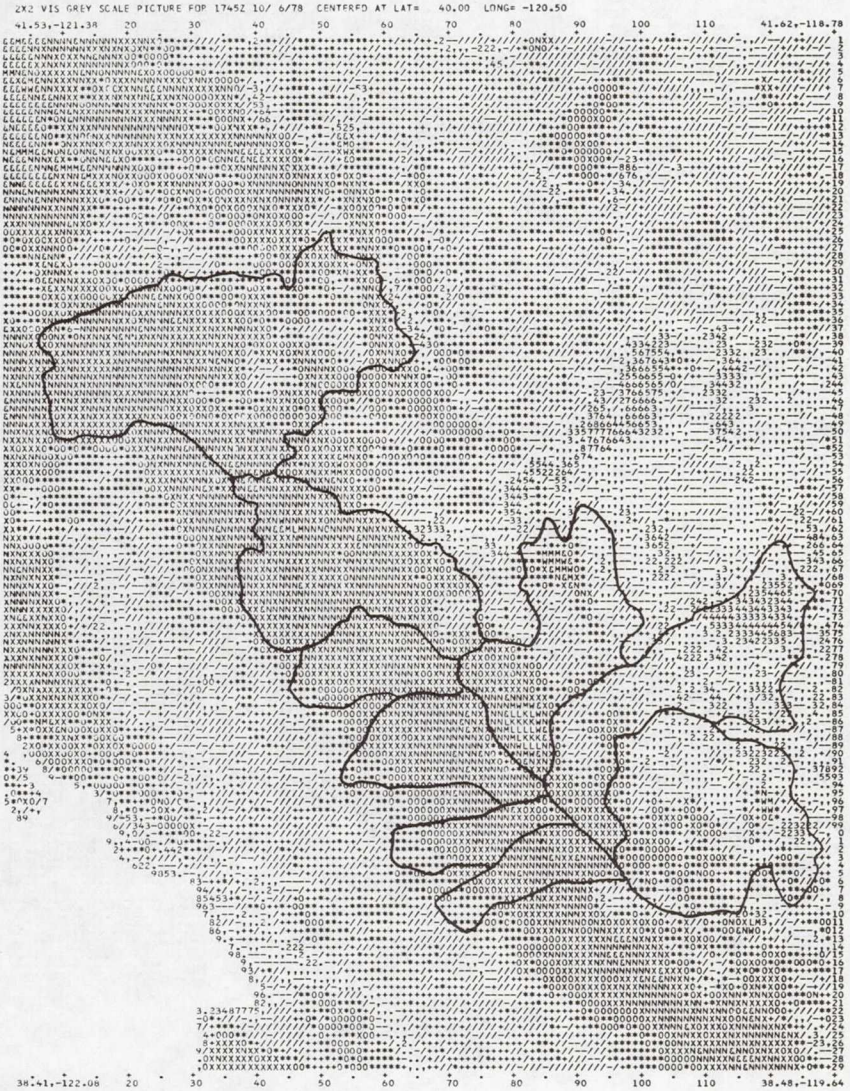


Fig. 2--Alphanumeric printout with each character representing a 4-km pixel element. Basin boundaries drawn with aid of a ZTS.

Fig. 3--Digital basin masks

In processing the digital data for snowcover, it is essential that the digital mask and data array be exactly aligned with respect to one another. Misalignment can easily be detected by comparing location of the aforementioned landmarks on mask and data array. In case of misalignment, the data array can be shifted by line and pixel (up/down or right/left) so that it is properly registered to the mask.

## Determination of Snow-Free Brightness

The heart of the automatic snow-mapping procedure is computation of the brightness of each pixel in a basin under cloud-free, snow-free conditions. The most important quantities determining the brightness of a scene are the illumination angles (local solar zenith angle and azimuth angle between sun and satellite) and ground cover. The brightness values for all pixels in the Feather, Carson, and Walker basins are shown as histograms in Figure 4 to illustrate surface brightness variations within basins. For each basin, the histogram at the top shows the brightness distribution at 0945 local standard time on a clear day in August 1978; the distribution on the same day at 1245 is on the bottom. Increasing count values indicate increasing brightness. The Feather River drainage, mostly covered with forest except for a small grassy plain in the southeastern corner, has a sharply peaked distribution, representative of its uniform ground cover. The Carson and Walker basins are on the east side of the Sierra and contain contrasting climate zones and vegetative cover. The histograms from these two basins are broad, particularly that of the Carson, which has ground cover ranging from pine-juniper forest through desert scrubland to bright salt flats. The Walker histogram is bimodel, reflecting the two predominant types of ground cover in the basin, pine-juniper woodlands and scrub-covered desert. From morning to noon, each basin brightens by 4 or 5 counts but the histogram shapes change very little, indicating that the different types of terrain and ground cover brighten by the same amount. This fact suggests a practical method of computing the clear brightness of each pixel.

If the brightness of each pixel in a basin is known relative to that of a reference area within the basin, then one has only to obtain the brightness of the reference area, which when added to the relative brightness gives the clear value for each pixel. Choosing the reference area to be the darkest region, we can express the brightness count of any basin pixel, $B_i$, as

$$B_i = B_d + R_i \quad ,$$

where $B_d$ is the brightness count of the darkest area and $R_i$ is the brightness of the ith pixel relative to $B_d$.

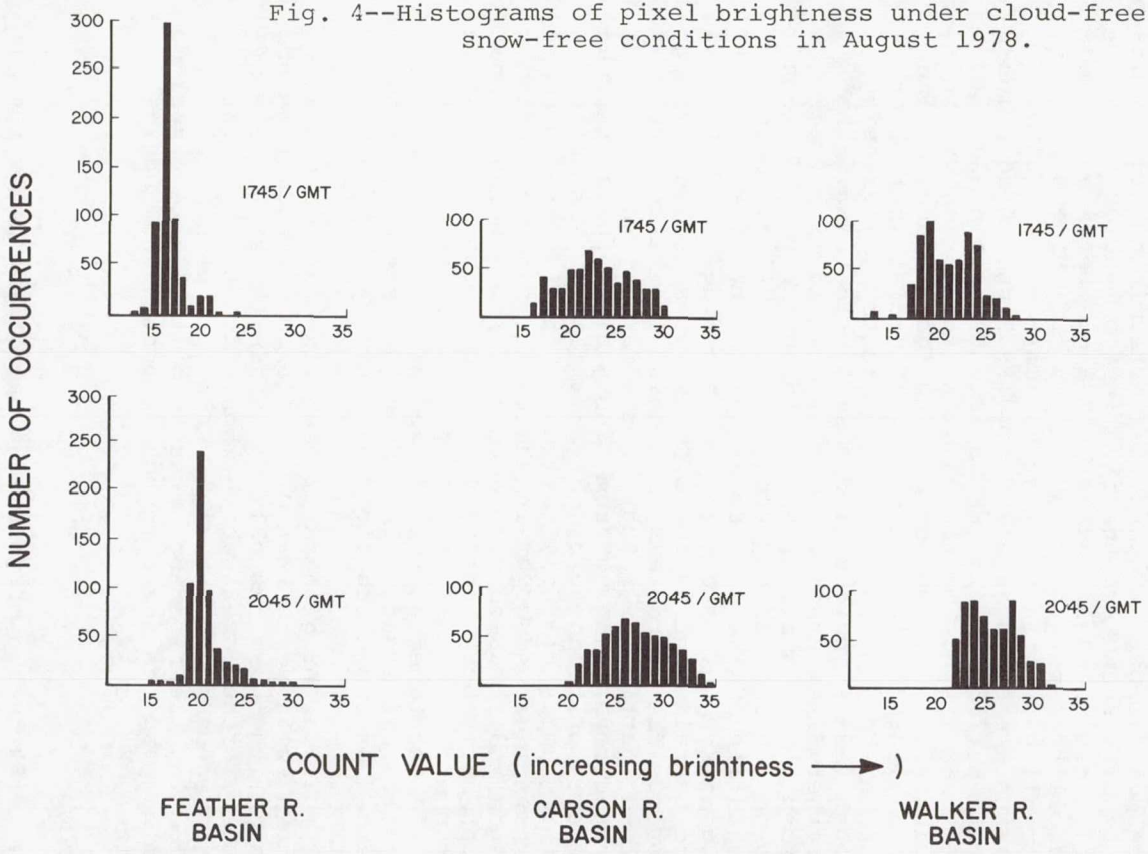


Fig. 4--Histograms of pixel brightness under cloud-free, snow-free conditions in August 1978.

To calculate $B_d$, a regression equation of the following form was used:

$$B_d = a + b \cos\chi + c \sin\chi \cos\phi + d \sin\chi \cos^2\phi \quad ,$$

where $\chi$ is the local solar zenith angle, $\phi$ is the azimuth angle between the sun and satellite, and a, b, c, and d are regression coefficients. Regression coefficients were derived for each basin from clear data collected from August through early November 1978. The regressions are accurate to within 1 count for most pictures as long as the sensor response is stable (Tarpley et al., 1978).

## Construction of the Relative Brightness Mask

A relative brightness mask was constructed for each basin from data collected at 0945 local time on a cloud-free, snow-free day in August 1978. The darkest area in each basin (excluding lakes) was chosen by visual examination. In the Sierra, the darkest area is the most densely forested part of the basin. The digital count of the darkest area, $B_d$, was then subtracted from the value of each pixel in the basin, yielding the relative brightness value, $R_i$, for each pixel. The relative brightness mask for the Walker basin is shown in Figure 5. These data have the same distribution (excluding lakes) as the 0945 histogram in Figure 4. Note that high numbers in the relative brightness mask correspond to bright features in the picture in Figure 1, while numbers 0 to about 4 are located in forested regions. Since relative brightness in a basin is nearly independent of solar illumination angles, as shown in the histograms, the relative brightness mask was generated for only one hour (0930) but used at other hours during the day.

## Determination of Snowcover

A threshold value is added to the predicted clear brightness of each pixel to give a value, $T_i$,

$$T_i = B_i + \Delta \quad ,$$

where $\Delta$ is the threshold. If the measured count exceeds $T_i$, then the pixel is assumed to be snow-covered. The value of $\Delta$ is empirically determined and varies by basin for different illumination conditions and types of ground cover.

Computer-printed snowcover maps, illustrated in Figure 6, are produced by filling a 129x129 array with

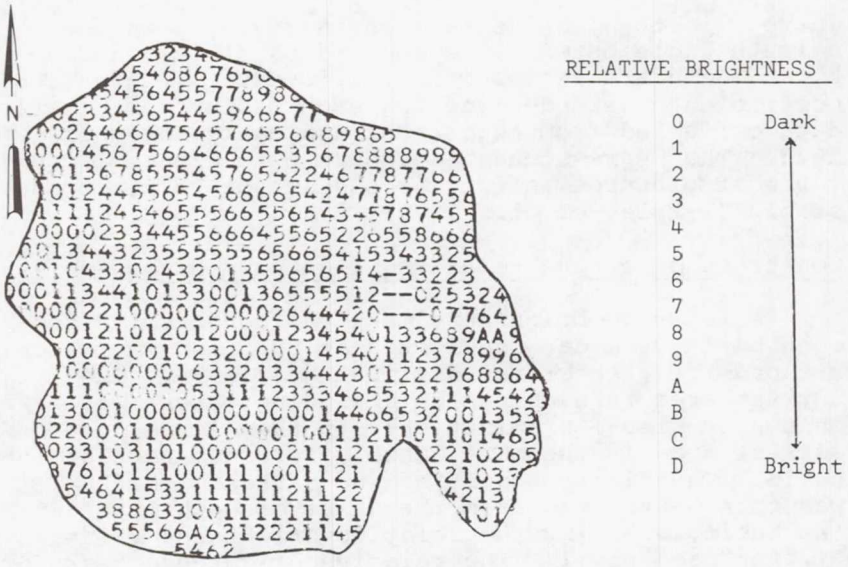


Fig. 5--Relative brightness mask for the Walker River basin

dots, basin number, and blanks, depending on whether or not the corresponding pixel in the data array is outside the basins of interest, snow-free (brightness count $\leq T_i$) or snow-covered (brightness $> T_i$), respectively. Snowcover can be determined from any of four pictures resident on the VDB (at 1645, 1745, 2045, and 2145 GMT) and for any combination of the nine Sierra basins. The snowcover in a basin is the number of snow-covered pixels expressed as a percentage of the total number of pixels in the basin.

## PRELIMINARY RESULTS

Digital snow maps for the nine Sierra River basins have been generated experimentally at NESS since November 3, 1978. The results are compared to snowcover measurements produced photointerpretively as part of the NESS Operational Snowmapping Program. Over 100 cases have been studied as of this writing. The critical parameter has proven to be $\Delta$, the number of counts by which snow brightens up a basin pixel.

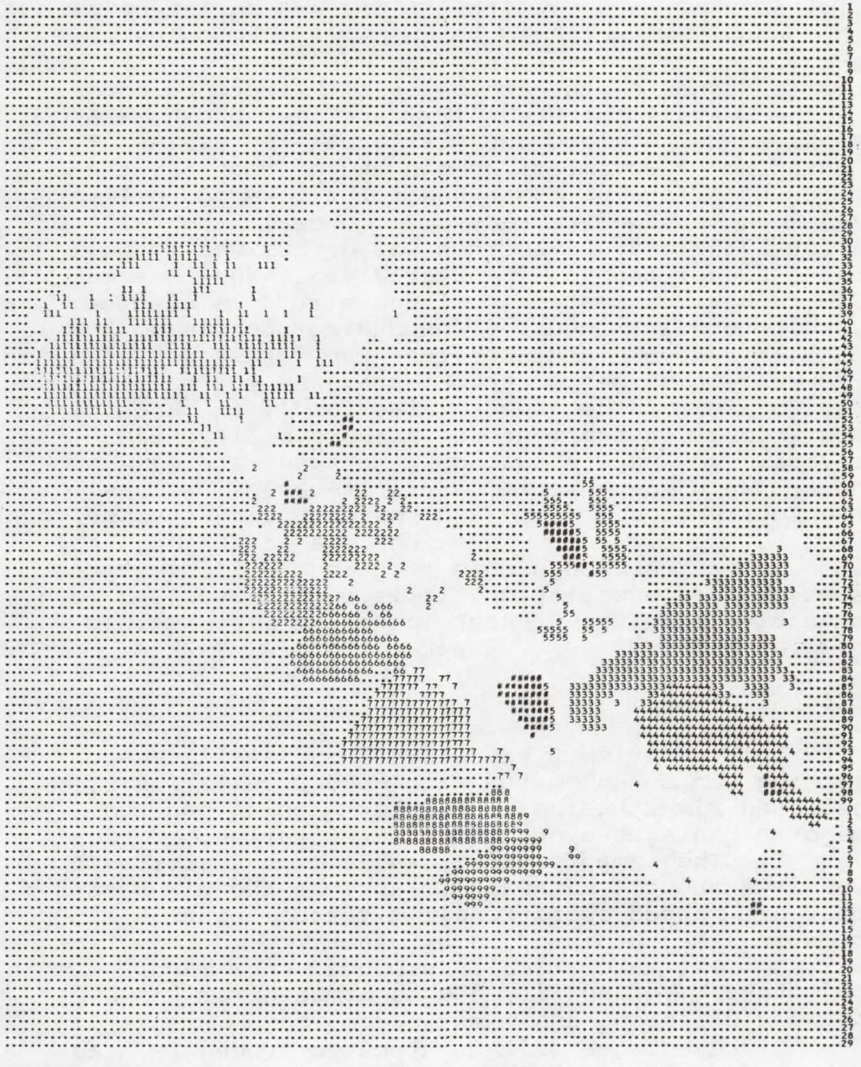

| RIVER | PERCENT SNOW COVERED |
|---|---|
| SACRAMENTO | 57.7 |
| FEATHER | 57.0 |
| CARSON | 42.7 |
| WALKER | 61.6 |
| TRUCKEE | 64.2 |
| YUBA | 34.1 |
| AMERICAN | 33.3 |
| MOKELUMNE | 29.4 |
| STANISLAUS | 47.4 |

PICTURE TIME 1745

Fig. 6--Printout of digital snow maps with corresponding basin snowcover percentages

In every case, a Δ was identified that brought the digital snow maps to within 5 percent agreement with the manual product. For each basin, the value of Δ producing the correct snow map was found to vary with terrain, snow depth, and solar illumination angles. In the heavily forested American River basin, a Δ of 4 was found to yield the most accurate results at the beginning of November; by the end of December the value of Δ for the basin had to be lowered to 1 to achieve the same accuracy. In general, the value of Δ for 1745Z and 2045Z cases was determined to be 1 count higher than at 1645Z or 2145Z. The eastern Sierra basins, containing large stretches of open desert terrain, required (depending upon season) a Δ from 1 to 3 counts higher than the forested basins on the western slopes of the Sierra. As yet there is no way to predict the proper value for Δ, so in an operational environment the authors believe that several snow maps should be generated with each computer run using a series of first-guess Δ values. The "correct" snow map (and corresponding Δ value) can then be identified by checking it against the satellite image. Although this technique still requires some photointerpretation, it is much faster and more objective than the present manual analysis method used at NESS.

## DISCUSSION

This experiment has shown that satellite snow mapping can be automated with good results for selected river basins. Computer mapping has two major advantages over photointerpretation:

1. The computer analysis is much faster. It requires about 4 manhours to analyze the six basins that are mapped operationally, versus about 30 minutes for the automatic technique.
2. The automatically produced snow maps are more objective. Variability due to human error and bias between different analysts is removed.

Disadvantages of the automated procedure are:

1. The program cannot discriminate between snow and cloud or fog, so basins cannot be mapped unless they are completely cloud-free.
2. Very light or patchy snow may not brighten a scene sufficiently to be detected.
3. Digital data are available from the VDB for only 24 hours after the observation so there are deadlines within which the program has to be successfully run. Retrospective snow mapping would have to be done from archived data.

The data used in this study were of sufficient resolution to map snow cover in the Sierra basins. However, it probably would not be possible to use 4-km data to monitor snowcover in basins that are smaller, are farther away from the satellite's subpoint, or have more complex snowlines than the Sierra basins. In order to completely automate snow mapping at NESS, 2-km or even 1-km VISSR data would have to be used to insure good results in all basins.

ACKNOWLEDGMENT

The authors wish to express their appreciation to Michael Oncale and Robert Carey of NESS for programming support.

REFERENCES

Bristor, C.L., 1975: Central processing and analysis of geostationary satellite data. *NOAA Technical Memorandum NESS 64*, National Oceanic and Atmospheric Administration, U.S. Department of Commerce, Washington, D.C., 155 p.

Schneider, S.R., D.R. Wiesnet, and M.C. McMillan, 1976: River basin snow mapping at the National Environmental Satellite Service. *NOAA Technical Memorandum NESS 83*, National Oceanic and Atmospheric Administration, U.S. Department of Commerce, Washington, D.C., 19 pp.

Tarpley, J.D., S.R. Schneider, J.E. Bragg, and M.P. Waters, 1978: Satellite data set for solar incoming radiation studies. *NOAA Technical Memorandum NESS 96*, National Oceanic and Atmospheric Administration, U.S. Department of Commerce, Washington, D.C., 36 pp.

**Page intentionally left blank**

# A REVIEW OF LANDSAT-D AND OTHER ADVANCED SYSTEMS RELATIVE TO IMPROVING THE UTILITY OF SPACE DATA IN WATER-RESOURCES MANAGEMENT

V. V. Salomonson and D. K. Hall, Laboratory for Atmospheric Sciences, Goddard Space Flight Center, Greenbelt, Maryland

## ABSTRACT

Substantial progress has been made in applying remote sensing data from spacecraft to water-resources management and hydrologic problems. Landsat-D and the primary instrument, the thematic mapper, offer substantial potential for providing improved information for a wide range of applications. In particular, significant technological advantages are: (1) the spatial resolution (30 meters in the reflected solar-radiation bands) and the greater spectral coverage (seven bands) and narrower bands relative to previous Landsat instruments and (2) the radiometric resolution (256 versus 64 levels over the sensor dynamic range). Technological advances such as that typified by Landsat-D and planned microwave sensors indicate that significantly more applications to water-resources studies are possible. This growth in the use of remotely sensed data from spacecraft must be closely coupled to advances in data processing and delivery technology and methodology before routine and widespread use of the information observations is possible.

## INTRODUCTION

The use of remotely sensed data, particularly from spacecraft, in activities related to water-resources management and studies of the hydrologic cycle is continuing to grow. The launch in the early 1970's of the Landsat series of satellites by the National Aeronautics and Space Administration (NASA) and the flight of the Very High Resolution Radiometer (VHRR) on the National Oceanic and Atmospheric Administration (NOAA) polar-orbiting, operational, environmental satellite series are examples of space missions that have provided useful data to hydrologists and water-resources managers (Salomonson, et.al., 1979).

The observations provided from space have, nevertheless, gained rather slow acceptance because they are still lacking in several respects. For example, they may not have the spatial resolution or spectral resolution necessary for identifying key hydrologic features. The processing of the high volumes of data provided by remote

sensors is often too expensive or too difficult to make their use attractive. Finally, the use of remotely sensed data has often been limited by the speed with which it can be ordered from a data archival center and applied by a water-resources manager. Although progress has been made in each of these areas, much remains to be done before the application of satellite data will become "routine" and widespread.

It is believed that a need exists and that there are substantive reasons for making substantive efforts to improve the utility of satellite data. The need arises from the perception that water resources and the associated hydrologic processes must be managed in an increasingly effective manner and must be better understood over larger and larger areas or regions because of expanding populations and increased industrial and agricultural activity, both in the United States and abroad. A key reason for attempting to better apply satellite data is that satellites and the associated sensors are particularly suited for providing repetitive, high spatial density, uniform observations over large areas. It is believed that these observations have and can be increasingly used to most effectively augment or complement conventional observation networks and data-gathering techniques.

The purpose of this paper is to review systems that NASA is now implementing or developing and to briefly consider other systems or approaches that may substantially affect the frequency of use and effective application of satellite data in hydrology and related fields.

## LANDSAT-D

A new experimental Earth-resources monitoring system, Landsat-D, is scheduled for launch in the third quarter of 1981. Landsat-D includes several technological advances over the capabilities provided by Landsats 1, 2, and 3. In essence, the Landsat-D system is designed to be a complete, highly automated, data-gathering and processing system that should substantially contribute to more effective remote sensing of Earth resources and to the management of these resources, including water resources, on a local, regional, continental, and global basis.

The four major objectives of the Landsat-D project and program are:

1. To assess the capability of the thematic mapper (TM) to provide improved information for Earth-resources management.

2. To provide a transition for both domestic and foreign users from multispectral scanner subsystem (MSS) data to the higher resolution and data rate of the TM.

3. To provide system-level feasibility demonstrations in concert with user agencies to define the need for, and characteristics of, an operational system.

4. To encourage continued foreign participation in the program.

## Flight Segment

The two major segments of the overall Landsat-D system are the flight segment and the ground segment. The flight segment (Figure 1) is being configured for compatibility with the operations of the Shuttle Transportation System (STS). A backup spacecraft, including sensors, is being planned that is called Landsat-D′ (D-prime). It is to be prepared for launch, as needed to ensure continuity of data, by the second quarter of 1982.

The launch vehicle for Landsat-D will be a Delta 3910 rocket. It will carry the Landsat-D payload to an orbital altitude slightly above 700 km. This altitude is compatible with the retrieval and replacement capabilities planned in conjunction with the STS during the Landsat-D project timeframe. The Landsat-D payload, including the spacecraft, instruments, and other equipment, is expected to weigh nearly 1630 kg (3600 lb). The present launch capability of the Delta 3910 is 1723 kg (3800 lb). This leaves a weight margin of approximately 5 percent.

It is expected that the Landsat-D flight segment will be placed into one of two Sun-synchronous orbits. Figure 2 shows the coverage patterns for these orbits. The orbit described in Figure 2a is the closest approximation permitted by orbital mechanics to the "minimum-drift" orbit associated with Landsats 1 through 3. It is essentially an "inventory" type of orbit that, pending minimum cloudcover, can permit large areas to be observed and image mosaics to be prepared with minimum surface-cover change during the observing period. The orbit described in Figure 2b is more what is termed as "skipping or sampling" orbit. It permits samples of observations (scenes) over very large areas to be acquired in a minimum amount of time.

The advantages of the orbit in Figure 2a are most realizable in the lower latitudes in which clear skies tend to persist for longer periods of time (e.g., areas within large semipermanent atmospheric high-pressure regions). The advantages of the orbit described in Figure 2b are most realized in the higher latitudes (above 45 degrees) because of the orbit sidelap coverage. Barring cloudcover, observations would be available at least every 9 to 11 days at latitudes higher than 45 degrees in the Figure 2b orbit. This attribute makes this orbit attractive for monitoring snowcover variations and other dynamic features that occur at the higher latitudes. The decision of which orbit to use should be made by the summer of 1979 so that complete systems and error-budget studies can be completed..

The spacecraft component of the flight segment will be the Multimission Modular Spacecraft (MMS). This spacecraft will perform the basic functions of providing power, altitude control, and the command and data-handling systems. The MMS has improved attitude-control capability over previous systems. The pointing accuracy is specified to be 0.01 degrees (1-sigma value), and the stability is $10^{-6}$ degrees/second (1-sigma value). To appreciate the advantages afforded by the MMS in this area, one can compare these performance values to the 0.7-degree pointing accuracy and 0.01-degree/second stability values associated with Landsats 1 through 3.

The solar panels shown in Figure 1 will provide ample power. The individual outboard panels are approximately 1.5 by 2.3 meters in dimension. The solar array

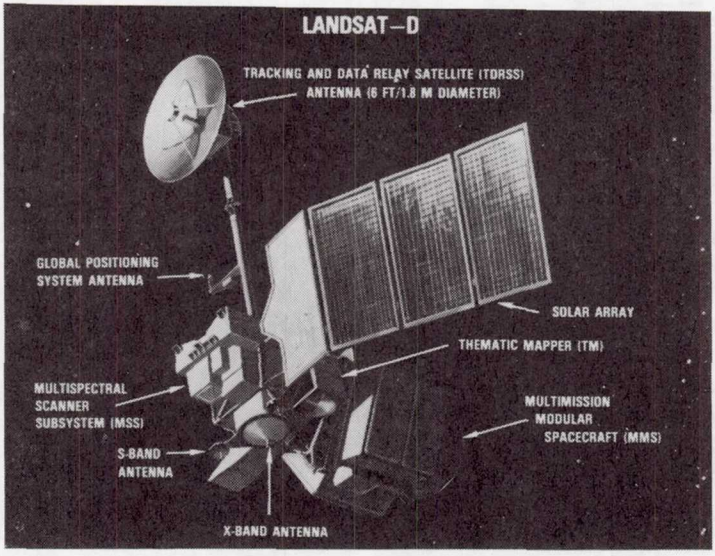


Fig. 1–Landsat-D flight segment

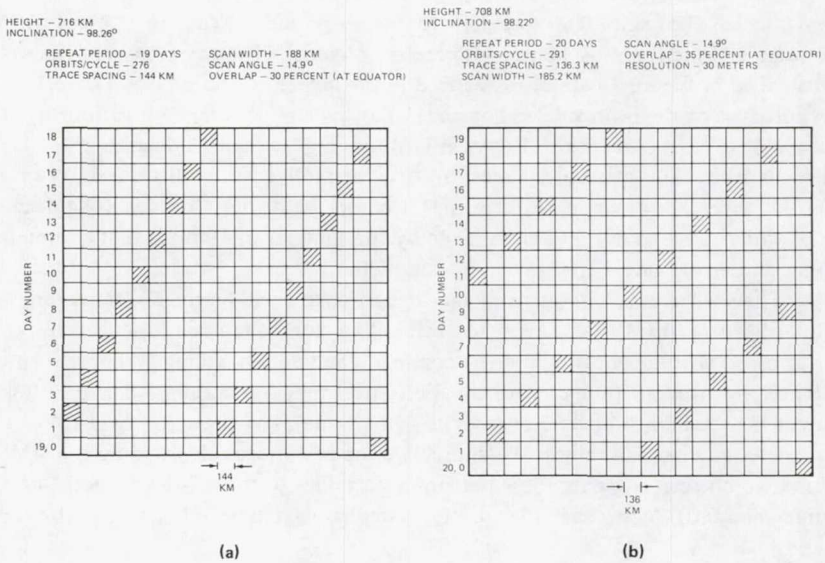


Fig. 2–Major choices available for Landsat-D orbits (9:30 a.m. equator crossing time in both cases)

will be capable of providing 790 watts of average power at the end of the Landsat-D mission, in contrast to the conservative estimate of 760 watts of average power that may be needed to sustain the operations of the various components, including the Earth-observing instruments.

One of the major aspects of the Landsat-D system and the subsequent operations is the compatibility with and use of the Tracking and Data Relay Satellite (TDRS) system. The use of this system will eliminate the need to rely on tape recorders. This is a positive step forward in concept because tape recorders have frequently been one of the satellite subsystems that have failed earliest in past Earth-observing space missions. Certainly, previous Landsat missions have had this problem.

The TDRS antenna shown in Figure 1 will permit command signals, telemetry signals, and sensor observations to be relayed to data-processing centers through one of two geosynchronous satellites in the TDRS system placed at 41° and 171°W. Data from these satellites will be received at White Sands, New Mexico, and relayed to the Landsat-D data-processing center at the Goddard Space Flight Center (GSFC) by a communications satellite. Figure 3 gives an overall view of the communications process for Landsat-D. To handle the high data rates associated with Landsat-D, the STS, and other space missions, the TDRS system uses a Ku-band (≈15 GHz) frequency for communications. Because this frequency is somewhat more affected by atmospheric conditions than previously applied communications links, a relatively cloud-free location (White Sands, New Mexico) was chosen as the point for receiving TDRS information.

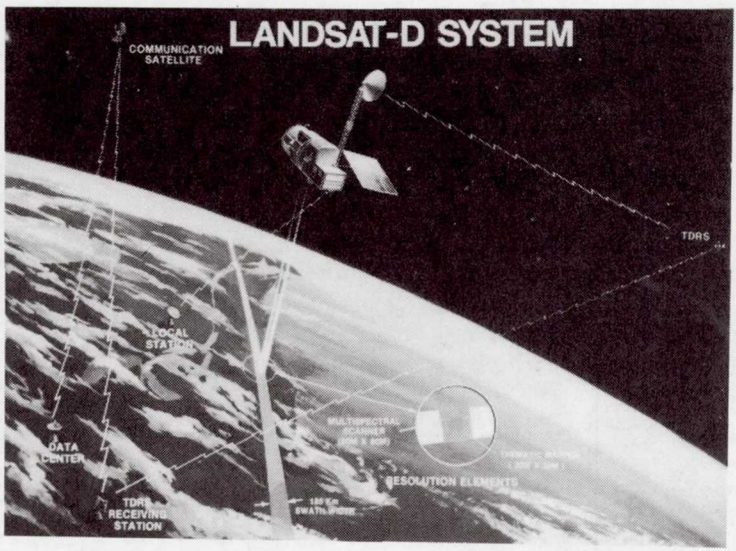


Fig. 3—An illustration depicting the overall communications and data-gathering process for Landsat-D

Landsat-D will also be able to directly communicate with and send data to ground receiving stations. For this purpose, X-band (8.025 to 8.4 GHz) and S-band (2206 to 2300 MHz) frequencies will be used. Although S-band has been used for previous Landsat missions, a high-frequency X-band link is required for handling the TM data stream. As a result, stations that intend to receive TM data must add some capabilities that were not previously required for receiving Landsat MSS data.

Landsat-D will fly a position-location device that receives and processes data from the Global Positioning System (GPS) (Fuchs and Pajerki, 1978). The GPS experiment is expected to provide a very accurate position location, nominally 10 meters for the portion of the orbit when Landsat-D is in view of the GPS satellites that are now available. The complete GPS will eventually employ 24 satellites, using doppler techniques to provide the 10-meter accuracy on a global basis. In the initial stages, Landsat-D will be able to use only six of the 24 satellites. Because these six are more or less in a cluster, they will be in view for only part of the orbit. GPS should provide more accurate data than standard tracking networks and contribute substantially to more autonomous operations of satellites and improved onboard data processing in the future.

The instrument payload (Table 1) consists of the familiar MSS of Landsats 1 and 2; that is, it is the four-band instrument and does not have the fifth band (thermal infrared) that was included on Landsat-3. The TM provides narrower bands similar to those on the MSS and adds 0.45 to 0.52, 1.55 to 1.75, and 2.08 to 2.35 $\mu$m bands, plus the thermal band (10.5 to 12.5 $\mu$m). Table 1 lists the spectral intervals and radiometric sensitivity of each of the sensors. Table 2 provides the radiometric

Table 1
Landsat-D Earth-Observing Instrumentation
(March 1979)

| | THEMATIC MAPPER (TM) | | MULTISPECTRAL SCANNER SUBSYSTEM (MSS) | |
|---|---|---|---|---|
| | MICROMETERS | RADIOMETRIC SENSITIVITY (NE$\Delta$P) | MICROMETERS | RADIOMETRIC SENSITIVITY (NE$\Delta$P) |
| SPECTRAL BAND 1 | 0.45 - 0.52 | 0.8% | 0.5 - 0.6 | .57% |
| SPECTRAL BAND 2 | 0.52 - 0.60 | 0.5% | 0.6 - 0.7 | .57% |
| SPECTRAL BAND 3 | 0.63 - 0.69 | 0.5% | 0.7 - 0.8 | .65% |
| SPECTRAL BAND 4 | 0.76 - 0.90 | 0.5% | 0.8 - 1.1 | .70% |
| SPECTRAL BAND 5 | 1.55 - 1.75 | 1.0% | | |
| SPECTRAL BAND 6 | 2.08 - 2.35 | 2.4% | | |
| SPECTRAL BAND 7 | 10.40 - 12.50 | 0.5K (NE$\Delta$T) | | |
| GROUND IFOV | | 30M (BANDS 1 - 6)<br>120M (BAND 7) | 82M (BANDS 1 - 4) | |
| DATA RATE | | 85 MB/S | 15 MB/S | |
| QUANTIZATION LEVELS | | 256 | 64 | |
| WEIGHT | | 227 KG | 68 KG | |
| SIZE | | 1.1 X 0.7 X 2.0M | 0.35 X 0.4 X 0.9 M | |
| POWER | | 320 WATTS | 50 WATTS | |

Table 2
Radiometric Performance Requirements

| BAND | SPECTRAL WIDTH ($\mu$M) | DYNAMIC RANGE (MW/CM$^2$ — STER) | LOW LEVEL INPUT (MW/CM$^2$ — STER) | SNR |
|---|---|---|---|---|
| 1 | 0.45 — 0.52 | 0 — 1.00 | 0.28 | 32 |
| 2 | 0.52 — 0.60 | 0 — 2.33 | 0.24 | 35 |
| 3 | 0.63 — 0.69 | 0 — 1.35 | 0.13 | 26 |
| 4 | 0.76 — 0.90 | 0 — 3.00 | 0.16 | 32 |
| 5 | 1.55 — 1.75 | 0 — 0.60 | 0.08 | 13 |
| 6 | 2.08 — 2.35 $\mu$M | 0 — 0.43 | 0.05 | 5 |
| 7 | 10.40 — 12.50 | 260K — 320K | 300K | 0.5K (NET D) |

- ABSOLUTE CHANNEL ACCURACY < 10% OF FULL SCALE
- BAND TO BAND RELATIVE ACCURACY < 2% OF FULL SCALE
- CHANNEL TO CHANNEL ACCURACY < 0.25% RMS OF SPECIFIED NOISE LEVELS

performance requirements for the TM. A more in-depth description of the TM is provided by Blanchard and Weinstein (1979).

In terms of basic design, there is at least one fundamental difference between the two instruments (TM and MSS). The MSS scans and obtains data in one direction only. The TM, however, scans and obtains data in both directions. The TM approach is necessary for reducing the scan rate for providing the dwell time needed to produce improved radiometric accuracy. Figure 4 illustrates the scanning strategy of the TM. Figure 5 sketches the optics configuration for the TM. The potential applicability of the TM for various applications with emphasis on water-resources management and hydrology is discussed in a later section.

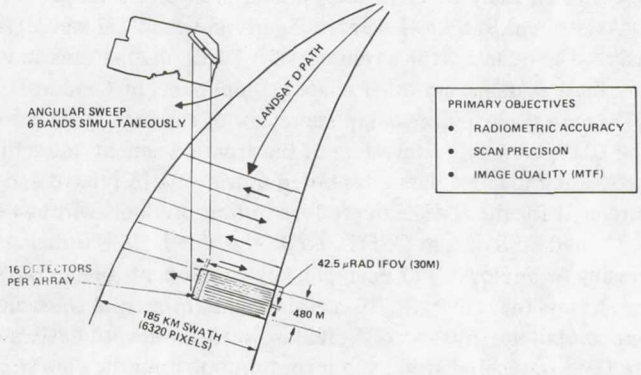


Fig. 4—A sketch illustrating how the thematic mapper will scan the Earth

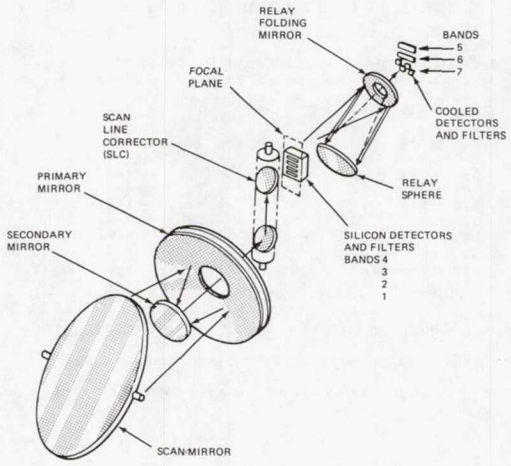


Fig. 5—Thematic mapper optical system

Ground Segment

The ground segment, a major part of the overall Landsat-D system, is being assembled for NASA by the General Electric Company. The ground system faces substantial challenges that are largely a function of the high data rate of the TM and MSS combined (≈100 megabits/second) that must be rapidly processed. The ground segment of the Landsat-D system consists of three major subsystems. The Operations Control Center (OCC) handles all communications with the flight segment, including the commanding and scheduling of the various subsystems of the flight segment and the monitoring of their performance. The Data Management System (DMS) processes all the data from the TM and MSS into final products. The Landsat-D Assessment System (LAS) is a facility in which TM and MSS observations will be analyzed to quantify the advantages for Earth observations and applications afforded by these systems and other related components of Landsat-D. Smith and Webb (1979) have made a more complete review of the Landsat-D ground segment.

The DMS, the major subsystem of the ground segment, faces the major challenge of processing the high data rates noted previously. A related and key performance requirement for the DMS is to produce output products within 48 hours after receipt of TM and MSS data at GSFC. To do this, the DMS is utilizing advanced data-processing technology. For example, key components of the DMS will be two pipeline processors that are in the 10-megainstructions/second class, along with advanced minicomputers. Advanced digital-tape read-and-record devices will also be used in the DMS to receive, store, and record output from the data stream generated by the TM and the MSS. For example, 42-track, 20,000-bits/inch tape recorders will be used to handle the data rate (≈85 megabits/second) and to record multiple scenes

from the TM that involve approximately $250 \times 10^6$ bytes per scene. Use of this technology in the DMS will continue the primarily digital approach (as opposed to film) to processing and archiving data established with Landsat-3 and will maintain or improve the total processing and output production time even in the face of the increased data rates.

Table 3 summarizes the input and output products of the DMS as of March 1979. The output products will be put into a long-term archive facility that will produce and deliver products on order to the general public. The long-term archive facility is expected to be the EROS Data Center in Sioux Falls, South Dakota, operated by the U.S. Department of Interior.

The LAS and OCC will also make use of the data-processing technology used in the DMS. The OCC will use three advanced minicomputer systems to perform its functions. The LAS will use one advanced minicomputer and one pipeline processor to analyze TM and MSS data. As in the DMS, high-speed, very high-density multitrack tape recorders will record and store data and output results.

As already indicated, the DMS is the key component of the ground segment in that it produces the major output products going to the long-term archival facility and eventually to the user community and the public at large. The four major components of the DMS are: (1) the information management subsystem (IMS), (2) the data receive, record, and transmit subsystem (DRRTS), (3) the image-processing subsystem (IPS), and (4) the product generation subsystem (PGS).

Table 3
Data-Management System

| INPUT | OUTPUT (PUBLIC DOMAIN) |
|---|---|
| • 100 TM SCENES (IMAGE DATA) PER DAY<br>– ALL SCENES PARTIALLY PROCESSED (RADIOMETRICALLY CORRECTED)<br>– PUT ON HIGH DENSITY TAPES ($HDT_A$)<br>– $HDT_A$ ARCHIVED FOR SIX MONTHS AT GODDARD SPACE FLIGHT CENTER | • 200 MSS SCENES<br>–FULLY CORRECTED (RADIOMETRICALLY AND GEOMETRICALLY) TAPES ($HDT_P$)<br>– ALL SCENES TRANSMITTED TO EROS DATA CENTER SIOUX FALLS, SOUTH DAKOTA FOR LONG-TERM ARCHIVING |
| • 200 MSS SCENES ( IMAGE DATA) PER DAY<br>– ALL SCENES PARTIALLY PROCESSED (RADIOMETRICALLY CORRECTED)<br>– PUT ON HIGH DENSITY TAPES ($HDT_A$)<br>– $HDT_A$ ARCHIVED FOR SIX MONTHS AT GODDARD SPACE FLIGHT CENTER | • 50 SELECTED TM SCENES<br>– FULLY CORRECTED (RADIOMETRICALLY AND GEOMETRICALLY) TAPES ($HDT_P$)<br>– ALL SCENES TRANSMITTED TO EROS DATA CENTER FOR LONG-TERM ARCHIVING<br>– FIRST GENERATION FILM MASTERS (241 MM X 241 MM, = $1:10^6$ SCALE) SENT TO EDC<br>– 10 TM SCENES PER DAY CAN BE PRODUCED ON COMPUTER COMPATIBLE TAPES (CCT'S) |
| • ANCILLARY DATA<br>– SPACECRAFT EPHEMERIS AND ALTITUDE<br>– RADIOMETRIC CORRECTION DATA<br>– GEOMETRIC/GROUND CONTROL POINT DATA | |
| • PROCESS CONTROL DATA<br>– PROCESSING, CONTROL, AND OPERATIONAL COMMANDS | |
| • DATA BASE UPDATES<br>– AGENCY AND USER FILES, ETC. | |

Data processing in the DMS is performed in these four subsystems through five fundamental steps (Figure 6). In steps 1 and 2, raw sensor data are accumulated from the spacecraft through the communications links already discussed and are processed to produce radiometrically corrected data that are stored on high-density tapes that are designated HDT-A tapes. In these same steps, computations are performed in preparation for making the sensor data compatible with map projections and a ground-control point (reference location) library is developed. In step three, the sensor data are processed and stored on high-density tapes that are designated HDT-P tapes, indicating that they have been fully processed and geometrically and radiometrically corrected. The sensor data are geometrically compatible with map projections such as the universal transverse mercator (UTM) projection, the space oblique mercator (SOM), or the lambert conformal conic (LCC) projections. Here, the data are to be processed to meet goals such as a geodetic accuracy for TM observations of 15 meters (90 percent of the time) and registration of observations from different times to each other of 9 meters (90 percent of the time). In step 4, the output products described in Table 4 will be produced in the PGS. In step 5, the HDT stored data are transmitted to the archival facility at Sioux Falls, South Dakota, by a communications satellite. Images or other products are mailed to this facility.

## Advances in Application Using TM Data

Tables 1 and 2 compare the characteristics of the TM and the MSS. In essence, the TM offers advantages over the MSS in terms of spatial resolution, spectral resolution and numbers of spectral bands, and radiometric resolution.

In quantitative terms, the TM resolution element ("pixel" instantaneous field-of-view) covers 0.09 hectares on the ground. For mensuration and classification, several pixels must fall within a field or feature. If one assumes that 25 pixels are necessary for accurate work, then the field size involved is approximately 2.5 hectares. The corresponding figure for the MSS is over 16 hectares. For example, in urban situations in which stormwater management and watershed planning are activities for which satellite data have proved to be useful (Ragan and Jackson, 1975), the TM spatial resolution is roughly equal to the standard lot size (30 by 30 meters or approximately 100 feet by 100 feet). The identification of urban features, therefore, should be markedly facilitated by the use of TM data.

The TM spatial-resolution advantage and the attendant data processing for geodetic accuracy of pixel location should also produce map products from satellite imagery that are satisfactory or applicable at larger map scales than are possible with MSS data. Landsat 1, 2, and 3 MSS data can be used to compile a planimeter map that meets map accuracy standards at scales of 1:500,000 to 1:250,000. For Landsat-D, maps at 1:100,000 scale should be possible.

Figure 7 shows the spectral and radiometric capability of the TM relative to some typical spectral reflectivity curves. The new TM bands will enhance spaceborne remote sensing capability for mapping both surface and subsurface water

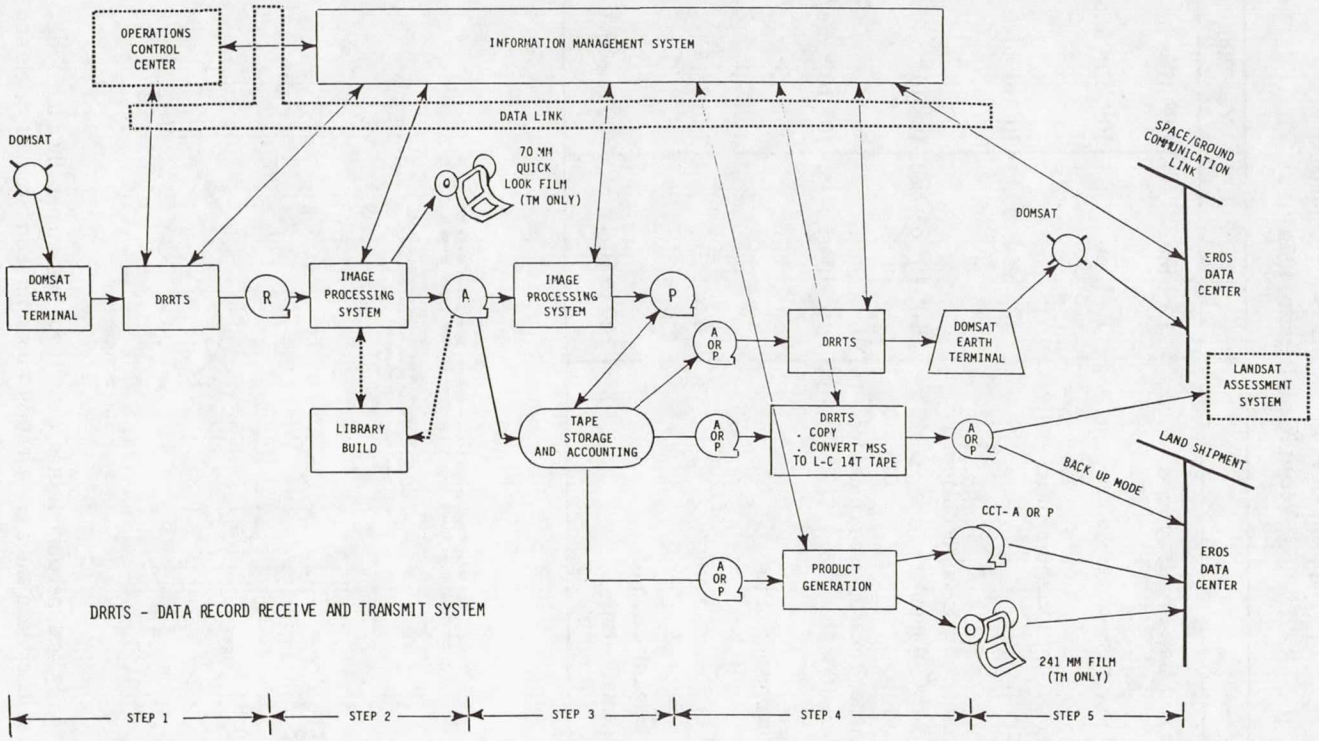


Fig. 6—Data flow within the Landsat-D data-management system

Table 4
Apparent Prognosis for Relevant Technologies
Versus Needs (Hearth, 1976)

| | Now | Year 2000 |
|---|---|---|
| Earth-based mass-storage systems | $10^{12}$ bits | $10^{17}$-$10^{21}$ bits |
| Spaceborne mass-storage systems | $10^{11}$ bits | $10^{14}$-$10^{15}$ bits |
| Transfer rate for spaceborne mass-storage systems | $10^{7}$ bits/sec | $10^{9}$-$10^{10}$ bits/sec |
| Performance of spaceborne computers (Navy AADC Computer) | $10^{6}$-$10^{7}$ ops/sec | $10_{8}$-$10^{9}$ ops/sec |
| Performance of earth-based computers (CDC Star-100, Illiac IV) | $10^{8}$-$10^{9}$ ops/sec | $10^{9}$-$10^{10}$ ops/sec |
| Data compression ratio | | |
| Exact reconstruction | 4 to 5:1 | 7 to 8:1 |
| Reconstruction of thematic map | 60 to 60:1 | 300 to 400:1 |

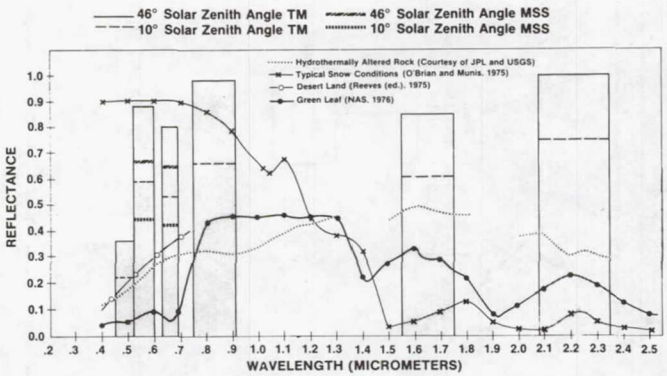


Fig. 7—Typical spectral reflectance curves for hydrothermally altered rock, snow, desert land and a green leaf showing saturation levels for visible and near-infrared bands of the thematic mapper (saturation of bands)

features. TM bands 5 and 6 should be useful in geological studies related to groundwater exploration. TM band 1 should be useful in bathymetry studies. Previous work (Barnes and Bowley, 1977) indicates that TM band 5 will be useful in objectively separating snow from clouds in monitoring regions. In comparison with the radiometric resolution, the TM suite of bands should permit more classes of land cover to be effectively delineated for urban hydrology studies or should be helpful in situations in which detection of moisture stress of crop is the objective, such as for irrigation efficiency studies. Overall, it is projected that the TM spectral capabilities should provide a basic dimensionality of at least 4 in the data compared to the dimensionality of 2 generally experienced in Landsat 1 and 2 MSS data.

Figure 7 also illustrates that the dynamic range of the TM data is larger in some key spectral intervals than that of the MSS. The TM will be less prone to saturate in the 0.63- to 0.69-m and 0.52- to 0.60-m region than the MSS. For example, saturation over clouds and snow, a common occurrence with the MSS, should happen less frequently in TM observations.

One of the major challenges in the Landsat-D timeframe is the high data rate associated with the TM. This high data rate conflicts with the need for rapid turnaround of data and ease in data processing. The Landsat-D ground segment, particularly the DMS and LAS, will be testing data-processing equipment and procedures to ease the problems associated with the TM data rates that arise from desirable increases in spatial resolution and spectral capabilities. From the viewpoint of water-resources management, the 48-hour turnaround goal is very desirable and needs to be improved whenever possible. The following section addresses some of the studies that are in progress to better handle the increased data rates and data-processing complexity associated with remote sensors and, thereby, to improve the utility of this type of data.

## FUTURE THRUSTS

The application of remotely sensed information acquired by spaceborne sensors is growing, and future growth may be expected for reasons indicated in the introduction. This growth, however, will come about and arrive at the point where this type of data are routinely and conventionally applied in water resources, depending on the success achieved in developing sensors that provide information that meets user requirements and the progress made in simplifying and expediting the processing of remotely sensed data and delivering it in optimally usable form to water-resources managers and hydrologists.

Figure 8 shows curves of relative effort versus time that represent the views of the authors as to how progress and timing in the areas noted previously may be achieved on the basis of current NASA planning and modest optimism as to the evolution of technology related to remote sensing and data processing.

The information extraction curve in Figure 8 addresses not only sensor development but also interpretation technique development that must be applied to remotely sensed data. Landsat-D represents technology that extracts new spectral information and spatial resolution by using sensors that respond to reflected solar

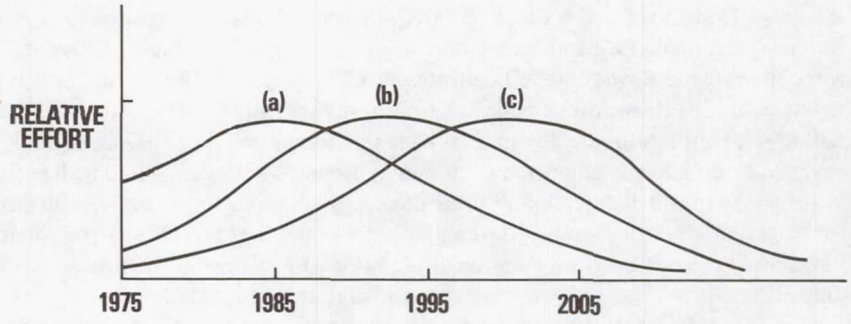


a) INFORMATION EXTRACTION
b) DATA PROCESSING/FORMATTING AND DELIVERY
c) ROUTINE APPLICATION IN RESOURCES MANAGEMENT AND SCIENTIFIC RESEARCH

Fig. 8—Technology development and applications development

and emitted thermal infrared radiation. However, work needs to be done on these data to determine how to extract the maximum information in an efficient manner. Information in the reflected and thermal infrared will probably be further exploited in the next few years by using mechanical scanners or, more likely, solid-state technology and the development of pointable sensors that will permit temporal changes in selected areas or situations to be observed at resolutions higher than the thematic mapper while, at the same time, controlling or keeping the data within the 10 megabits/second order of magnitude.

The microwave portion of the electromagnetic spectrum will also be, or should be, exploited further because of the more nearly all-weather capability of these sensors and their greater sensitivity to variations in the moisture contained within the atmosphere (e.g., cloud liquid-water content and precipitation), the snow pack (e.g., moisture equivalent and wetness), and the upper layers of the soil surface or within vegetation (e.g., soil moisture). The possibility of extracting information related to fundamental flux and storage terms in the hydrologic cycle, such as precipitation and soil moisture, makes research and development of microwave systems and interpretation techniques appear to be very attractive, if not imperative, given the increasing need to better manage water resources and understand climatic processes that either are strongly related to or impact hydrologic processes. The factors noted previously indicate that effort and support for information extraction efforts must continue to grow into the mid-1980's and comprise a substantive portion of technology and applications development into the 1990's.

The sensors mentioned previously will not only provide new information in themselves but, in order to extract the most pertinent and useful information, will most likely necessitate the combining of data from different sensors on the same space vehicle and also different vehicles. In addition, high data volumes will be produced by these sensors that will be in the $10^7$ to $10^8$ bits/second orders of magnitude and the $10^{11}$ to $10^{12}$ bits/day range. To make these data volumes at all tractable for application to water-resources management and hydrological studies,

considerable emphasis must be placed on developing data processing, formatting, and delivery technologies and methodologies. This is suggested in the second curve of Figure 8. This problem has been likened to "learning to drink water from a fire-hose."

There is considerable hope that the challenges associated with data processing and applications of remotely sensed data will be met. Table 4 shows the expected growth in ground-based and spaceborne computer systems and mass-storage systems (Hearth, 1976). The steps forward suggested in Table 4 appear to be promising in terms of handling the data volumes previously suggested.

Specific efforts in the near term include the Global Positioning System noted earlier. This is a step toward the autonomous operation of spacecraft. This capability, accompanied by improved onboard computers and storage, may possibly lead to the onboard processing of data so as to include not only reformatting and calibration, but also the geographic location of each observation so that minimal processing would be required on the ground at receiving stations before having applicable results.

Studies that are evaluating the various methods and alternatives to expedite and simplify the use and processing of satellite data both in conjuction with and independently of conventional data sources include the NASA end-to-end data systems (NEEDS) study (Sos, 1979) and the Applications Data Service (ADS) (Brown, 1979) concept. These efforts are not only assessing the volumes of data involved and the technologies needed, but also studying and developing strategies and approaches to formatting and assessing data so as to simplify its use and diminish costs involved as much as possible.

It appears certain that an increasing effort to develop the data-processing and delivery techniques alluded to previously will be necessary before routine and continued use of remotely sensed data over a wide spectrum of activities occurs. Figure 8 suggests that the peak in this kind of effort may be projected into the 1990's time frame with routine use occurring by the 21st century. It is clear that this schedule could be different, depending on a host of development and alternatives. However, the main point is that routine use of remotely sensed data will occur pending the joint development of accurate information that is expeditiously delivered to the user community.

## ACKNOWLEDGMENTS

The authors acknowledge the contributions of many people who are part of the Landsat-D Project and who have provided material and understanding that have made the preparation of this paper possible. They particularly thank some of the key Landsat-D Project personnel such as Charles Gunn (Project Manager), L. Gonzales (Deputy Project Manager-Technical), O. Weinstein (thematic mapper development), P. L. Smith (ground systems manager), and W. Webb (ground systems engineer).

REFERENCES


1. Barnes, J. C., and Bowley, C. J., "Study of Near Infrared Reflectance Using Skylab S192 Multispectral Scanner Data," *ERT Document No. 1474F, Final Report,* Environmental Research and Technology Inc., Boston, Mass., 48 pp., 1977.

2. Blanchard, L. E., and O. Weinstein, "Thematic Mapper Development," *Proceedings of the 1979 Machine Processing of Remotely Sensed Data Symposium,* Purdue University, West Lafayette, Indiana, 1979.

3. Brown, L. E., "NASA Applications Data Service," *Proceedings of the IEEE/International Conference on Communications (ICC),* Boston, Mass., 1979.

4. Fuchs, A. J., and R. S. Pajerki, "The Role of Autonomous Satellite Navigations in the NEEDS Program," *Proceedings of the AIAA/NASA Conference on "Smart" Sensors,* Hampton, Virginia, November 14-16, *American Institute of Aeronautics and Astronautics,* New York, 1978.

5. Hearth, D. P., *A Forecast of Space Technology, 1980-2000,* NASA SP-387, National Aeronautics and Space Administration, Washington, D.C., 1976.

6. National Academy of Sciences (NAS), *Resource and Environment Surveys from Space with the Thematic Mapper in the 1980's,* Report of the Committee on Remote Sensing for Earth Resources Surveye (CORSPERS), Washington, D.C., 1976.

7. O'Brien, H. W., and R. H.. Munis, "Red and Near-Infrared Spectral Reflectance of Snow," *Proceedings of the Workshop on Operational Applications of Satellite Snowcover Observations,* NASA SP-391, Washington, D.C., pp. 71-85, 1975.

8. Ragan, R. M., and T. J. Jackson, "Use of Satellite Data in Urban Hydrologic Models," *Journal of the Hydraulics Division, ASCE,* 101, pp. 1469-1475, 1975.

9. Reeves, R. G., A. Anson, D. Landen, *Manual of Remote Sensing,* American Society of Photogrammetry, Falls Church, Virginia, 1975.

10. Salomonson, V. V., V. R. Algazi, and D. R. Wiesnet, "Applicability of Space Acquired Data for Water Resources Management," *Proceedings of the Conference on "Improved Hydrologic Forecasting—Why and How,"* Pacific Grove, California, 1979, 16 pp.

11. Smith, P. L., and W. C. Webb, "Landsat-D Acquisition and Data Processing System," *Proceedings of the 1979 Machine Processing of Remotely Sensed Data Symposium,* Purdue University, West Lafayette, Indiana, 1979.

12. Sos, J., *NASA End-to-End Data System Concept,* Goddard Space Flight Center, NASA, Greenbelt, Maryland, 1979, 68 pp.

FINAL WORKSHOP ON OPERATIONAL APPLICATIONS
OF
SATELLITE SNOWCOVER OBSERVATIONS

## ROSTER OF PARTICIPANTS

WORKSHOP DIRECTOR
Albert Rango
Senior Research Hydrologist
NASA/Goddard Space Flight Center
Code 913, Greenbelt, MD 20771

PROGRAM COORDINATOR
Jan Dunbar-Douglass
Conferences and Institutes/Continuing Education
University of Nevada - Reno
Reno, NV 89557

---

ABRAHAM, C. E.
U.S. Corporation of Engineers
125th and Center
Omaha, NE 68144

ARMSTRONG, Betsy R.
WDC-A, INSTAAR,
University of Colorado
Boulder, CO 80309

ARMSTRONG, Richard L.
University of Colorado
PSRB 1
Boulder, CO 80309

BAIRD, G. H.
U.S. Bureau of Reclamation
7680 Sierra Drive
Roseville, CA 95678

BARNES, James C.
ERT, Inc.
696 Virginia Road
Concord, MA 01742

BARTON, Manes
USDA Soil Conservation Service
511 NW Broadway, Rm. 510
Portland, OR 97209

BEARD, Gerald
Soil Conservation Service
3108 Barr Street
Boise, ID 83703

BILELLO, Michael A.
U.S. Army - CRREL
Snow and Ice Branch
Hanover, NH 03755

BISSELL, Vern
NWS
121 Custom House
Portland, OR 97232

BOGART, Gene
City of Bakersfield
1501 Truxton Avenue
Bakersfield, CA 93301

BOWLEY, Clinton
ERT, Inc.
696 Virginia Road
Concord, MA 01742

BOYNE, H. S.
National Bureau of Standards
325 Broadway
Boulder, CO 80302

BROOKS, Kenneth N.
University of Minnesota
110 Green Hall
St. Paul, MN 55108

BROWN, A. J.
Calif. Department of Water Resources
1416 9th Street
Sacramento, CA 95814

BURNS, Joseph I.
Murray, Burns, and Kienlen
600 Forum Building
Sacramento, CA 95814

CASTRUCCIO, P.
ECOsystems International, Inc.
Box 261
Gambrills, MD 21108

CLINE, Terry
University of Idaho
Dept. EE
Moscow, ID 83843

COULSON, C. H.
B C Environment
Parliament Building
Victoria, BC
CANADA

COX, Lloyd
USDA SEA AR
1175 So. Orchard, Suite 116
Boise, ID 83705

CROZIER, Al
Weather Measure Corporation
4451 Osprey Street
San Diego, CA 92107

DAVIS, Robert
University of California
Santa Barbara, CA 93106

DAVIS, Robert T.
Soil Conservation Service
Rm. 360 U.S. Courthouse
Spokane, WA 99201

DEETS, Neil A.
U.S.D.A. Ashley N.F.
Vernal, UT 84078

DILLARD, John
Bonneville Power Administration
P.O. Box 3621
Portland, OR 97208

DOBSON, Don A.
Water Survey of Canada
502 1001 W. Pender Street
Vancouver, BC
CANADA

DOZIER, Jeff
University of California
Santa Barbara, CA 93106

FALLEK, Hank
Handar
3327 Kifer Road
Santa Clara, CA 95051

FARNES, Phillip
Soil Conservation Service
P.O. Box 98
Bozeman, MT 59745

FETTY, Carl W.
Leopold and Stevens, Inc.
P.O. Box 688
Beaverton, OR 97005

FFOLLIOTT, Peter
University of Arizona
SRNR, College of Agriculture
Tucson, AZ 85721

FRAMPTON, Mike
University of California
Santa Barbara, CA 93106

FREDEN, Stanley C.
Goddard Space Flight Center
Missions Utilization Office
Greenbelt, MD 20771

FREW, James
Computer Systems Lab
University of California
Santa Barbara, CA 93106

GIRD, Ron
National Environmental Satellite Service
World Weather Bldg., Rm. 510
Washington, DC 20233

GORDON, Bill
Bonneville Power Administration
P.O. Box 3621
Portland, OR 97208

HAEFNER, Harold
Department of Geography
University of Zurich
Zurich, CH-8006
SWITZERLAND

HANNAFORD, J. F.
Sierra Hydrotech
P.O. Box 169
Placerville, CA 95667

HART, Mike
Pennzoil Vermigo Park Corporation
Drawer E
Raton, NM 87740

HEDGES, Delbert
Nevada Irrigation District
Grass Valley, CA 95945

HUFFMAN, Don
SCS Snow Surveys
Bozeman, MT 59715

JOLLY, Wallace
Soil Conservation Service
Bozeman, MT 59715

JONES, E. Bruce
Resource Consultants, Inc.
Ft. Collins, CO 80522

KAHAN, Archie M.
Bureau of Reclamation
Lakewood, CO 80228

KEITH, Sandra
University of California
Santa Barbara, CA 93106

KIRDAR, Edib
Salt River Project
P.O. Box 1980
Phoenix, AZ 85001

KLIEFORTH, Harold
Desert Research Institute
Reno, NV 89506

KUEHL, Don
River Forecast Center
Portland, OR

LEAF, Charles
Consulting Hydrologist
201 1/2 Main #241
Sterling, CO 80751

LEAVESLEY, George
U.S. Geological Survey
M.S. 412 Denver Fed. Center
Lakewood, CO 80225

LUKE, Dan
U.S. Bureau of Reclamation
Boise, ID 83724

MARKS, Danny
University of California
Santa Barbara, CA 93106

MARRON, James
Soil Conservation Service
Broomfield, CO 80020

MARTINEC, J.
Federal Institute for Snow and
Avalanche Research
Davos
SWITZERLAND

MATZLER, Christian
Inst. of Applied Physics
Berne
SWITZERLAND

MEIMAN, Jim
Colorado State University
Ft. Collins, CO 80549

MEISNER, Douglas
University of Minnesota
110 Green Hall
St. Paul, MN 55108

MERRY, Carolyn J.
Cold Regions Research &
Engineering Lab.
P.O. Box 282
Hanover, NH 03755

MORAVEC, George F.
Colorado Division of Water Res.
Denver, CO 80005

MORELAND, Ron
USDA SCS
P.O. Box 4850
Reno, NV 89505

MUSTAPHA, A. Majeed
Alberta Environment
(1031) 9820 106 Street
Edmonton, Alberta
CANADA

NEWELL, Shawn
Salt River Project
Box 1980
Phoenix, AZ 85001

ODEGAARD, Helge
IBM
P.O. Box 1329 Vika
Oslo 1
NORWAY

ORIG, Ming
Department of Water Resources
9 & O Streets
Sacramento, CA 95814

ORWIG, Chuck
National Weather Service
121 Custom House
Milwaukie, OR 97222

OUTCALT, Sam
University of Michigan
Ann Arbor, MI 48001

PETERSON, Ralph
GE
5030 Herzel Place
Beltsville, MD 20705

PFANKUCH, Dale
U.S. Forest Service
11177 W. 8th Avenue
Lakewood, CO 80225

PUGNER, Paul E.
U.S. Army Corps of Engineers
650 Cantol Mall
Sacramento, CA 95814

RAETZ, Roland
National Weather Service
Salt Lake City, UT 11188

RIDD, Merrill
University of Utah
270 Orson
Salt Lake City, UT 84112

ROLPH, David
Humboldt State University
Arcata, CA 95521

SALOMONSON, Vincent
NASA/Goddard Space Flight Center
Greenbelt, MD 20771

SCHNEIDER, Stanley
Department of Commerce
World Weather Bldg., Rm. 510
Washington, DC 20233

SCHOLEFIELD, Peter
Atmospheric Environment Service
4905 Dufferin Street
Downsview, Ontario
CANADA

SCHUMANN, Herbert
U.S. Geological Survey
Suite 1880 Valley Ctr.
Phoenix, AZ 85073

SHAFER, Bernie
Soil Conservation Service
2490 W. 26th Avenue
Denver, CO 80212

SHERRETS, Ray
Sacramento Municipal Utility Dist.
6201 "S" Street
P.O. Box 15830
Sacramento, CA 95813

STRIFLER, William D.
Colorado State University
Dept. of Earth Resources
Ft. Collins, CO 80523

SULLIVAN, Howard J.
State of California
9th & O Streets
Sacramento, CA 95814

TANGBORN, Wendell
URS
4th and Vine Bldg.
Seattle, WA 98121

TAYLOR, Mike
U.S. Forest Service
Challenge, CA

THOMAS, I. L.
Physics and Engineering Laboratory
Department of Scientific and
Industrial Research
Private Bag, Lower Hutt,
NEW ZEALAND

THOMAS, Billy J.
U.S.C.E.C.
4800 N.W. 186
Portland, OR 97229

THOMSEN, Anton
Colorado State University
Dept. of Earth Resources
Ft. Collins, CO 80523

WASHICHEK, Jack N.
Soil Conservation Service
1200 Del Mar
Ft. Collins, CO 80521

WENDLER, Gerd
University of Alaska
Fairbanks, AK 99701

WERNER, Jon G.
USDA Soil Conservation Service
3 Janguit
Casper, WY 82601

WHALEY, Bob L.
USDA Soil Conservation Service
Fed. Bldg. 125
S. State Rm. 4012
Salt Lake City, UT 84138

WHITSEL, Gerald
U.S.B.R.
Wilson Avenue
Loveland, CO 80537

WIESNET, D. R.
NOAA/NESS
S-33
Washington, DC 20233

WILSON, Jack A.
Soil Conservation Service
304 N. 8th, Rm. 345
Boise, ID 83702

WILSON, T. T.
Salt River Project
P.O. Box 1980
Phoenix, AZ 85001

YOUNG, Gordon
Federal Government, Canada
Ottawa K1R OE7
CANADA

ZUZEL, John F.
USDA SEA
1175 S. Orchard
Boise, ID 83705

| 1. Report No. | 2. Government Accession No. | 3. Recipient's Catalog No. |
|---|---|---|
| NASA CP-2116 | | |

| 4. Title and Subtitle | 5. Report Date |
|---|---|
| OPERATIONAL APPLICATIONS OF SATELLITE SNOWCOVER OBSERVATIONS | May 1980 |
| | 6. Performing Organization Code |

| 7. Author(s) | 8. Performing Organization Report No. |
|---|---|
| Albert Rango and Ralph Peterson, Editors | |
| | 10. Work Unit No. |

| 9. Performing Organization Name and Address | 11. Contract or Grant No. |
|---|---|
| NASA Goddard Space Flight Center<br>Greenbelt, Maryland 20771 | |
| | 13. Type of Report and Period Covered |

| 12. Sponsoring Agency Name and Address | 13. Type of Report and Period Covered |
|---|---|
| National Aeronautics and Space Administration<br>Washington, DC 20546<br>and<br>The University of Nevada, Reno, Nevada | Conference Publication |
| | 14. Sponsoring Agency Code |

15. Supplementary Notes

Albert Rango, Goddard Space Flight Center
Ralph Peterson, General Electric Company

The requirement for the use of the International System of Units (SI) has been waived for this document under the authority of NPD 2220.4, paragraph 5.d.

16. Abstract

The proceedings of the final workshop on Operational Applications of Satellite Snowcover Observations, held at Sparks, Nevada, on April 16-17, 1979, are reported in this NASA conference proceedings. Research progress in extracting meaningful snow information from satellite data led to the initiation of a NASA Applications Systems Verification and Transfer (ASVT) project. Nine operational water management agencies in the western United States participated in this ASVT in cooperation with NASA. By the spring snowmelt seasons of 1978 and 1979, many of the agencies were using the satellite snowcover data in a quasi-operational mode. In order to conclude the project, the agency participants were brought together to exchange investigation results at the Final Workshop on Operational Applications of Satellite Snowcover Observations. Seventeen scientific papers were presented over the two day period covering various techniques for interpreting Landsat and NOAA satellite data, the status of future systems for continuing snow hydrology applications, the use of snowcover observations in streamflow forecasts by both ASVT participants and selected foreign investigators, and the benefits of using satellite snowcover data in runoff forecasting.

| 17. Key Words (Suggested by Author(s)) | 18. Distribution Statement |
|---|---|
| Satellite snowcover data<br>Snow hydrology<br>Streamflow forecasts<br>Benefits | Unclassified - Unlimited<br><br>Subject Category 43 |

| 19. Security Classif. (of this report) | 20. Security Classif. (of this page) | 21. No. of Pages | 22. Price* |
|---|---|---|---|
| Unclassified | Unclassified | 302 | $11.75 |

* For sale by the National Technical Information Service, Springfield, Virginia 22161

NASA-Langley, 1980